

A Project Report on

PERFORMANCE OF VARIOUS ANTENNAS FOR

WIRELESS IMAGE TRANSFER USING

SOFTWARE-DEFINED RADIO

Of

Master of Science

In

Electronics



Under the guidance of
Prof. Kamlesh Patel

Submitted by
Rounak DEB

Department of Electronic Science
University of Delhi South Campus New Delhi-110021
2023-2025

CERTIFICATE

This is to certify that the thesis entitled "**Performance of Various Antennas for Wireless Image Transfer Using Software-Defined Radio**" submitted by **Rounak Deb**, Roll No. **232517490**, in partial fulfillment of the requirements for the award of the degree of **Master of Science in Electronics** at **University of Delhi, South Campus, New Delhi** during January 2025 to May 2025, is a bonafide record of original work carried out under the supervision and guidance of the undersigned. The work has not been submitted previously in part or full to any other university or institute for the award of any degree or diploma.

**Prof. Kamlesh Patel
(Project Guide)**

Department of Electronic Science
University of Delhi
South Campus New Delhi-110021

**Dr. Amit Birwal
(Project Coordinator)**

Department of Electronic Science
University of Delhi
South Campus New Delhi-110021

**Prof. Harsupreet Kaur
(Head of the Department)**

Department of Electronic Science
University of Delhi
South Campus New Delhi-110021

DECLARATION

I hereby declare that the thesis entitled "**Performance of Various Antennas for Wireless Image Transfer Using Software-Defined Radio**", submitted in partial fulfillment of the requirements for the award of the degree of Master of Science in Electronics, is the result of my original research work carried out under the supervision of **Prof. Kamlesh Patel**, Department of Electronic Science University of Delhi from January 2025 to May 2025. This thesis has not been submitted previously, in part or full, to any other university or institution for the award of any degree or diploma. All the sources of information used in this thesis have been duly acknowledged.

Mr. Rounak Deb
M.Sc. Electronics
23251749020
Department of Electronic Science
University of Delhi
South Campus New Delhi-110021

ACKNOWLEDGEMENT

I would like to express my sincere gratitude to all those who have supported me throughout the completion of my M.Sc. project titled **“Performance of Various Antennas for Wireless Image Transfer Using Software-Defined Radio”**. I am deeply thankful to my project supervisor, **Prof. Kamlesh Patel**, for his invaluable guidance, support, and encouragement at every stage of the project. His expertise and constant motivation played a vital role in the successful execution of this work.

I would also like to thank **Dr. Amit Birwal**, Project Coordinator, for his timely support, feedback, and guidance throughout the duration of the project. I would like to express my special thanks to **Prof. Harsupreet Kaur**, Head of the Department, for facilitating an academic environment conducive to research and learning.

My sincere thanks to **Mr. Ravi**, PhD Scholar, and **Dr. Shailesh**, Post-Doctoral Researcher, for their technical inputs and helpful discussions that enhanced the quality of this work

I extend my appreciation to the faculty and staff of the **Department of Electronic Science, University of Delhi, South Campus**, for their support and cooperation during this project. Lastly, I am grateful to my family and friends for their unwavering encouragement, patience, and moral support throughout this journey.

Mr. Rounak Deb

M.Sc. Electronics

23251749020

Department of Electronic Science

University of Delhi

South Campus, New Delhi – 110021

ABSTRACT

This project looks at how different antennas perform when sending pictures wirelessly using a system called **Software-Defined Radio (SDR)**. We focused on the **5.8 GHz** frequency because it's commonly used in wireless communication. It's really important to know how the design of an antenna affects how well signals and data travel through the air.

For our tests, we set up a reliable system using a special piece of hardware called **USRP (Universal Software Radio Peripheral)**. This hardware works easily with **LabVIEW**, which is a visual programming tool. We carefully checked how well our system could send and receive signals using different antennas.

We used a **Metamaterial Double Negative Index antenna** to send the pictures. For receiving, we tested four different types of antennas: a **Metamaterial Epsilon Near Zero antenna**, a **Parasitic Patch antenna** (made from Rogers RO3003 material), a **Slot Cut Patch antenna** (also from Rogers RO3003), and a regular **Patch antenna** (made from FR4 material).

First, we took digital pictures, prepared them using **Python**, and then encoded and modulated them with **QPSK (Quadrature Phase Shift Keying)** in LabVIEW to prepare signals for wireless sending. After the signal traveled wirelessly, LabVIEW received and decoded it. Then, the data went back to Python, where the original image was put back together.

To see how good the received images were, we used several important measurements. These included the **Peak Signal-to-Noise Ratio (PSNR)**, the **Structural Similarity Index (SSIM)**, the **Root Mean Squared Error (RMSE)**, the **Pearson Correlation Coefficient**, and the **Normalized Cross-Correlation (NCC)**.

Our study clearly shows that the type of antenna chosen has a big impact on how successfully digital pictures are sent wirelessly. Our setup, which used **USRP B210** hardware controlled by LabVIEW and analyzed with Python, showed that each antenna delivered different levels of signal quality and image clearness. This research provides useful information for picking the best antennas for **5.8 GHz** wireless systems, especially where reliable data transfer is key. We found that the reconstructed pictures were consistently good when compared to the originals, proving that our method works well.

TABLE OF CONTENTS

Section No.	Title	Page No.
CHAPTER 1	INTRODUCTION	1
1.1	Wireless Image Transfer	1
1.1.1	What Wireless Image Transfer Is	1
1.1.2	Basic Wireless Image Transfer System	1
1.1.2.1	Basic Operations of Wireless Image Transfer	2
1.2	Image Transfer Methods	4
1.2.1	Efficient Digital Modulation Technique for Image Transmission	4
1.2.2	Secure Image Transmission with Chaotic Encryption and Turbo Codes	5
1.2.3	Robust Wireless Image Transmission	6
1.2.4	Performance Analysis of Image Transmission with Various Channel Conditions/Modulation Techniques	8
1.2.5	Wireless Image Transfer with Real-Time Antenna Comparison	9
1.3	Comparison of Image Transfer Methods and Their Characterization Parameters	11
1.4	Project Objectives	12

CHAPTER 2	SYSTEM COMPONENTS AND METHODOLOGY	13
2.1	Software Defined Radio (SDR)	13
2.1.1	What is Software Defined Radio (SDR)?	13
2.1.2	Basic Operation of SDR	13
2.1.3	Strengths of SDR	14
2.1.4	Challenges of SDR	15
2.1.5	Features of SDR	15
2.2	Hardware: Universal Software Radio Peripheral (USRP) B210	16
2.2.1	Installation of USRP B210	16
2.2.2	Figure of USRP B210	17
2.2.3	Operation of USRP B210	18
2.2.4	Physical Setup of the USRP B210 for Wireless Image Transfer	20
2.3	Software: LabVIEW	21
2.3.1	Installation Steps for LabVIEW	21
2.3.2	System Operation and Control	22
2.3.3	LabVIEW System Interface and Program Architecture	23

2.3.3.1	LabVIEW Front Panel During Operation	25
2.4	Software: Python	26
2.4.1	Python Libraries Utilized	26
2.4.2	Python Code Description	27
CHAPTER 3	ANTENNA CHARACTERIZATION AND MEASUREMENT	36
3.1	Vector Network Analyzer	36
3.1.1	S-Parameter	36
3.1.2	Libre-VNA	38
3.1.2.1	LibreVNA Software and Installation	39
3.1.2.2	LibreVNA Experimental Setup	40
3.1.2.3	LibreVNA Calibration Procedure	40
3.1.3	Rohde & Schwarz ZVH8 VNA	45
3.1.3.1	Rohde & Schwarz VNA: System Architecture	46
3.1.3.2	Rohde & Schwarz VNA Calibration Procedure	47
3.2	Antenna Characteristics and Performance	52
3.2.1	Physical Image of Antennas Used	52

3.2.2	Antenna Physical and Performance Characteristics	54
3.2.3	Return Loss (S11) Performance	56
3.2.3.1	LibreVNA S11 Measurements	56
3.2.3.2	Rohde & Schwarz ZVH8 VNA S11 Measurements	59
3.2.4	Radiation Patterns	61
3.2.5	Comparison of Antenna S11 and Frequency Performance	64
CHAPTER 4	SYSTEM IMPLEMENTATION AND EXPERIMENTAL RESULTS	65
4.1	System Design and Operational Principles	65
4.1.1	Transmitting Module	65
4.1.2	Receiving Module	66
4.2	Experimental Setup and Performance Evaluation	68
4.2.1	Single USRP Experimental Arrangement and Results	68
4.2.2	Two USRPs Experimental Arrangement and Results	92
4.3	Discussion and Comparative Analysis	182
4.3.1	Understanding Image Quality Metrics	182
4.3.2	Graphical Performance Comparisons	183

4.3.3	Overall Discussion of Antenna Performance	185
CHAPTER 5	CONCLUSION AND FUTURE WORK	186
5.1	Conclusion	186
5.2	Future Work	187
REFERENCES		188

CHAPTER 1

INTRODUCTION

1.1 Wireless Image Transfer

Wireless image transfer has become a fundamental aspect of modern communication, allowing for the quick and easy sharing of visual information without the need for physical connections. This technology underpins many everyday applications, from mobile phone photography to advanced surveillance systems and remote monitoring. As such, understanding and optimizing the process of sending digital pictures through the air is crucial for reliable and efficient data exchange.

1.1.1 What Wireless Image Transfer Is

Wireless image transfer involves sending digital pictures from one device to another without using any physical cables. This technology relies on radio waves or other invisible signals that travel through the air. It's a fundamental part of many everyday applications, from sharing photos on mobile phones to more specialized uses in remote monitoring or security systems.

For effective wireless image transfer, especially in important applications, it's crucial to transmit a large amount of data both quickly and dependably. This requires good wireless connections that provide sufficient bandwidth, allow for multiple signals to share the same medium (through multiplexing), and support high-speed data transfer with minimal loss. The system also needs to be adaptable, capable of using different modulation techniques without requiring changes to the physical equipment.

1.1.2 Basic Wireless Image Transfer System

A typical system for sending images wirelessly is made up of several interconnected components, working together to ensure that visual data can be sent from a source to a destination without physical wires. This process can be broadly divided into three main conceptual parts: the sending side (often called the transmitter), the medium through which the signals travel (the wireless channel or airwaves), and the receiving side (the receiver). Each part plays a vital role in transforming an image into a transmittable signal, sending it across the air, and then reassembling it accurately at the other end. The fundamental steps and components involved in this process are visually represented and detailed in a block diagram.

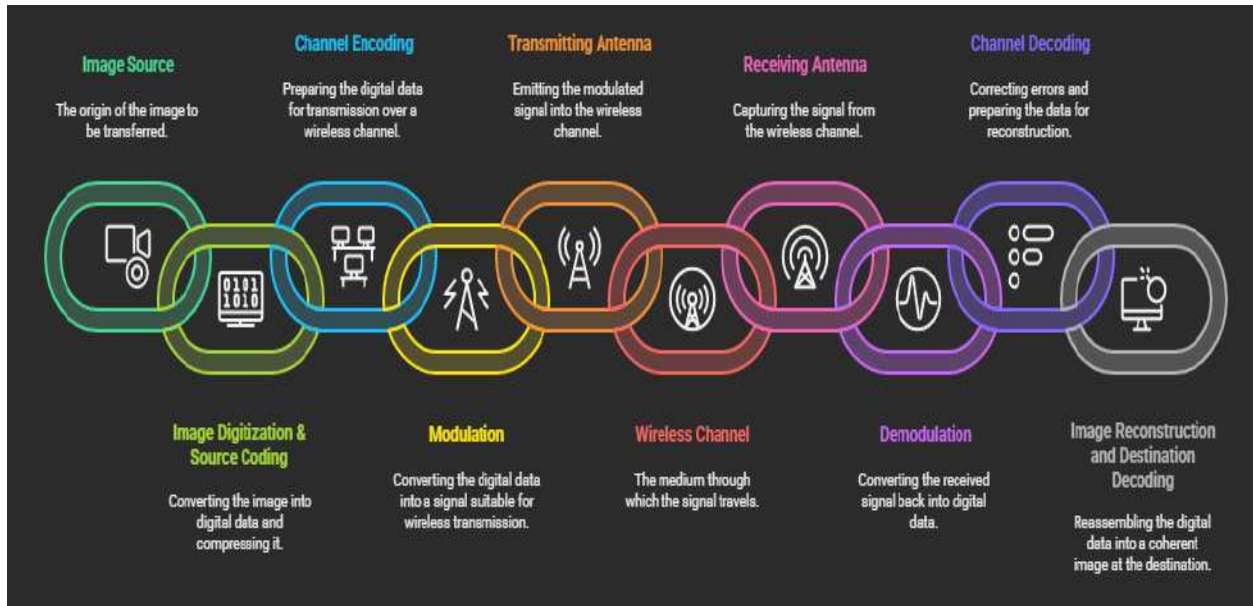


Fig. 1.1 Basic Block Diagram of Wireless Image Transfer

1.1.2.1 Basic Operations of Wireless Image Transfer

Each stage in the diagram shows an important step needed to send a picture accurately and efficiently from where it starts to where it ends up wirelessly.

- **Image Source:** This is simply where the picture comes from. It could be a camera taking a photo, a picture file on a computer, or an image created by software.
- **Image Digitization & Source Coding:**
 - **Image Digitization:** Real-world pictures are often in an analog form. To send them digitally, they need to be turned into numbers. This involves breaking the picture into tiny squares called pixels and then giving each pixel a number to represent its brightness or color.
 - **Source Coding:** After being turned into numbers, picture data often has repeated information. Source coding, or compression, removes this extra information. This reduces the amount of data to send, making the transfer faster and more efficient without losing too much quality.
- **Channel Encoding:** Wireless connections are naturally noisy and can have interference, which can mess up the data. Channel encoding, also called Forward Error Correction (FEC), adds extra, specially designed bits to the data. These extra bits help the receiving end find and fix errors that happen during the transmission, making the communication more reliable. Convolutional coding is a common technique used here.

- **Modulation:** The digital picture data needs to be converted into a form that can travel through the air. Modulation does this by changing a property (like strength, frequency, or phase) of a high-frequency radio wave, based on the digital data. This turns the digital 0s and 1s into a continuous electrical signal that the antenna can send out. Phase-Shift Keying (PSK) is a popular method for sending digital data this way.
- **Transmitting Antenna:** The electrical signal, which now carries the picture data, is made stronger and sent to the transmitting antenna. The antenna's job is to turn this electrical signal into radio waves that spread out into the air.
- **Wireless Channel:** This is simply the air or space through which the radio waves travel. It's not a perfect path; it can add noise (like random static, called AWGN), suffer from interference from other devices, cause the signal to get weaker (fading), or make the signal take multiple paths to reach the receiver (multipath), all of which can mess up the picture data.
- **Receiving Antenna:** At the other end, the receiving antenna catches the radio waves coming through the air and turns them back into an electrical signal.
- **Demodulation:** This step does the opposite of modulation. It takes the received electrical signal and processes it to pull out the original digital data. This involves filtering the signal and figuring out what each changed radio wave meant. Special filters, called matched filters, are often used here to make sure the signal is detected as clearly as possible, improving its quality.
- **Channel Decoding:** The digital data that came out of demodulation might still have some errors. The channel decoder uses the extra bits added during channel encoding to find and fix as many errors as possible. Viterbi decoding is a commonly used method for this, especially if convolutional coding was used before.
- **Image Reconstruction & Destination Decoding:** Finally, the corrected digital data is put back together to re-create the original picture. This also involves undoing any compression that was applied earlier. Computer programs (like Python with image libraries) are often used for this last step. The result is the picture, ready to be shown on a screen or saved.

1.2 Image Transfer Methods

Wireless image transfer is a critical domain in modern communication, enabling the transmission of visual data without physical connections. Over time, various methodologies have been developed to enhance the efficiency, reliability, and security of image transmission over wireless channels. This section presents five distinct image transfer methods, drawn from recent academic research, detailing their operational principles, system architectures, and key performance outcomes.

1.2.1 Efficient Digital Modulation Technique for Image Transmission

This method focuses on comparing the performance of different digital modulation techniques for image transmission over a wireless channel, specifically analyzing their behavior across varying Signal-to-Noise Ratio (SNR) conditions. The study is conducted using MATLAB simulations.

Source Paper: Raghavendra Singh Chadhar, Prof. Avinash Rai. "An Efficient Digital Modulation Technique for Image Transmission over Wireless Channel." INTERNATIONAL JOURNAL OF SCIENTIFIC PROGRESS AND RESEARCH (IJSR), Volume 24, Number 01, 2016.

Operation:

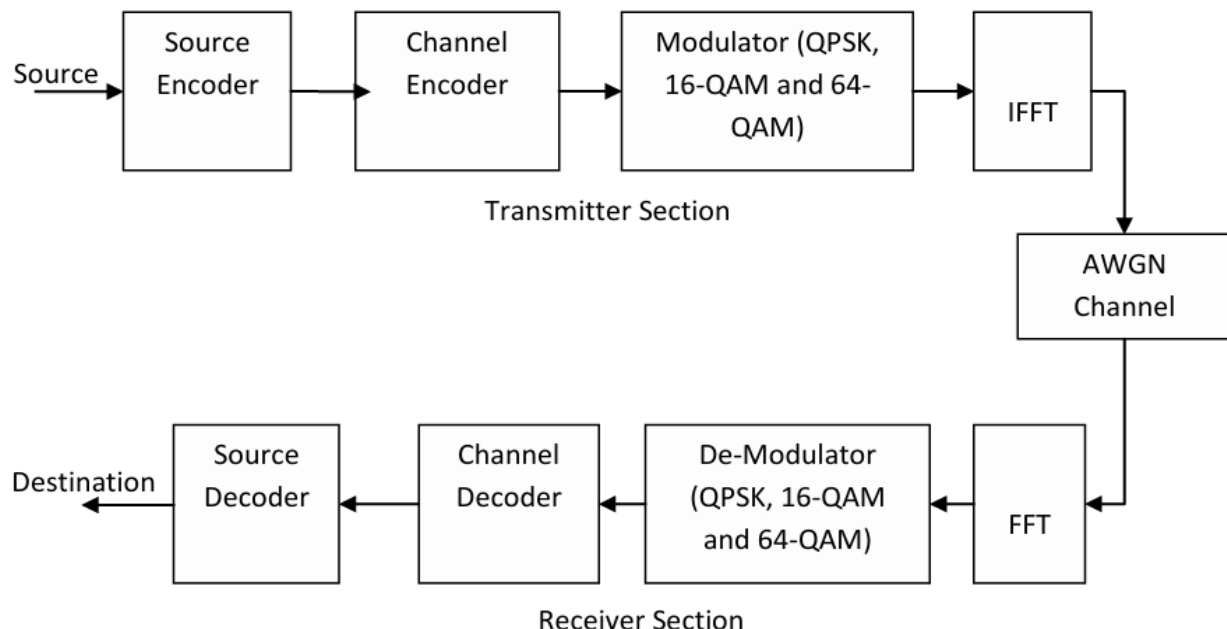


Fig. 1.2 Block Diagram for Efficient Digital Modulation Technique

The primary goal is to evaluate the impact of different modulation schemes, including QPSK, 16-QAM, and 64-QAM, on the quality of received images. The simulation models a simplified wireless digital communication system. It processes an input image, converting it into a binary sequence via a source encoder. This binary sequence is then modulated by the chosen technique, passed through an Inverse Fast Fourier Transform (IFFT) block, and transmitted over an Additive White Gaussian Noise (AWGN) channel. At the receiver, the process is reversed, involving a Fast Fourier Transform (FFT), demodulation, and source decoding to reconstruct the image. The simulation investigates image transmission quality rather than audio signal transmission.

Results: The quality of the received image varied depending on the modulation technique and SNR. Simulations were performed at SNR values of 5 dB, 10 dB, and 50 dB. Findings indicated that 64-QAM generally provided superior results compared to QPSK and 16-QAM at 5 dB and 10 dB SNR. However, at 50 dB SNR, all tested techniques exhibited comparable good performance. The system's design allowed for degraded image quality rather than complete loss of the transmitted image, even under high noise conditions.

1.2.2 Secure Image Transmission with Chaotic Encryption and Turbo Codes

This method introduces a robust and secure image transmission system designed for noisy wireless networks, integrating techniques for image compression, chaotic encryption, and advanced channel coding using Turbo codes.

Source Paper: Salah A. Aliesawi, Dena S. Alani, Abdullah M. Awad. "Secure image transmission over wireless network." International Journal of Engineering & Technology, 7(4), 2758-2764, 2018.

Operation: The system prioritizes security and robustness for image transfer over wireless channels. It begins with image compression to reduce data size and convert the image from a 2D to a 1D matrix. This compression involves steps like RGB to YCbCr conversion, Discrete Cosine Transform (DCT), quantization, zigzag scanning, Run-Length Encoding (RLE), and shift coding. The compressed image is then encrypted using a model that combines a key generator with a Chaotic Henon map. The encrypted data is further protected by Turbo coding, a powerful error correction code that uses two identical convolutional codes and an interleaver. This coded data is then modulated and transmitted wirelessly. At the receiver, the process is reversed, involving demodulation, Turbo decoding (using Soft-Input Soft-Output (SISO) decoders), decryption, and decompression to reconstruct the image.

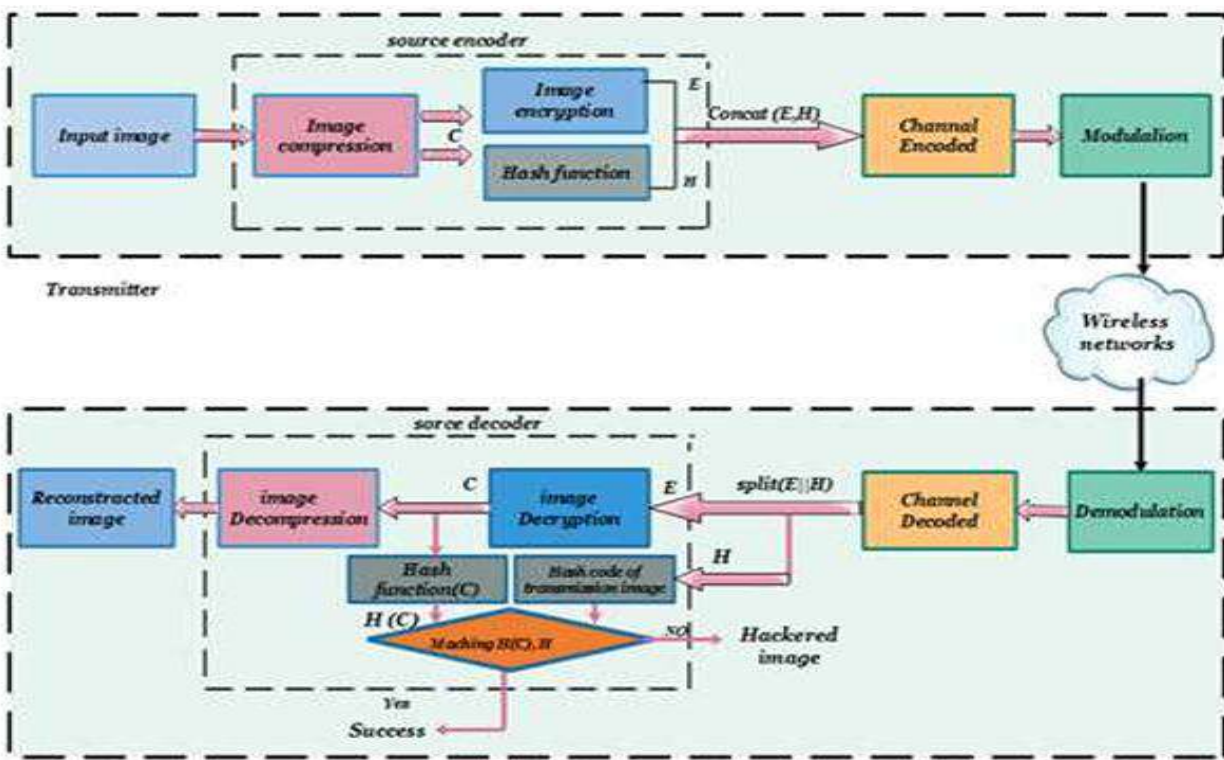


Fig. 1.3 Block Diagram for Secure Image Transmission

Results: Simulation outcomes indicated that the proposed system achieved high robustness against various attacks and channel impairments. The integration of Turbo codes significantly reduced the Bit Error Rate (BER) by effectively correcting transmission errors. Comparisons demonstrated that the quality of transmitted data was superior when transferred through a Turbo-coded channel compared to an uncoded channel. The study showed that images reconstructed using Turbo codes were clear and efficient even at lower SNR values, where uncoded images were distorted.

1.2.3 Robust Wireless Image Transmission

This method proposes a robust image transmission system that integrates Orthogonal Frequency Division Multiplexing (OFDM) with Reed-Solomon (RS) channel coding and a jointly optimized Vector Quantization (VQ) source encoder alongside 16-QAM modulation.

Source Paper: Angela Doufexi, Andrew Nix, David Bull. "Robust Wireless Image Transmission using Jointly-Optimized Modulation and Source Coding." VTC2000, 2000.

Operation:

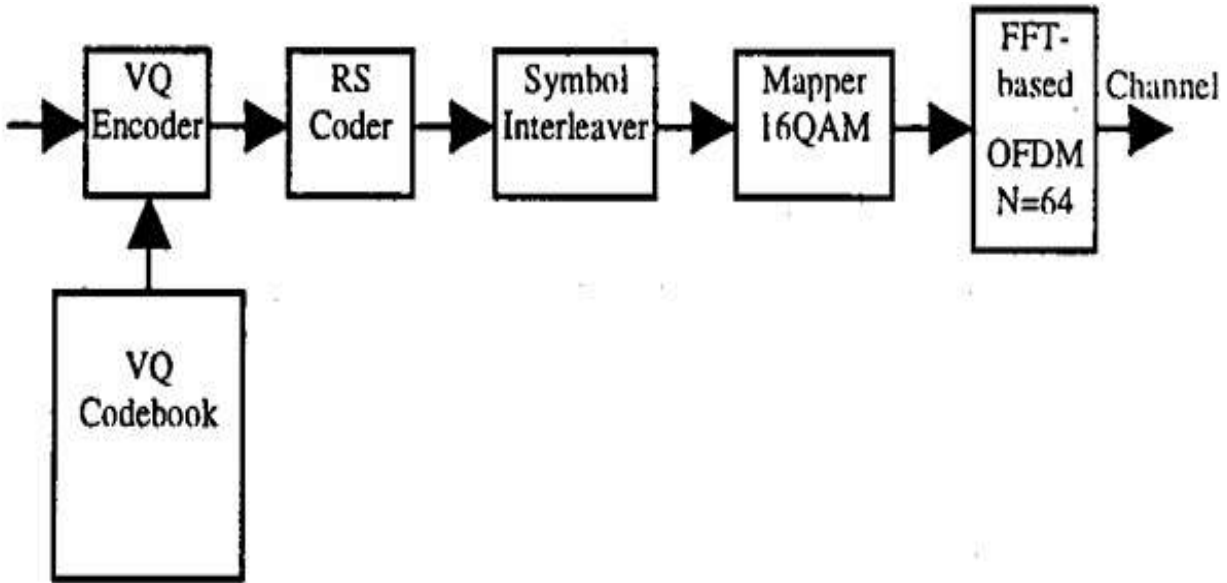


Fig.1.4 Block Diagram of Robust Wireless Image Transmission

The system is designed for robust image transmission, particularly over wideband multipath fading channels. It utilizes Vector Quantization (VQ) for image compression, which reduces the bit rate by leveraging statistical redundancy among pixels. The VQ encoder generates codevector indices, which are then Reed-Solomon (RS) encoded for channel error protection. These encoded indices are mapped onto a 16-QAM Orthogonal Frequency Division Multiplexing (OFDM) constellation. Symbol interleaving is incorporated to minimize the effects of burst errors. OFDM is employed to combat frequency-selective fading and random burst errors by distributing data over multiple orthogonal subcarriers, thereby mitigating Inter-Symbol Interference (ISI). The channel is modeled as a wideband multipath Rayleigh fading channel. The core principle involves a joint optimization of the source coding (VQ) and 16-QAM modulation to reduce visual artifacts caused by channel errors.

Results: Simulations demonstrated that the combination of OFDM and Reed-Solomon coding made the system highly robust to transmission errors. The proposed scheme achieved reliable image transmission even at relatively low Signal-to-Noise Ratios (SNRs). A key finding was that the joint optimization of the VQ source encoder with 16-QAM, combined with OFDM's inherent ability to degrade gracefully, resulted in a smooth degradation of image quality as the SNR decreased, resembling an analog system. For instance, a PSNR (Peak Signal-to-Noise Ratio) of 28.25 dB was observed at an SNR of 18 dB (with a Bit Error Rate (BER) of 3×10^{-4}), indicating near-unimpaired image transmission over a wideband Rayleigh fading channel. The ordered codebook property of the VQ coder was instrumental in reducing visual artifacts, thus maintaining good subjective image quality even at higher BERs.

1.2.4 Performance Analysis of Image Transmission with Various Channel Conditions/Modulation Techniques

This method presents a MATLAB-based simulation study that analyzes the performance of image transmission using different QAM-based modulation techniques (QPSK, 16-QAM, 64-QAM) across both AWGN and Rayleigh fading channels, incorporating the use of Wiener and Median filters at the receiver.

Source Paper: Marwa Jaleel Mohsin, Wasan Kadhim Saad, Bashar J. Hamza, Waheb A. Jabbar. "Performance analysis of image transmission with various channel conditions/modulation techniques." TELKOMNIKA Telecommunication, Computing, Electronics and Control, Vol. 18, No. 3, June 2020, pp. 1158-1168.

Operation:

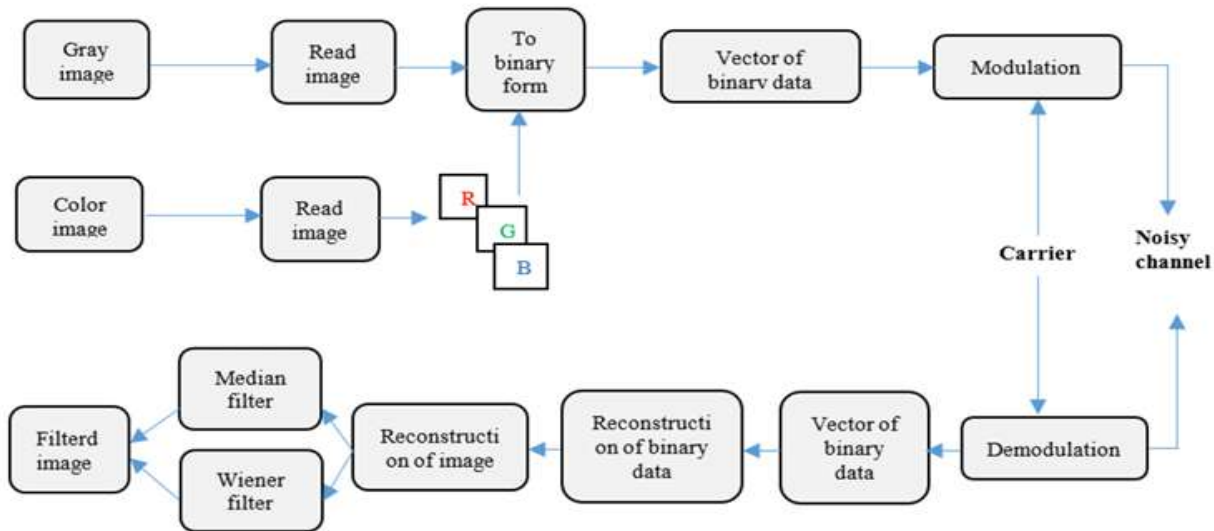


Fig.1.5 Block Diagram for Performance Analysis of Image Transmission

This study evaluates the transmission of two-dimensional (2D) grayscale and color (RGB) images. The process involves initial image preprocessing to convert the 2D image into a one-dimensional (1D) binary vector. This data is then modulated using one of the chosen techniques: QPSK, 16-QAM, or 64-QAM, where higher-order QAM schemes transmit more bits per symbol. The modulated signal is then transmitted through simulated AWGN or Rayleigh fading channels. At the receiver, the inverse operations are performed, including demodulation and image reconstruction. Wiener and Median filters are optionally applied after reception to mitigate impulsive noise in the recovered image. Performance is quantitatively assessed using Peak Signal-to-Noise Ratio (PSNR) and Mean Squared Error (MSE).

Results: Simulation results, conducted across various Signal-to-Noise Ratio (SNR) values (5, 10, and 15 dB), consistently showed that the system performs better in AWGN channels compared to Rayleigh fading channels. Higher PSNR values were directly correlated with improved image quality. The application of Median and Wiener filters at the receiver generally increased PSNR, indicating improved image clarity. Notably, the QPSK modulation technique yielded superior received image quality and demonstrated greater immunity to noise compared to 16-QAM and 64-QAM, especially in Rayleigh fading environments. This is attributed to the fact that higher-order QAM techniques are more susceptible to interference and Inter-Symbol Interference (ISI). The system was designed to gracefully degrade image quality rather than lose the image completely under high noise conditions.

1.2.5 Wireless Image Transfer with Real-Time Antenna Comparison

This method proposes an inexpensive technique for real-time wireless image transfer, focusing on evaluating the comparative performance of various antenna types at 5.8 GHz using a no-reference image quality assessment method.

Source Paper: Gobind Rai, Puneet Sehgal, Kamlesh Patel. "Wireless image transfer by various antennas using transmitter and receiver modules at 5.8 GHz." International Journal of Microwave and Wireless Technologies, 16(7), 1248-1259, 2024.

Operation:

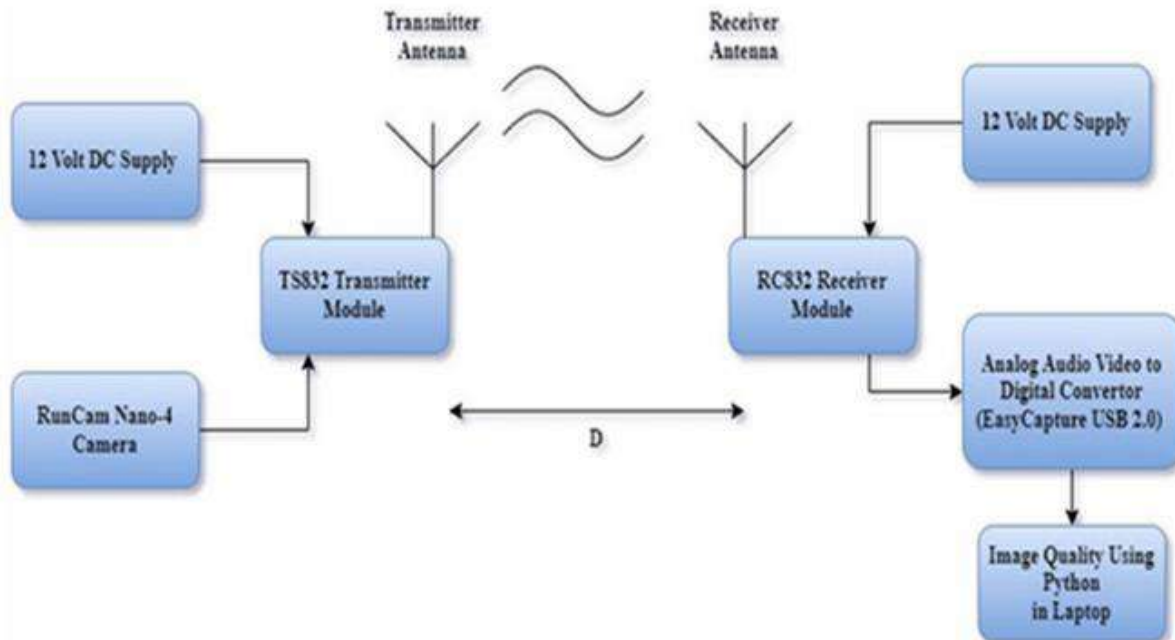


Fig.1.6 Block Diagram of Wireless Image Transfer with Real-Time Antenna Comparison

The system employs commercial 5.8 GHz transmitter (TS832 audio/video) and receiver (RC832 audio/video) modules for real-time wireless image transfer. A camera (Run Cam Nano 4) captures real-time images, which are then transmitted via Frequency Modulation (FM) at 5.8 GHz. The received analog signals are converted to digital via a USB converter for storage on a laptop or desktop computer. A custom Python code-based Graphical User Interface (GUI) application is developed for real-time image capturing and storage. Image quality assessment is performed using the Blind/Referenceless Image Spatial Quality Evaluator (BRISQUE) method, which is implemented in Python. BRISQUE generates an Image Quality Score (IQS) (ranging from 0 for very good quality to 100 for very bad quality) by analyzing image pixel information and Natural Scene Statistics (NSS), without requiring a reference image. The performance of different antenna types, including dipole, circular split-ring resonators (C-SRR), hexagonal split-ring resonators (H-SRR), and metamaterial antennas, is comparatively evaluated across various distances and orientations.

Results: The research concluded that images transferred using metamaterial antennas generally exhibited higher quality (indicated by lower IQS scores) compared to those transferred with other antenna types. While dipole antennas demonstrated good performance at very close distances, metamaterial antennas showed superior performance at longer ranges. This suggests that higher-gain, narrow-beamwidth antennas, such as the metamaterial ones, are optimal for wireless image transfer over extended distances due to more efficient radiated power transmission and focused reception. The system demonstrated functionality even in the presence of obstructions, confirming its suitability for security and surveillance applications.

1.3 Comparison of Image Transfer Methods and Their Characterization Parameters

Table 1.1

Reference No.	Image Transfer Method	Primary Characterization Parameters
1.2.1	Efficient Digital Modulation Technique for Image Transmission	SNR, Image Quality (Visual), PSNR, MSE
1.2.2	Secure Image Transmission with Chaotic Encryption and Turbo Codes	NPCR, UACI (for encryption sensitivity), BER, Image Quality
1.2.3	Robust Wireless Image Transmission	PSNR, BER
1.2.4	Performance Analysis of Image Transmission with Various Channel Conditions/Modulation Techniques	PSNR, MSE, SNR (image)
1.2.5	Wireless Image Transfer with Real-Time Antenna Comparison	BRISQUE Image Quality Score (IQS)

1.4 Project Objectives

The main aim of this project is to thoroughly investigate and show the capabilities of various antennas working in the 5.8 GHz frequency band for wireless image transfer. This will be done using an integrated USRP-LabVIEW system.

To achieve this overall goal, we have set the following specific objectives:

- **Development of an SDR-based Image Transfer Method:** This objective involves creating a complete and functional system that can convert digital image data into a suitable format for wireless transmission, manage its processing through a communication link, and accurately reconstruct the image at the receiving end.
- **Characterization of 5.8 GHz Antennas:** This involves experimentally evaluating the operational characteristics and efficiency of specific antenna types. The antennas under study include a Metamaterial Double Negative Index antenna for transmission, and for reception, a Metamaterial Epsilon Near Zero antenna, a Parasitic Patch Antenna on Rogers RO3003, a Slot Cut Patch Antenna on Rogers RO3003, and a standard Patch Antenna on FR4.
- **Implementation of Wireless Image Transfer:** This objective focuses on practically integrating the characterized antennas into the developed SDR-based image transfer system to facilitate the actual transmission and reception of images wirelessly.
- **Quantitative Assessment of Transferred Image Quality:** This final objective involves evaluating the fidelity of the received images against the original transmitted images. This assessment will employ recognized image quality metrics, such as Peak Signal-to-Noise Ratio (PSNR), Structural Similarity Index (SSIM), Root Mean Squared Error (RMSE), Pearson Correlation Coefficient, and Normalized Cross-Correlation (NCC), to determine the effectiveness and integrity of the wireless image transfer process under different antenna configurations.

CHAPTER 2

SYSTEM COMPONENTS AND METHODOLOGY

2.1.1 What is Software Defined Radio (SDR)?

Software-defined radio (SDR) is a radio system where the main parts that handle radio signals – like the mixers, filters, amplifiers, and modulators – are controlled by software instead of being fixed circuits. This design lets one piece of hardware act like many different radios just by running different software programs. It swaps out many special analog circuits with digital processing, which makes it very adaptable. Typically, an SDR system has a part that connects to antennas (the RF front-end, which handles analog signals) linked to a computer or a special digital signal processor (DSP) that takes care of all the complicated signal work.

2.1.2 Basic Operation of SDR

The core idea behind SDR is to turn analog radio signals into digital data so software can work with them, and then turn them back again when needed. This cycle is shown in Fig. 2.1.

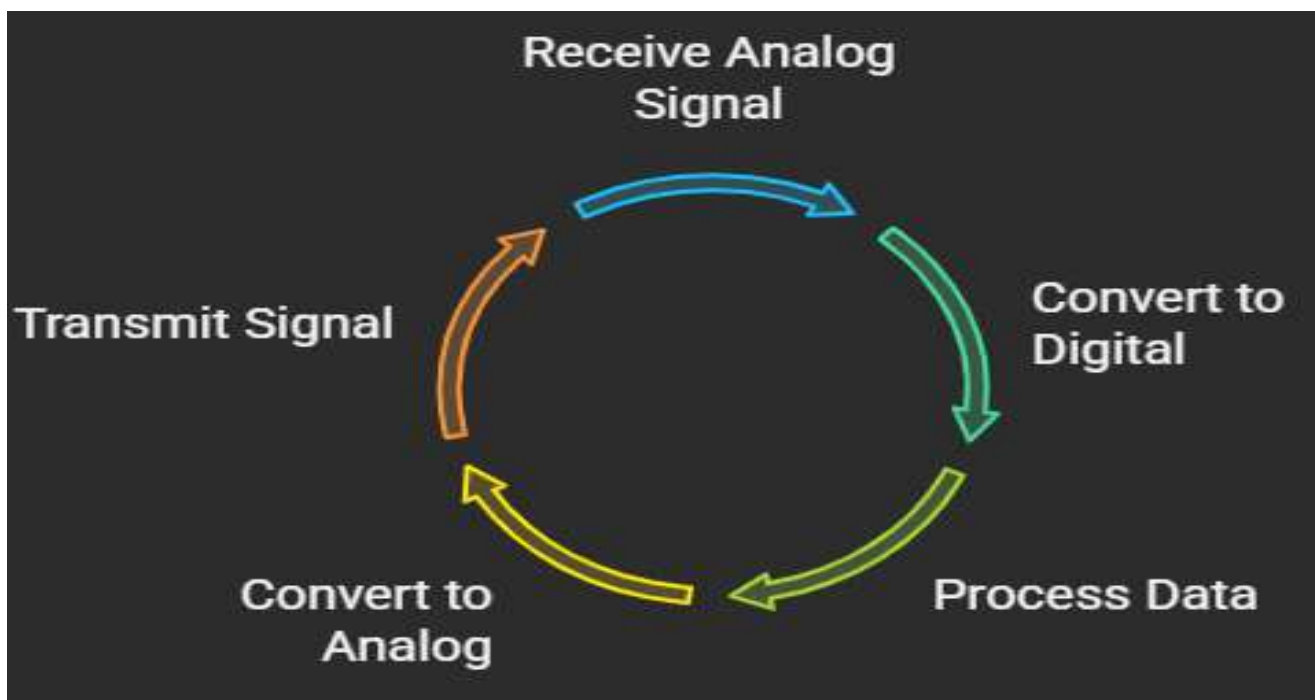


Fig.2.1

- **Analog-to-Digital Conversion (ADC):** When the radio is receiving a signal, its antenna picks up the analog radio waves. This analog signal then goes into an analog-to-digital

converter (ADC). The ADC takes samples of the analog wave and changes them into a stream of digital numbers.

- **Digital Signal Processing (DSP) (Software):** These digital numbers are then sent to a powerful computer processor, like a main computer chip or a dedicated DSP chip. Here, computer programs do all the jobs a traditional radio would: they filter out unwanted frequencies, pull the original information out of the signal (demodulation), and correct any errors that might have happened during transmission.
- **Digital-to-Analog Conversion (DAC):** When the radio needs to send something, the digital information (like voice, an image, or video) is first prepared by software (encoded and modulated). This digital signal then goes to a digital-to-analog converter (DAC). The DAC changes these digital numbers back into an analog wave.
- **Analog Radio Frequency (RF) Front-End:** This analog wave is then amplified and sent to the transmitting antenna, which sends it out as a radio signal.

2.1.3 Strengths of SDR

SDRs come with several big advantages:

- **Very Flexible:** SDRs can quickly change how they work. They can support different wireless standards, types of signals, or frequency ranges just by updating their software.
- **Quick to Develop:** They make it much faster to design and test new ways to send and receive signals, saving a lot of time and money in research and development.
- **Many Uses in One:** A single SDR device can handle many different communication tasks or easily switch between them.

2.1.4 Challenges of SDR

Even with their strengths, SDRs do have some difficulties:

- **Need Powerful Computers:** Because so much of the radio's work is done by software, SDRs need very fast and strong computer processors. These powerful processors can use a lot of electricity.
- **Possible Delays:** The processing done by software can sometimes cause tiny delays in the signal. This could be a problem for systems that need to react instantly.
- **Expensive Core Parts:** While SDRs are flexible, the main components that turn radio signals into digital data and back need to be very high-performing. These key parts can be quite expensive.

2.1.5 Features of SDR

SDR systems are known for several key features that highlight how versatile and advanced they are:

- **Works Across Many Frequencies:** Many SDRs can operate over a wide range of frequencies, supporting multiple bands without needing any physical changes to the hardware.
- **Supports Advanced Designs:** Modern SDRs can easily work with multiple antennas for MIMO (Multiple-Input Multiple-Output) setups. This can greatly improve data speeds and how reliably a connection works.
- **Customizable Signals:** Researchers and developers have the freedom to design and implement new and custom radio waveforms and communication rules directly through software.
- **Built-in Spectrum Analysis:** SDR platforms often include powerful tools for looking at the radio spectrum in real-time. This helps in identifying signals and detecting interference.
- **Easy Software Integration:** SDR hardware is often designed to work smoothly with high-level programming environments like LabVIEW and MATLAB, offering easy-to-use interfaces for complex radio operations.

2.2 Hardware: Universal Software Radio Peripheral (USRP) B210

The Universal Software Radio Peripheral (USRP) B210 is the main piece of hardware used in this project. It makes it possible to build a Software Defined Radio (SDR) system specifically for sending images wirelessly. USRP devices are flexible and popular in research because they provide a versatile radio part (RF front-end) that's perfect for SDR projects.

2.2.1 Installation of USRP B210

Properly installing and setting up the USRP B210 is crucial for it to work smoothly with the chosen software, mainly LabVIEW, in this project. Following the installation steps correctly ensures that the computer can communicate effectively with the USRP hardware.

Installation Steps for USRP Driver:

- **Get the Drivers and Software:** First, download the official drivers and the software development kit (SDK) for the USRP B210. You can usually find these important software packages on the official websites of National Instruments (NI) or Ettus Research, as NI often provides complete solutions for systems using LabVIEW and USRP.
- **Run the Installer:** Find the downloaded installer file and run it. The installer will guide you through a series of questions. It's usually best to stick with the default installation choices unless your system has specific needs.
- **Install USB 3.0 Driver:** During the installation, make sure to select and install the specific USB 3.0 drivers for the USRP B210. These drivers are essential for creating a fast data link between your computer and the USRP device.
- **Restart Your System (if asked):** After the installation finishes, the installer might ask you to restart your computer. It's a good idea to do this to make sure all the driver parts are properly set up and recognized by your computer's operating system.
- **Connect the USRP:** Once your system has restarted, connect the USRP B210 to a fast USB 3.0 port on your computer using the USB 3.0 cable provided. Also, make sure the USRP device is turned on.
- **Check the Installation:** To confirm that the drivers are installed correctly and communication is working, use the utility tools or example programs provided by the manufacturer. For NI-USRP drivers, this often means using the NI-USRP Configuration Utility or running a simple example program within LabVIEW to see if it detects the connected USRP device. If it's detected, the drivers are working correctly.

2.2.2 Figure of USRP B210

Pictures of the USRP B210 from different angles are available in Figures 2.2, 2.3, and 2.4. A general diagram showing how a USRP device is built internally is displayed in Figure 2.5.



Fig. 2.2 USRP B210 (Front View)



Fig. 2.3 USRP B210 (Angled)



Fig. 2.4 USRP B210 (Side View)

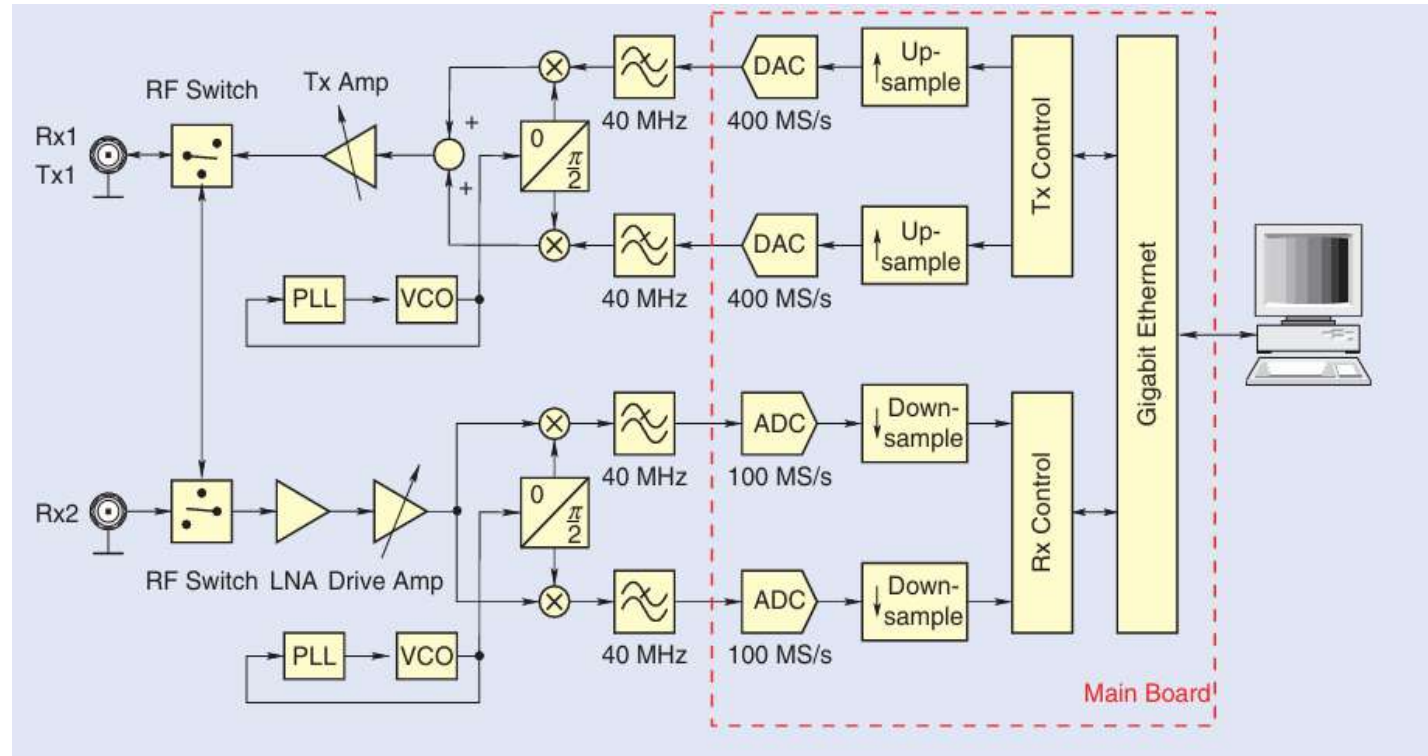


Fig. 2.5 Typical Block Diagram of USRP B210 Device

2.2.3 Operation of USRP B210

The USRP B210 acts as a versatile device that can both send and receive radio signals for Software-defined Radio (SDR) applications. It works by precisely controlled software. Its operation involves a constant back-and-forth between its internal hardware and the software on the computer it's connected to.

➤ Transmitting Operation

- **Making the Digital Signal:** The sending process starts on the computer, where the digital waveforms (like the image signal prepared in LabVIEW) are created as two parts: In-phase (I) and Quadrature (Q) components.
- **Sending Data to USRP:** These digital I/Q parts are then sent from the computer to a special chip inside the USRP B210 called an FPGA (Field-Programmable Gate Array), using a fast connection like Gigabit Ethernet.
- **Digital-to-Analog Conversion and Upconversion:** Inside the USRP's FPGA, the speed of the digital signal is adjusted. Then, two 16-bit DACs (Digital-to-Analog Converters) change the digital I/Q parts into analog signals. These analog I/Q signals then go into a mixer, which combines them to create the radio frequency (RF) signal ready for transmission.
- **Amplifying and Sending the RF Signal:** This newly created RF signal is then amplified by a power amplifier that can change its strength. Finally, this amplified RF signal is sent out through a small connector (like Tx1) to the connected antenna, which radiates it wirelessly.

➤ Receiving Operation

- **Catching the RF Signal and Converting Down:** The USRP's antenna picks up incoming RF signals from the air. This weak incoming signal first goes into a Low-Noise Amplifier (LNA) to reduce any unwanted noise and boost the signal's strength. The signal then goes into a mixer to separate it back into its analog I/Q components.
- **Analog-to-Digital Conversion:** After going through a filter to prevent unwanted signals, the analog I/Q parts are turned into digital signals by ADCs (Analog-to-Digital Converters), typically 14-bit ones that sample at 100 million times per second.
- **Sending Data to Computer:** The rate of these digital samples from the ADCs is adjusted for sending over the Gigabit Ethernet connection. These digital I/Q samples are then sent back to the computer.
- **Software Processing:** Once on the computer, this stream of digital data undergoes further processing by software, such as demodulation (to get the original information back), error decoding, and finally preparing the data to rebuild the image, often done by another program like Python.

2.2.4 Physical Setup of the USRP B210 for Wireless Image Transfer

The actual physical arrangement of the USRP B210 with the transmitting and receiving antennas can be seen in Figures 2.6 and 2.7.



Fig. 2.6 USRP B210 with Transmitting Antenna



Fig. 2.7 USRP B210 with Receiving Antenna

2.3 Software: LabVIEW

LabVIEW (Laboratory Virtual Instrumentation Engineering Workbench), created by National Instruments (NI), is a well-known graphical programming environment. It is used a lot in many fields, like testing and measuring things, controlling industrial machines, and developing custom engineering systems. Its easy-to-use graphical interface, where you connect function blocks with virtual "wires," makes it very effective for complex signal processing tasks and for interacting with hardware. In this project, LabVIEW acts as the main software platform. It controls the Universal Software Radio Peripheral (USRP) B210 and manages the entire wireless image transfer system.

2.3.1 Installation Steps for LabVIEW

Installing LabVIEW and its extra toolkits correctly is essential to make sure it can talk to the USRP B210 and handle all the necessary signal processing.

- **Get the Software:** Start by getting the main LabVIEW development software along with any modules and toolkits you need. For working with USRP, the NI-USRP driver and the NI LabVIEW Modulation Toolkit are key parts, usually available from the National Instruments website.
- **Run the Installer:** Run the LabVIEW installer program. This big installer will guide you through choosing and installing the main LabVIEW software, important modules (like Digital Signal Processing), and specific toolkits (including NI-USRP and the Modulation Toolkit). It's very important to pick all the parts that are needed for Software Defined Radio (SDR) and wireless communication.
- **Activate License:** After installation, you'll need to activate the LabVIEW software and its toolkits using the license keys you were given. This makes sure everything works fully.
- **Restart Your System (if asked):** You might need to restart your computer after installation to finish the process and ensure all software parts are correctly set up and recognized by the operating system.
- **Check the Installation:** Open LabVIEW and confirm that the VIs (Virtual Instruments, which are LabVIEW's program files) for NI-USRP and the Modulation Toolkit can be found in the Functions Palette. This step confirms that the installation was successful and the software is ready for your project.

2.3.2 System Operation and Control

LabVIEW serves as the central brain for controlling and processing everything in the wireless image transfer system. It operates the USRP B210 hardware and manages the signal path from start to finish.

➤ How LabVIEW Controls USRP B210

- **Setting Up and Controlling Hardware:** LabVIEW provides visual screens, called Front Panels, where users can easily set up and control different working settings of the USRP B210. These settings include the carrier frequency, how often samples are taken, the power of the transmitted signal, and how much the receiver boosts the signal. This ability is like a "USRP management service" that lets you change how the hardware works in real-time directly from the software.
- **High-Speed Data Transfer (I/Q Components):** LabVIEW helps move digital I (In-phase) and Q (Quadrature) signal parts at high speed between the computer and the USRP device. Specific LabVIEW programs, called VIs, like "Fetch I/Q Data" (for receiving) and "Write I/Q Data" (for transmitting), handle this "USRP data service".
- **Generating and Processing Signals:** Inside LabVIEW's visual programming setup, complex signal processing steps are built by connecting function blocks with wires. For sending signals, LabVIEW creates the modulated waveforms that carry the image information. For receiving signals, it processes the incoming digital I/Q data stream, doing important jobs like demodulation and channel decoding.
- **Complete Transmitting Process:** The digital data that represents the image signal (after being encoded and modulated within LabVIEW) is prepared by the software on the computer. This data is then streamed through LabVIEW's connection to the USRP B210. The USRP's internal hardware then changes this digital stream into an analog radio frequency (RF) signal, which is sent wirelessly through the connected antenna.
- **Complete Receiving Process:** The USRP B210's antenna picks up incoming RF signals. The hardware then changes these into digital I/Q baseband samples. These digital samples are streamed back to the computer, where LabVIEW processes them. This processing includes demodulation (getting the original signal back), correcting any errors, and finally preparing the data for the image to be put back together, often by another software like Python.

2.3.3 LabVIEW System Interface and Program Architecture

The LabVIEW Front Panel of the Transmitting Module, which shows the controls and displays for sending the image data, is depicted in Figure 2.8. Similarly, the LabVIEW Block Diagram of the Transmitting Module, illustrating the internal wiring and logic for the transmission process, is presented in Figure 2.9.

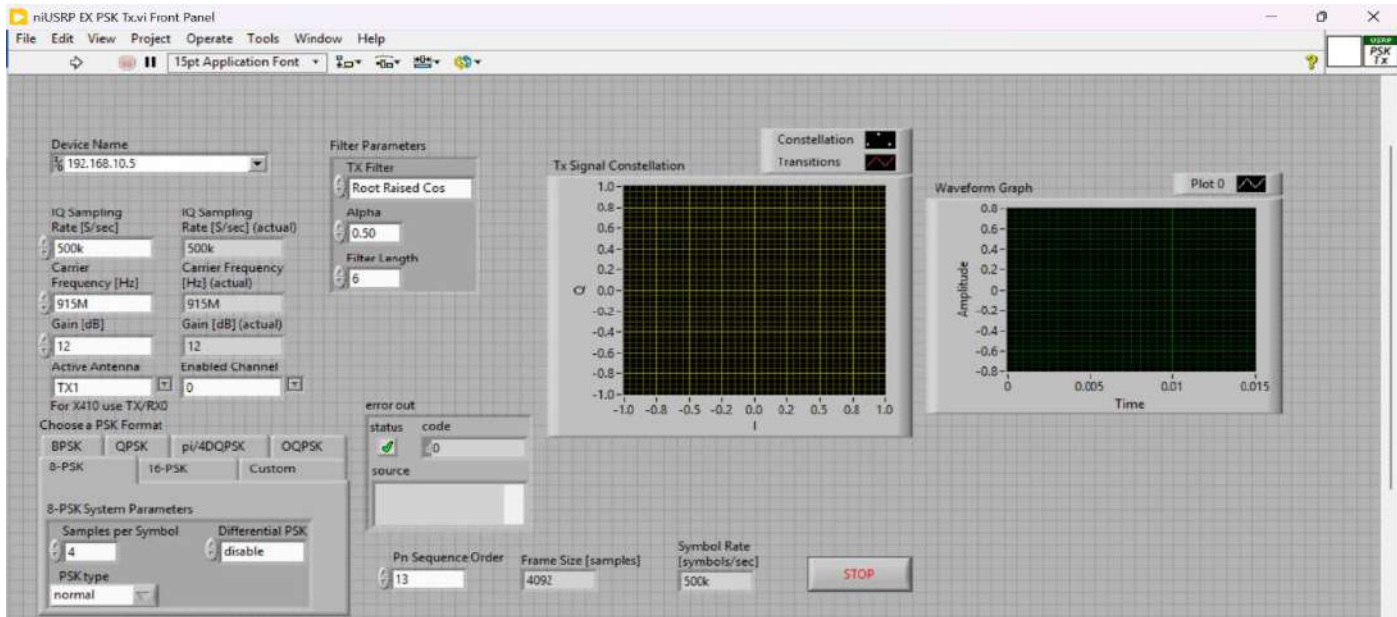


Fig. 2.8 LabVIEW Front Panel of the Transmitting Module

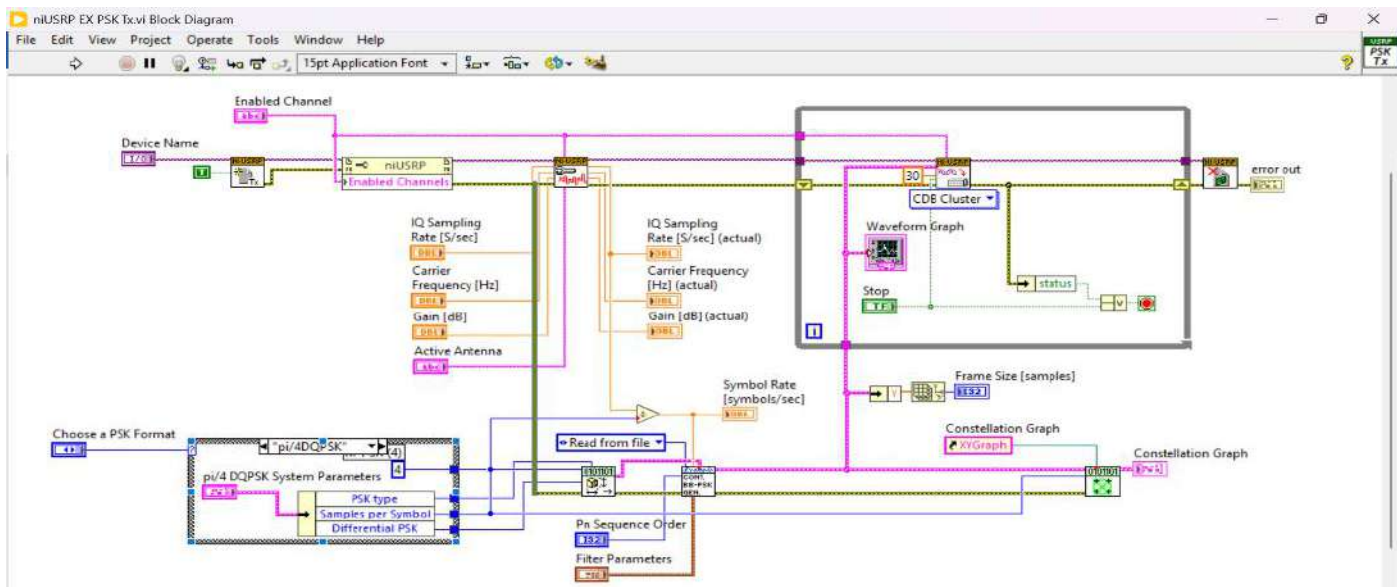


Fig. 2.9 LabVIEW Block Diagram of the Transmitting Module

For the receiving side, the LabVIEW Front Panel of the Receiving Module, providing the user interface for managing signal reception and observing parameters, is shown in Figure 2.10. Its corresponding internal wiring and processing flow are detailed in the LabVIEW Block Diagram of the Receiving Module, presented in Figure 2.11. These figures visually represent how the LabVIEW environment is set up to handle both sending and receiving wireless image data.

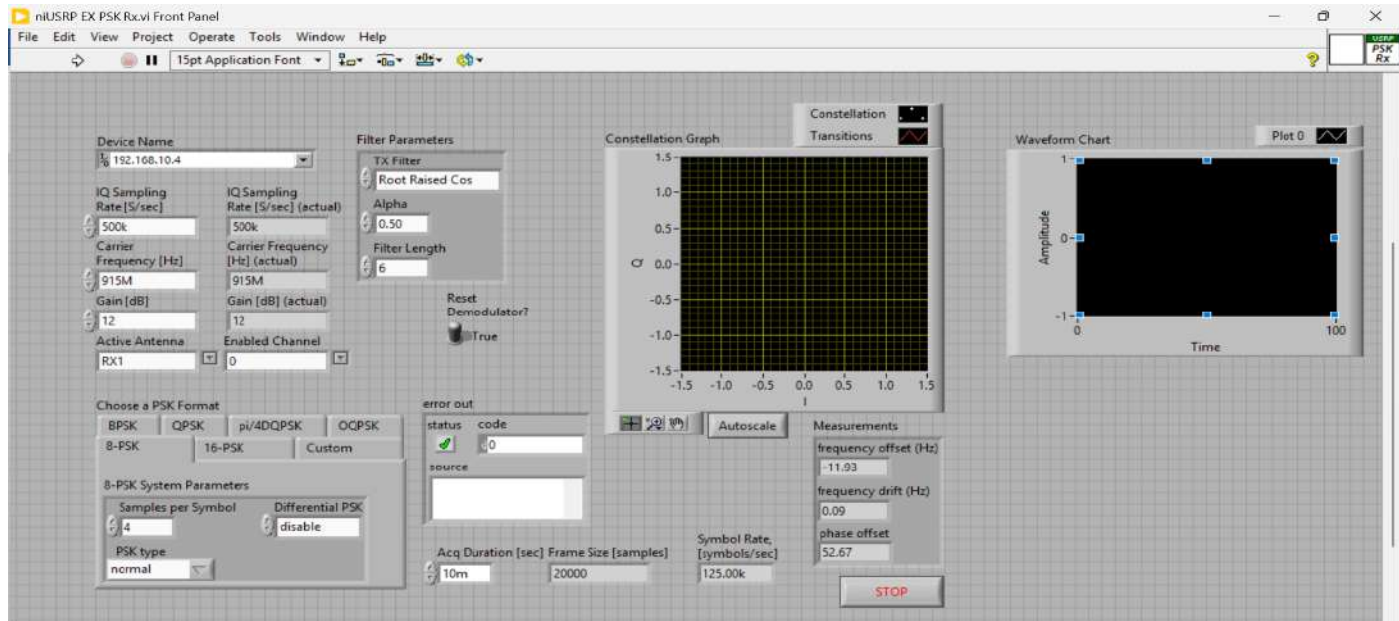


Fig. 2.10 LabVIEW Front Panel of the Receiving Module

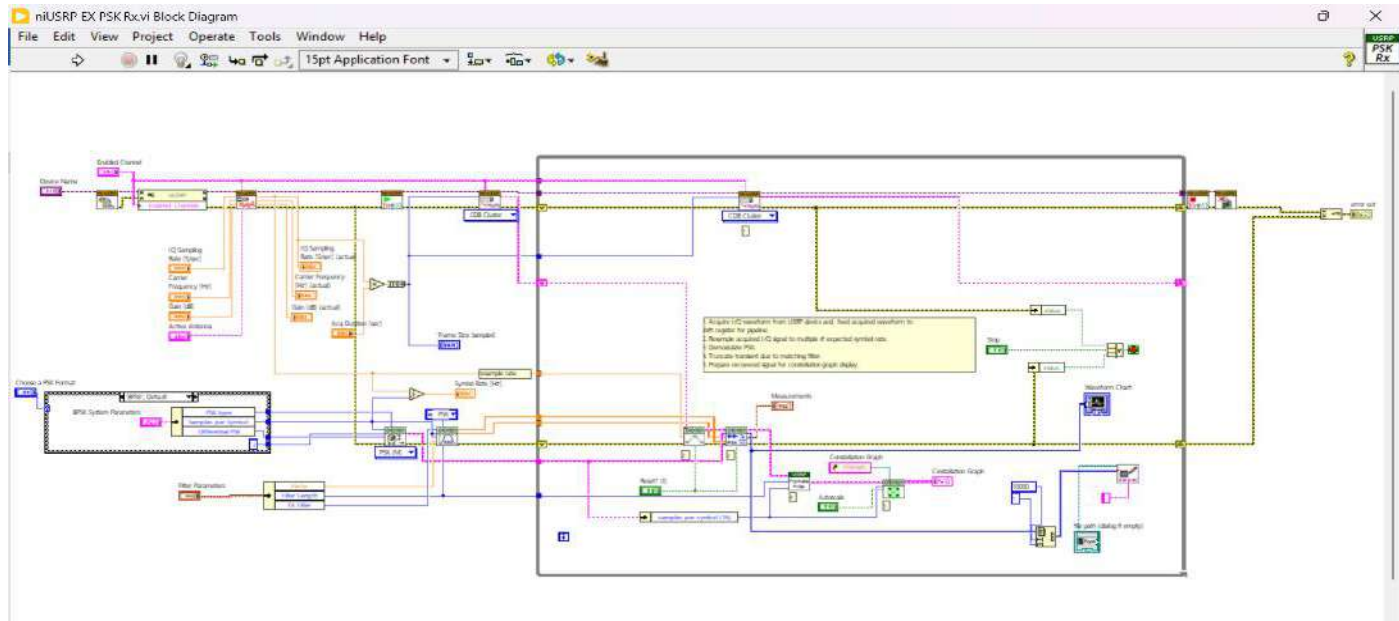


Fig. 2.11 LabVIEW Block Diagram of the Receiving Module

2.3.3.1 LabVIEW Front Panel During Operation

Figure 2.12 displays the LabVIEW Transmitting Module's front panel while it's actively sending data, showing live signal details. Figure 2.13 shows the Receiving Module's front panel during active reception, giving a real-time look at signal characteristics and measurements.

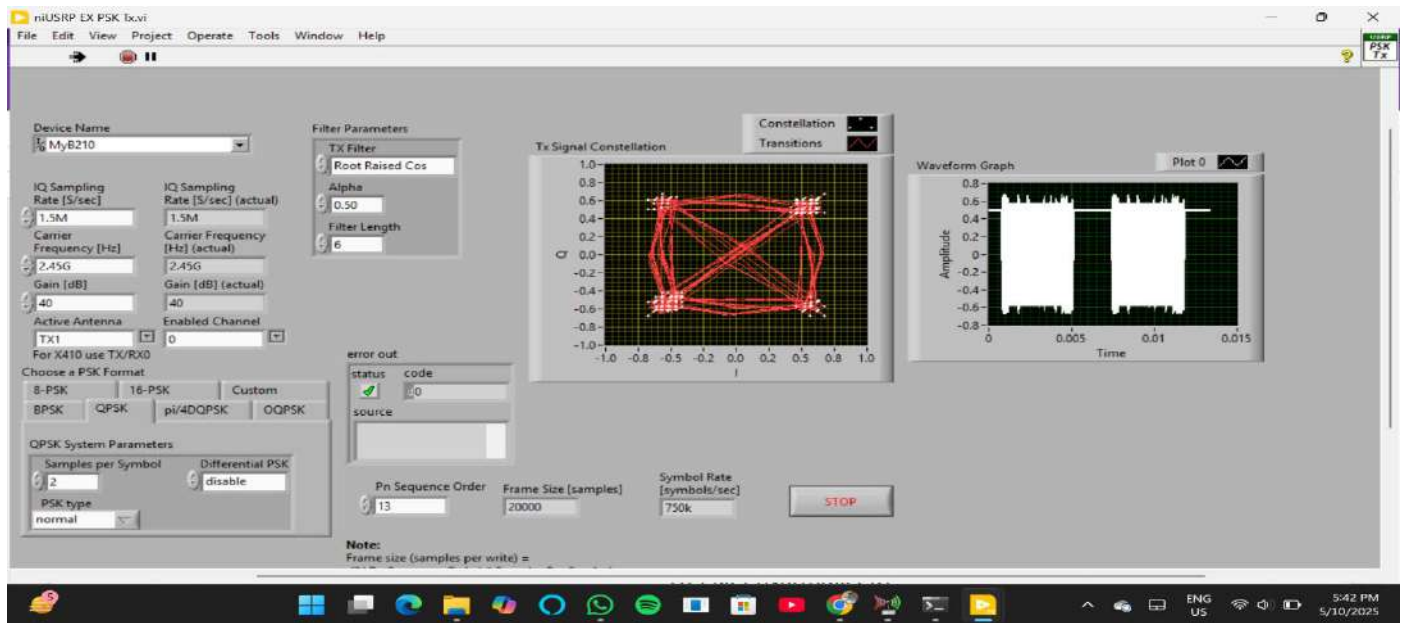


Fig. 2.12 LabVIEW Transmitting Module Front Panel During Active Transmission

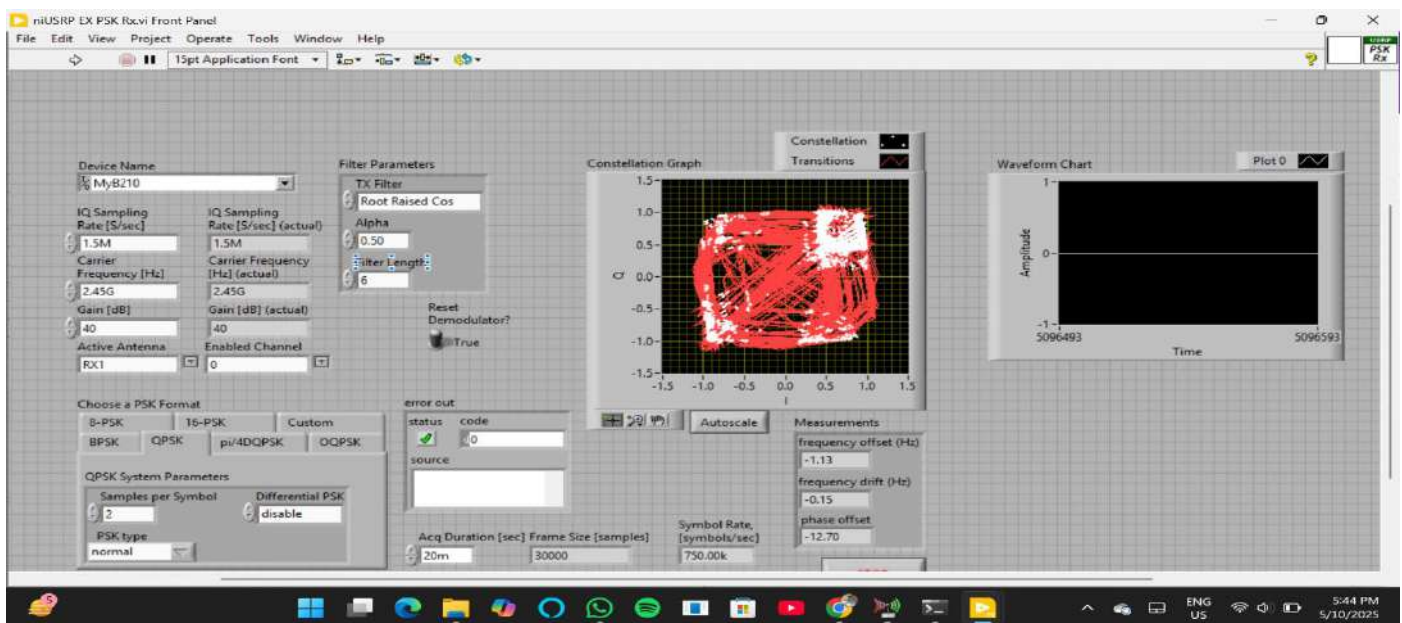


Fig 2.13 LabVIEW Receiving Module Front Panel During Active Reception

2.4 Software: Python

Python is a high-level, easy-to-use programming language well-liked for its clear way of writing code and its huge collection of ready-made tools (libraries). Because it can be used for so many different things, it's a very important tool in areas like data analysis, scientific calculations, and image processing. In this project, Python is key for getting image data ready, rebuilding received images, and performing detailed measurements to check image quality. The code for this project is written and run in a Jupyter Notebook environment.

2.4.1 Python Libraries Utilized

Python's abilities in this project are greatly expanded by several specialized libraries. These provide pre-built parts for specific tasks. Table 2.1 lists the main Python libraries used in this research.

Table 2.1 Python Libraries for Wireless Image Transfer Project

Library (Alias)	Primary Function in Project
cv2 (OpenCV)	Used for basic image processing actions, like reading images, changing them to grayscale, and making them black and white (binary thresholding).
pandas (pd)	Essential for organizing and working with data, especially for reading from and writing to CSV and Excel files, which store the image's bitstream data.
numpy (np)	Key for numerical calculations, offering support for multi-dimensional arrays needed to handle and reshape image pixel data.
PIL.Image (im)	Used to create image objects from number arrays, change image formats, and save images for looking at and comparing.
matplotlib.pyplot (plt)	Used for making graphs and visualizations, specifically for showing the relationship between pixel strengths in transmitted and received images.
skimage.metrics.structural_similarity (ssim)	Calculates the Structural Similarity Index (SSIM), a main measurement for how similar two images look in terms of structure.
os	Provides tools for working with the computer's operating system, such as making folders to keep output files like CSVs and images organized.
csv	Used for reading and writing data in CSV format, ensuring that pixel data is stored and retrieved efficiently and in a standard way.

2.4.2 Python Code Description

This part explains what each section of the Python code does in this project.

```
# Importing Libraries needed for image processing, handling data, and plotting
import cv2 # for image processing
import pandas as pd # to work with excel and csv files
import numpy as np # to handle arrays
from PIL import Image as im # to create image
import matplotlib.pyplot as plt # For plotting graphs
from skimage.metrics import structural_similarity as ssim # For comparing images using SSIM
import os # for file operations
import csv # Used to save values in a CSV file

# reading the image in grayscale mode (2 stands for grayscale)
img = cv2.imread(r"C:\Users\Rounak Deb\Downloads\Final_Jupyter_project_10th_may\Image_1.jpg", 2)

img # just checking the image matrix
```

➤ Cell 1

Fig. 2.14 Python Code - Cell 1 (Libraries & Image Loading)

This code block starts the Python environment by bringing in all the necessary libraries for handling images, managing data, creating plots, and performing file operations. After that, it loads the first image file (specifically, "Image_1.jpg" from a local folder) into the computer's memory, converting it to grayscale during the loading process. This foundational step prepares the Python workspace and brings in the raw image data to be processed.

```
# applying binary thresholding to the image
bwimg = cv2.threshold(img, 127, 255, cv2.THRESH_BINARY)

bwimg # checking threshold output

# showing the binary image using OpenCV
cv2.imshow('Binary', bwimg[1])
cv2.waitKey(0) # waits for any key press
cv2.destroyAllWindows() # closes all OpenCV windows
```

➤ Cell 2

Fig. 2.15 Python Code - Cell 2 (Binary Thresholding)

The grayscale image that was loaded is then changed into a binary (black and white) image using a fixed threshold of 127. Any pixel with a brightness value above 127 becomes white (represented by 255), while those below become black (represented by 0). The new binary image is then temporarily shown in a separate window using OpenCV for a quick visual check. This step converts the image into a simpler, two-tone format, which is perfect for representing it as a stream of bits in a communication system.

➤ Cell 3

```
bwimg[1].shape # checking the shape of the thresholded (binary) image
```

Fig. 2.16 Python Code - Cell 3 (Image Dimensions Check)

This code block performs a quick check by looking at and displaying the dimensions (shape) of the binary image created in the previous step. This makes sure that the image data has the expected size before continuing with other operations that rely on its structure, like flattening it or changing its shape.

➤ Cell 4

```
a = [] # this will store pixel values in 1D

# storing only the first 100 rows into a
for i in range(100):
    a.extend(bwimg[1][i]) # flattening row-wise

a # checking the list
```

Fig. 2.17 Python Code - Cell 4 (Partial Data Extraction)

A specific part of the binary image is chosen for processing: the first 100 rows of pixels. These chosen rows are then "flattened," meaning their 2D layout is changed into a single, continuous 1D list of pixel values. This action acts like preparing a piece of the image data for sending, by turning it into a stream of information.

➤ Cell 5

```
len(a) # checking total number of elements

# converting all white pixels (255) to 1
for i in range(len(a)):
    if a[i] == 255:
        a[i] = 1

a # verifying the modified list
```

Fig. 2.18 Python Code - Cell 5 (Pixel to Bitstream Conversion)

This code block continues to process the 1D list of pixel values obtained in Cell 4. It goes through each item in the list, changing all the white pixels (which were originally 255) into the number '1'. Black pixels (which are 0) stay the same. This step specifically turns the image pixel data into a compact, standard stream of binary bits (made only of 0s and 1s), which is the usual format for digital communication.

➤ Cell 6

```
bitstream = pd.DataFrame(a) # converting the list into a DataFrame

bitstream # checking the data

bitstream.shape # checking rows and columns
```

Fig. 2.19 Python Code - Cell 6 (Bitstream to Data Frame)

The 1D list of binary pixel values (which is now a bitstream) is converted into a Pandas Data Frame. A Data Frame is a way to store data in rows and columns, like a table, and it's very good for handling and saving data efficiently. Putting the bitstream into a Data Frame gives it a structured and convenient form, getting it ready for saving to files later.

➤ Cell 7

```
# creating a folder to save csv and excel
os.makedirs("tx_rx_csv_files", exist_ok=True)

# saving the bitstream in excel and csv formats
bitstream.to_excel("tx_rx_csv_files/transmit1.xlsx", index=False, header=False)
bitstream.to_csv("tx_rx_csv_files/transmit1.csv", index=False, header=False)
```

Fig. 2.20 Python Code - Cell 7 (Transmitted Bitstream Saving)

This code block first makes sure that a specific folder named "tx_rx_csv_files" exists to keep all the output files organized. Then, the bitstream, which is stored in the Pandas Data Frame, is saved into both an Excel file ("transmit1.xlsx") and a CSV file ("transmit1.csv"). This step effectively simulates the "transmission" of the prepared bitstream by saving it to outside files that another system could use.

➤ Cell 8

```
x = [] # This list will store the received bitstream data

# Reading the CSV file from the 'tx_rx_csv_files' folder where we saved the received.csv
dataframe = pd.read_csv("outputs_tx_rx/received.csv") # Load CSV containing received data

# Converting the column values to a Python List
x = dataframe["0"].tolist() # Extract the values of column '0' as a list

# Inserting a 0 at the beginning of the list
x.insert(0, 0) # Add a 0 at the start for formatting or structure

len(x) # Check the total number of elements in the list

x # Show the List to verify the content
```

Fig. 2.21 Python Code - Cell 8 (Received Bitstream Loading)

This code block starts the process for the "received" data. It loads a CSV file named received.csv (which should contain the bitstream data after it's been received and initially processed by LabVIEW/USRP) into a Pandas Data Frame. It then pulls out the values from the column labeled "0" and puts them into a Python list. A '0' is also added right at the very beginning of this list, which might be for a specific way of formatting or aligning the data for later steps.

➤ Cell 9

```
# converting all 1s to 225 to reconstruct image
for i in range(len(x)):
    if x[i] == 1:
        x[i] = 225

a_arr1 = [] # will store pixels

# storing first 10000 values only
for i in range(10000):
    a_arr1.append(x[i])
```

Fig. 2.22 Python Code - Cell 9 (Received Data Preparation)

The received bitstream values are converted back into pixel brightness values that are suitable for displaying an image. Specifically, any '1's found in the received list are changed to the value '225' (a high grayscale value, representing white). After this, a specific part of this processed data, limited to the first 10,000 values, is taken out and stored in a new list. This step is part of reversing the transmission process, getting the received data ready to be seen as an image.

➤ Cell 10

```
a_arr = np.array(a_arr1) # converting list to array
a_arr.resize(100, 100) # resizing into 100x100 image

a_arr.shape # checking shape

x # checking received list again

a_arr # checking image array
```

Fig. 2.23 Python Code - Cell 10 (Image Reshaping)

The list of prepared received pixel values from Cell 9 is changed into a NumPy array. This 1D array is then dynamically reshaped into a 2D format, specifically 100 rows by 100 columns. This matches the expected size of the original image part that was "sent". This step changes the straight line of received pixel data back into a two-dimensional grid, which is how images are usually organized.

➤ Cell 11

```
# Convert array to uint8 format if not already
image_array = np.uint8(a_arr)

# Show image in a separate popup window using OpenCV
cv2.imshow("Reconstructed Image", image_array)

# Wait for any key to be pressed
cv2.waitKey(0)

# Close all OpenCV windows
cv2.destroyAllWindows()
```

Fig. 2.24 Cell 11 (Reconstructed Image Display)

The NumPy array that represents the rebuilt image is changed into an unsigned 8-bit integer format (uint8), which is the standard for displaying images. The rebuilt image is then opened and shown in a separate pop-up window using OpenCV. The program will pause until you press any key, after which the image window will close automatically. This gives an immediate visual check of how good the received image looks after the wireless transfer and reconstruction process.

➤ Cell 12

```
# create folder to save images
os.makedirs("outputs_tx_rx", exist_ok=True)

# converting both TX and RX to proper image format
tx_image = im.fromarray(bwimg[1]) # original transmitting image
rx_image = im.fromarray(a_arr.astype(np.uint8)) # received image

# saving both images
tx_image.save("outputs_tx_rx/transmitting_image.jpg")
rx_image.save("outputs_tx_rx/receiving_image.jpg")
```

Fig. 2.25 Cell 12 (Saving TX and RX Images)

This code block first creates a folder named "outputs_tx_rx" if it doesn't already exist. This helps keep all the output images organized. Then, it converts both the original (prepared for sending) binary image and the rebuilt received image into standard image objects. Finally, these two images are saved as JPEG files, named "transmitting_image.jpg" and "receiving_image.jpg", inside the created output folder. This step makes permanent visual records of both the input and output images, which is useful for documentation and for comparing them later.

➤ Cell 13

```
# create new blank image of double width
combined = im.new('L', (tx_image.width + rx_image.width, tx_image.height))

# paste both images side-by-side
combined.paste(tx_image, (0, 0))
combined.paste(rx_image, (tx_image.width, 0))

# save comparison image
combined.save("outputs_tx_rx/tx_rx_comparison_image.jpg")

# show in notebook
display(combined)
```

Fig. 2.26 Cell 13 (Side-by-Side Comparison)

A new, blank image is created. Its width is double the width of a single image, and it has the same height. The original transmitted image and the reconstructed received image are then placed side-by-side onto this new blank image. This combined image is saved as "tx_rx_comparison_image.jpg" and also shown directly within the Jupyter Notebook output. This action makes it easy to visually compare the image that was conceptually "sent" with the image that was "received".

➤ Cell 14

```
# Using the transmitting image (TX) as it is since it is already in grayscale
tx_image_gray = np.array(tx_image)

# Using the receiving image (RX) as it is since it is also grayscale
rx_image_gray = a_arr # RX image is already in the required format

# Convert both images to uint8 to avoid any data type issues while calculating pixel differences
tx_image_gray = np.uint8(tx_image_gray)
rx_image_gray = np.uint8(rx_image_gray)

# Calculate Pearson's Correlation Coefficient
correlation_coefficient = np.corrcoef(tx_image_gray.flatten(), rx_image_gray.flatten())[0, 1]
print(f"Pearson Correlation Coefficient: {correlation_coefficient}")

# Calculate RMSE (Root Mean Squared Error)
rmse_value = np.sqrt(np.sum((tx_image_gray - rx_image_gray) ** 2) / tx_image_gray.size)
print(f"RMSE: {rmse_value}")

# Calculate PSNR (Peak Signal-to-Noise Ratio)
max_pixel_value = 255.0 # Maximum pixel value for uint8 images
psnr_value = 20 * np.log10(max_pixel_value / rmse_value)
print(f"PSNR: {psnr_value} dB")

# Calculate Normalized Cross-Correlation (NCC)
norm_tx = tx_image_gray.flatten() - np.mean(tx_image_gray)
norm_rx = rx_image_gray.flatten() - np.mean(rx_image_gray)
ncc_value = np.sum(norm_tx * norm_rx) / np.sqrt(np.sum(norm_tx**2) * np.sum(norm_rx**2))
print(f"Normalized Cross-Correlation (NCC): {ncc_value}")

# Calculate SSIM (Structural Similarity Index)
ssim_value, _ = ssim(tx_image_gray, rx_image_gray, full=True)
print(f"SSIM: {ssim_value}")
```

Fig. 2.27 Cell 14 (Quality Metrics Calculation)

This important code block measures the quality of the received image compared to the transmitted image using several well-known metrics. These include the Pearson Correlation Coefficient, Root Mean Squared Error (RMSE), Peak Signal-to-Noise Ratio (PSNR), Normalized Cross-Correlation (NCC), and Structural Similarity Index (SSIM). The calculated values for each measurement are then printed on the screen. This provides objective numbers to accurately evaluate how well the image transfer process performed.

➤ Cell 15

```
# Flatten the grayscale images
tx_flat = tx_image_gray.flatten()
rx_flat = rx_image_gray.flatten()

# Linear fit: RX = m * TX + c
m, c = np.polyfit(tx_flat, rx_flat, 1)

# Create the figure
plt.figure(figsize=(8, 6), dpi=300) # High DPI for clear export

# Scatter plot of RX vs TX
plt.scatter(tx_flat, rx_flat, s=1, alpha=0.3, color='blue', label='Pixel Data (RX vs TX)')

# Best-fit Line
plt.plot(tx_flat, m * tx_flat + c, color='red', linewidth=2, label=f'Fit: RX = {m:.2f} * TX + {c:.2f}')

# Labels and Title
plt.xlabel('Transmitted Pixel Intensity (TX)', fontsize=12)
plt.ylabel('Received Pixel Intensity (RX)', fontsize=12)
plt.title('Linear Relationship Between Transmitted and Received Images', fontsize=14)

# Grid and legend
plt.grid(True, linestyle='--', alpha=0.5)
plt.legend(fontsize=10)

# Save the figure
plt.tight_layout()
plt.savefig('outputs_tx_rx/linear_fit_rx_vs_tx_presentable.jpg')
plt.show()
```

➤ **Fig. 2.28** Python Code - Cell 15 (Pixel Intensity Scatter Plot)

This code block gets the image data ready for a visual check of how the pixels match up. It flattens both the transmitted and received image pixel values into single-line arrays and then creates a scatter plot of these values. A straight line (linear regression) is calculated and added to this scatter plot, showing the mathematical relationship between the pixel brightness levels. The plot is given proper labels and a title, then saved as a high-quality JPEG image. This graph clearly shows how consistently the received pixel brightness matches the transmitted ones.

➤ Cell 16

```
# Save all metrics and Linear fit values to a CSV
comparison_data = {
    'Pearson Correlation Coefficient': [correlation_coefficient],
    'RMSE': [rmse_value],
    'PSNR (dB)': [psnr_value],
    'Normalized Cross-Correlation (NCC)': [ncc_value],
    'SSIM': [ssim_value],
    'Linear Fit Slope (m)': [m],
    'Linear Fit Intercept (c)': [c]
}

# Create a DataFrame
comparison_df = pd.DataFrame(comparison_data)

# Save to CSV in output folder
comparison_df.to_csv("outputs_tx_rx/comparison_parameters.csv", index=False)
```

Fig. 2.29 Python Code - Cell 16 (Saving Metrics to CSV)

All the image quality measurements calculated in Cell 14 (Pearson Correlation, RMSE, PSNR, NCC, SSIM), along with the slope and intercept of the straight line from Cell 15, are put into a Pandas Data Frame. This organized data is then saved into a CSV file named "comparison_parameters.csv" inside the "outputs_tx_rx" folder. This step systematically records all the key performance numbers in an organized, easy-to-access format for analysis and reporting.

CHAPTER 3

ANTENNA CHARACTERIZATION AND MEASUREMENT

3.1 Vector Network Analyzer

A Vector Network Analyzer (VNA) is a very important tool in the field of microwave and radio frequency (RF) engineering. It's used to measure how well high-frequency parts and systems work electrically. Unlike simpler tools that only measure the strength of signals, VNAs measure both the strength (magnitude) and the timing (phase) of signals. This makes them extremely valuable for getting a complete picture of how linear electrical networks behave.

A VNA has a few main parts: a source, a receiver, a test set, and a processor/display. The RF signal that the source creates is sent through the test set to the device being tested (DUT). Signals that bounce back (reflected) and signals that pass through (transmitted) are then picked up by special couplers and receivers. These signals are processed to figure out complex values called S-parameters, which include both amplitude and phase over a range of frequencies.

The VNA works by sending a known RF signal into the device being tested (DUT) and then measuring how much of that signal is reflected and how much passes through at each connection point (port). This behavior is described using S-parameters (scattering parameters), which explain how a network with multiple connection points responds to incoming radio waves. In this project, the S11 parameter is especially important. It tells us how efficiently the antenna is taking in energy and how well it matches the system.

3.1.1 S-Parameter

At very high frequencies, especially in microwave engineering, trying to analyze circuits using basic rules like Ohm's Law (which works with voltage and current) becomes very difficult. Instead, we use S-parameters (scattering parameters), which describe how signals act when they meet different parts like antennas, filters, amplifiers, or sensors. S-parameters help us understand how much of a signal bounces back, how much goes through, and how the signal changes as its frequency changes. This information is extremely important when designing and testing antennas and sensors that work in the RF/microwave range.

For a common 2-port network (most RF components like amplifiers, filters, antennas, and cables can be thought of this way), there are four S-parameters, often shown in a matrix form (S-matrix).

$$\begin{pmatrix} S_{11} & S_{12} \\ S_{21} & S_{22} \end{pmatrix} \quad (1)$$

- **S11 (Input Reflection Coefficient):** This parameter shows what portion of the signal that is sent into Port 1 of the Device Under Test (DUT) bounces back. It's important for checking how well the antenna matches the system; a lot of reflection means there's a mismatch. It's typically used to see if the antenna is taking in energy efficiently. An ideal value is generally -10 dB or even lower, which means very little signal is reflected.
- **S21 (Forward Transmission):** This parameter measures how much of the signal successfully travels from Port 1 to Port 2 of the DUT. It's crucial for determining if the signal passes through the device successfully. This measurement is commonly used for parts like filters, amplifiers, or two-port sensing systems. An ideal value close to 0 dB means that most of the signal is transmitted through the device.
- **S12 (Reverse Transmission):** This parameter measures the signal passing from Port 2 to Port 1. Its importance is similar to S21, but it evaluates the signal flow in the opposite direction. It is used to find out if the device is reciprocal, meaning it behaves the same way in both directions. In devices that are symmetric, the ideal value for S12 should be similar to S21.
- **S22 (Output Reflection Coefficient):** This parameter shows the portion of the signal that reflects back from Port 2 of the DUT. It's important for understanding how well the impedance is matched at Port 2. This measurement is especially relevant for parts like amplifiers or other devices with two ports where the characteristics of both the input and output are critical. An ideal value is usually -10 dB or lower, meaning low reflection at the output port

The relationship between these S-parameters is summarized in Table 3.1

Table 3.1 S-Parameter Table

S-Parameter	What it Tells	Simple Formula
S11	Reflection at Port 1 (input port)	$S11 = \text{Reflected wave at Port 1} / \text{Incident wave at Port 1}$
S21	Transmission from Port 1 to Port 2	$S21 = \text{Transmitted wave at Port 2} / \text{Incident wave at Port 1}$
S12	Transmission from Port 2 to Port 1	$S12 = \text{Transmitted wave at Port 1} / \text{Incident wave at Port 2}$
S22	Reflection at Port 2 (output port)	$S22 = \text{Reflected wave at Port 2} / \text{Incident wave at Port 2}$

3.1.2 Libre-VNA

LibreVNA is an affordable, open-source Vector Network Analyzer that can perform measurements on two ports. It works across a wide frequency range, from 100 kHz to about 6 GHz. This makes it suitable for checking the performance of the 5.8 GHz antennas used in this study. It is portable, powered by USB, and works with custom software. Because it's open-source, it can be easily changed and connected with other systems. This tool was used to collect S11 readings for the antennas, which helps understand their impedance matching and resonance at specific frequencies. It provides a good balance between being affordable and functional, making it ideal for academic and lab-scale experiments. The LibreVNA device is shown in Figure 3.1.



Fig. 3.1 Libre-VNA

3.1.2.1 LibreVNA Software and Installation

The LibreVNA software was installed from GitHub, which made the setup easy to configure and customize. The software offers features like real-time viewing of signal traces, marker analysis, and the ability to export data as CSV files, which was helpful for further analysis of antenna performance. Its open-source nature provided better control over data collection and made it a good platform for checking results obtained from a more advanced commercial VNA, the R&S ZVH8. It was installed using the official repository available on GitHub. For Windows systems, the installation is straightforward and does not require any special drivers or setup tools. The latest release zip file was downloaded from the LibreVNA GitHub page. The zip file was extracted to a convenient folder. The application was launched by running LibreVNA-GUI.exe directly from the folder. An example of the GitHub installation instructions is shown in Figure 3.2.

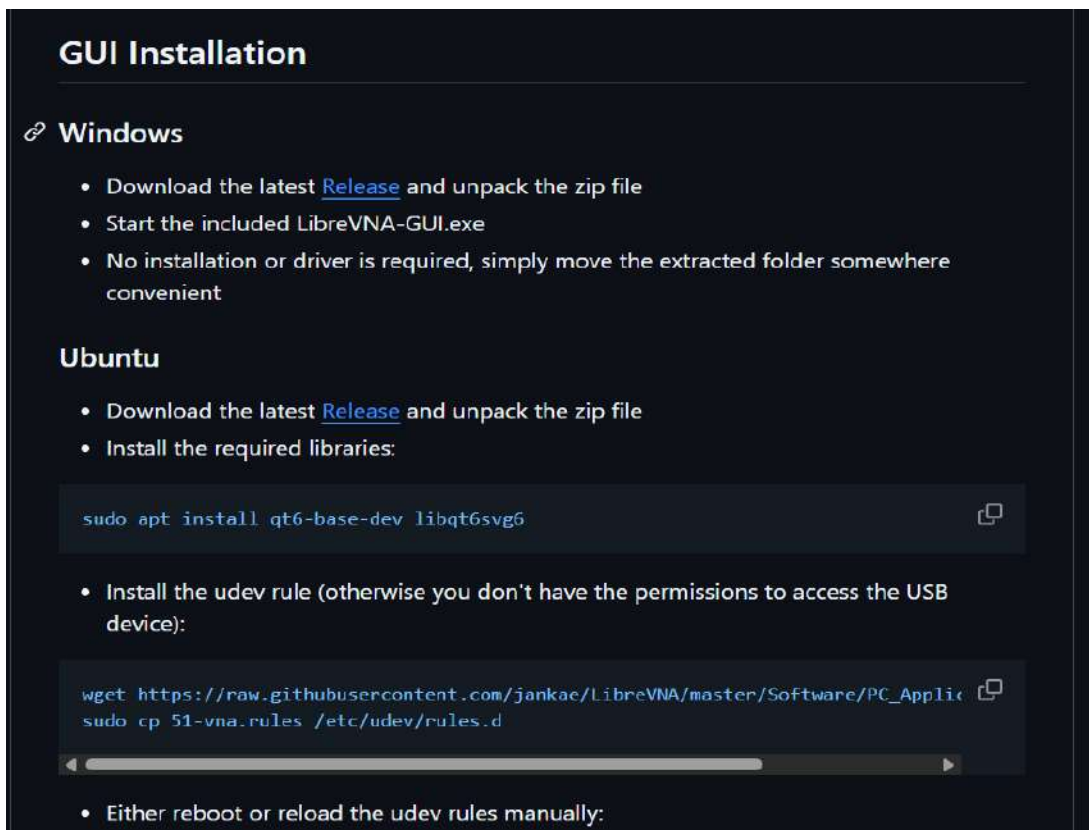


Fig. 3.2 GitHub

3.1.2.2 LibreVNA Experimental Setup

Figure 3.3 shows the basic experimental setup used for collecting S-parameter data using the LibreVNA. The device has two connection points: Port 1 and Port 2. These ports are connected to the antenna or device being tested using coaxial cables with SMA connectors. The LibreVNA itself is connected to a laptop via a USB cable, which powers the device and also provides the user interface for controlling measurements.

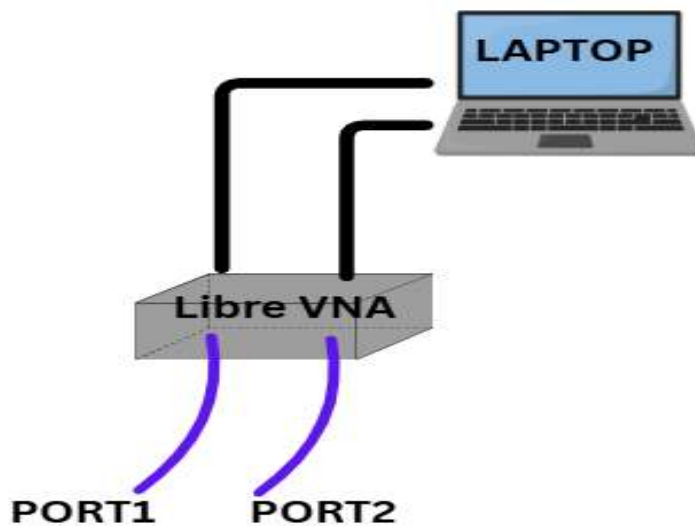


Fig. 3.3 General Set-Up

3.1.2.3 LibreVNA Calibration Procedure

Before taking any VNA measurement, it's very important to perform a calibration. This process removes systematic errors that come from the cables, connectors, and adapters used in the setup. Calibration makes sure that the S-parameter measurements are accurate by correcting for any reflections, losses, and mismatches in the test arrangement. Figure 3.4 shows the three standard calibration loads typically used in the SOL (Short-Open-Load) method. The steps for calibration are outlined in Table 3.2.



Fig. 3.4 Calibration Kit used for SOL Calibration—Load, Open, and Short Standards (from left to right).

Table 3.2 Steps for Calibration

Title	Description	Figure No.
Software Interface	LibreVNA opens to its default interface with a Smith chart and response panels	Fig 3.5
Changing Chart View to XY	The Smith chart is changed to XY view for better analysis of S-parameters	Fig 3.6
Selecting S-Parameter	The user selects S11, S21, S12, or S22 from the measurement options	Fig 3.7
Displaying All Four S-Parameters	All four S-parameters are shown simultaneously in split view mode	Fig 3.8
Starting Calibration Process	The user initiates the calibration process via the calibration menu	Fig 3.9
Choosing 2-Port Calibration	The selection of a 2-port SOLT calibration is made from the options	Fig 3.10
Short Standard on Port 1	The short standard is connected to Port 1 and selected in the software	Fig 3.11
Measuring Short on Port 1	Measurement is taken after connecting the short to Port 1	Fig 3.12
Open Standard on Port 1 & Measuring	Open standard is connected to Port 1 for the next calibration step & measurement is taken	Fig 3.13
Load Standard on Port 1 & Measuring	Load (50Ω) is connected to Port 1 for the final calibration step of that port. & taken measurement	Fig 3.14
Short Standard on Port 2 & Measuring	The short standard is now connected to Port 2 for calibration	Fig 3.15
Open Standard on Port 2 & Measuring	The open standard is connected to Port 2	Fig 3.16
Load Standard on Port 2 & Measuring	The load is connected to Port 2 for the final step on that port	Fig 3.17
Through Connection Between Ports & Measuring	Ports 1 and 2 are connected directly using an SMA adapter or cable	Fig 3.18
Selecting SOLT	SOLT calibration is selected, completing the full 2-port setup	Fig 3.19
Activating Calibration	Activating the SOLT PORT 1 2	Fig 3.20
Libre-VNA Software Interface	Readings to be taken	Fig 3.21
Disconnect	Disconnect from the laptop before removing the USB	Fig 3.22

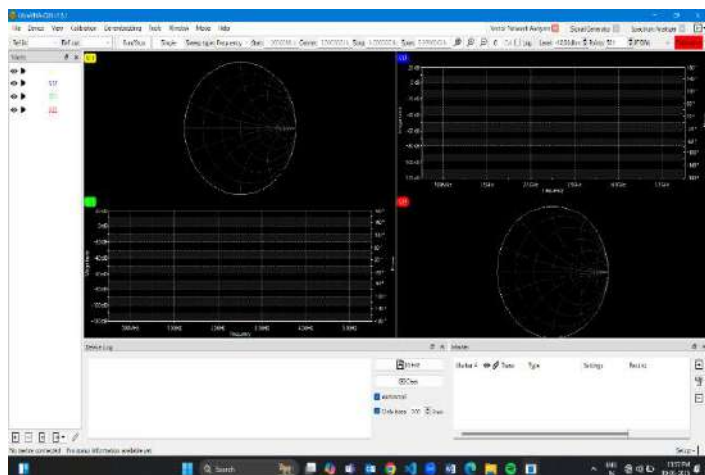


Fig. 3.5 Software Interface

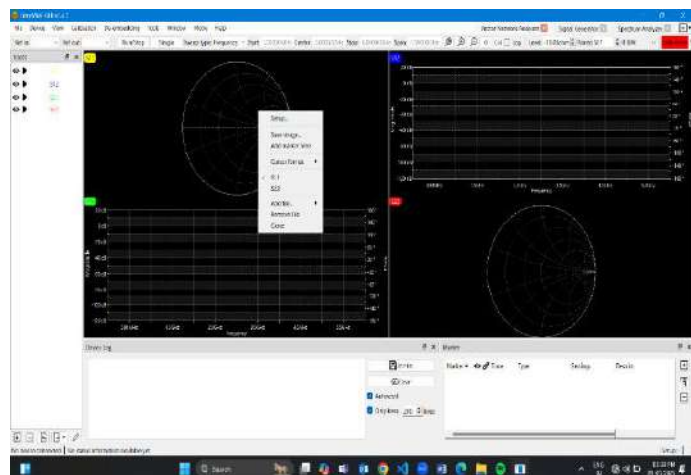


Fig. 3.6 Changing Chart View to XY

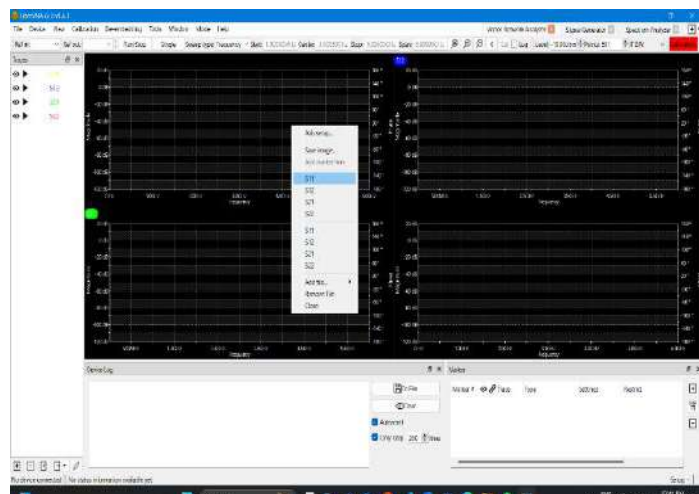


Fig. 3.7 Selecting S-Parameter

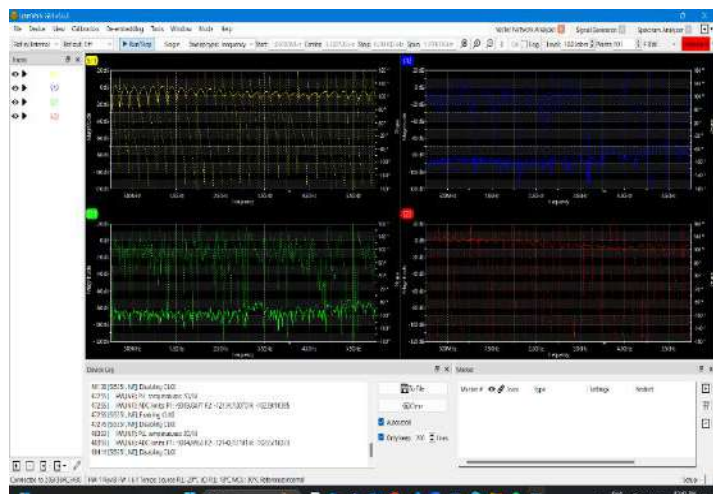


Fig. 3.8 Displaying All Four S-Parameters

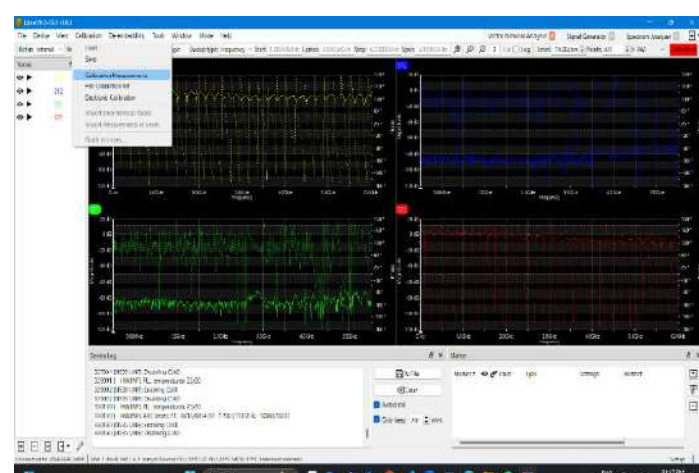


Fig. 3.9 Starting Calibration Process

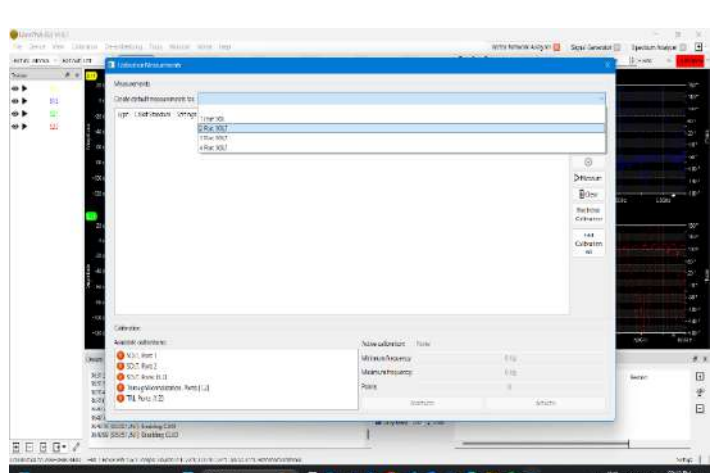


Fig. 3.10 Choosing 2-Port Calibration

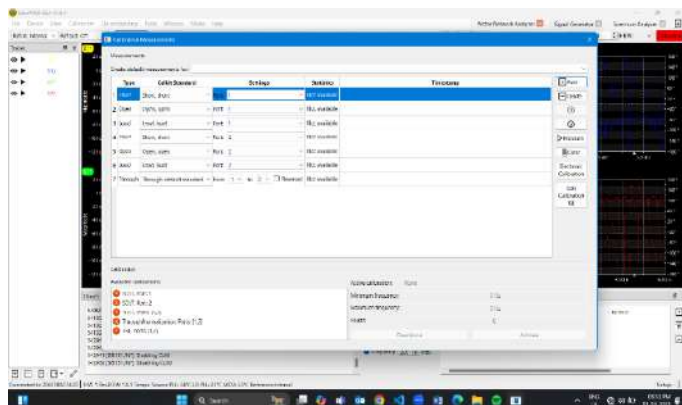


Fig. 3.11 Short Standard on Port 1

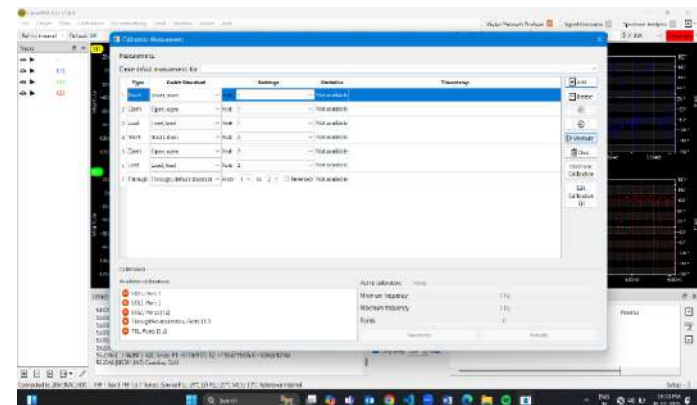


Fig. 3.12 Measuring Short on Port 1

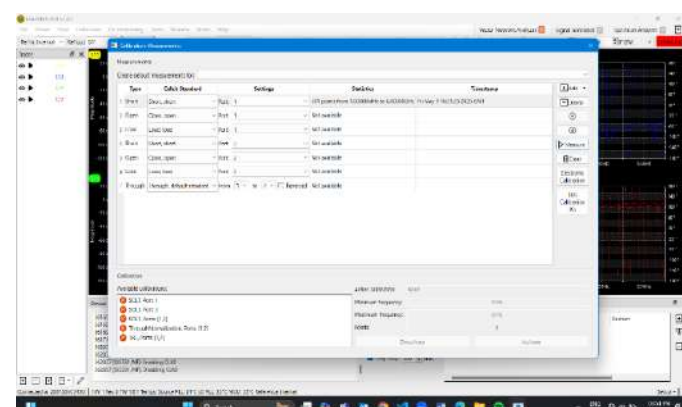


Fig. 3.13 Open Standard on Port 1 & Measuring

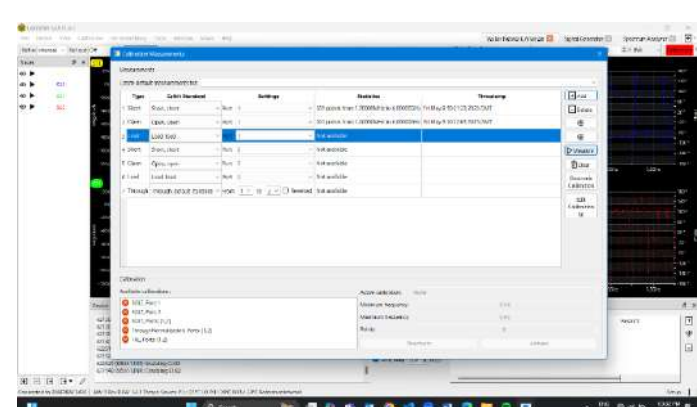


Fig. 3.14 Load Standard on Port 1 & Measuring

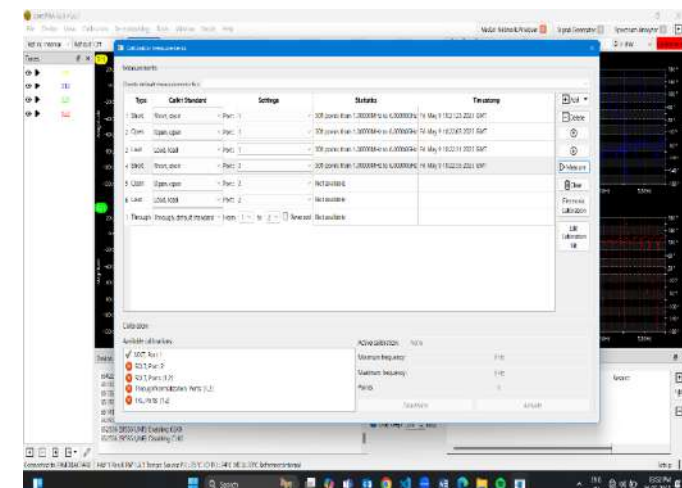


Fig. 3.15 Short Standard on Port 2 & Measuring

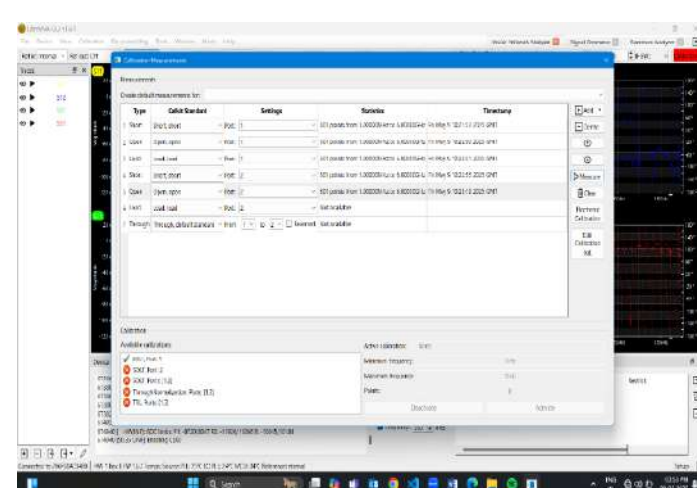


Fig. 3.16 Open Standard on Port 2 & Measuring

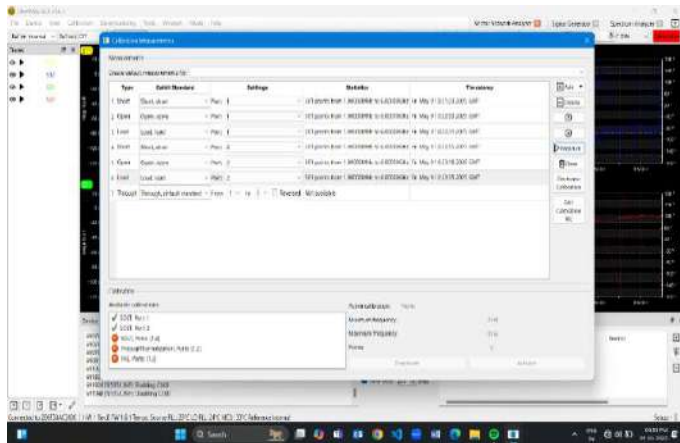


Fig. 3.17 Load Standard on Port 2 & Measuring

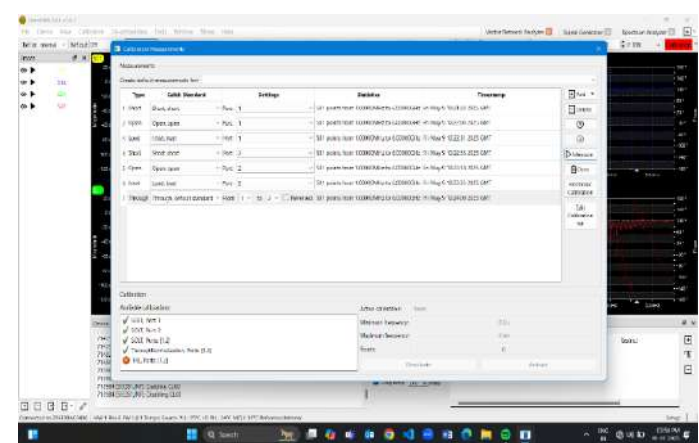


Fig. 3.18 Through Connection Between Ports & Measuring

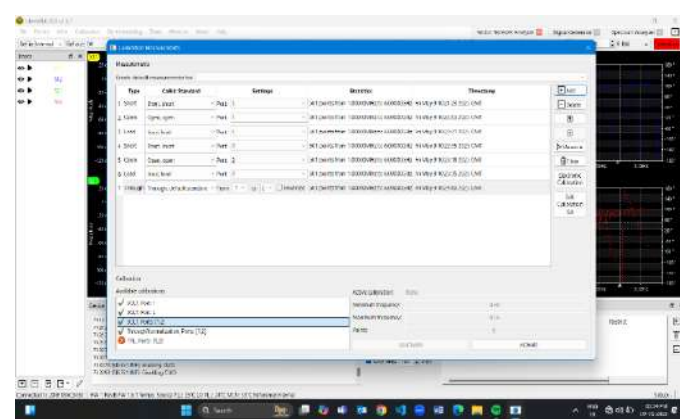


Fig. 3.19 Selecting SOLT

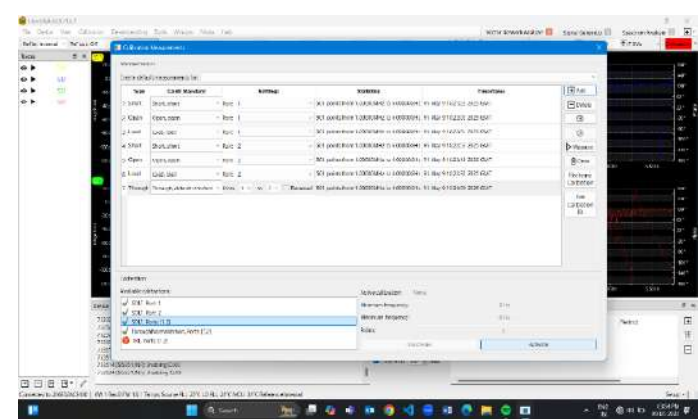


Fig. 3.20 Activating Calibration

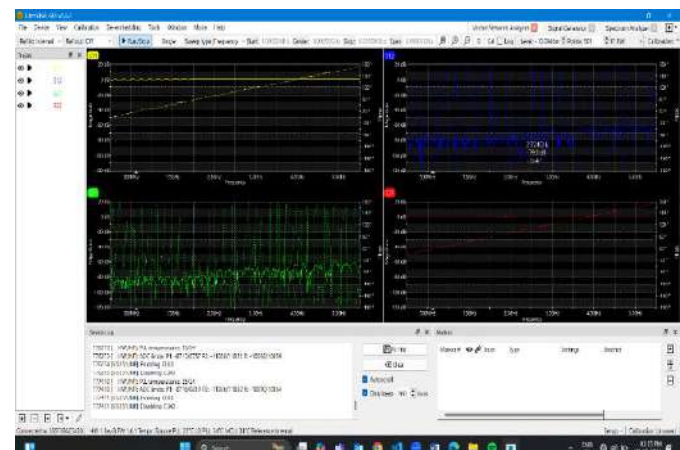


Fig. 3.21 Libre-VNA Software Interface

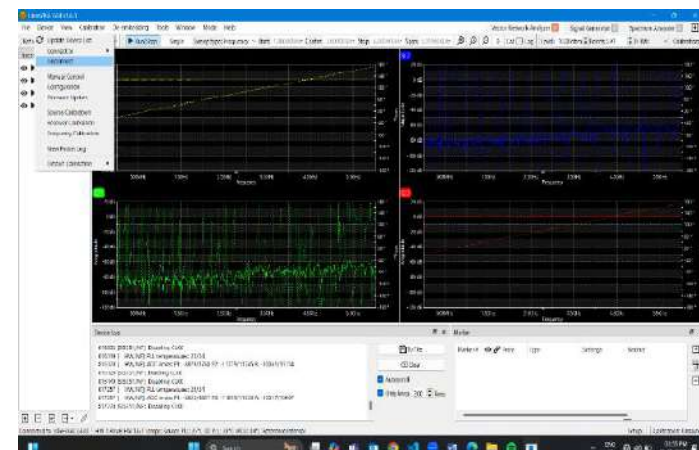


Fig. 3.22 Disconnect

3.1.3 Rohde & Schwarz ZVH8 VNA

The Rohde & Schwarz ZVH8 is a high-performance, handheld cable and antenna analyzer that also has extensive Vector Network Analyzer (VNA) capabilities. It operates across a broad frequency range from 100 kHz to 8 GHz. This wide range makes it suitable for many different uses in setting up, maintaining, and fixing RF systems. It's very portable, which means it can be used for reliable measurements even in tough outdoor or industrial settings. Its full VNA functionality allows for precise S-parameter measurements to check various RF components like antennas, cables, filters, and amplifiers within its specified frequency range. The ZVH8 also includes advanced features such as Distance-to-Fault (DTF) analysis for pinpointing cable damage and optional spectrum analysis capabilities. It provides a powerful and versatile solution for professional RF engineers and technicians, balancing precision with practical field usability within its operational frequency window. The Rohde & Schwarz ZVH8 VNA is shown in Figure 3.23.

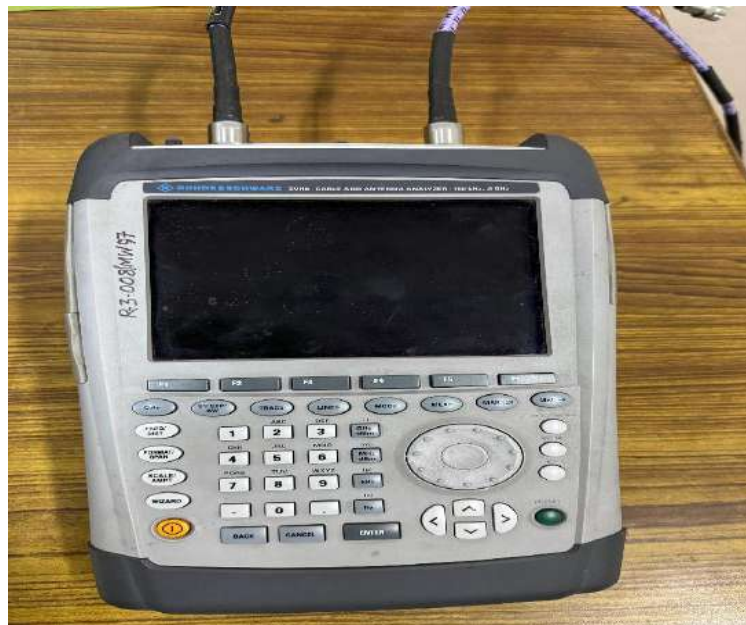


Fig. 3.23 Rohde & Schwarz ZVH8 VNA

3.1.3.1 Rohde & Schwarz VNA: System Architecture

The way the Rohde & Schwarz ZVH8 works, as shown in its block diagram, is mainly based on the principles of Vector Network Analysis (VNA). A VNA works by checking a Device Under Test (DUT) by looking at the signals that go into it and the signals that come out (reflected and transmitted) at its connection points. The core idea follows these steps, which are carried out by the different parts of the system.

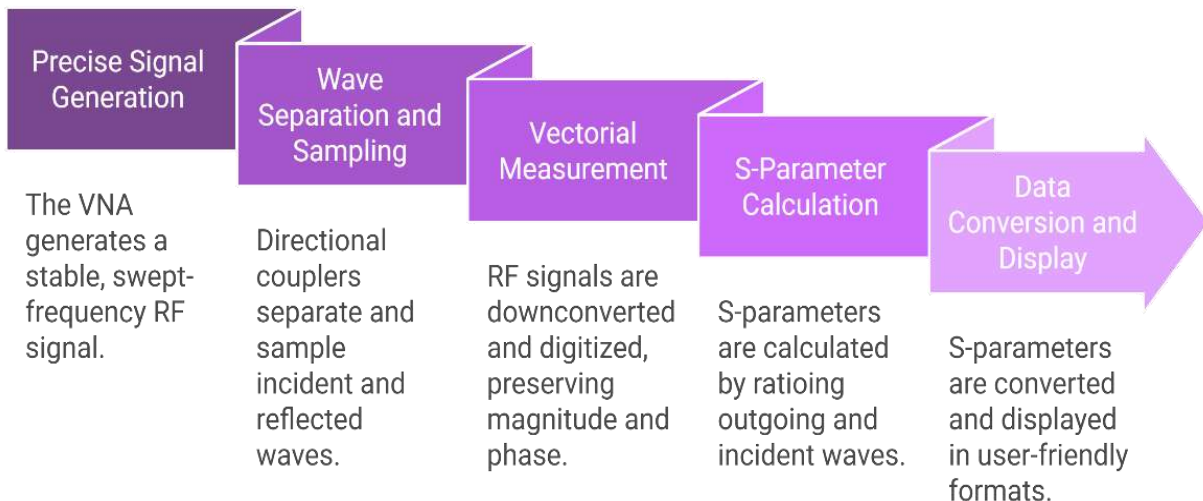


Fig. 3.24 Block Diagram VNA

- **Precise Signal Generation:** The VNA starts by creating a steady RF signal that changes across frequencies. This signal is sent to the device under test (DUT). This ensures accurate measurements that depend on frequency.
- **Wave Separation and Sampling:** Special directional couplers are used to separate the signals that go into the device from the signals that bounce back at each connection point. This allows the VNA to see what goes into and comes out of the DUT at the same time.
- **Vectorial Measurement:** The RF signals are converted to a lower frequency and then digitized, while making sure both their strength and timing (magnitude and phase) are kept. This allows for vector-based analysis, which is more detailed than just measuring amplitude.

- **S-Parameter Calculation (Rationing):** The VNA calculates S-parameters by comparing the outgoing signals to the incoming signals. This process removes common errors and provides accurate information about how the DUT reflects and transmits signals.
- **Data Conversion and Display:** The calculated S-parameters are then changed into easy-to-understand formats, like return loss (in dB), VSWR (Voltage Standing Wave Ratio), or Smith charts. The display unit shows this data as graphs for easy interpretation.

In simple terms, the R&S ZVH8's block diagram represents a complex system built to accurately create, separate, measure, and process radio waves. This allows for a full understanding of RF and microwave components and systems using S-parameter measurements.

3.1.3.2 Rohde & Schwarz VNA Calibration Procedure

Calibration is a very important step to do before any measurement using a Vector Network Analyzer (VNA). Rohde & Schwarz VNAs, like the ZVH8, need careful calibration to get rid of errors that are caused by the cables, connectors, and adapters. These errors can really affect how accurate the S-parameter readings are, especially at high frequencies. The ZV-Z135 female calibration unit is a standard tool used for this purpose. It is shown in Figure 3.25.



Fig. 3.25 ZV-Z135 female Calibration kit

During the calibration process:

- The Short, Open, and Load standards are connected one by one to each port to measure and correct for errors caused by signal reflections.
- The Through connection is used between ports to calibrate the signal paths and to isolate errors that happen between the ports.

This process results in a mathematically corrected measurement area right at the device under test (DUT), allowing for very accurate checks of how the device reflects (S11, S22) and transmits (S21, S12) signals. The R&S software makes this process easier by guiding the user through each calibration step and automatically saving the correction values. This helps ensure that RF measurements are repeatable, reliable, and of high quality. The steps for calibration are outlined in Table 3.3.

Table 3.3 Steps for Calibration

Title	Description	Figure No.
Clicking the Calibration Button	The user opens the calibration menu from the VNA interface.	Fig 3.26
Selecting Calibration Kit (F6)	Cal kit selection is initiated by pressing the F6 key.	Fig 3.27
Choosing ZV-Z135 Female Calibration Kit	ZV-Z135 female cal kit selected for 2-port SOLT calibration.	Fig 3.28
Selecting Full 2-Port Calibration	The full 2-port calibration method is chosen.	Fig 3.29
Starting Calibration	The calibration process started by clicking Continue.	Fig 3.30
Open Standard to Port 1	Open standard connected to Port 1 and confirmed.	Fig 3.31
Open Standard to Port 2	Open standard connected to Port 2 and confirmed.	Fig 3.32
Short Standard to Port 1	Short standard connected to Port 1 and confirmed.	Fig 3.33
Short Standard to Port 2	Short standard connected to Port 2 and confirmed.	Fig 3.34
Load Standard to Port 1	Load standard connected to Port 1 and confirmed.	Fig 3.35
Load Standard to Port 2	Load standard connected to Port 2 and confirmed.	Fig 3.36
Through Calibration	Final through connection made between Ports 1 and 2 to complete calibration.	Fig 3.37

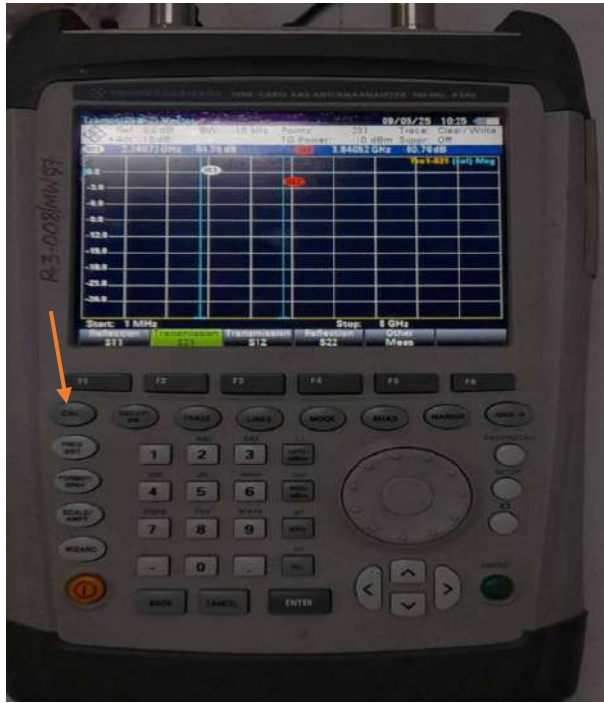


Fig.3.26 Clicking the Calibration Button

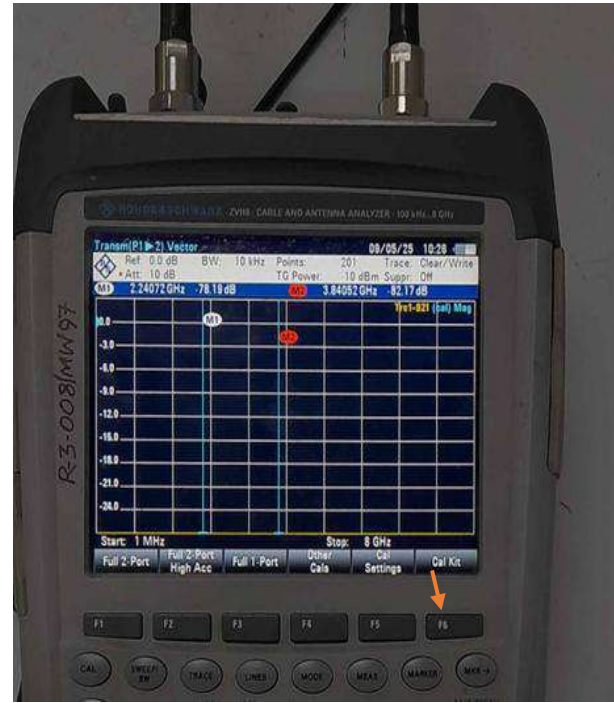


Fig. 3.27 Selecting Calibration Kit (F6)



Fig.3.28 Choosing ZV-Z135 Female Calibration Kit

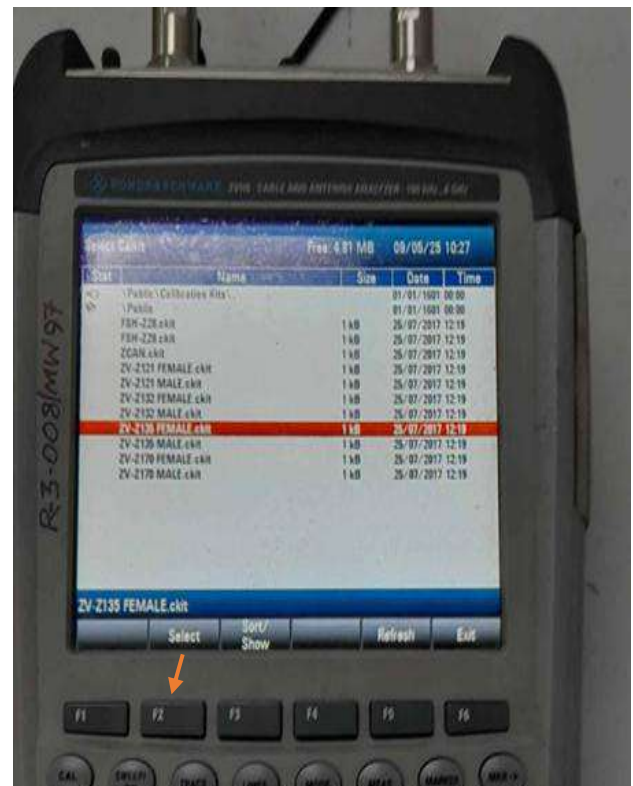


Fig. 3.29 Selecting Full 2-Port Calibration

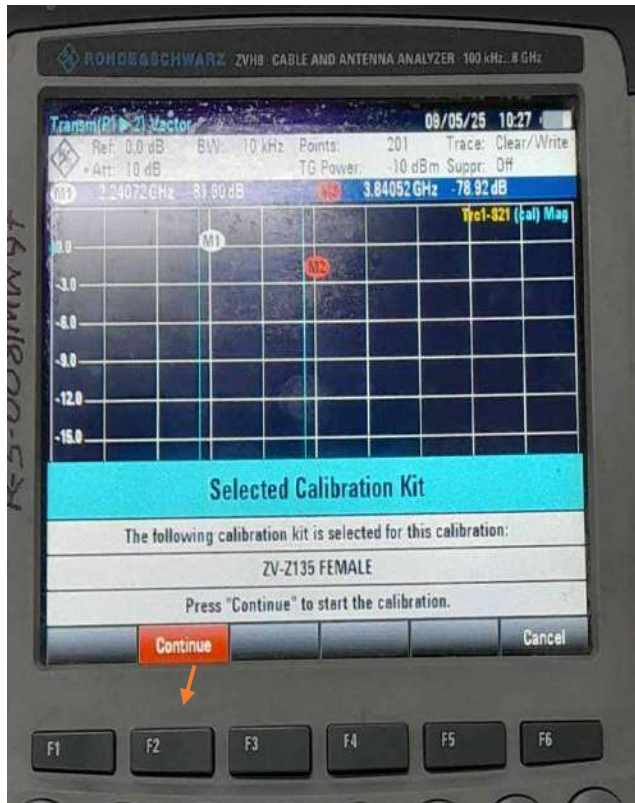


Fig.3.30 Starting Calibration

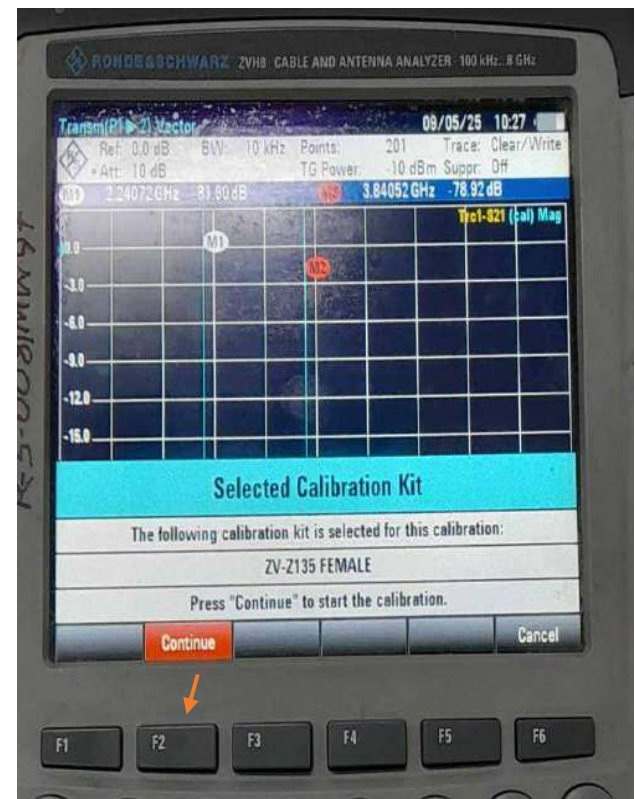


Fig. 3.31 Open Standard to Port 1



Fig.3.32 Open Standard to Port 2

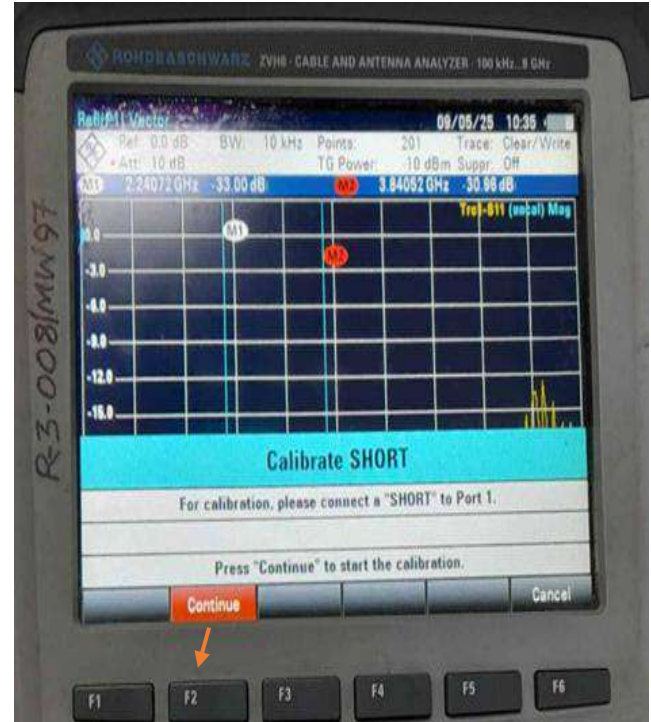


Fig. 3.33 Short Standard to Port 1

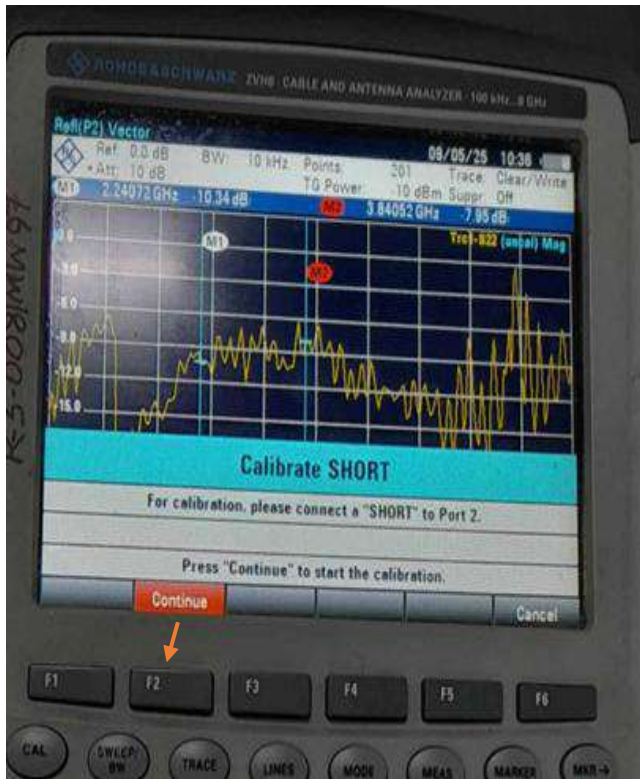


Fig.3.34 Short Standard to Port 2

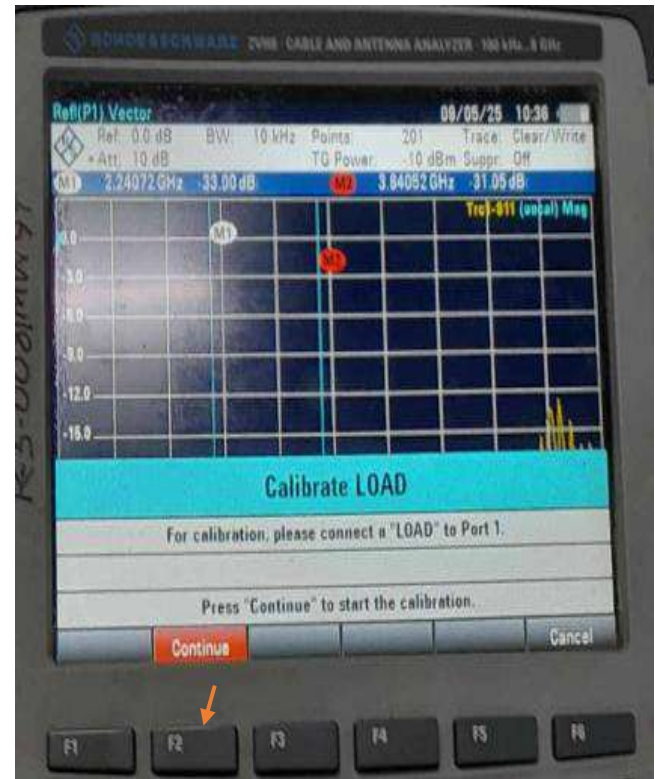


Fig. 3.35 Load Standard to Port 1

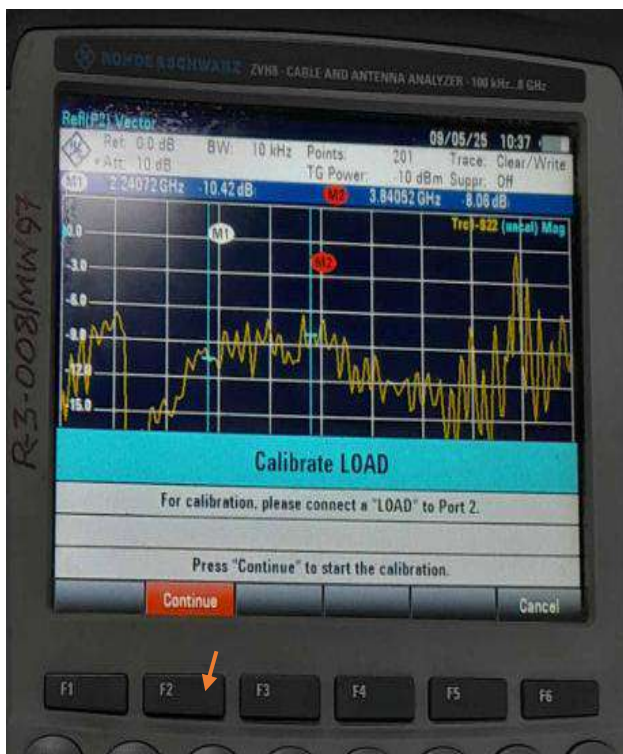


Fig.3.36 Load Standard to Port 2

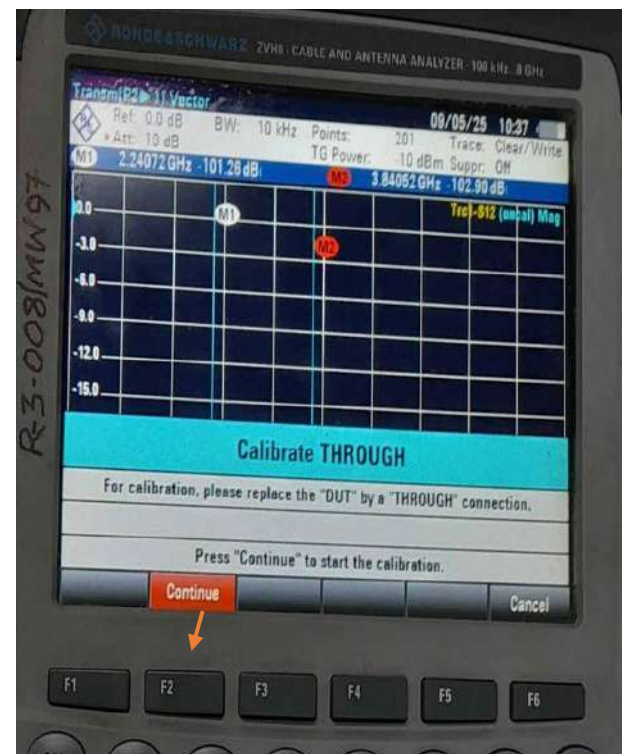


Fig. 3.37 Through Calibration

3.2 Antenna Characteristics and Performance

This section provides a detailed look at the characteristics and performance of each of the five antennas specifically designed and used in this project. The information is organized by each antenna feature, giving a clear and easy-to-compare overview of their physical details, design specifics, and measured performance.

3.2.1 Physical Image of Antennas Used

This subsection shows pictures of the antennas we used in our study.

- **Metamaterial Double Negative Index (DNI) Transmit Antenna:** You can see the front and back views of this antenna in Figures 3.38 and 3.39.

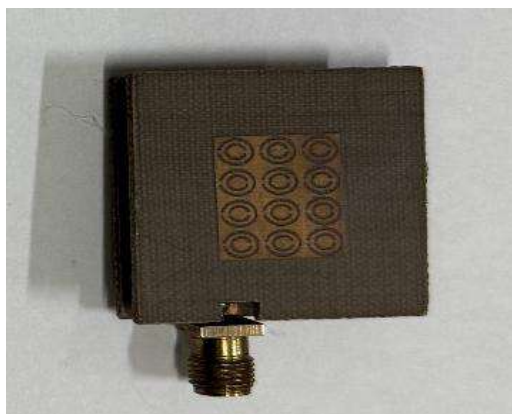


Fig 3.38 Front View

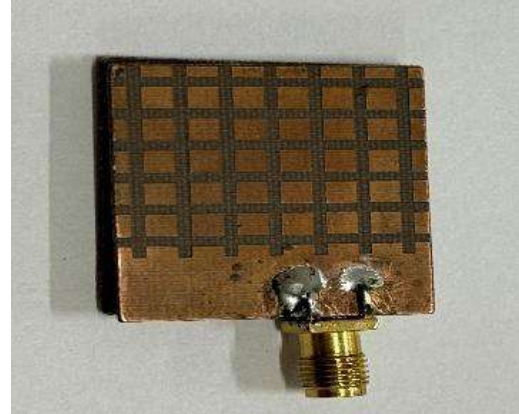


Fig. 3.39 Back View

- **Metamaterial Epsilon Near Zero (ENZ) Receive Antenna:** The front and back views of this antenna are shown in Figures 3.40 and 3.41.



Fig. 3.40 Front View



Fig. 3.41 Back View

- **Slot Cut Patch Antenna (Rogers RO3003):** Figures 3.42 and 3.43 show the front and back views of this antenna.

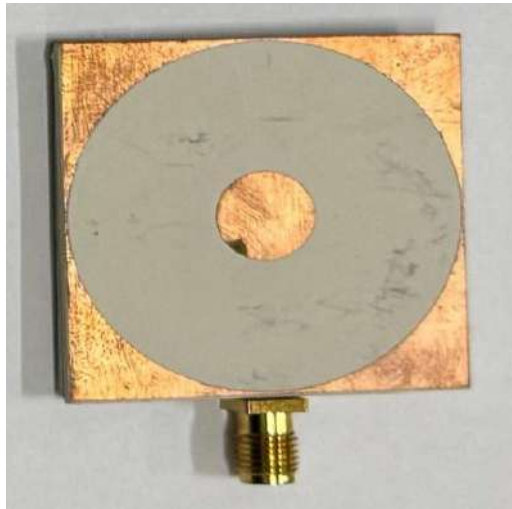


Fig. 3.42 Front View



Fig. 3.43 Back View

- **Parasitic Patch Antenna (Rogers RO3003):** The front and back views of this antenna are presented in Figures 3.44 and 3.45.



Fig. 3.44 Front View



Fig. 3.45 Back View

- **Patch Antenna (FR4 Material):** Figures 3.46 and 3.47 display the front and back views of this antenna.

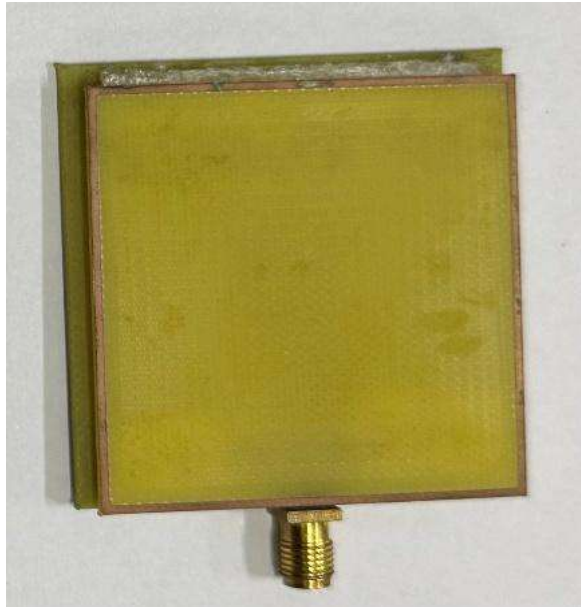


Fig. 3.46 Front View

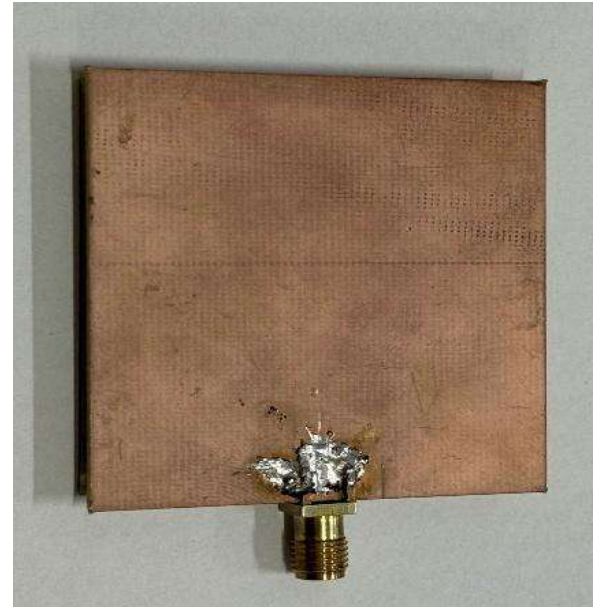


Fig. 3.47 Back View

3.2.2 Antenna Physical and Performance Characteristics

This table combines the key physical dimensions, fabrication details, and measured gain for each antenna, offering a consolidated view of their properties and performance.

Table 3.5 Antenna Physical and Performance Characteristics

Antenna	Dimensions (W×L in mm)	Substrate Used	Fabrication Details	Gain (dBi)
Metamaterial Double Negative Index (DNI) Transmit Antenna	28×32	Rogers RO3003 Thickness: 1.52 mm Relative perm. = 3 $\tan\delta=0.002$	Fabricated on Roger RO3003 substrate. Design includes Square Grid Patterns (SGP) on bottom, Complementary Split Ring Resonator (CSRR) arrays on top, and microstrip lines in middle for proximity-coupled feeding.	5.59 dBi at 5.8 GHz

Metamaterial Epsilon Near Zero (ENZ) Receive Antenna	105×105	Rogers RO-3003 Thickness: 1.52 mm	Fabricated on Roger RO-3003 substrate. Design incorporates a circular grid structure with etched circles for ENZ layer on both sides. Includes 19 mm-thick foam layer (air gap) between metamaterial layers and patch, secured with plastic stripes.	11.4 dBi at 5.8 GHz
Slot Cut Patch Antenna (Rogers RO3003)	40×40 (60% size reduction) Patch: 10.5×9 mm Microstrip feed: 1×18 mm Circular parasitic ring width: 1.2 mm	Rogers RO3003 Thickness: 1.52 mm Relative perm. = 3 Optimized superstrate height: 9 mm	Fabricated in college laboratory. Process used Circuit Pro CAD Tool, Board Master software, and a 3D Antenna Fabrication CNC Machine. Connectors soldered, S-parameters measured using VNA.	8.49 dBi at 5.8 GHz (with FSS: +11.12% gain)
Parasitic Patch Antenna (Rogers RO3003)	52.5×52.5	Rogers RO3003 Substrate/Superstrate Thickness: 1.52 mm Relative perm. = 3 $\tan\delta=0.001$	Fabricated in college laboratory. Process involved Circuit Pro CAD Tool, Board Master software, and a 3D Antenna Fabrication CNC Machine. Connectors soldered, S-parameters measured using VNA.	8.93 dBi at 5.8 GHz (with FSS: +11.9% gain)
Patch Antenna (FR4 Material)	52.5×52.5	FR4 Thickness: 1.6 mm Relative perm. = 4.3 $\tan\delta=0.025$ Superstrate: 50×50 mm	Fabricated in college laboratory. Process involved Circuit Pro CAD Tool, Board Master software, and a 3D Antenna Fabrication CNC Machine. Connectors soldered, S-parameters measured using VNA.	6.13 dBi at 5.8 GHz (with FSS: +57.1% gain)

3.2.3 Return Loss (S11) Performance

Measurements for return loss (S11) were taken using two different Vector Network Analyzers: the LibreVNA and the Rohde & Schwarz ZVH8 VNA. This was done to ensure a thorough check of their performance.

3.2.3.1 LibreVNA S11 Measurements

The LibreVNA was used for S11 measurements.

- The setup for the DNI Transmit Antenna with the LibreVNA is shown in Figure 3.48. The S11 graph for the Metamaterial Double Negative Index (DNI) Transmit Antenna is shown in Figure 3.49.

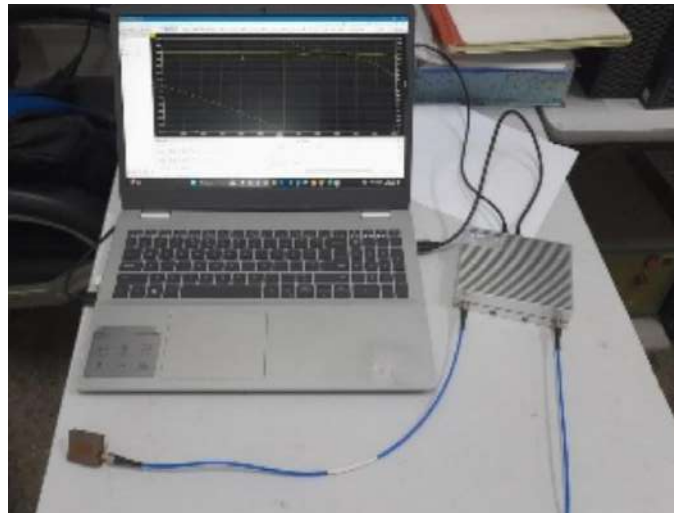


Fig. 3.48 DNI Tx Antenna

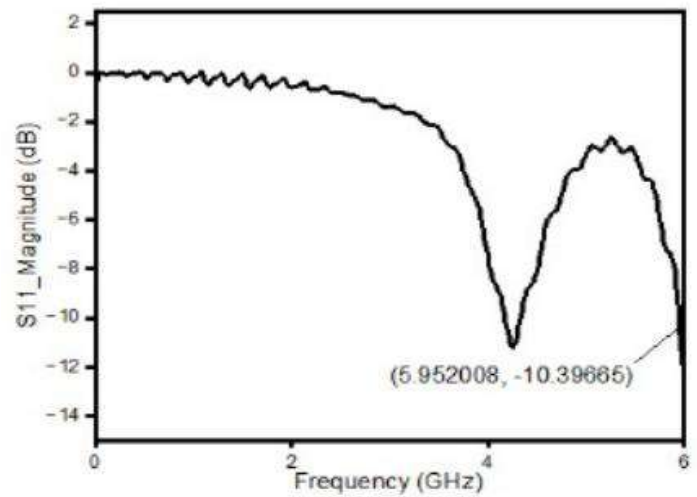


Fig. 3.49 DNI Tx Antenna S11 Graph

- The setup for the ENZ Receive Antenna with the LibreVNA is shown in Figure 3.50. The S11 graph for the Metamaterial Epsilon Near Zero (ENZ) Receive Antenna is shown in Figure 3.51.

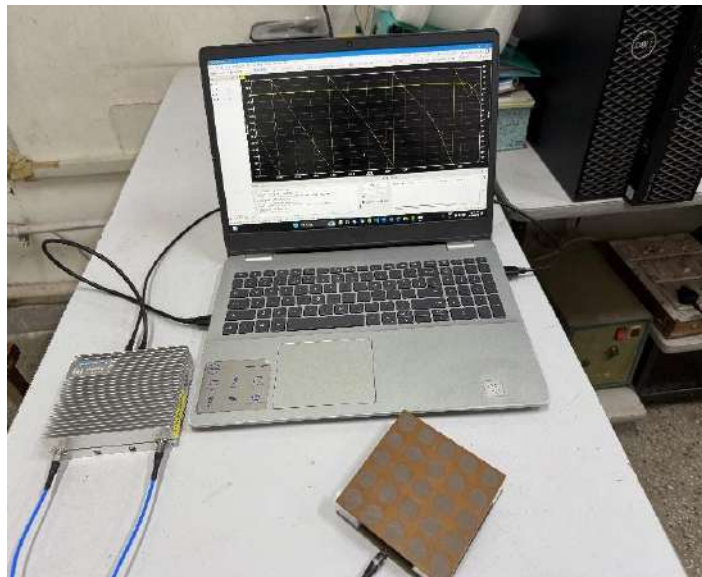


Fig. 3.50 ENZ Rx Antenna

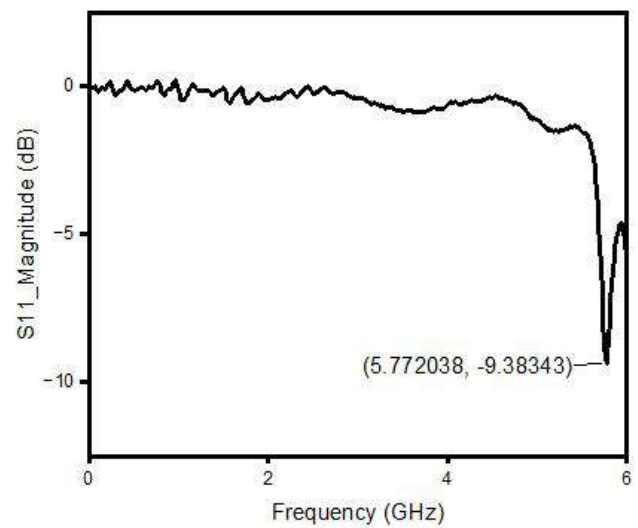


Fig. 3.51 ENZ Rx Antenna S11 Graph

- The setup for the Slot Cut Patch Antenna with the LibreVNA is shown in Figure 3.52. The S11 graph for the Slot Cut Patch Antenna (Rogers RO3003) is shown in Figure 3.53.

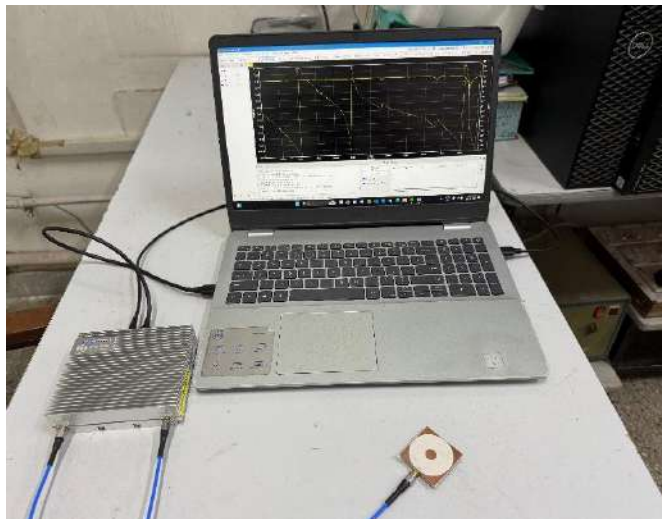


Fig. 3.52 Slot Cut Patch Antenna

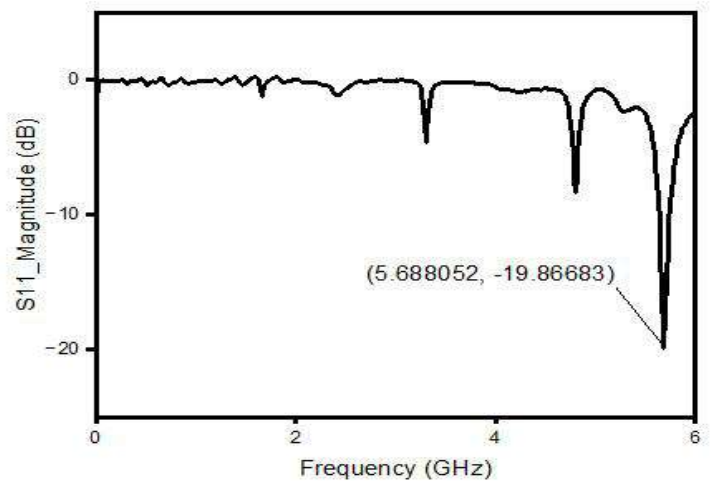


Fig. 3.53 Slot Cut Patch Antenna S11 Graph

- The setup for the Parasitic Patch Antenna with the LibreVNA is shown in Figure 3.54. The S11 graph for the Parasitic Patch Antenna (Rogers RO3003) is shown in Figure 3.55.

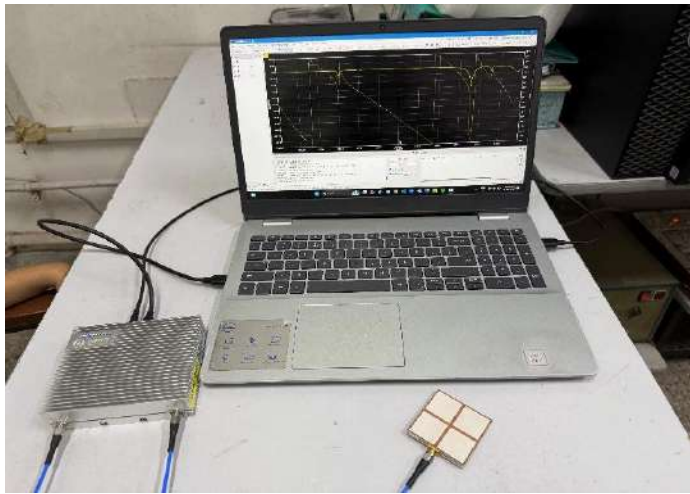


Fig. 3.54 Parasitic Patch Antenna

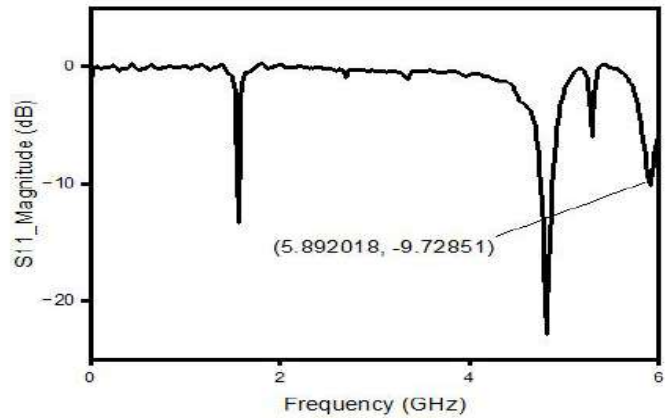


Fig. 3.55 Parasitic Patch Antenna S11 Graph

- The setup for the FR4 Patch Antenna with the LibreVNA is shown in Figure 3.56. The S11 graph for the Patch Antenna (FR4 Material) is shown in Figure 3.57.

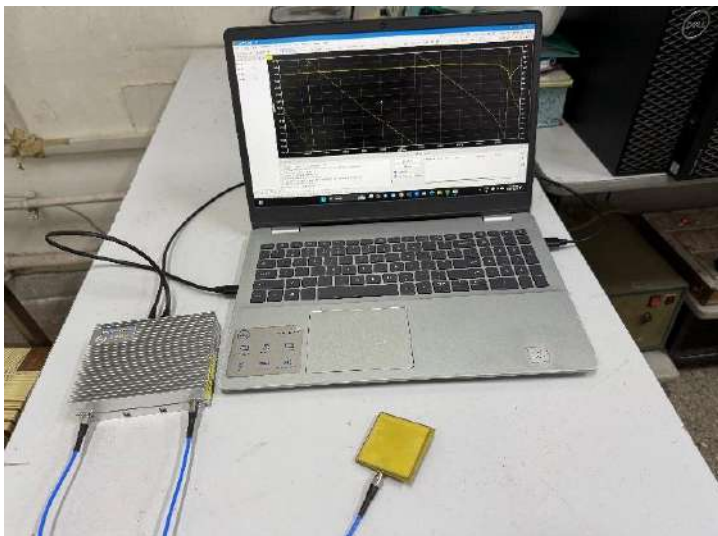


Fig. 3.56 FR4 Patch Antenna

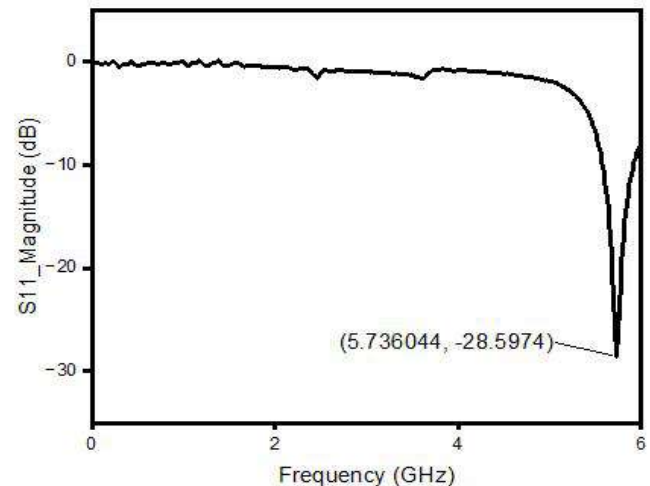


Fig. 3.57 FR4 Patch Antenna S11 Graph

3.2.3.2 Rohde & Schwarz ZVH8 VNA S11 Measurements

The Rohde & Schwarz ZVH8 VNA was also used for S11 measurements.

- The setup for the DNI Transmit Antenna with the R&S VNA is shown in Figure 3.58. The S11 graph for the Metamaterial Double Negative Index (DNI) Transmit Antenna measured with the R&S VNA is shown in Figure 3.59.



Fig. 3.58 DNI Tx Antenna

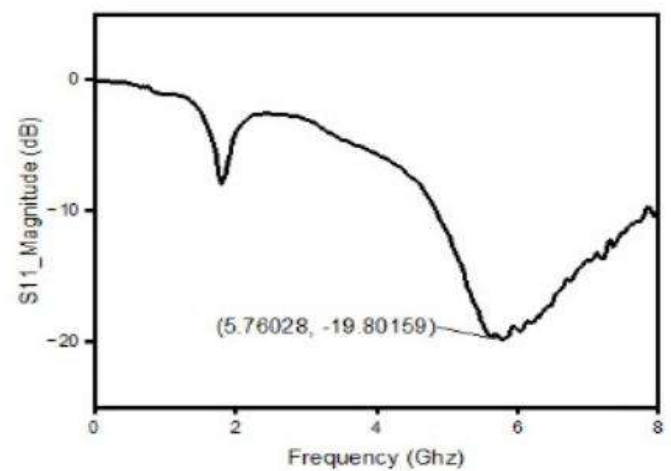


Fig. 3.59 DNI Tx Antenna S11 Graph

- The setup for the ENZ Receive Antenna with the R&S VNA is shown in Figure 3.60. The S11 graph for the Metamaterial Epsilon Near Zero (ENZ) Receive Antenna measured with the R&S VNA is shown in Figure 3.61.



Fig. 3.60 ENZ Rx Antenna

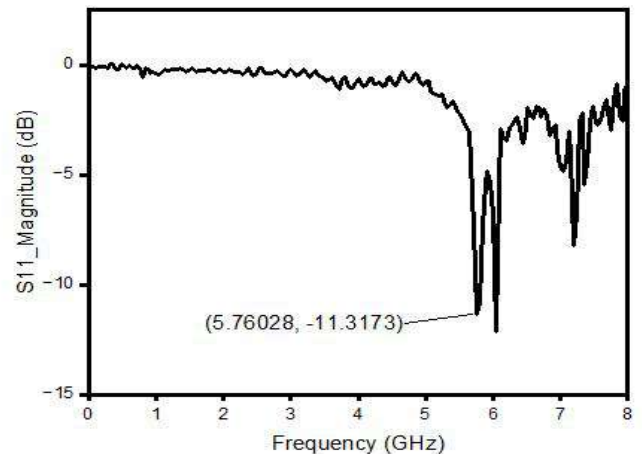


Fig. 3.61 ENZ Rx Antenna S11 Graph

- The setup for the Slot Cut Patch Antenna with the R&S VNA is shown in Figure 3.62. The S11 graph for the Slot Cut Patch Antenna (Rogers RO3003) measured with the R&S VNA is shown in Figure 3.63.



Fig. 3.62 Slot Cut Patch Antenna

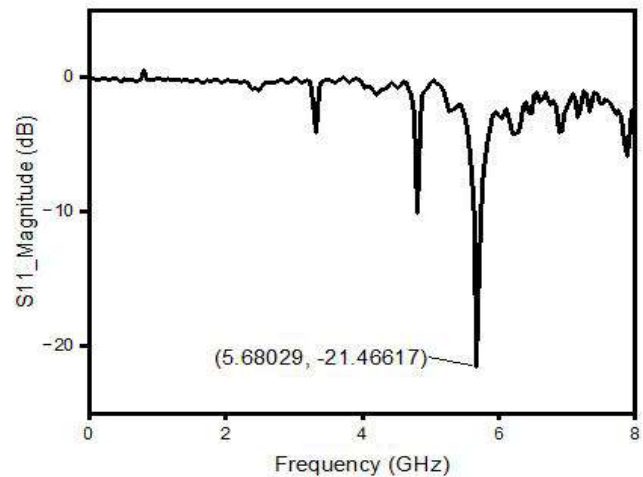


Fig. 3.63 Slot Cut Patch Antenna S11 Graph

- The setup for the Parasitic Patch Antenna with the R&S VNA is shown in Figure 3.64. The S11 graph for the Parasitic Patch Antenna (Rogers RO3003) measured with the R&S VNA is shown in Figure 3.65.

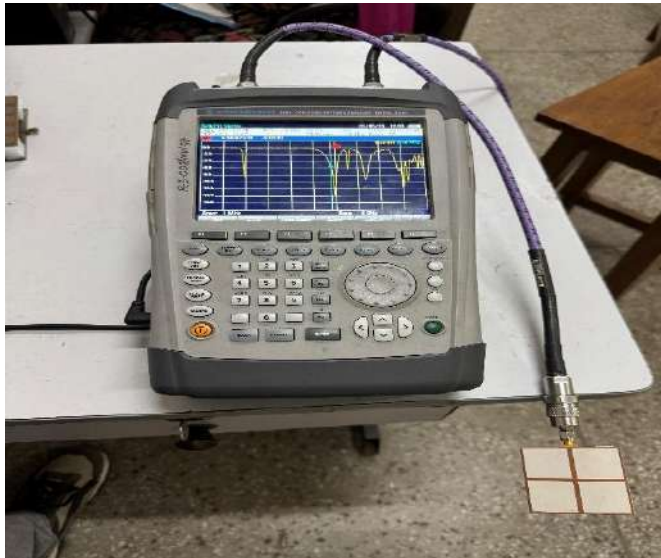


Fig. 3.64 Parasitic Patch Antenna

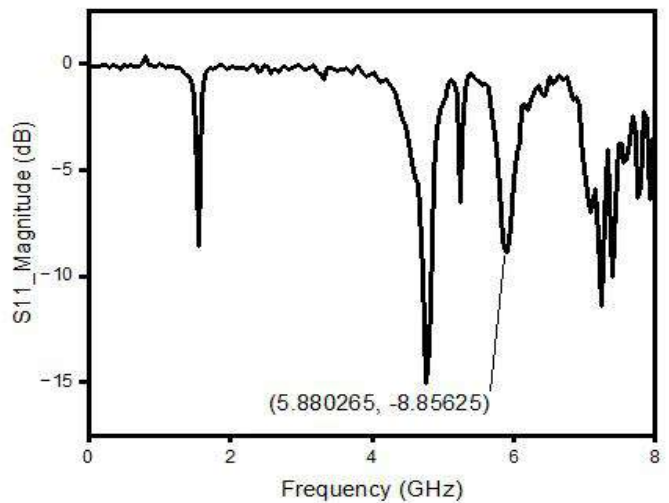


Fig. 3.65 Parasitic Patch Antenna S11 Graph

- The setup for the FR4 Patch Antenna with the R&S VNA is shown in Figure 3.66. The S11 graph for the Patch Antenna (FR4 Material) measured with the R&S VNA is shown in Figure 3.67.



Fig. 3.66 FR4 Patch Antenna

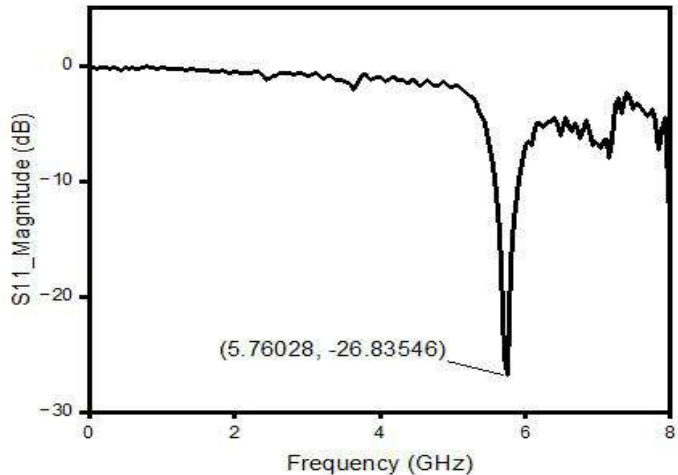


Fig. 3.67 FR4 Patch Antenna S11 Graph

3.2.4 Radiation Patterns

This section describes how each antenna spreads its radio waves.

- Metamaterial Double Negative Index (DNI) Transmit Antenna:** This antenna's radiation pattern shows a 3-dB beam width of 148° in the H-plane. It also exhibits backward wave propagation along the horizontal plane, which is a common feature of the left-handed materials used in its design. A 2D field pattern is shown in Figure 3.68.

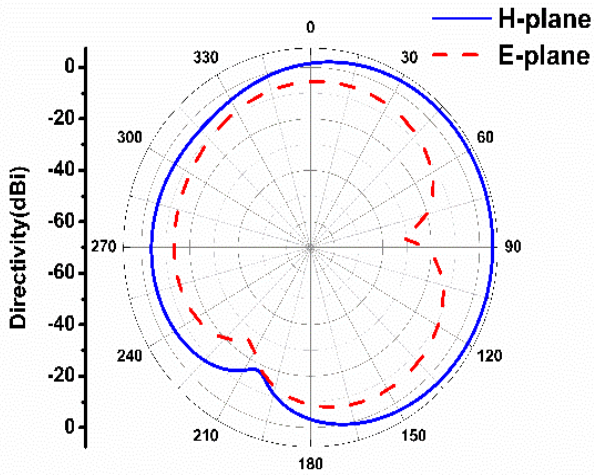


Fig. 3.68 2D Field Pattern

- **Metamaterial Epsilon Near Zero (ENZ) Receive Antenna:** This antenna's radiation pattern demonstrates excellent directivity, with a narrow 3-dB beam width of 32.5° in the H-plane. This narrow beamwidth is particularly good for getting the most signal from a distance and for precise angular location in wireless image transfer. A 2D field pattern is shown in Figure 3.69.

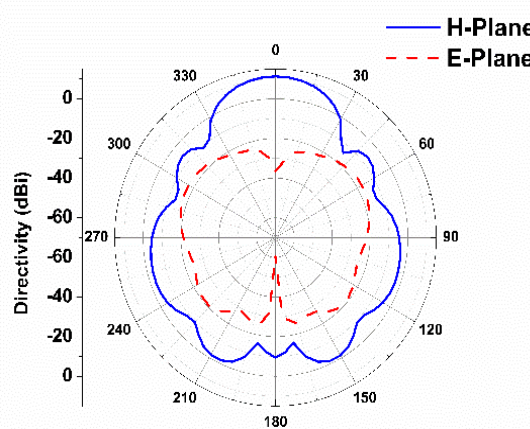


Fig. 3.69 2D Field Pattern

- **Slot Cut Patch Antenna (Rogers RO3003):** This antenna's radiation pattern shows how it sends and receives signals in both the E-plane and H-plane, indicating its directional properties. The E-plane pattern is in Figure 3.70 and the H-plane pattern is in Figure 3.71.

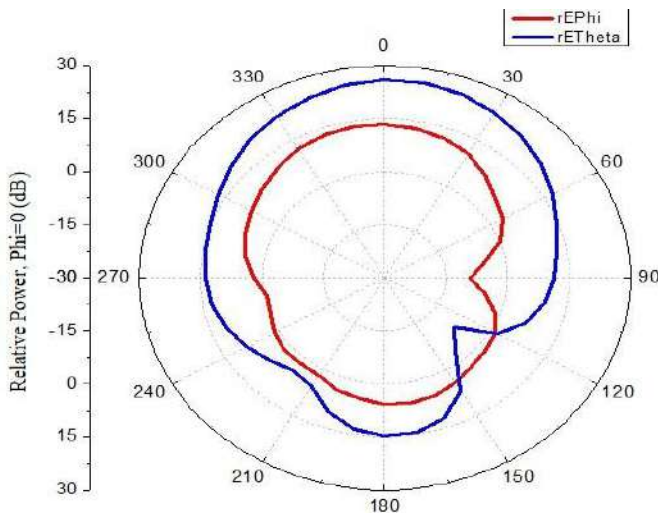


Fig. 3.70 E-Plane

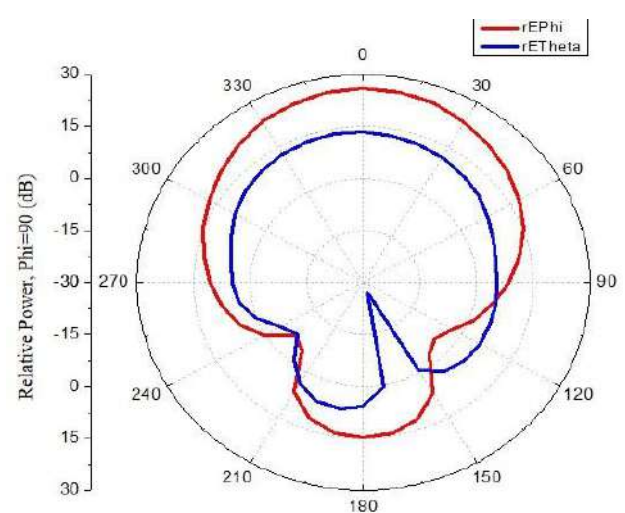


Fig. 3.71 H-Plane

- **Parasitic Patch Antenna (Rogers RO3003):** The radiation pattern for this antenna illustrates how its energy spreads in both the E-plane and H-plane. The E-plane pattern is in Figure 3.72 and the H-plane pattern is in Figure 3.73.

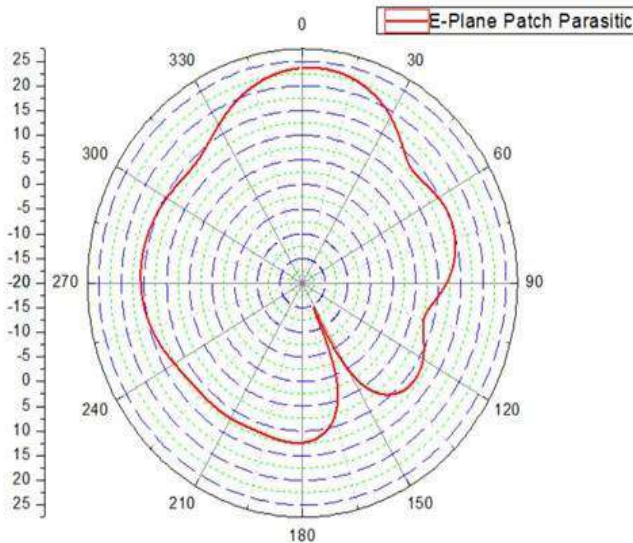


Fig. 3.72 E-Plane

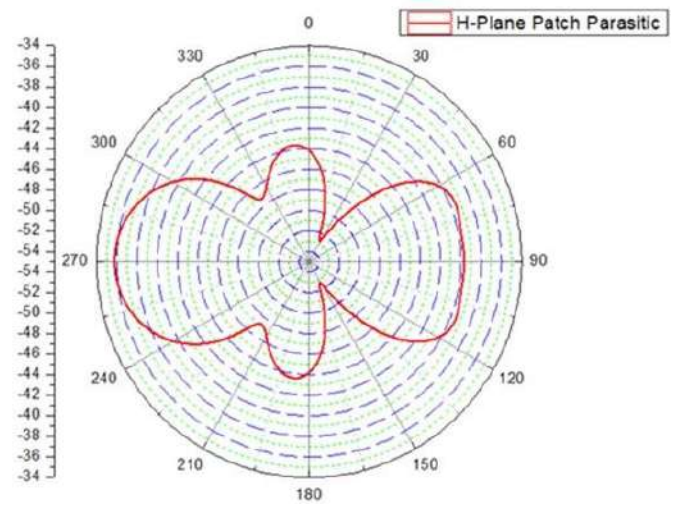


Fig. 3.73 H-Plane

- **Patch Antenna (FR4 Material):** The radiation pattern for this antenna provides insight into its directional characteristics in both the E-plane and H-plane. The E-plane pattern is in Figure 3.74 and the H-plane pattern is in Figure 3.75.

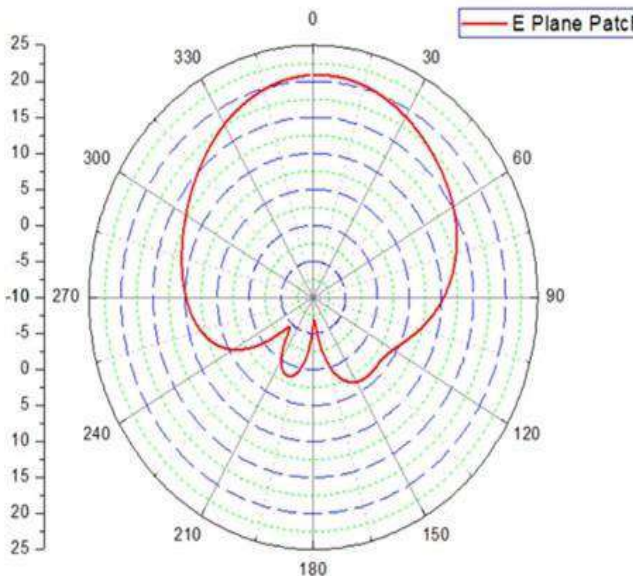


Fig. 3.74 E-Plane

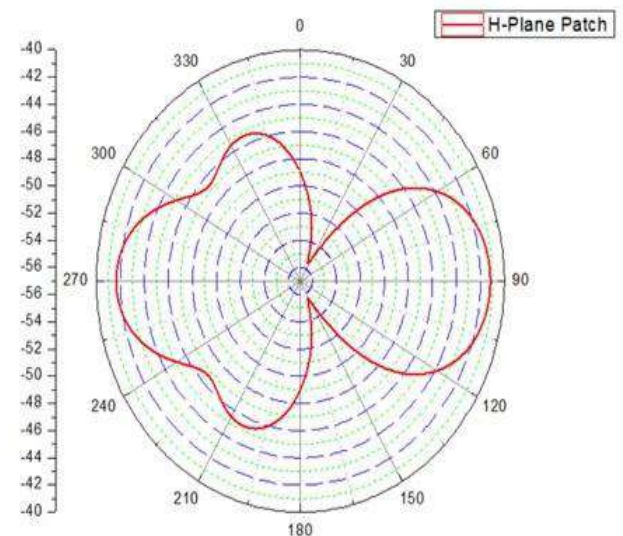


Fig. 3.75 H-Plane

3.2.5 Comparison of Antenna S11 and Frequency Performance

Table 3.4 summarizes the measured S11 and frequency performance for all antennas.

Table 3.4 Antenna S11 and Frequency Performance Summary

Antenna Type	S11 (LibreVNA) (dB)	Frequency (LibreVNA) (GHz)	S11 (R&S VNA) (dB)	Frequency (R&S VNA) (GHz)
Metamaterial Double Negative Index (DNI) Transmit Antenna	-10.39665	5.952008	-19.80159	5.76028
Metamaterial Epsilon Near Zero (ENZ) Receive Antenna	-9.38343	5.772038	-11.3173	5.76028
Slot Cut Patch Antenna (Rogers RO3003)	-19.86683	5.688052	-21.46617	5.68029
Parasitic Patch Antenna (Rogers RO3003)	-9.72851	5.892018	-8.85625	5.880265
Patch Antenna (FR4 Material)	-28.5974	5.736044	-26.83546	5.76028

CHAPTER 4

SYSTEM IMPLEMENTATION AND EXPERIMENTAL RESULTS

4.1 System Design and Operational Principles

The wireless image transfer system developed for this project is based on Software Defined Radio (SDR) principles. It uses Universal Software Radio Peripheral (USRP) B210 hardware, which is controlled by LabVIEW, and Python is used for preparing the images and analyzing the results. This way of working allows for digital image data to be sent from one end to the other over a wireless channel. The overall system is divided into two main parts: a transmitting module and a receiving module, both mainly set up and controlled within the LabVIEW environment.

4.1.1 Transmitting Module

The transmitting module is responsible for changing the digital image data into a radio frequency (RF) signal that can be sent wirelessly. The block diagram for the image transmission system is shown in Figure 4.1.

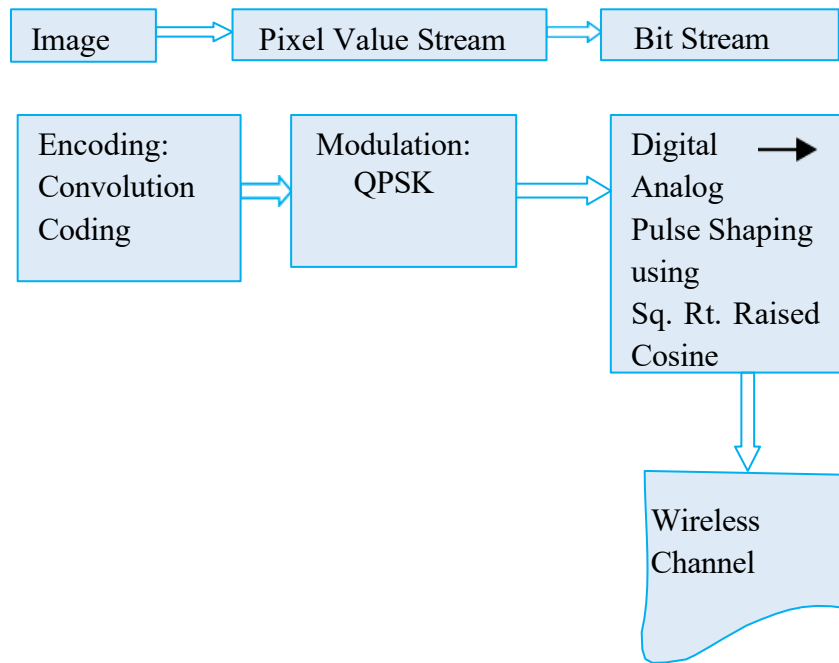


Fig. 4.1 Block Diagram of Image Transmission System

- **Encoding:** The process begins with the input image data, which has been prepared in Python. Inside LabVIEW, the image's bitstream goes through convolutional encoding for error protection. This encoding method helps to keep the data whole in wireless communications. It works by changing the input bits into output bits based on specific rules and a set length.
- **Modulation:** After encoding, the bitstream is modulated using Quadrature Phase-Shift Keying (QPSK). QPSK is a digital modulation technique where the phase of a steady carrier signal is shifted to represent different binary digit patterns, which allows for efficient data transfer. Digital pulse shaping, for example, using a Root Raised Cosine filter, is applied to the modulated signal to shape its waveform and get it ready for converting from digital to analog. This baseband signal is then sent to the USRP B210, which changes it to the desired 5.8 GHz RF frequency and sends it wirelessly through the connected antenna.

4.1.2 Receiving Module

The receiving module is responsible for capturing the wireless RF signal and changing it back into the original digital image data. The block diagram for the image reception system is shown in Figure 4.2.

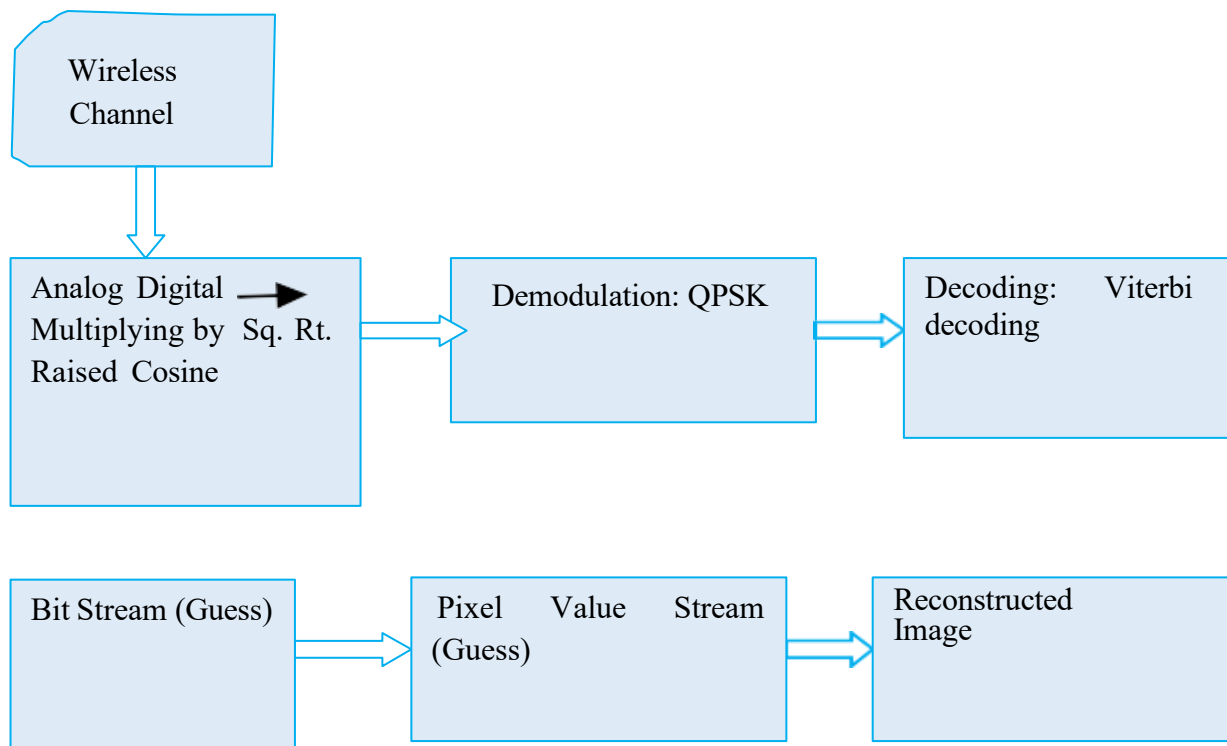


Fig. 4.2 Receiver Block for Image Reception

- **Demodulation:** Once the signal is received by the antenna and initially processed by the USRP B210, the digital baseband signal is sent to LabVIEW. Inside LabVIEW, QPSK demodulation is performed using a matched filter. This process reverses the modulation, pulling out the original data from the received signal, aiming to make the signal-to-noise ratio as high as possible at the output.
- **Decoding:** The demodulated bitstream, which might have errors from the wireless channel, then goes through Viterbi decoding. A Viterbi decoder efficiently decodes bitstreams that were encoded with a convolutional code, correcting errors that happened during transmission. The decoded bits are then typically saved in a CSV file for further processing.
- **Reconstruction Algorithm:** After decoding, Python is used to rebuild the image from the recovered data. The steps for this algorithm involve reading the CSV file that has the decoded binary data and changing this binary data back into an image format suitable for display and analysis. This includes changing binary values back to pixel strengths and reshaping the data into a 2D image.
- **LabVIEW Implementation:** LabVIEW plays a complete role in setting up both the transmitting and receiving parts of the system. For the transmitter, LabVIEW reads the image bitstream, performs convolutional encoding and QPSK modulation, and controls the USRP for sending the signal. For the receiver, LabVIEW handles QPSK demodulation, Viterbi decoding, and saves the decoded bits, which Python then uses for the final image reconstruction. The LabVIEW Front Panel and Block Diagram for both the transmitting and receiving modules are detailed in Figure 2.8 (Tx Front Panel), Figure 2.9 (Tx Block Diagram), Figure 2.10 (Rx Front Panel), and Figure 2.11 (Rx Block Diagram) of Chapter 2.3.

4.2 Experimental Setup and Performance Evaluation

This section describes the ways the experiments were set up for wireless image transfer. After that, it presents and analyzes the results obtained under various conditions. Data was collected in a laboratory setting, with additional measurements taken in different indoor and outdoor locations to simulate various real-world wireless signal conditions.

4.2.1 Single USRP Experimental Arrangement and Results

In this setup, a single USRP B210 device was connected to one laptop. Both the transmitting (Tx) and receiving (Rx) antennas were connected to this same USRP, which meant it had to switch between sending and receiving (time-division duplex mode) to handle both at once. LabVIEW software on this single laptop controlled the entire image transmission and reception process. All measurements for this arrangement were done inside the laboratory. The conceptual diagram for this setup is shown in Figure 4.3.

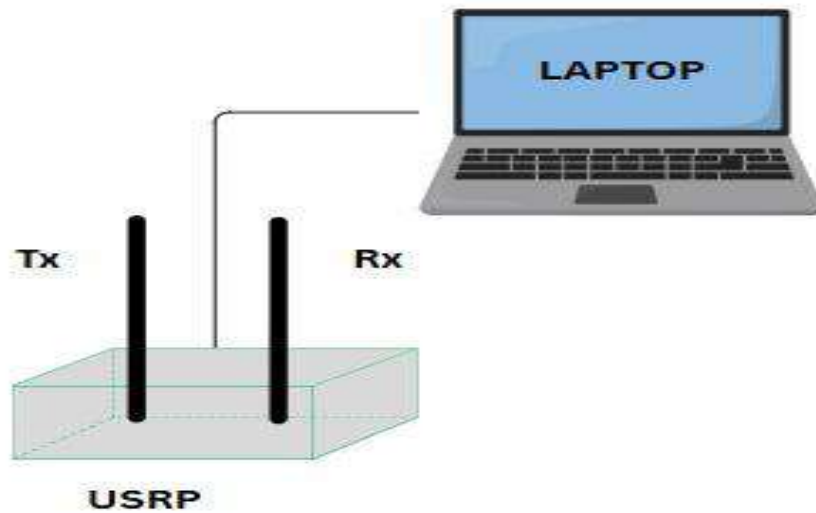


Fig. 4.3 Conceptual Diagram

- **Initial Testing with Dipole Antennas:** To check if the basic transmission and reception worked with the single USRP setup, standard dipole antennas (operating at 2.45 GHz) were used first for both sending and receiving. This served as a starting point for comparison. For this initial test, Image 1 was sent with an IQ sampling rate of 500k samples/second (S/sec), Image 2 with 1M S/sec, and Image 3 with 1.5M S/sec. The on-site experimental setup is shown in Figure 4.4. Visual results of these experiments are in Table 4.1. Quantitative performance metrics, including Pearson Correlation Coefficient, RMSE, PSNR, NCC, SSIM, Linear Fit Slope, and Linear Fit Intercept, are provided in Table 4.2.

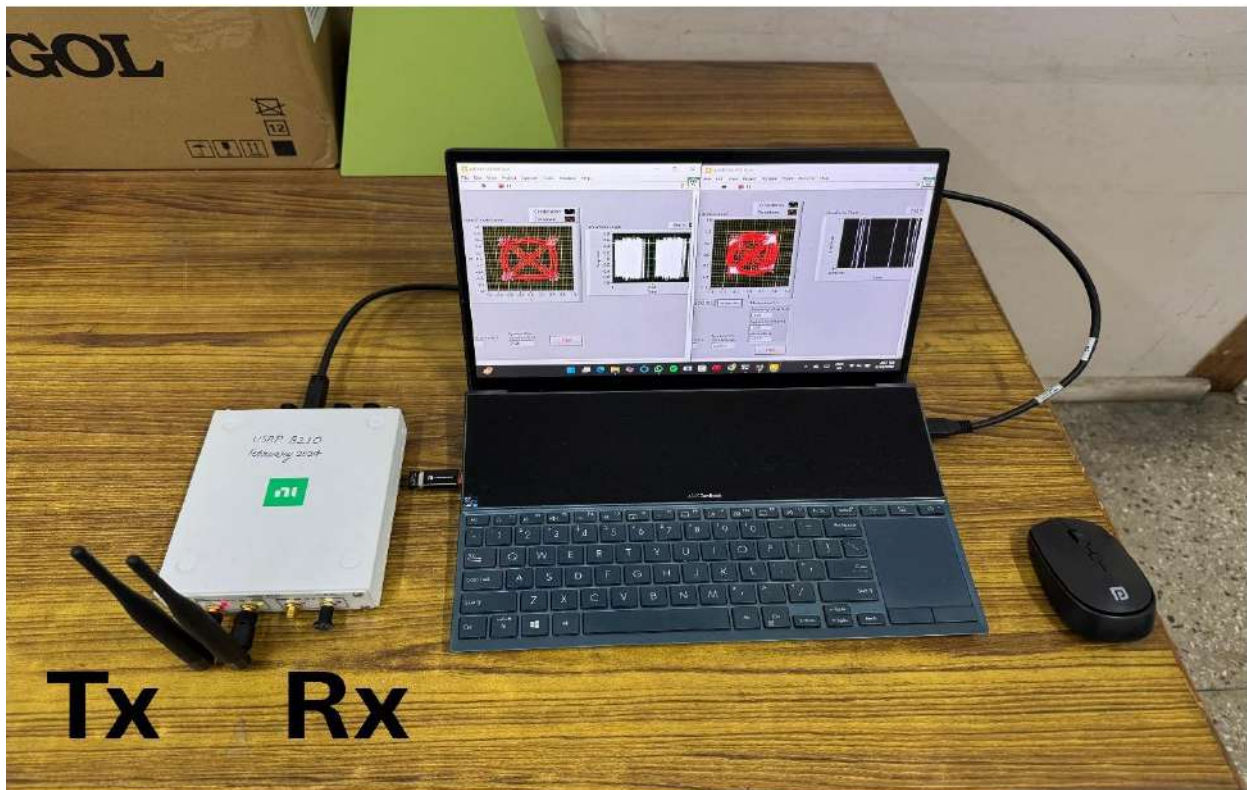


Fig. 4.4 On-site Experimental Setup

Table 4.1 (Single USRP Initial Testing with Dipole Antennas)

Image No.	Transmitted Image	Set Gain Value (dB)	Tx Front Panel	Rx Front Panel	Received Image
Image 1 (D1)		30			

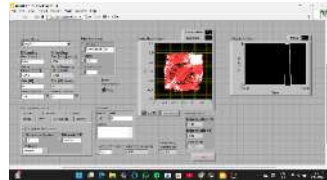
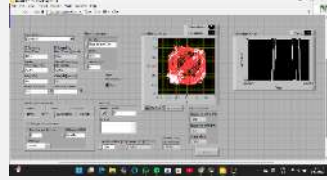
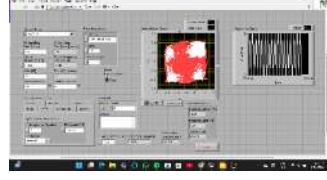
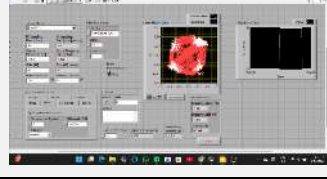
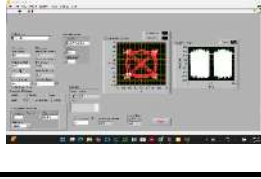
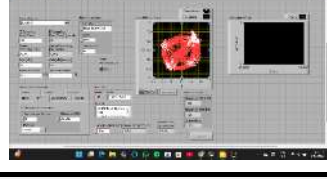
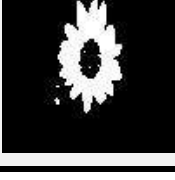
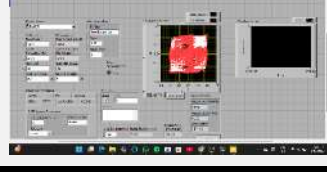
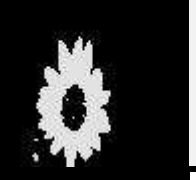
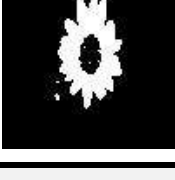
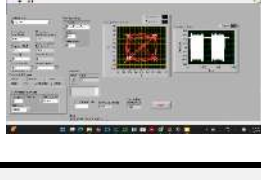
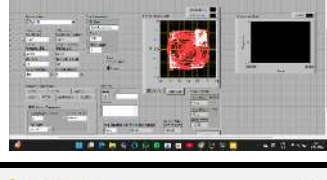
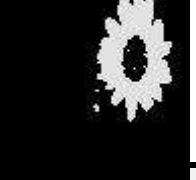
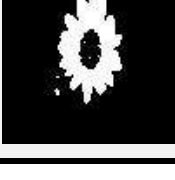
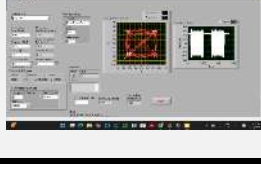
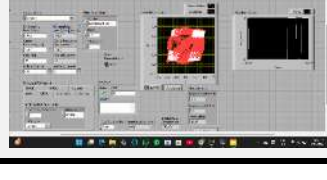
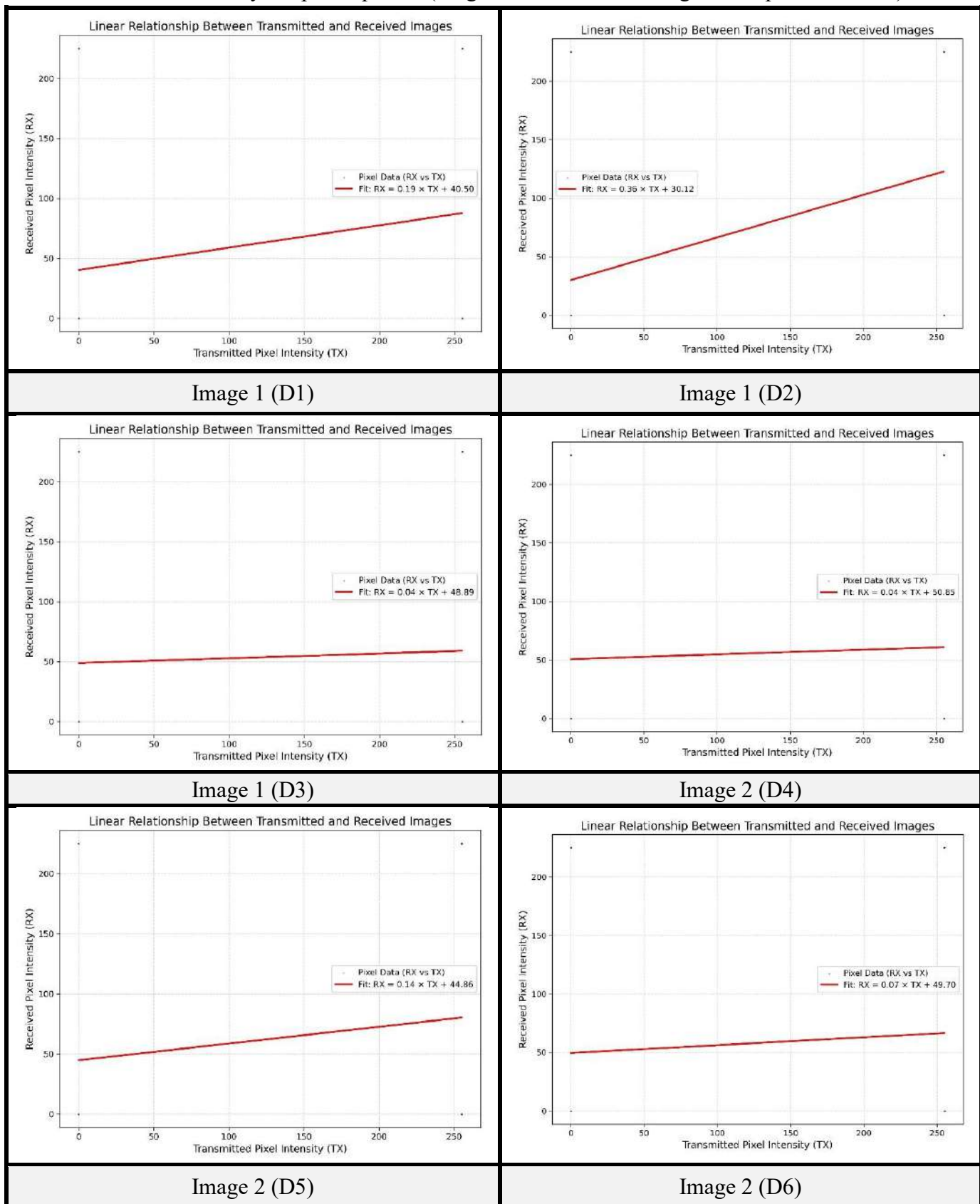
Image 1 (D2)		40			
Image 1 (D3)		50			
Image 2 (D4)		30			
Image 2 (D5)		40			
Image 2 (D6)		50			
Image 3 (D7)		30			
Image 3 (D8)		40			
Image 3 (D9)		50			

Table 4.2 Linearity Graph Properties (Single USRP Initial Testing with Dipole Antennas)

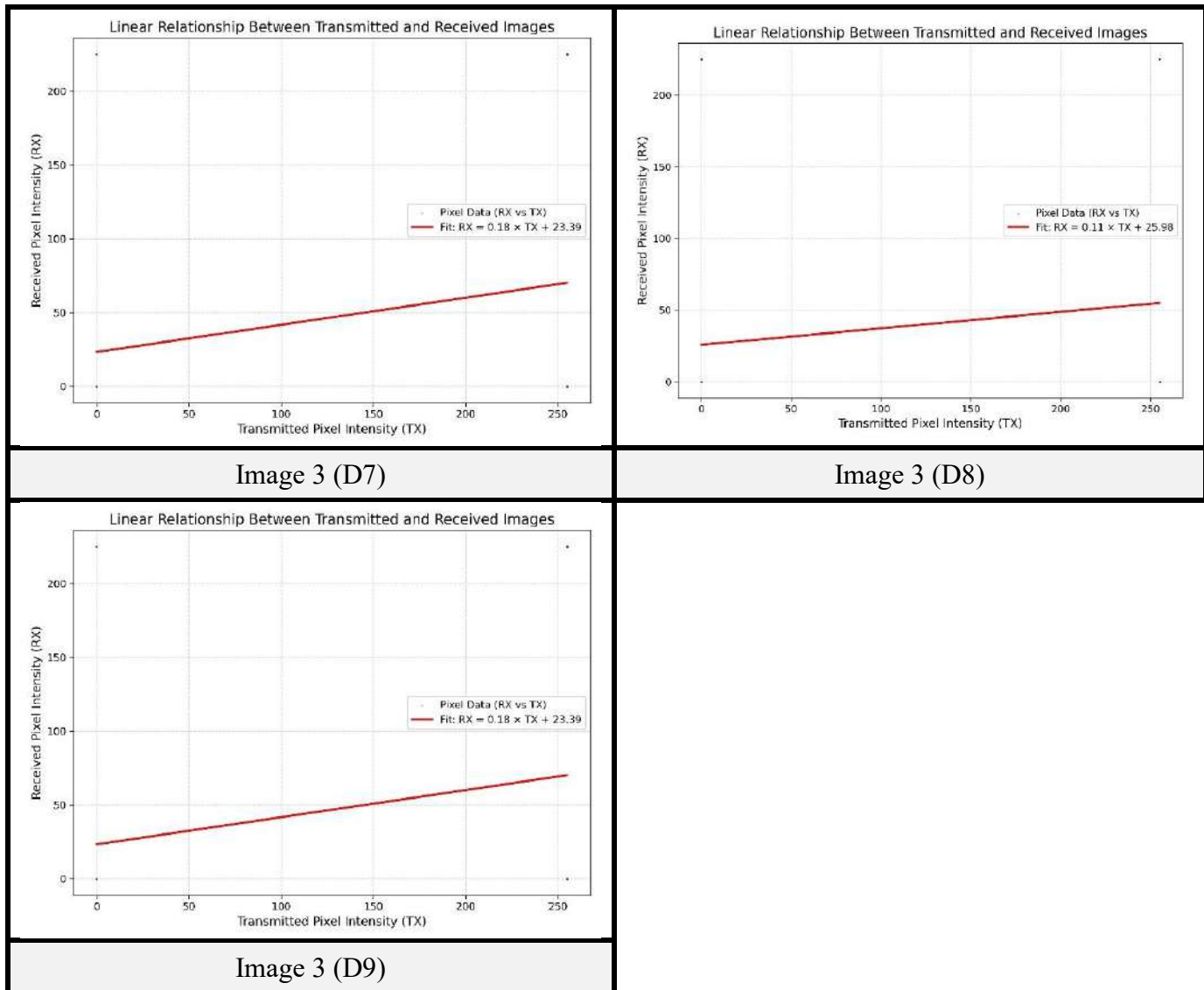


Table 4.3 Quantitative Performance Metrics (Single USRP with Dipole Antennas)

Image No.	Set Gain value (dB)	Pearson Correlation Coefficient	RMSE	PSNR (dB)	Normalized Cross-Correlation (NCC)	SSIM	Linear Fit Slope (m)	Linear Fit Intercept (c)
Image 1 (D1)	30	0.210379	6.220981	32.25363	0.210379	0.370635	0.185685994	40.49592127
Image 1 (D2)	40	0.412383	6.039892	32.51022	0.412383	0.441762	0.363924	30.1243
Image 1 (D3)	50	0.04536	6.359788	32.06195	0.04536	0.308716	0.040018	48.88644

Image 2 (D4)	30	0.045237	6.476064	31.90458	0.045237	0.31811 5	0.039915	50.84829
Image 2 (D5)	40	0.157595	6.37815	32.03691	0.157595	0.41332	0.139054	44.8644
Image 2 (D6)	50	0.075465	6.478634	31.90113	0.075465	0.33829 5	0.06679	49.69868
Image 3 (D7)	30	0.208314	4.788549	34.52673	0.208314	0.61690 7	0.183806	23.3884
Image 3 (D8)	40	0.12928032 9	4.86902454 3	34.3819643 4	0.12928032 9	0.57291 3	0.11451178 8	25.97847 358
Image 3 (D9)	50	0.208314	4.788549	34.52673	0.208314	0.60745 1	0.183806	23.3884

- **Experiment 1 [Fixed DNI Tx and Varied Rx Antennas (IQ 250k S/sec)]:** This experiment looked at how different receiving antennas affected image quality. The Metamaterial Double Negative Index (DNI) antenna stayed as the transmitting antenna for all tests. The IQ Sampling Rate was kept the same at 250k S/sec for all transmissions, and only the gain was changed (30 dB, 40 dB, 50 dB).
- For Metamaterial Epsilon Near Zero (ENZ) Receive Antenna: The on-site experimental setup for this antenna is shown in Figure 4.5. Visual results are presented in Table 4.4. Linearity graph metrics are provided in Table 4.5. Quantitative performance metrics are in Table 4.6.



Fig. 4.5 On-site Experimental Setup

Table 4.4 Visual Experiment Results (Single USRP ENZ Receive Antenna)

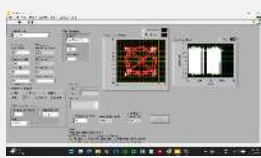
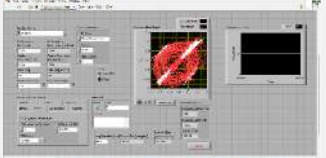
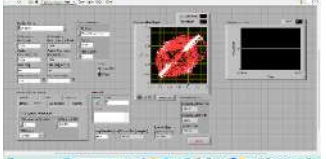
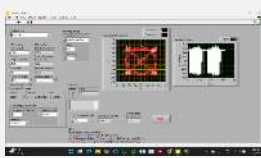
Image No.	Transmitted Image	Set Gain Value (dB)	Tx Front Panel	Rx Front Panel	Received Image
Image 1 (E1)		30			
Image 1 (E2)		40			
Image 1 (E3)		50			
Image 2 (E4)		30			
Image 2 (E5)		40			
Image 2 (E6)		50			
Image 3 (E7)		30			

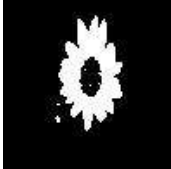
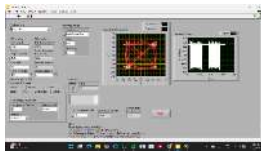
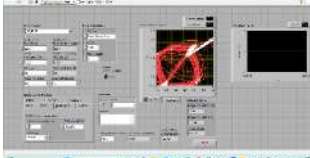
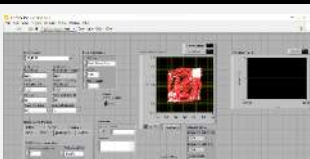
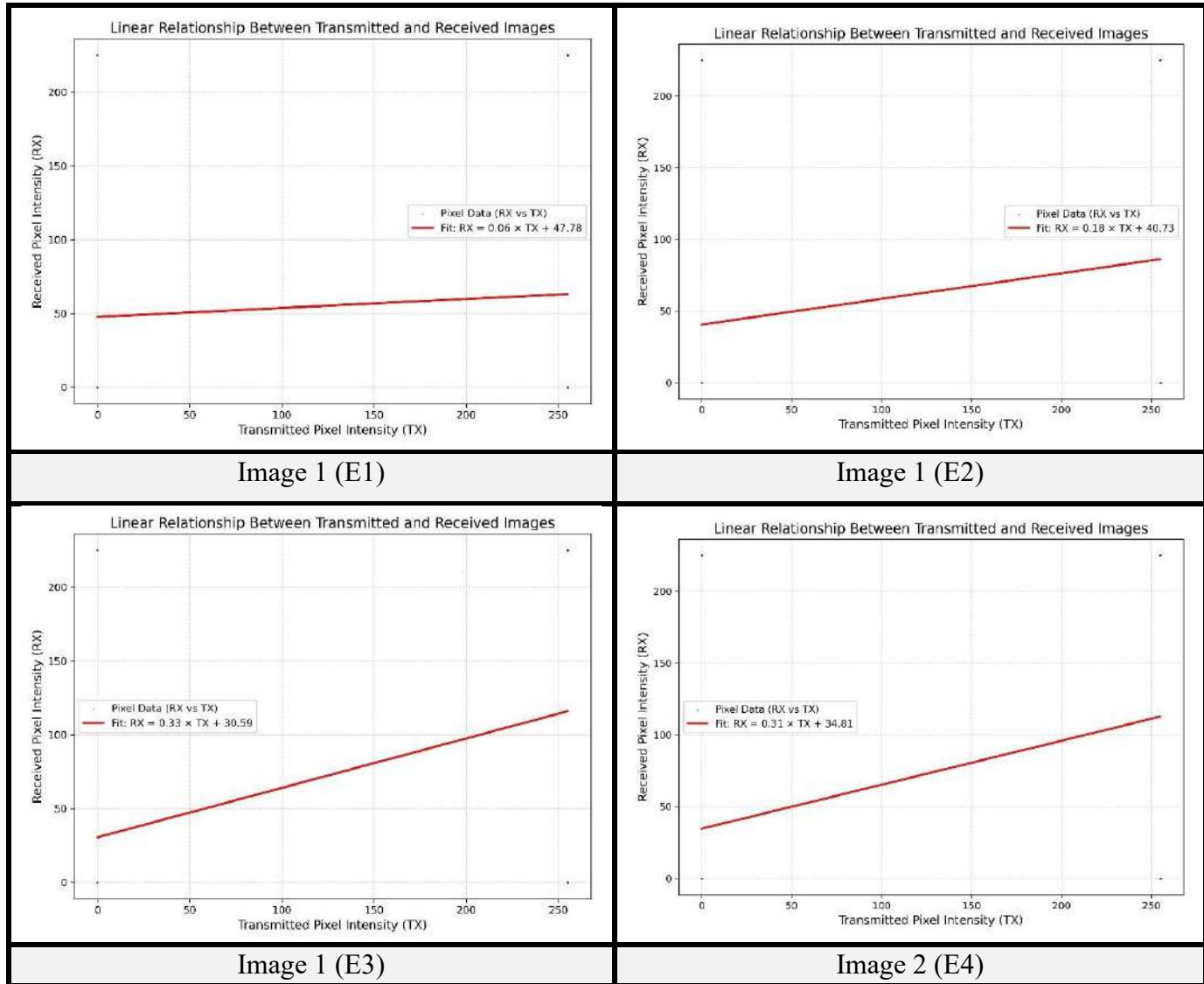
Image 3 (E8)		40			
Image 3 (E9)		50			

Table 4.5 Linearity Graph Metrics (Single USRP ENZ Receive Antenna)



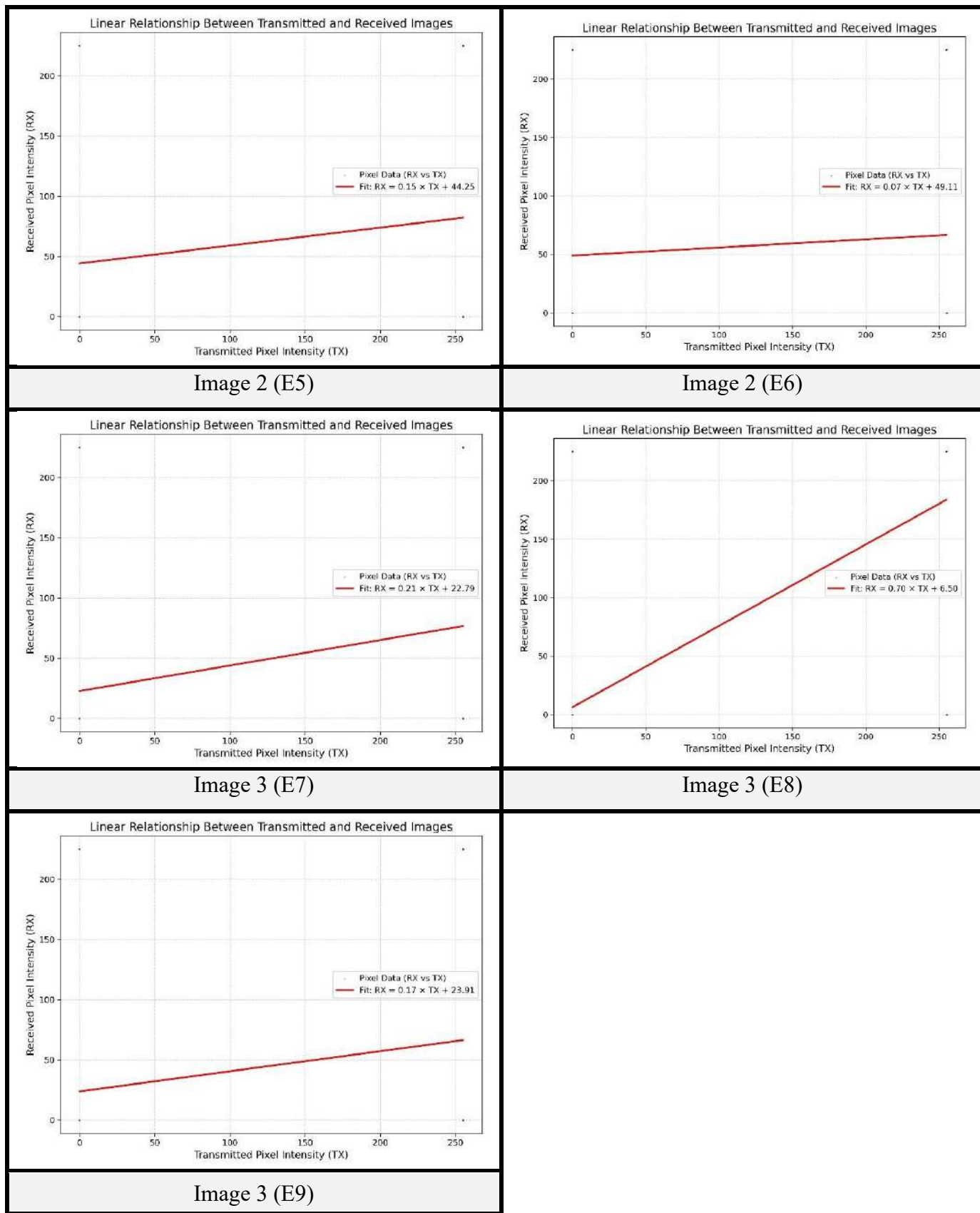


Table 4.6 Quantitative Performance Metrics (Single USRP ENZ Receive Antenna)

Image No.	Gain (dB)	Pearson Correlation Coefficient	RMSE	PSNR (dB)	Normalized Cross-Correlation (NCC)	SSIM	Linear Fit Slope (m)	Linear Fit Intercept (c)
Image 1 (E1)	30	0.068687	6.345368	32.08167	0.068687	0.325875	0.060634	47.77936
Image 1 (E2)	40	0.20257	6.216542	32.25983	0.20257	0.373331	0.178572	40.72899
Image 1 (E3)	50	0.382819	5.989332	32.58324	0.382819	0.419932	0.33497	30.59044
Image 2 (E4)	30	0.346705	6.211256	32.26722	0.346705	0.432996	0.305961	34.81266
Image 2 (E5)	40	0.16882	6.366907	32.05223	0.16882	0.375816	0.148937	44.24538
Image 2 (E6)	50	0.078715	6.449791	31.93989	0.078715	0.319161	0.069474	49.10913
Image 3 (E7)	30	0.23875	4.794174	34.51653	0.23875	0.624606	0.211679	22.79268
Image 3 (E8)	40	0.785535	4.362557	35.33598	0.785535	0.776162	0.695575	6.501094
Image 3 (E9)	50	0.189378	4.79875	34.50824	0.189378	0.60136	0.16699	23.90641

- **For Slot Cut Patch Antenna (Rogers RO3003):** The on-site experimental setup for this antenna is shown in Figure 4.6. Visual results are presented in Table 4.7. Linearity graph metrics are provided in Table 4.8. Quantitative performance metrics are in Table 4.9.

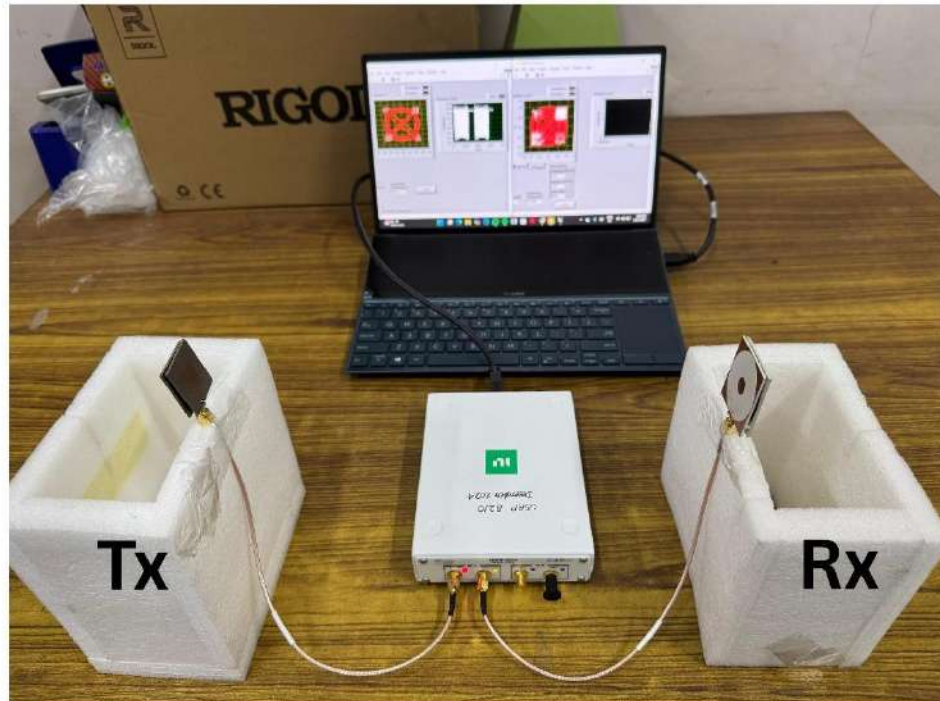


Fig. 4.6 On-site Experimental Setup

Table 4.7 Visual Experiment Results (Single USRP Slot Cut Patch Antenna)

Image No.	Transmitted Image	Set Gain Value (dB)	Tx Front Panel	Rx Front Panel	Received Image
Image 1 (S1)		30			
Image 1 (S2)		40			

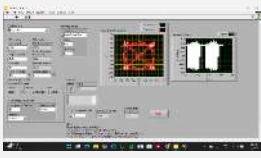
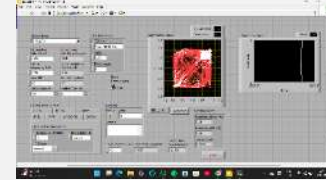
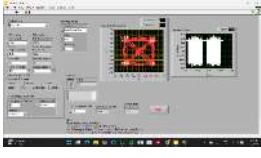
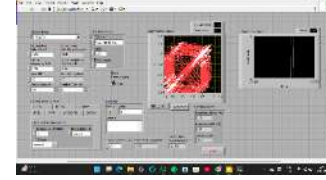
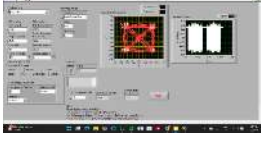
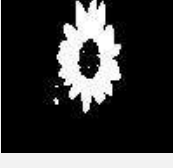
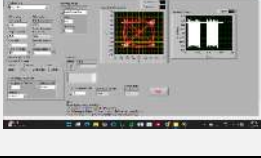
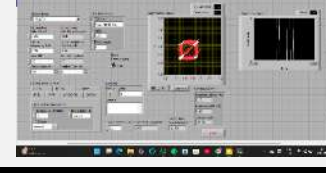
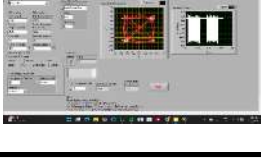
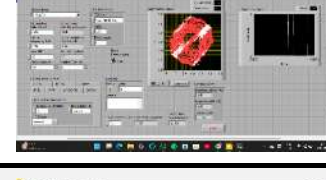
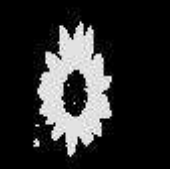
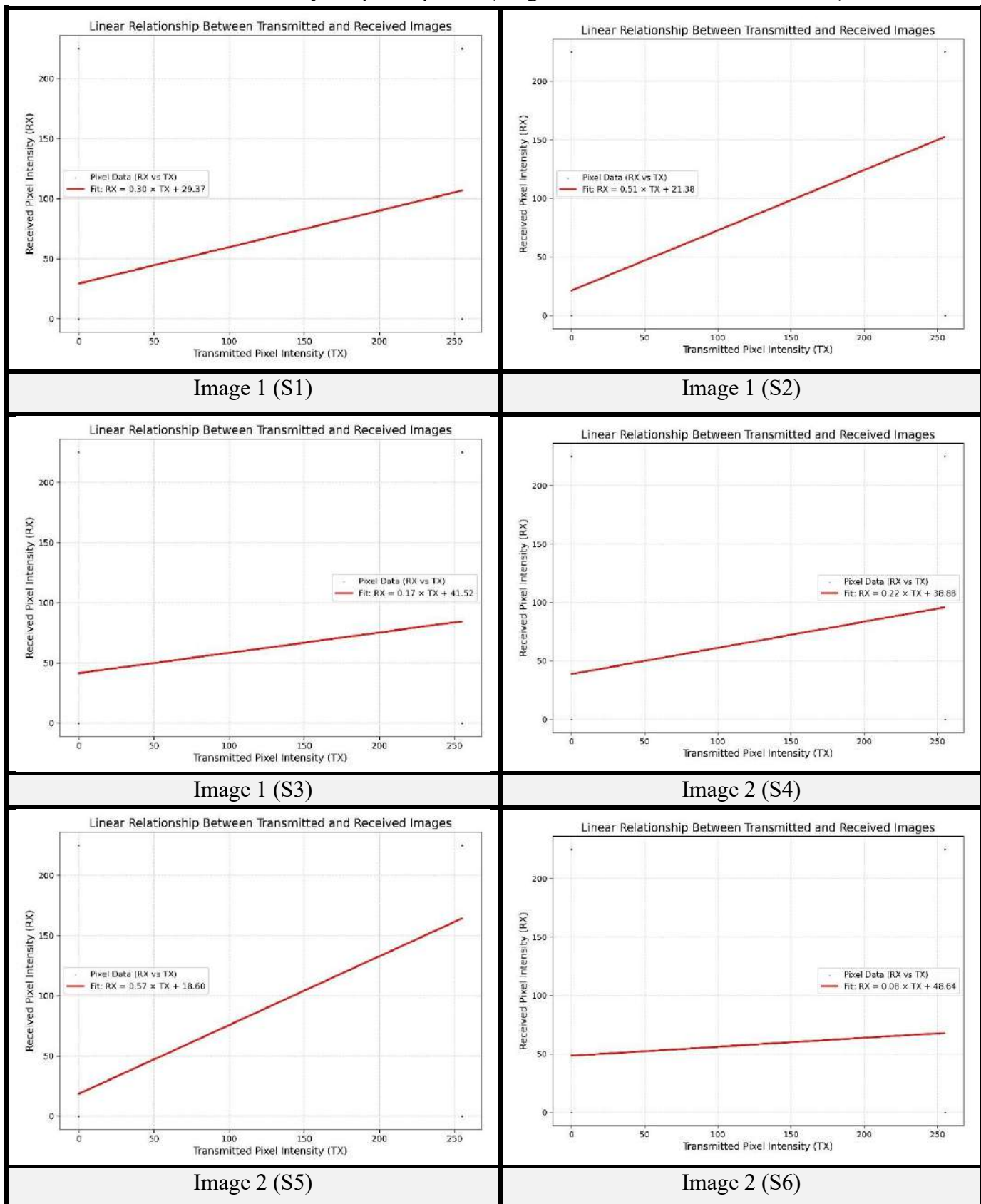
Image 1 (S3)		50	 	
Image 2 (S4)		30	 	
Image 2 (S5)		40	 	
Image 2 (S6)		50	 	
Image 3 (S7)		30	 	
Image 3 (S8)		40	 	
Image 3 (S9)		50	 	

Table 4.8 Linearity Graph Properties (Single USRP Slot Cut Patch Antenna)

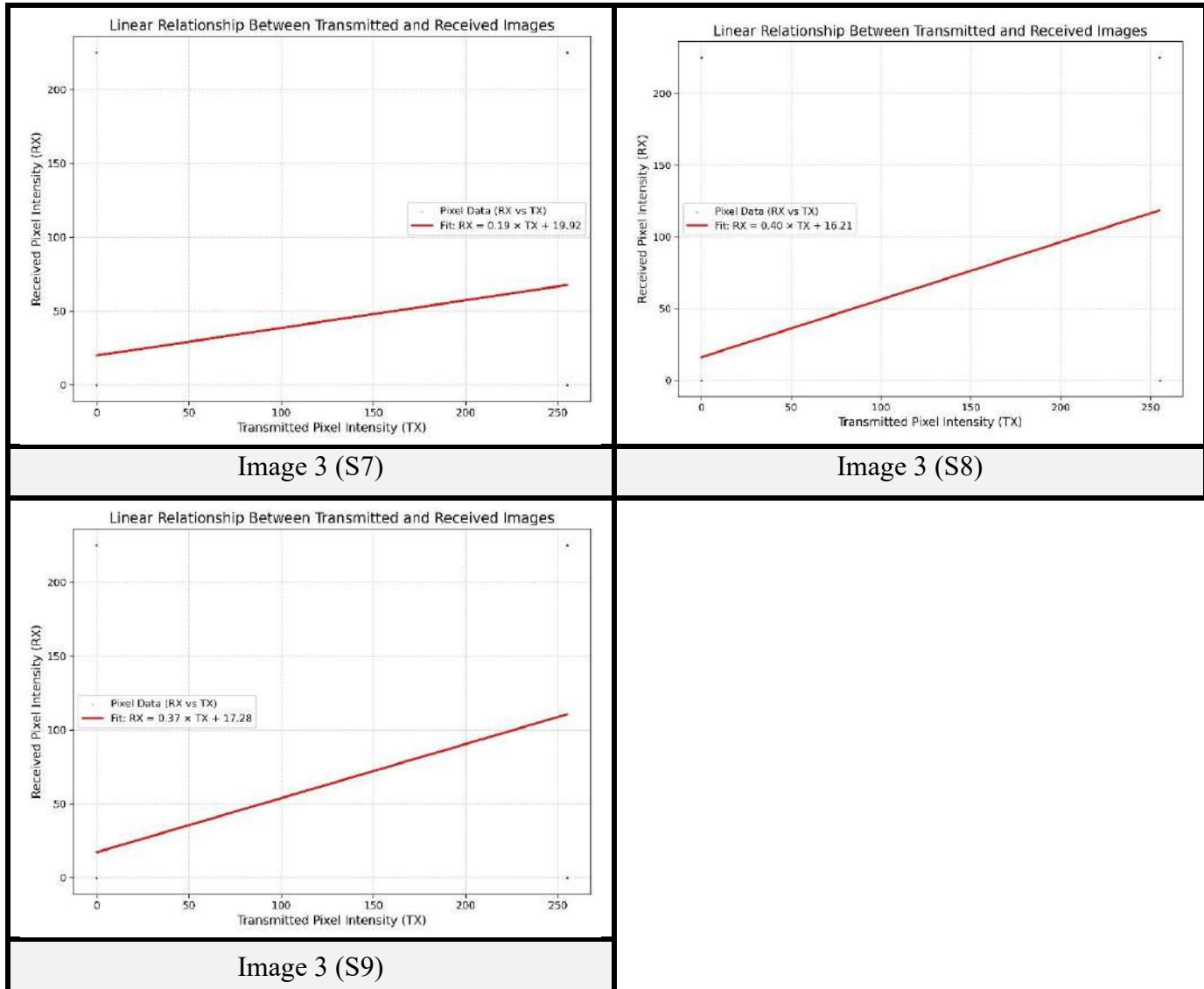


Table 4.9 Quantitative Performance Metrics (Single USRP Slot Cut Patch Antenna)

Image No.	Set Gain value (dB)	Pearson Correlation Coefficient	RMSE	PSNR (dB)	Normalized Cross-Correlation (NCC)	SSIM	Linear Fit Slope (m)	Linear Fit Intercept (c)
Image 1 (S1)	30	0.355088	5.817491	32.83609	0.355088	0.474446	0.303731	29.36683
Image 1 (S2)	40	0.582954	5.883902	32.7375	0.582954	0.50018	0.514451	21.38418
Image 1 (S3)	50	0.19171	6.241546	32.22496	0.19171	0.372587	0.169287	41.5156

Image 2 (S4)	30	0.255326	6.23894 2	32.2285 8	0.255326	0.43770 2	0.224028	38.88052
Image 2 (S5)	40	0.648456	5.92156 2	32.6820 8	0.648456	0.57712	0.571582	18.60016
Image 2 (S6)	50	0.086748	6.44006 2	31.953	0.086748	0.32707 8	0.076543	48.6375
Image 3 (S7)	30	0.223585	4.48859 7	35.0885 9	0.223585	0.63082 7	0.187336	19.91769
Image 3 (S8)	40	0.454243	4.61284 1	34.8514 3	0.454243	0.67074 7	0.401449	16.21388
Image 3 (S9)	50	0.415222	4.63324 9	34.8130 9	0.415222	0.66905 6	0.366372	17.27581

- **For Parasitic Patch Antenna (Rogers RO3003):** The on-site experimental setup for this antenna is shown in Figure 4.7. Visual results are presented in Table 4.10. Linearity graph properties are provided in Table 4.11. Quantitative performance metrics are in Table 4.12.



Fig. 4.7 On-site Experimental Setup

Table 4.10: Visual Experiment Results (Single USRP Parasitic Patch Antenna)

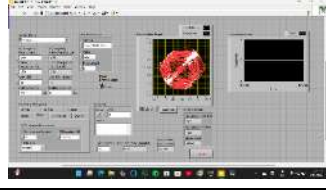
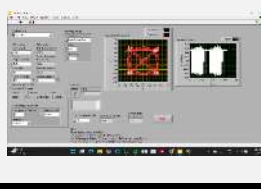
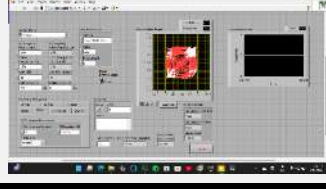
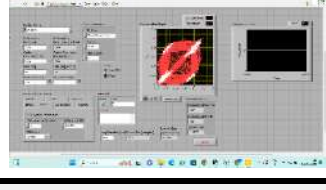
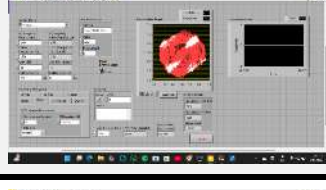
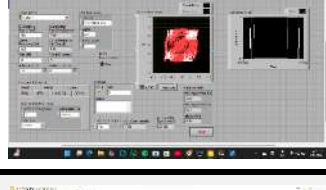
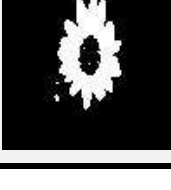
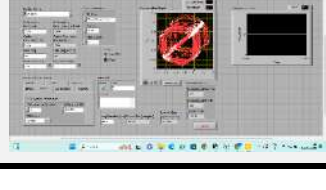
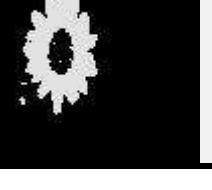
Image No.	Transmitted Image	Set Gain Value (dB)	Tx Front Panel	Rx Front Panel	Received Image
Image 1 (PP1)		30			
Image 1 (PP2)		40			
Image 1 (PP3)		50			
Image 2 (PP4)		30			
Image 2 (PP5)		40			
Image 2 (PP6)		50			
Image 3 (PP7)		30			

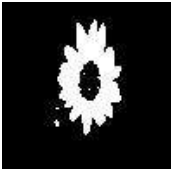
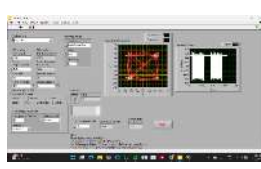
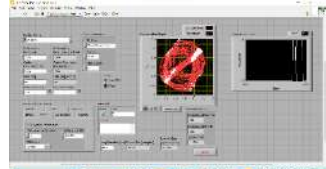
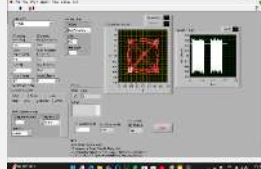
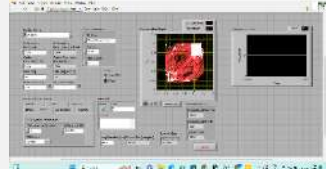
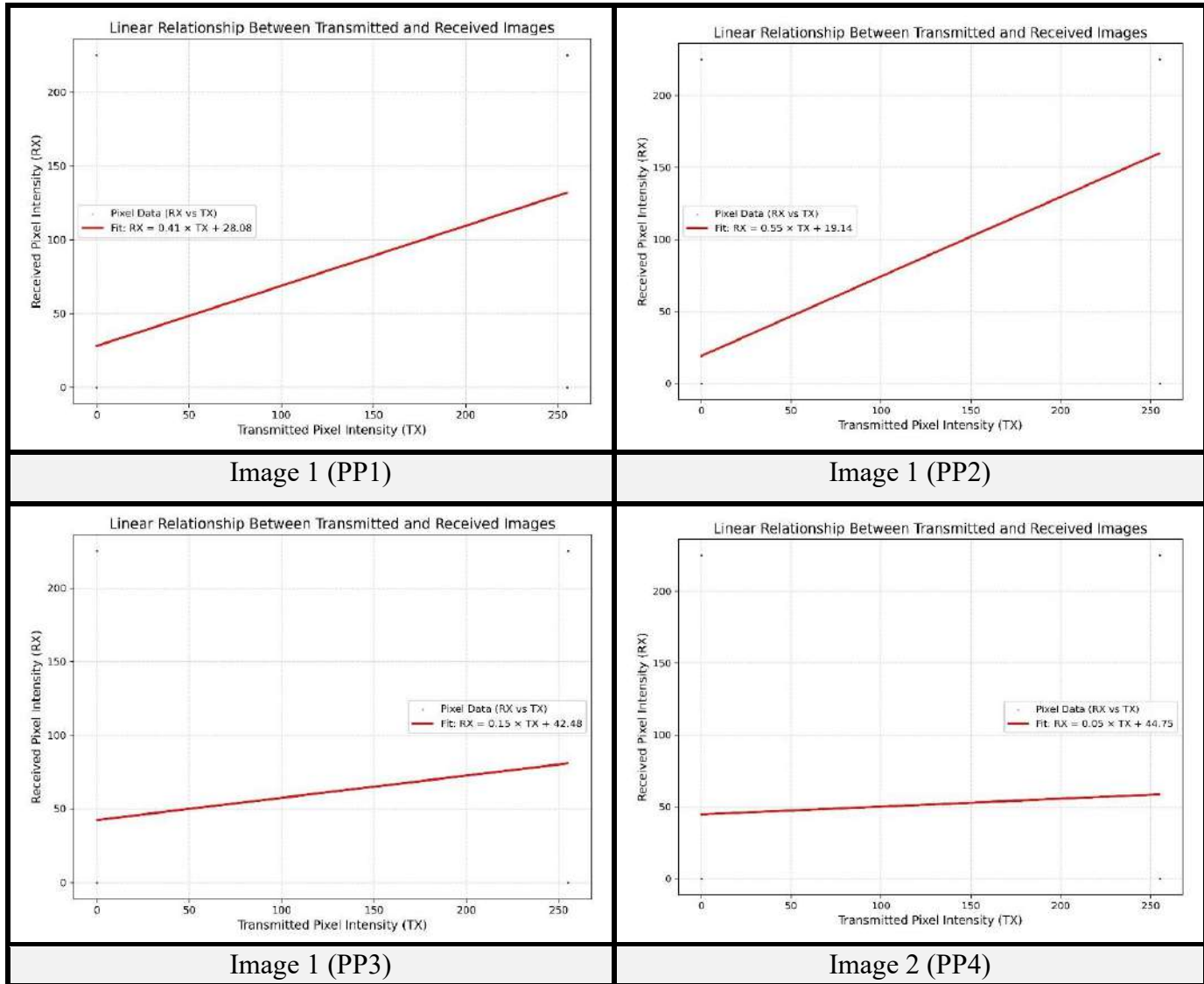
Image 3 (PP8)		40			
Image 3 (PP9)		50			

Table 4.11 Linearity Graph Properties (Single USRP Parasitic Patch Antenna)



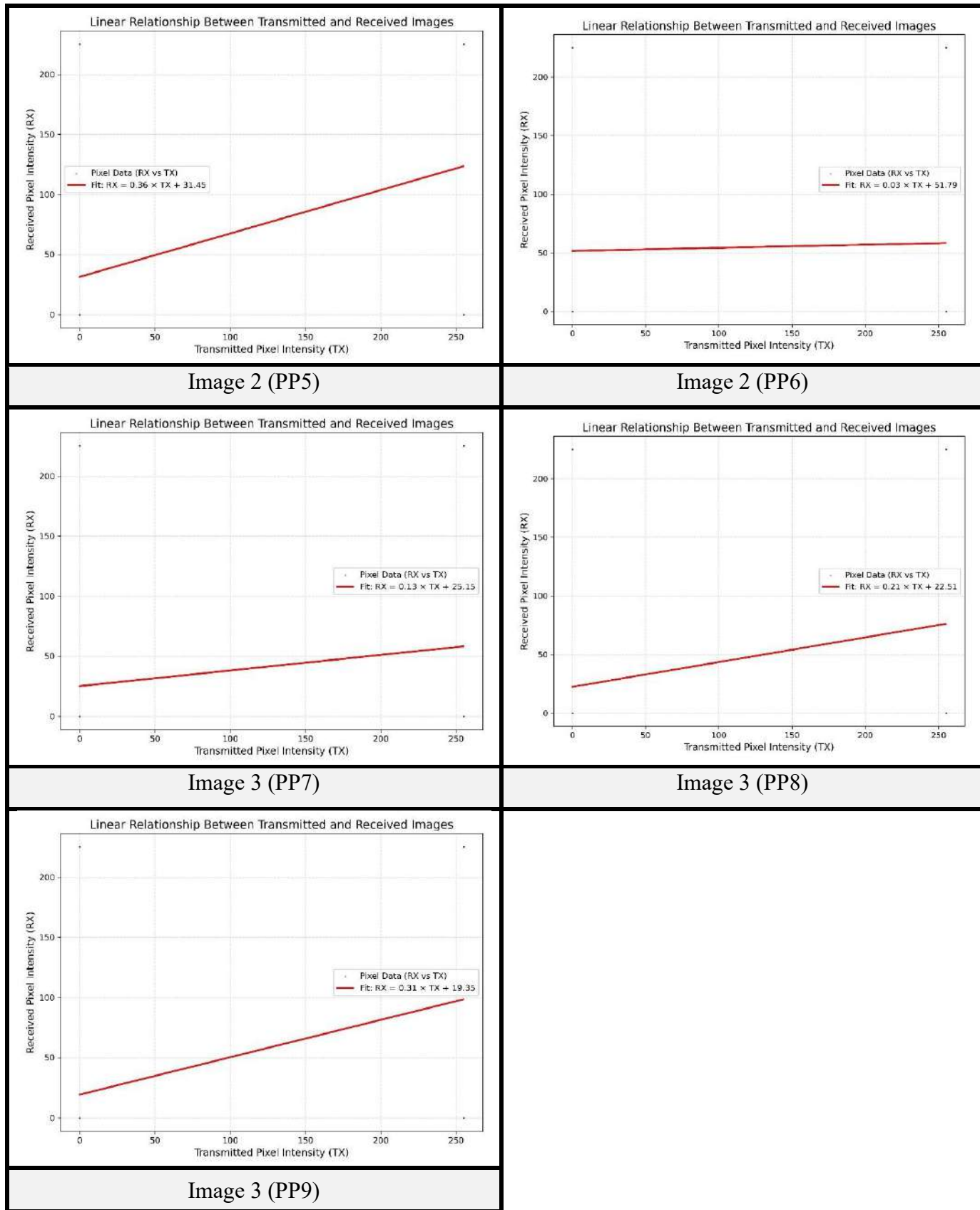


Table 4.12 Quantitative Performance Metrics (Single USRP Parasitic Patch Antenna)

Image No.	Set Gain value (dB)	Pearson Correlation Coefficient	RMSE	PSNR (dB)	Normalized Cross-Correlation (NCC)	SSIM	Linear Fit Slope (m)	Linear Fit Intercept (c)
Image 1 (PP1)	30	0.459918	6.026724	32.52918	0.459918	0.499789	0.407185	28.08494
Image 1 (PP2)	40	0.62605	5.84095	32.80113	0.62605	0.53505	0.552311	19.14088
Image 1 (PP3)	50	0.170897	6.252679	32.20948	0.170897	0.371036	0.150792	42.47702
Image 2 (PP4)	30	0.064098	6.133254	32.37699	0.064098	0.344728	0.054524	44.7465
Image 2 (PP5)	40	0.409431	6.153032	32.34902	0.409431	0.456885	0.361262	31.45225
Image 2 (PP6)	50	0.029198	6.495398	31.87869	0.029198	0.292081	0.025778	51.79156
Image 3 (PP7)	30	0.147268	4.829658	34.45248	0.147268	0.580051	0.129858	25.14965
Image 3 (PP8)	40	0.238807	4.767861	34.56433	0.238807	0.627991	0.21078	22.50777
Image 3 (PP9)	50	0.35092	4.699032	34.69064	0.35092	0.648631	0.310533	19.34788

- **For Patch Antenna (FR4 Material):** The on-site experimental setup for this antenna is shown in Figure 4.8. Visual results are presented in Table 4.13. Linearity graph properties are provided in Table 4.14. Quantitative performance metrics are in Table 4.15.



Fig. 4.8 On-site Experimental Setup

Table 4.13: Visual Experiment Results (Single USRP Patch Antenna - FR4 Material)

Image No.	Transmitted Image	Set Gain Value (dB)	Tx Front Panel	Rx Front Panel	Received Image
Image 1 (P1)		30			
Image 1 (P2)		40			

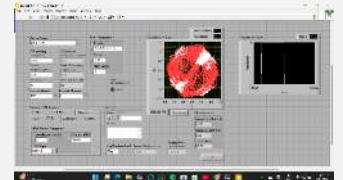
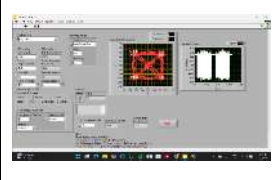
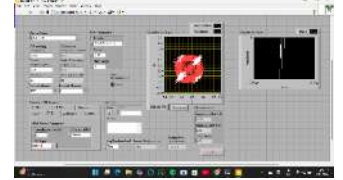
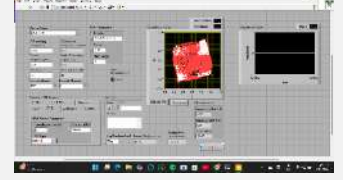
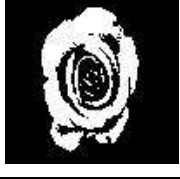
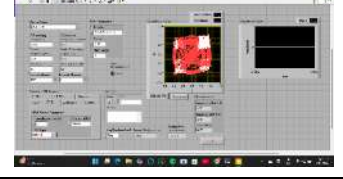
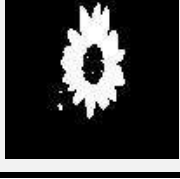
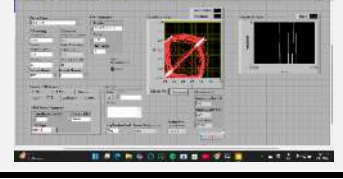
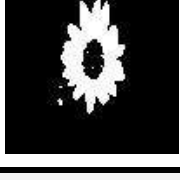
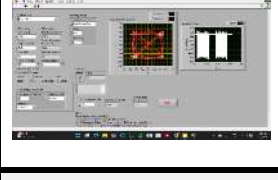
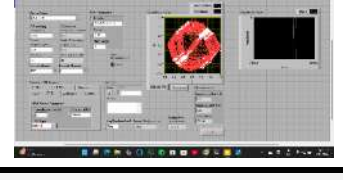
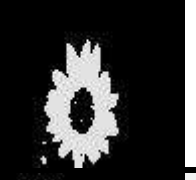
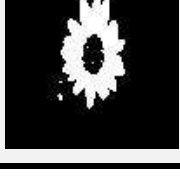
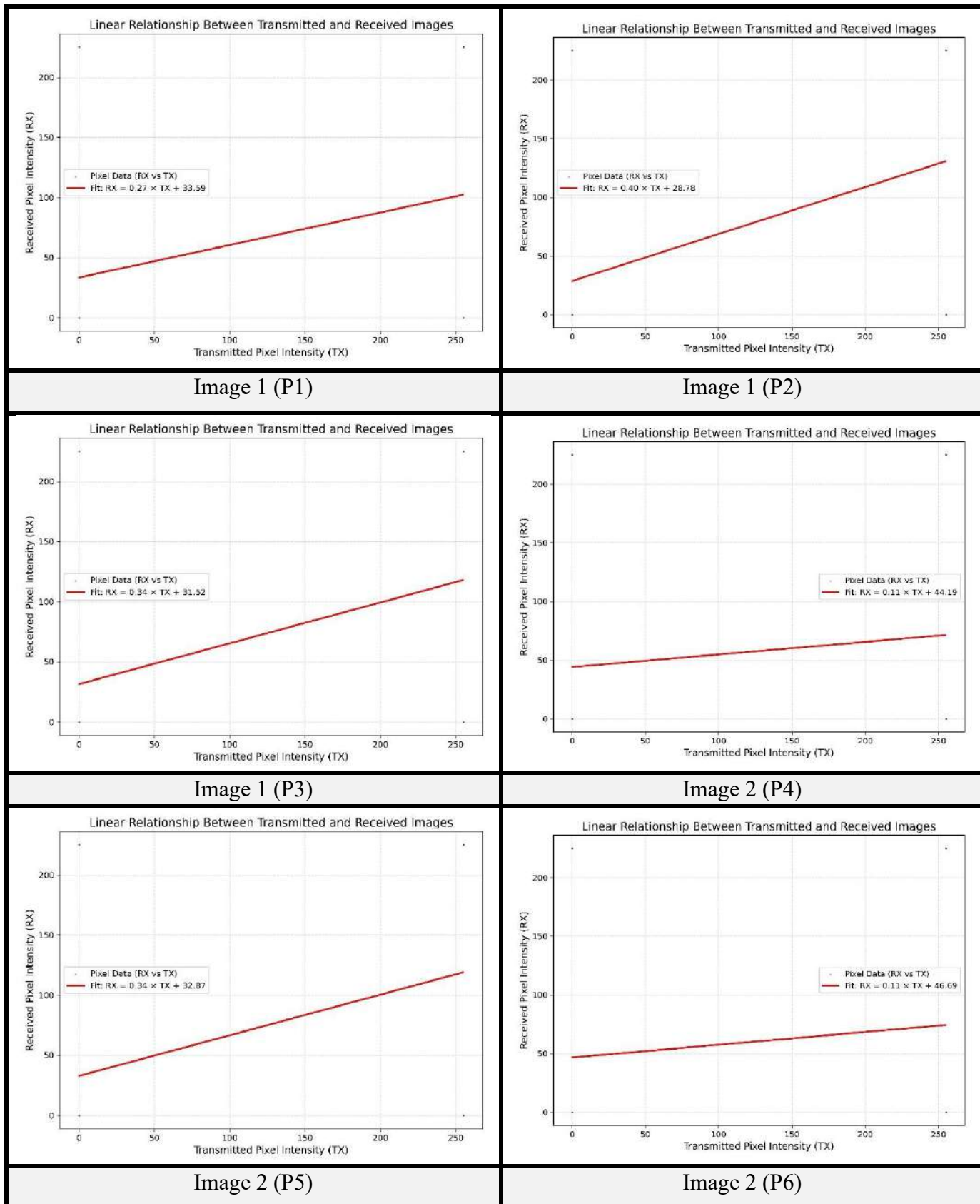
Image 1 (P3)		50			
Image 2 (P4)		30			
Image 2 (P5)		40			
Image 2 (P6)		50			
Image 3 (P7)		30			
Image 3 (P8)		40			
Image 3 (P9)		50			

Table 4.14 Linearity Graph Properties (Single USRP Patch Antenna - FR4 Material)

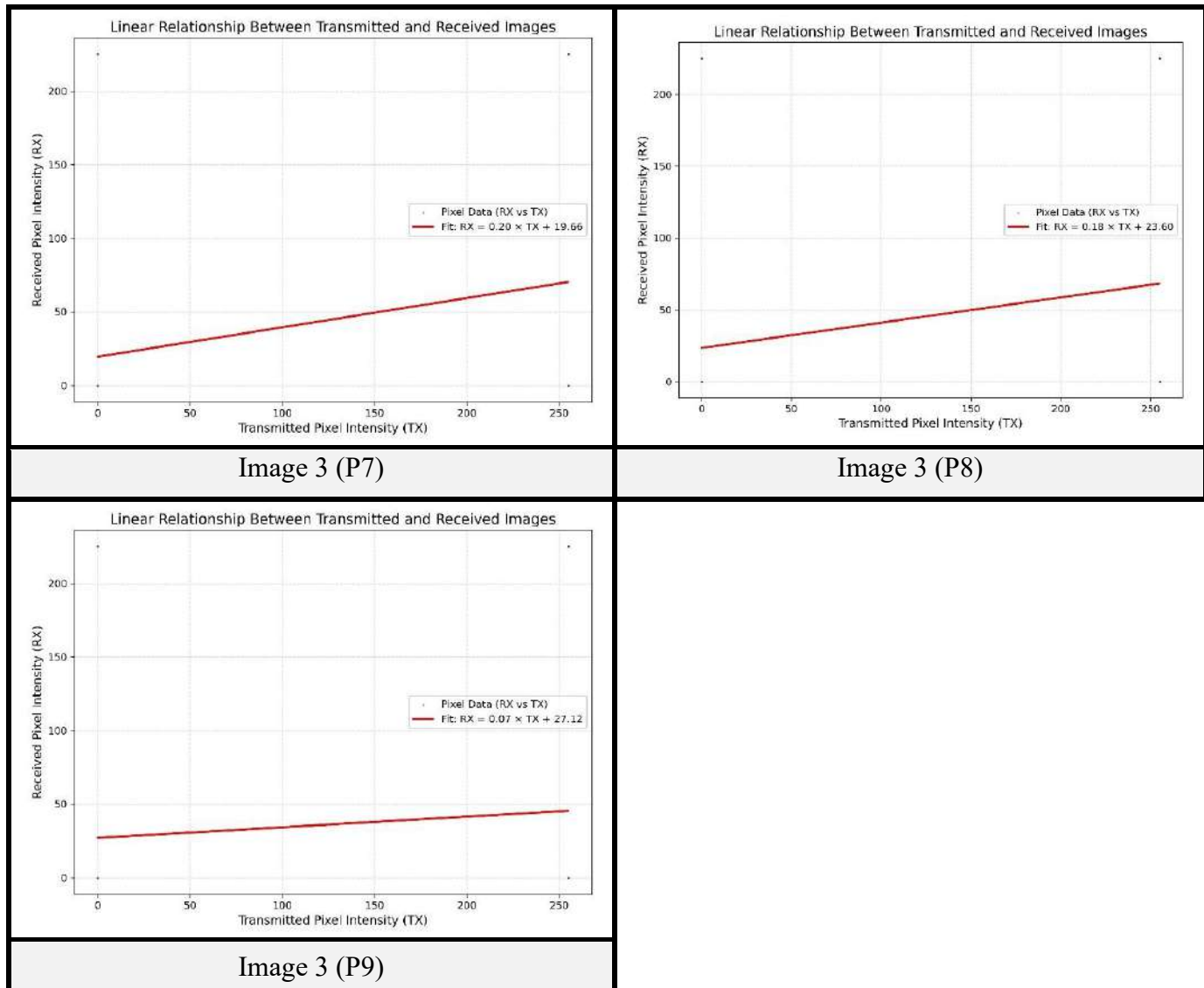


Table 4.15 Quantitative Performance Metrics (Single USRP Patch Antenna - FR4 Material)

Image No.	Set Gain value (dB)	Pearson Correlation Coefficient	RMSE	PSNR (dB)	Normalized Cross-Correlation (NCC)	SSIM	Linear Fit Slope (m)	Linear Fit Intercept (c)
Image 1 (P1)	30	0.310407	6.005439	32.55991	0.310407	0.44415	0.270114	33.59122
Image 1 (P2)	40	0.451115	6.05314	32.49119	0.451115	0.450014	0.40018	28.78415
Image 1 (P3)	50	0.384712	6.063398	32.47648	0.384712	0.419943	0.339452	31.52272

Image 2 (P4)	30	0.12347	6.24648 7	32.2180 9	0.12347	0.37012 6	0.107045	44.18643
Image 2 (P5)	40	0.382863	6.17716 8	32.3150 2	0.382863	0.44872	0.337821	32.86716
Image 2 (P6)	50	0.123279	6.40821 3	31.9960 6	0.123279	0.33435 1	0.108775	46.692
Image 3 (P7)	30	0.237101	4.49044 5	35.0850 2	0.237101	0.63961 9	0.199104	19.65869
Image 3 (P8)	40	0.199208	4.78962 4	34.5247 7	0.199208	0.62627 4	0.175601	23.5956
Image 3 (P9)	50	0.082065	4.88088 1	34.3608 4	0.082065	0.55408	0.07241	27.11811

4.2.2 Two USRPs Experimental Arrangement and Results

This setup used two separate USRP B210 devices, each connected to its own laptop. This created a dedicated transmitting station and a dedicated receiving station. This allowed for more flexibility in where antennas could be placed and how far apart they were. Measurements were taken in various locations both inside and outside the building. The conceptual diagram for this setup is shown in Figure 4.9.



Fig. 4.9 Conceptual Diagram

- **Initial Testing with Dipole Antennas (Line of Sight 195 cm):** To set a baseline for the two-USRP setup, dipole antennas were used on both the sending and receiving sides. The transmitting and receiving USRPs were placed in the laboratory with a direct line-of-sight (LOS) distance of 195 cm between them. For this initial test, Image 1 was sent with an IQ sampling rate of 250k S/sec, Image 2 with 500k S/sec, and Image 3 with 750k S/sec. This confirmed the basic transmission capability of the two-USRP system. The on-site experimental setup is shown in Figure 4.10. Visual results are in Table 4.16. Linearity graph properties are provided in Table 4.17. Quantitative performance metrics are in Table 4.18.

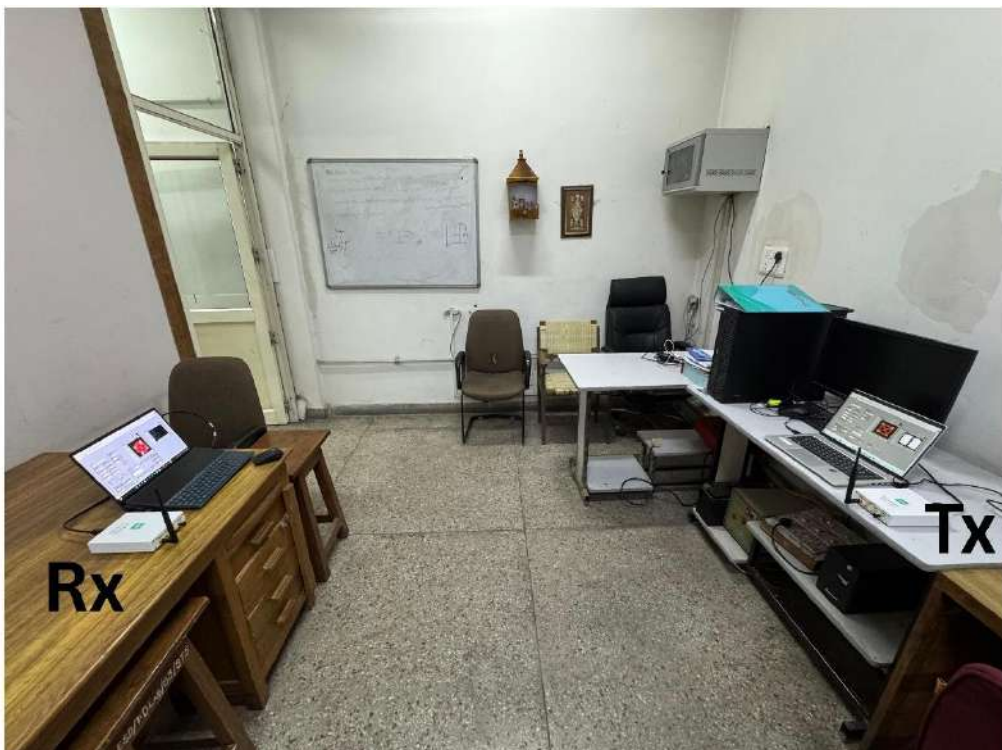


Fig. 4.10 On-site Experimental Setup

Table 4.16 Visual Experiment Results (Two USRPs Initial Testing with Dipole Antennas)

Image No.	Transmitted Image	Set Gain Value (dB)	Tx Front Panel	Rx Front Panel	Received Image
Image 1 (D1)		30			

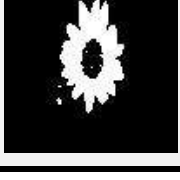
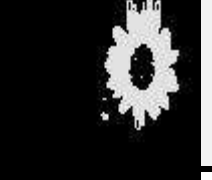
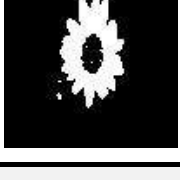
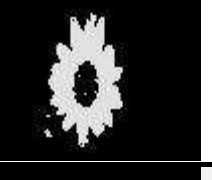
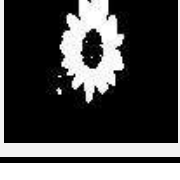
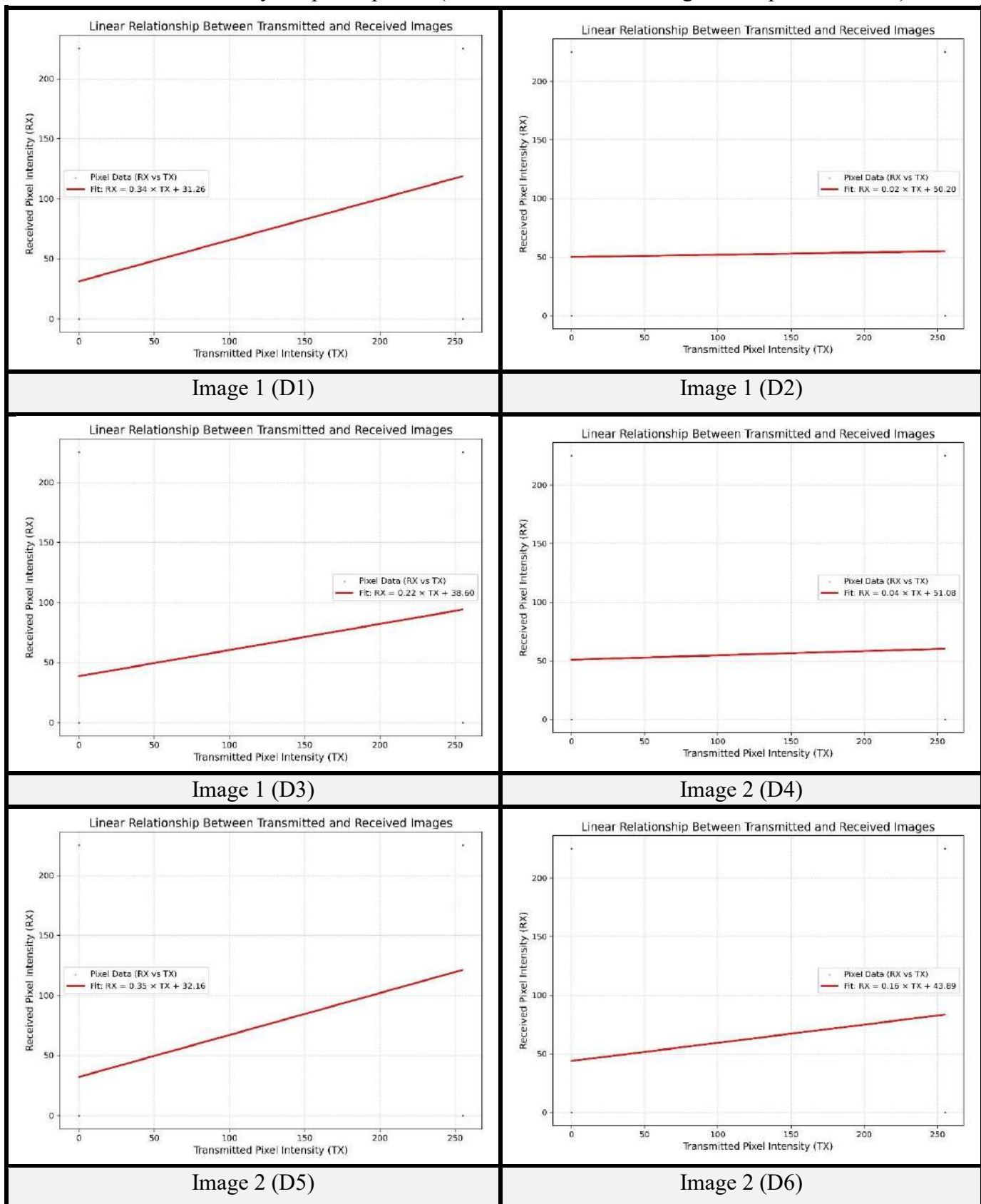
Image 1 (D2)		40	 	
Image 1 (D3)		50	 	
Image 2 (D4)		30	 	
Image 2 (D5)		40	 	
Image 2 (D6)		50	 	
Image 3 (D7)		30	 	
Image 3 (D8)		40	 	
Image 3 (D9)		50	 	

Table 4.17 Linearity Graph Properties (Two USRPs Initial Testing with Dipole Antennas)

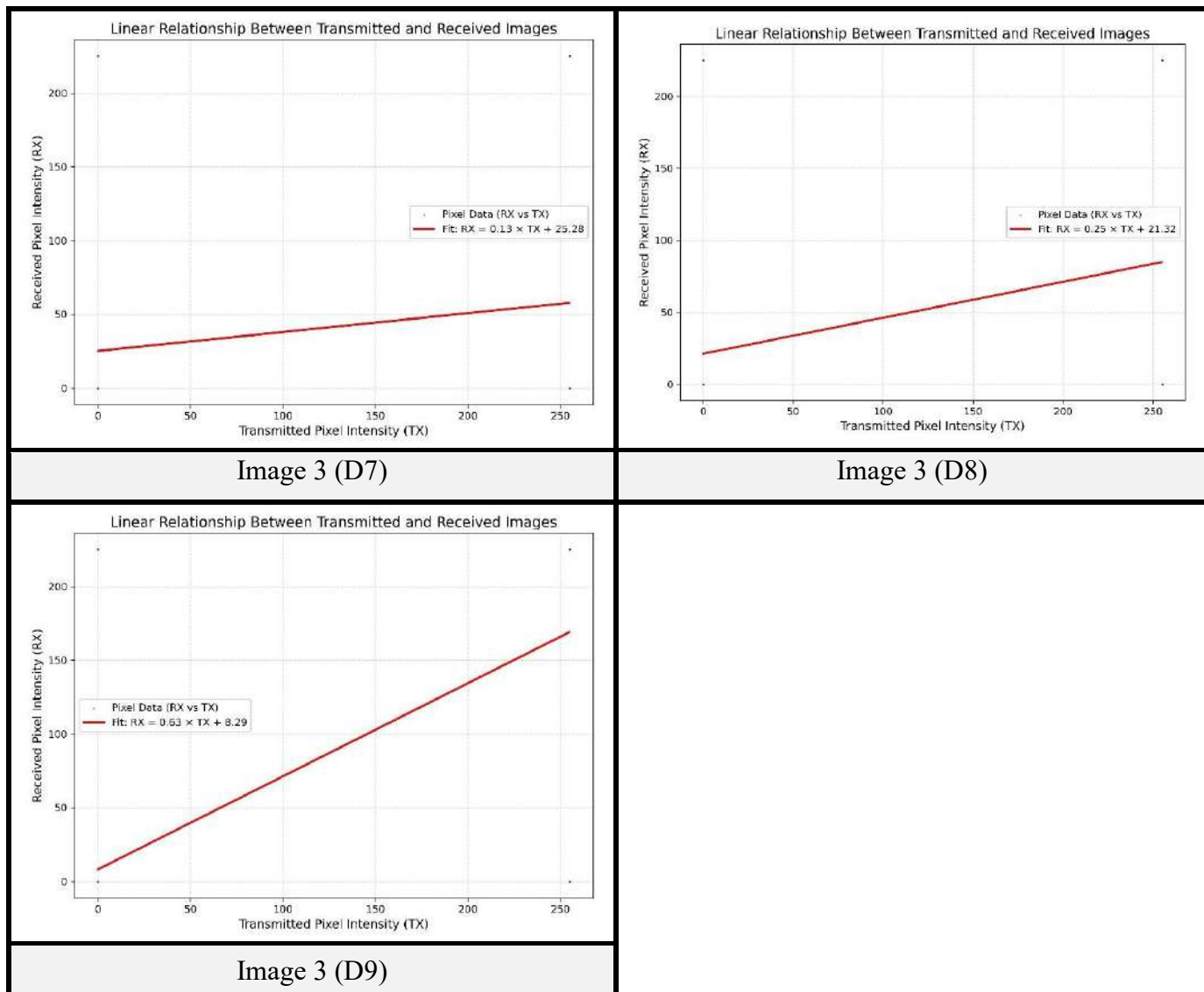


Table 4.18 Quantitative Performance Metrics (Two USRPs with Dipole Antennas)

Image No.	Set Gain value (dB)	Pearson Correlation Coefficient	RMSE	PSNR (dB)	Normalized Cross-Correlation (NCC)	SSIM	Linear Fit Slope (m)	Linear Fit Intercept (c)
Image 1 (D1)	30	0.389072	6.056633	32.48618	0.389072	0.427252	0.343193	31.26052
Image 1 (D2)	40	0.02151	6.385789	32.02651	0.02151	0.319342	0.018988	50.19746
Image 1 (D3)	50	0.246529	6.186388	32.30206	0.246529	0.392228	0.217525	38.60223

Image 2 (D4)	30	0.040809	6.47989 2	31.8994 5	0.040809	0.31376 6	0.036008	51.08411
Image 2 (D5)	40	0.396147	6.16511 2	32.3319 8	0.396147	0.48444 7	0.349541	32.1597
Image 2 (D6)	50	0.17586	6.36209 1	32.0588 1	0.17586	0.34959 6	0.15517	43.89165
Image 3 (D7)	30	0.145027	4.83693 1	34.4394 1	0.145027	0.57600 7	0.128006	25.27915
Image 3 (D8)	40	0.282475	4.74476 6	34.6065 1	0.282475	0.63055 9	0.249725	21.31633
Image 3 (D9)	50	0.716269	4.386	35.2894 3	0.716269	0.73644 4	0.630774	8.288247

- **Experiment 1 [Fixed DNI Tx, Varied Rx Antennas (LOS 195 cm, IQ 250k)]:** This experiment evaluated the impact of different receiving antennas on image quality. The Metamaterial Double Negative Index (DNI) antenna stayed as the transmitting antenna. The USRPs were kept at a fixed line-of-sight distance of 195 cm within the laboratory. The IQ Sampling Rate was fixed at 250k S/sec for all transmissions, and only the gain was changed (30 dB, 40 dB, 50 dB). The conceptual diagram for this setup is shown in Figure 4.11.

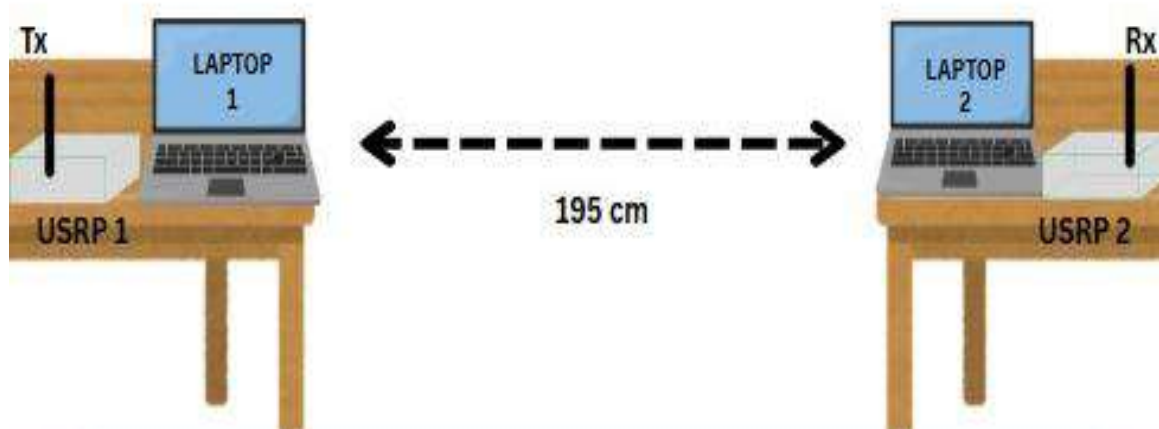


Fig. 4.11 Conceptual Diagram

- **For Metamaterial Epsilon Near Zero (ENZ) Receive Antenna:** The on-site experimental setup for this antenna is shown in Figure 4.12. Visual results are presented in Table 4.19. Linearity graph properties are provided in Table 4.20. Quantitative performance metrics are in Table 4.21.

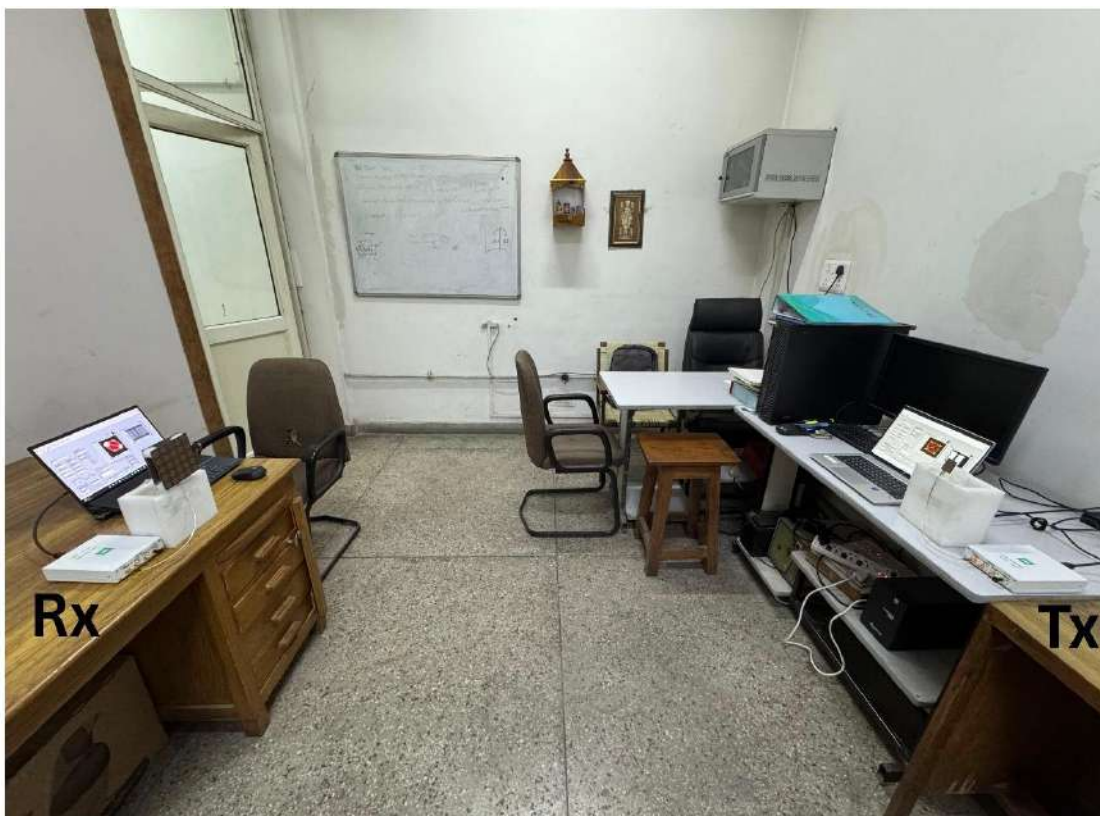


Fig. 4.12 On-site Experimental Setup

Table 4.19 Visual Experiment Results (Two USRPs ENZ Receive Antenna - LOS 195 cm)

Image No.	Transmitted Image	Set Gain Value (dB)	Tx Front Panel	Rx Front Panel	Received Image
Image 1 (E1)		30			
Image 1 (E2)		40			

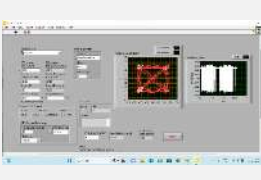
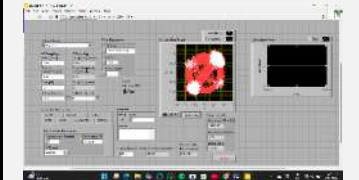
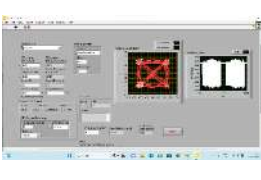
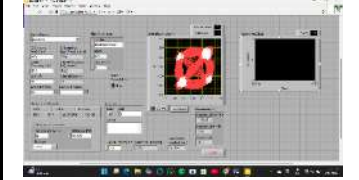
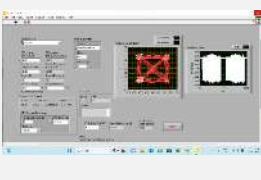
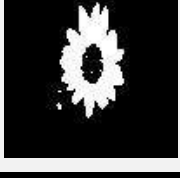
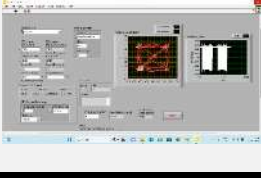
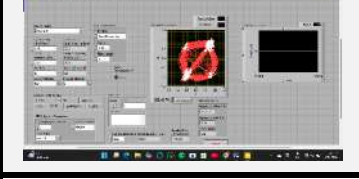
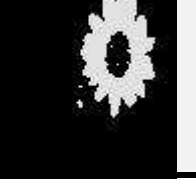
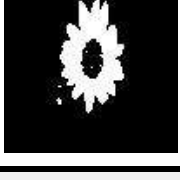
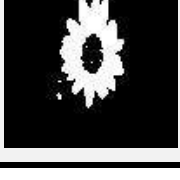
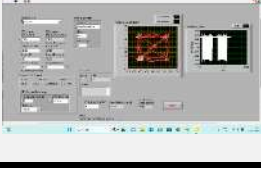
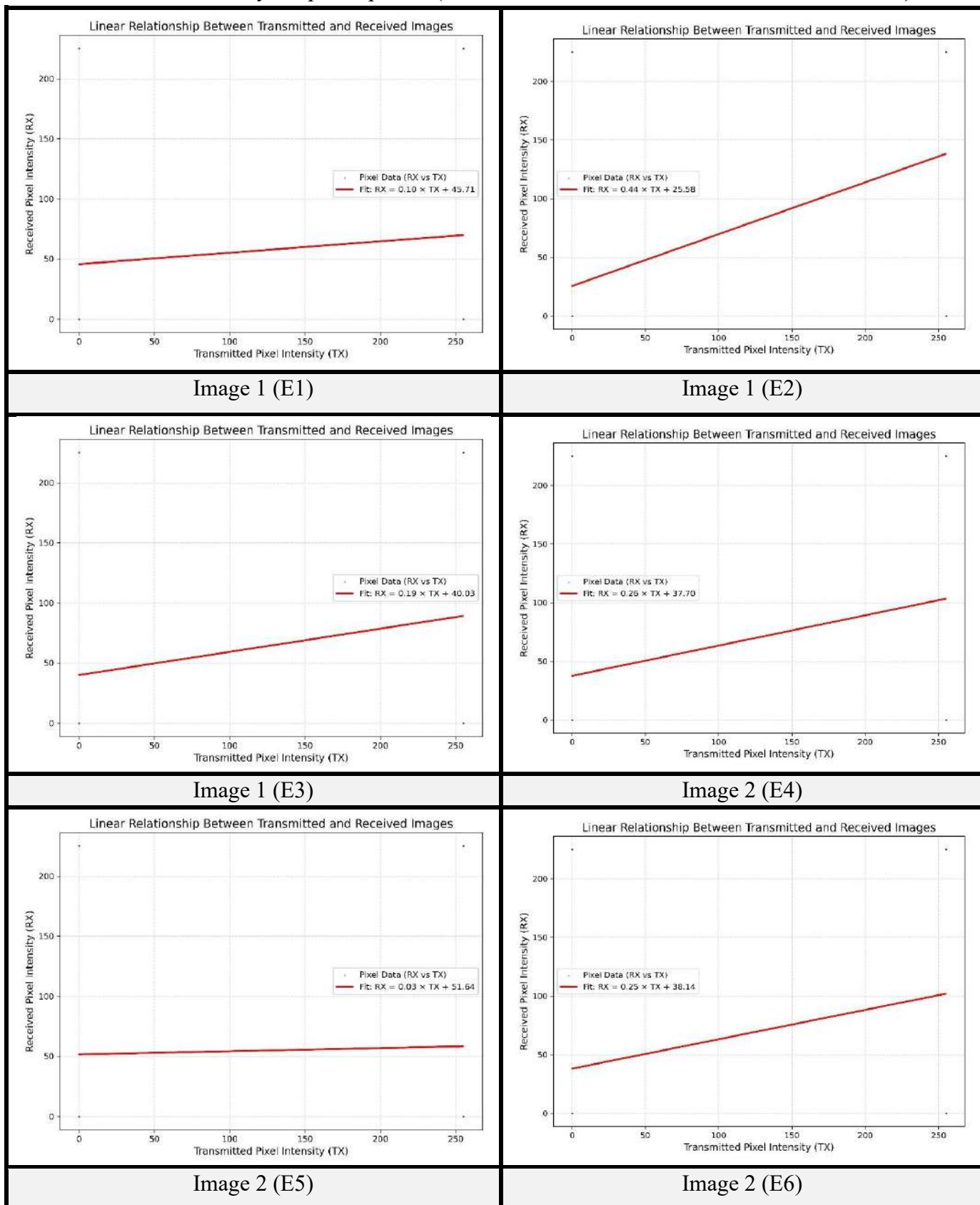
Image 1 (E3)		50			
Image 2 (E4)		30			
Image 2 (E5)		40			
Image 2 (E6)		50			
Image 3 (E7)		30			
Image 3 (E8)		40			
Image 3 (E9)		50			

Table 4.20 Linearity Graph Properties (Two USRPs ENZ Receive Antenna - LOS 195 cm)

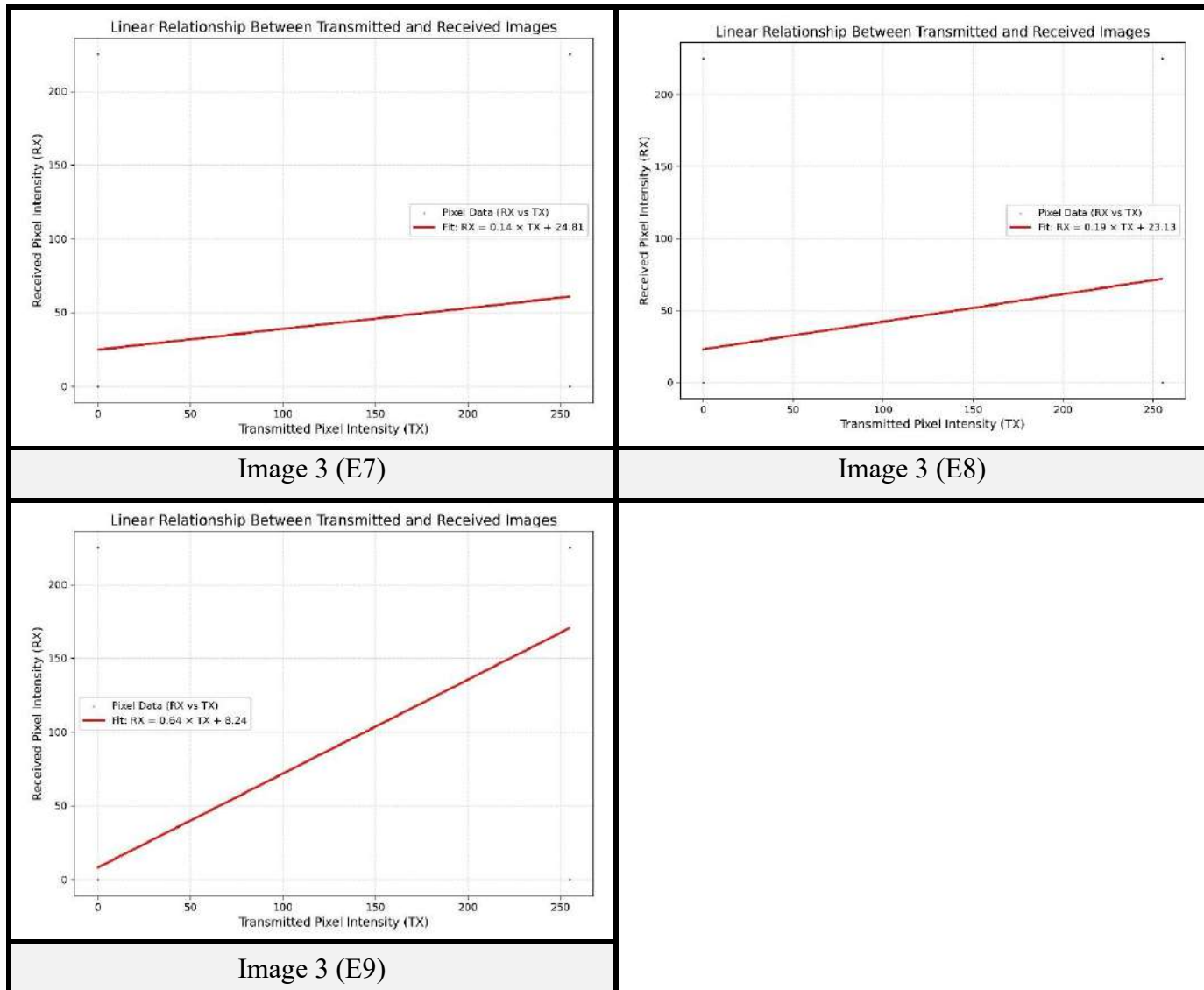


Table 4.21 Quantitative Performance Metrics (Two USRPs ENZ Antenna - LOS 195 cm)

Image No.	Set Gain value (dB)	Pearson Correlation Coefficient	RMSE	PSNR (dB)	Normalized Cross-Correlation (NCC)	SSIM	Linear Fit Slope (m)	Linear Fit Intercept (c)
Image 1 (E1)	30	0.107776	6.30747 ₂	32.1337	0.107776	0.35088 ₄	0.095097	45.71086
Image 1 (E2)	40	0.500719	5.95818 ₈	32.6285 ₂	0.500719	0.46235 ₄	0.44181	25.57944
Image 1 (E3)	50	0.218664	6.21089 ₄	32.2677 ₂	0.218664	0.38189 ₈	0.192939	40.02978

Image 2 (E4)	30	0.292092	6.25893	32.2008	0.292092	0.400129	0.257728	37.70143
Image 2 (E5)	40	0.030293	6.488975	31.88728	0.030293	0.308393	0.026729	51.64418
Image 2 (E6)	50	0.283789	6.266355	32.1905	0.283789	0.428931	0.250402	38.14359
Image 3 (E7)	30	0.160093	4.824023	34.46262	0.160093	0.584549	0.141259	24.81294
Image 3 (E8)	40	0.217081	4.782071	34.53848	0.217081	0.613233	0.191542	23.12939
Image 3 (E9)	50	0.7212	4.393541	35.27451	0.7212	0.742239	0.636353	8.236445

- **For Slot Cut Patch Antenna (Rogers RO3003):** The on-site experimental setup for this antenna is shown in Figure 4.13. Visual results are presented in Table 4.22. Linearity graph properties are provided in Table 4.23. Quantitative performance metrics are in Table 4.24.



Fig. 4.13 On-site Experimental Setup

Table 4.22 Visual Experiment Results (Two USRPs Slot Cut Patch Antenna - LOS 195 cm)

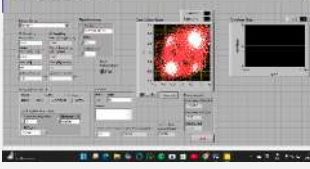
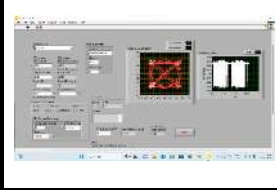
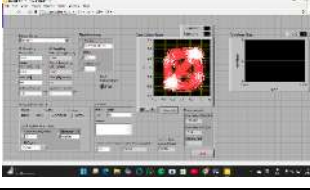
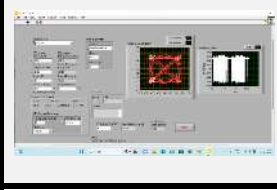
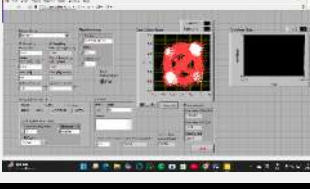
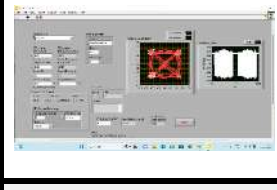
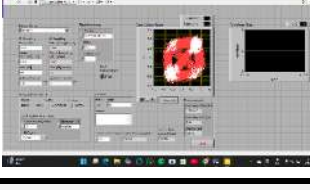
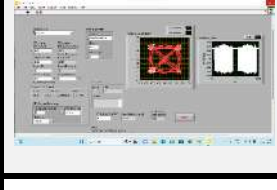
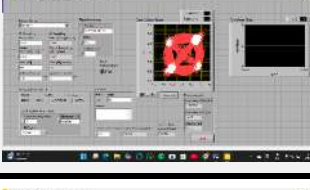
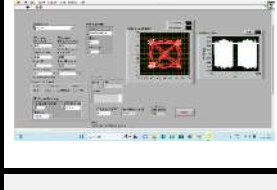
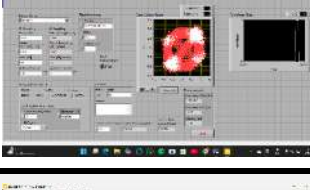
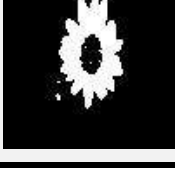
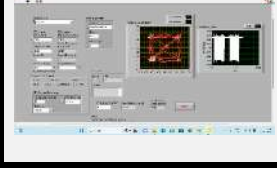
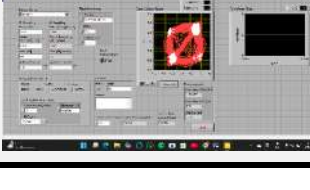
Image No.	Transmitted Image	Set Gain Value (dB)	Tx Front Panel	Rx Front Panel	Received Image
Image 1 (S1)		30			
Image 1 (S2)		40			
Image 1 (S3)		50			
Image 2 (S4)		30			
Image 2 (S5)		40			
Image 2 (S6)		50			
Image 3 (S7)		30			

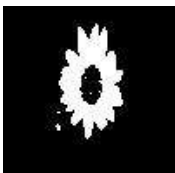
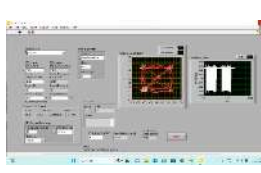
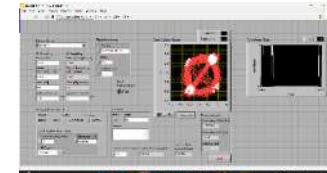
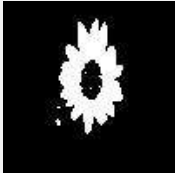
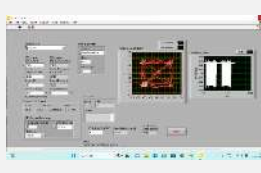
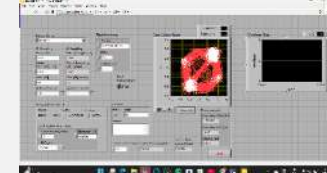
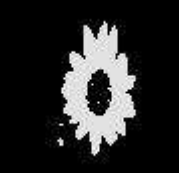
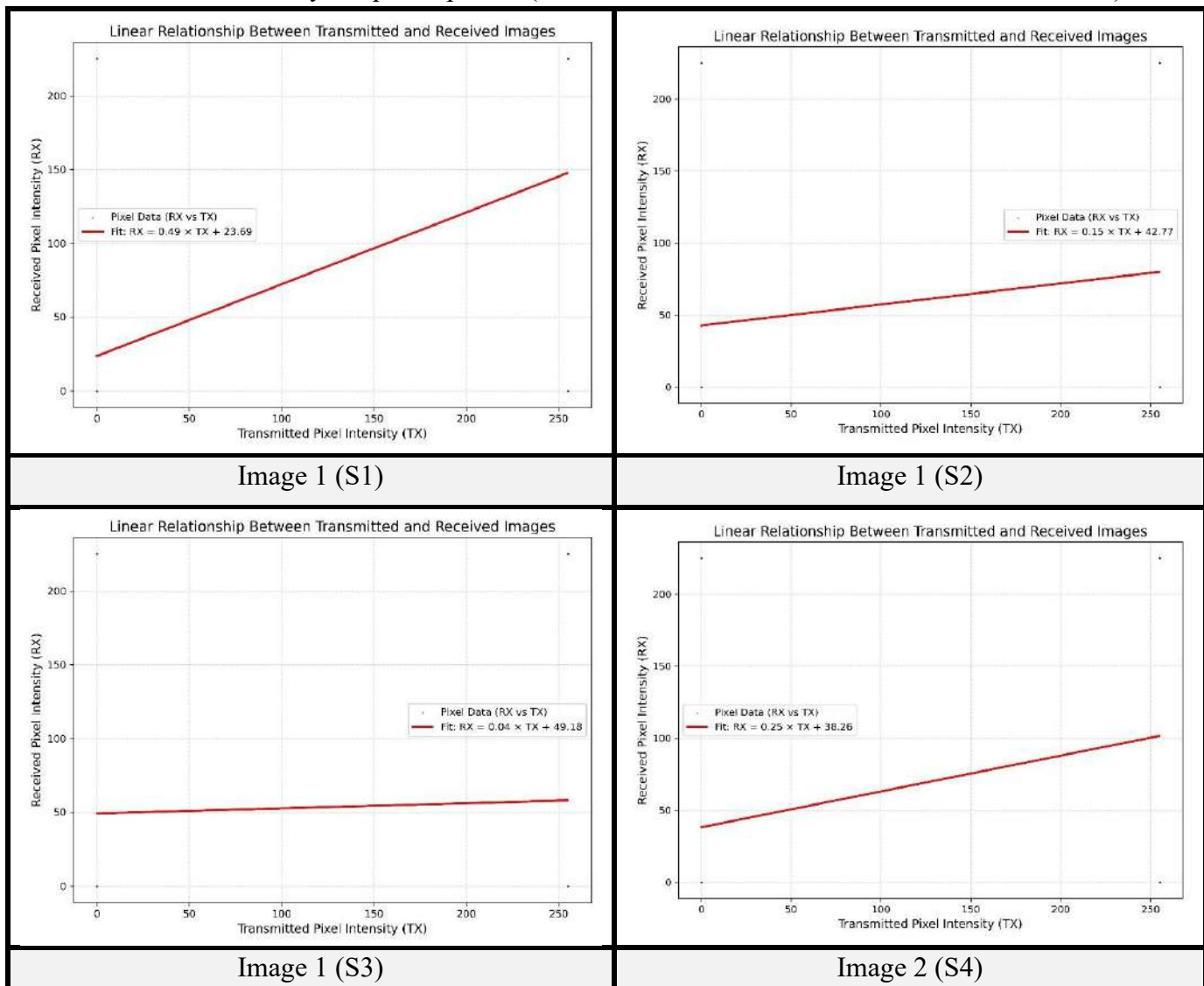
Image 3 (S8)		40			
Image 3 (S9)		50			

Table 4.23 Linearity Graph Properties (Two USRPs Slot Cut Patch Antenna - LOS 195 cm)



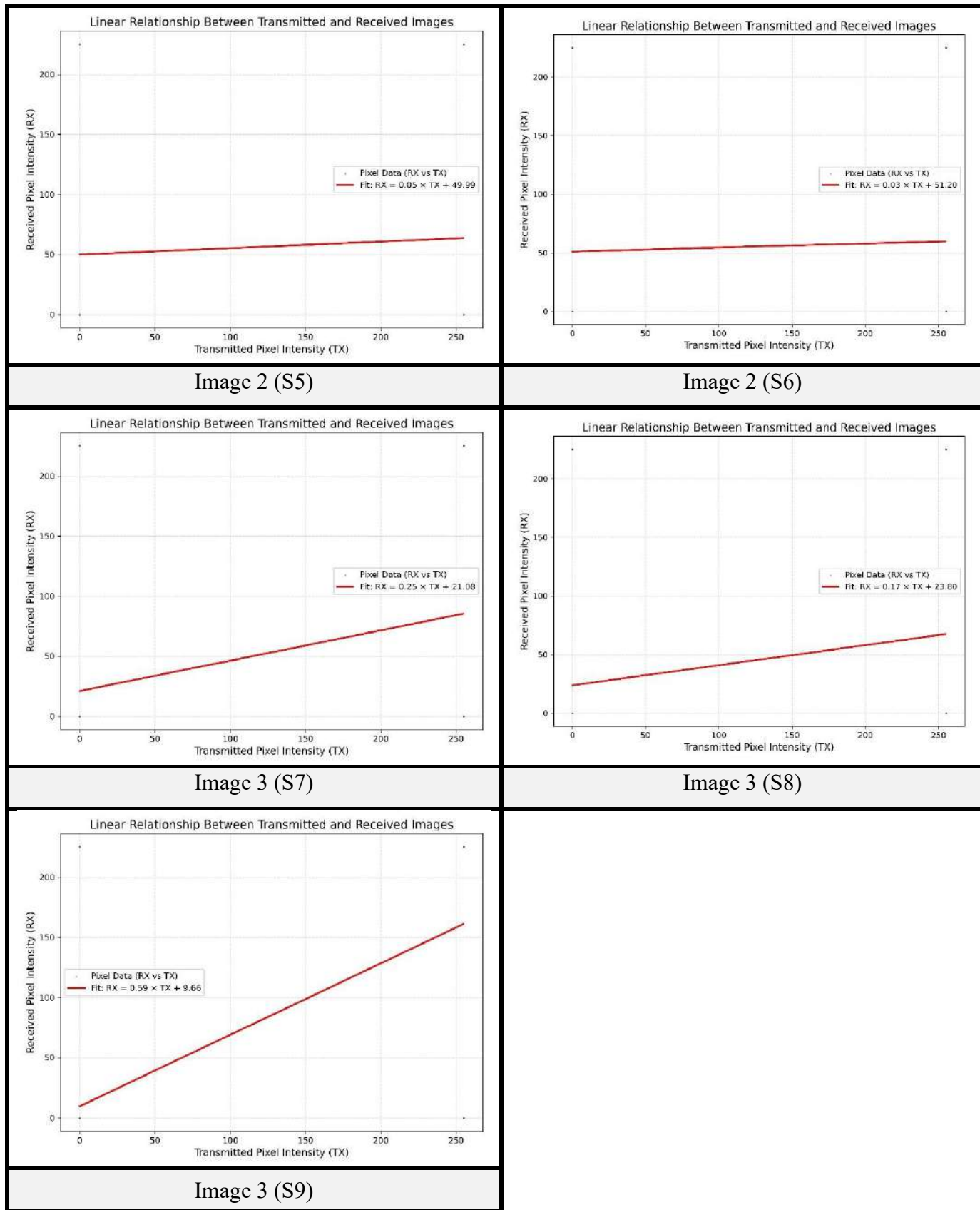


Table 4.24 Quantitative Performance Metrics (Two USRPs Slot Cut Patch - LOS 195 cm)

Image No.	Set Gain value (dB)	Pearson Correlation Coefficient	RMSE	PSNR (dB)	Normalized Cross-Correlation (NCC)	SSIM	Linear Fit Slope (m)	Linear Fit Intercept (c)
Image 1 (S1)	30	0.548683	5.958448	32.62814	0.548683	0.400223	0.486437	23.68574
Image 1 (S2)	40	0.165624	6.258682	32.20115	0.165624	0.363542	0.146161	42.76835
Image 1 (S3)	50	0.040106	6.365689	32.05389	0.040106	0.329819	0.035387	49.17778
Image 2 (S4)	30	0.281575	6.268333	32.18776	0.281575	0.419837	0.248449	38.2615
Image 2 (S5)	40	0.061288	6.462167	31.92324	0.061288	0.31578	0.054078	49.99345
Image 2 (S6)	50	0.038595	6.481805	31.89688	0.038595	0.307261	0.034055	51.20202
Image 3 (S7)	30	0.286342	4.730581	34.63251	0.286342	0.633737	0.252655	21.08323
Image 3 (S8)	40	0.194286	4.798896	34.50798	0.194286	0.596068	0.171429	23.80281
Image 3 (S9)	50	0.67298	4.432178	35.19846	0.67298	0.730673	0.593806	9.660988

- **For Parasitic Patch Antenna (Rogers RO3003):** The on-site experimental setup for this antenna is shown in Figure 4.14. Visual results are presented in Table 4.25. Linearity graph properties are provided in Table 4.26. Quantitative performance metrics are in Table 4.27.



Fig. 4.14 On-site Experimental Setup

Table 4.25 Visual Experiment Results (Two USRPs Parasitic Patch Antenna - LOS 195 cm)

Image No.	Transmitted Image	Set Gain Value (dB)	Tx Front Panel	Rx Front Panel	Received Image
Image 1 (PP1)		30			
Image 1 (PP2)		40			

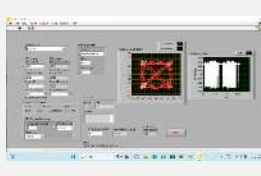
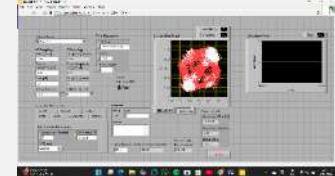
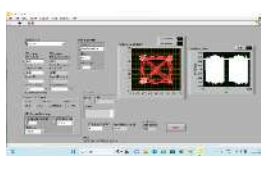
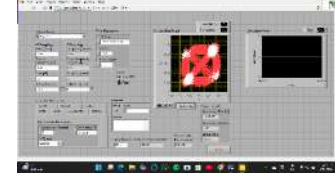
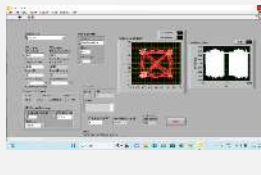
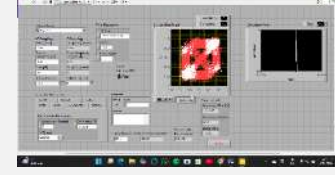
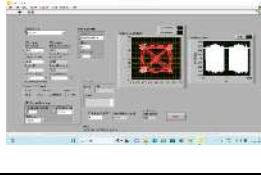
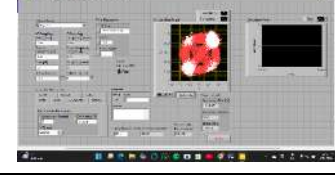
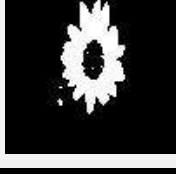
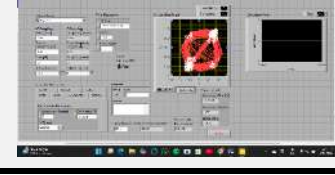
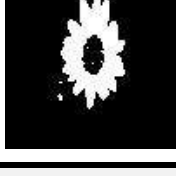
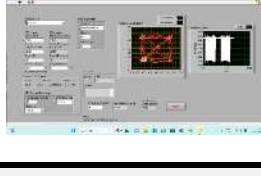
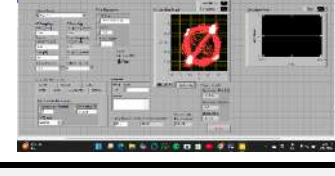
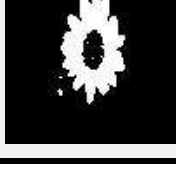
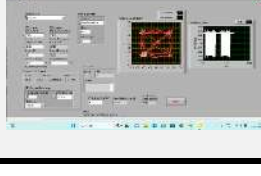
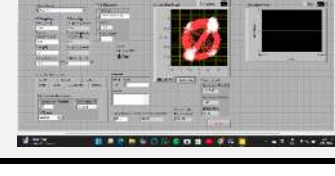
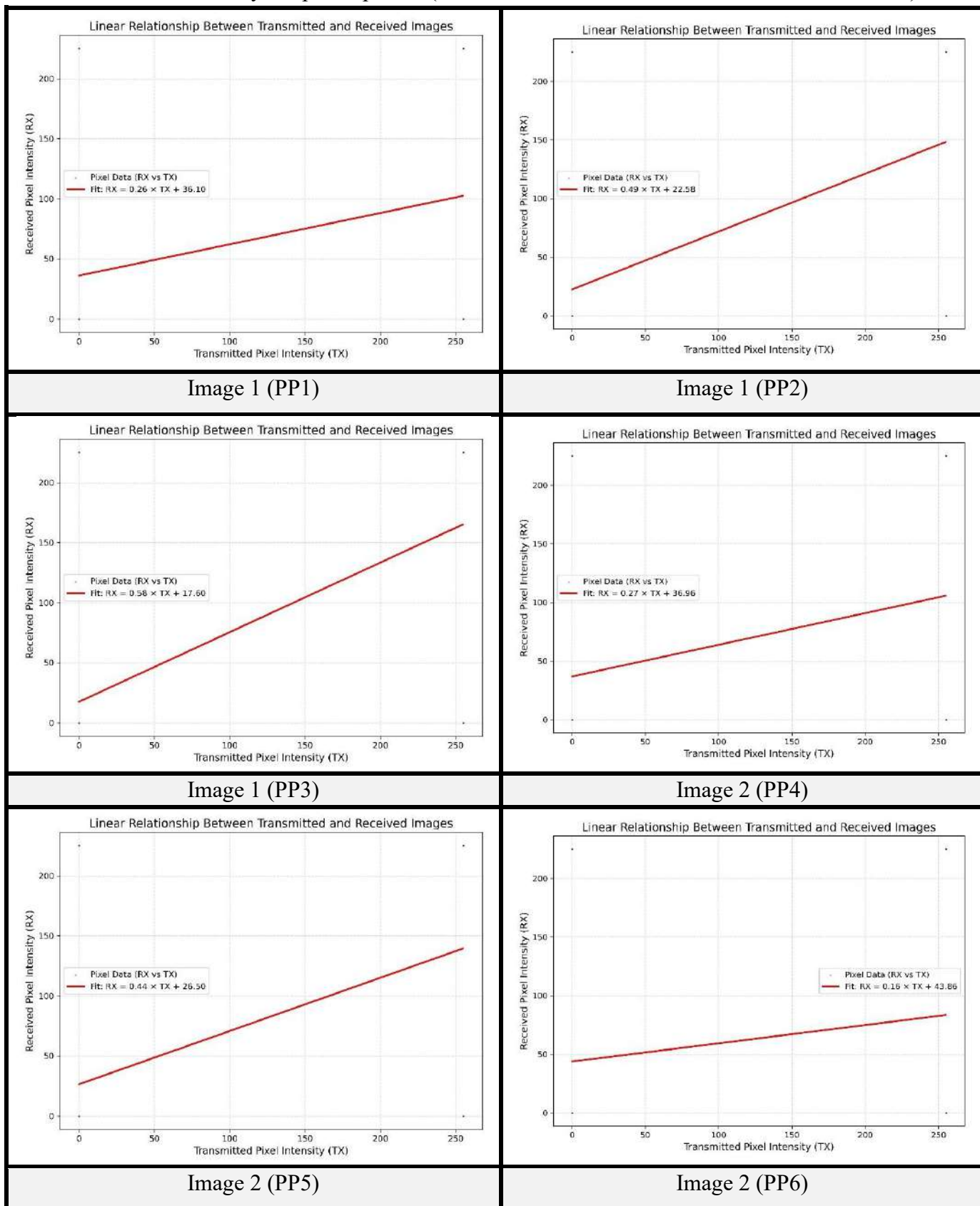
Image 1 (PP3)		50			
Image 2 (PP4)		30			
Image 2 (PP5)		40			
Image 2 (PP6)		50			
Image 3 (PP7)		30			
Image 3 (PP8)		40			
Image 3 (PP9)		50			

Table 4.26 Linearity Graph Properties (Two USRPs Parasitic Patch Antenna - LOS 195 cm)

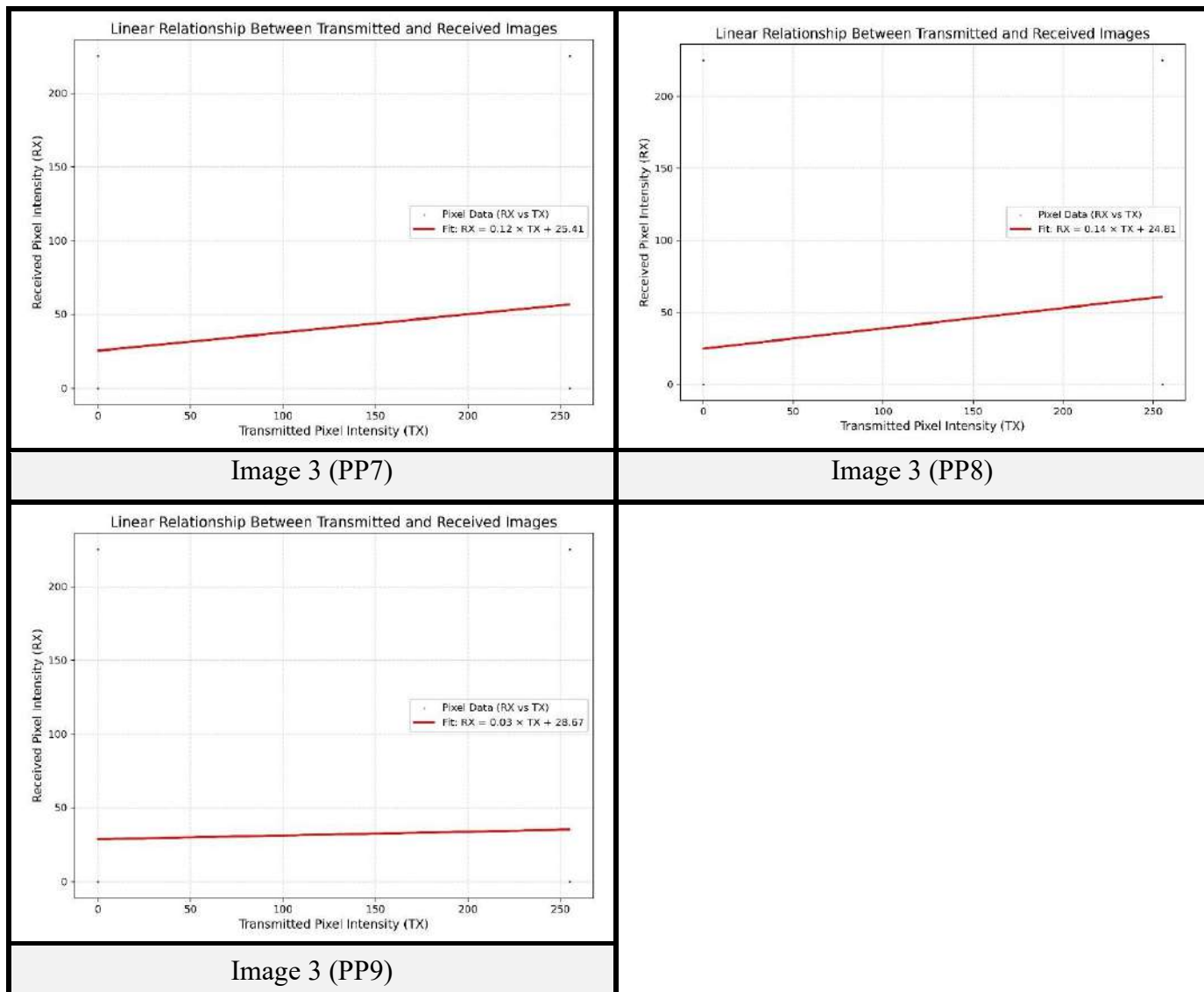


Table 4.27 Quantitative Performance Metrics (Parasitic Patch Antenna - LOS 195 cm)

Image No.	Set Gain value (dB)	Pearson Correlation Coefficient	RMSE	PSNR (dB)	Normalized Cross-Correlation (NCC)	SSIM	Linear Fit Slope (m)	Linear Fit Intercept (c)
Image 1 (PP1)	30	0.295433	6.143143	32.36299	0.295433	0.399028	0.260676	36.09672
Image 1 (PP2)	40	0.55929	5.904354	32.70736	0.55929	0.501369	0.493491	22.57866
Image 1 (PP3)	50	0.656531	5.81388	32.84148	0.656531	0.554231	0.579292	17.59679

Image 2 (PP4)	30	0.305929	6.246535	32.21802	0.305929	0.425503	0.269937	36.9645
Image 2 (PP5)	40	0.502416	6.0678	32.47018	0.502416	0.506145	0.443308	26.50007
Image 2 (PP6)	50	0.176413	6.361604	32.05947	0.176413	0.34982	0.155659	43.86218
Image 3 (PP7)	30	0.139929	4.838781	34.43608	0.139929	0.570292	0.123466	25.40866
Image 3 (PP8)	40	0.160093	4.824023	34.46262	0.160093	0.583519	0.141259	24.81294
Image 3 (PP9)	50	0.029461	4.918841	34.29355	0.029461	0.539728	0.025995	28.67215

- **For Patch Antenna (FR4 Material):** The on-site experimental setup for this antenna is shown in Figure 4.15. Visual results are presented in Table 4.28. Linearity graph properties are provided in Table 4.29. Quantitative performance metrics are in Table 4.30.



Fig. 4.15 On-site Experimental Setup

Table 4.28 Visual Experiment Results (Two USRPs Patch Antenna - LOS 195 cm)

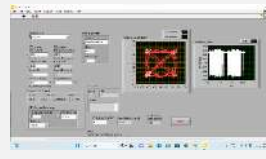
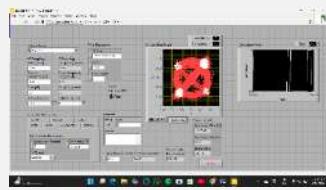
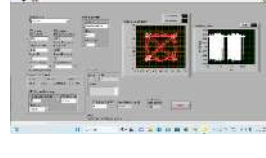
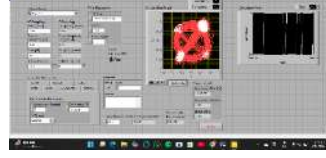
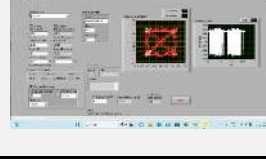
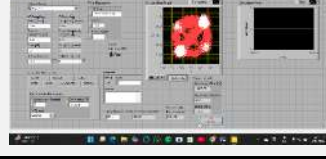
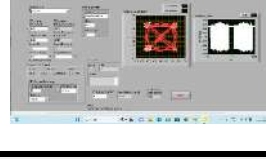
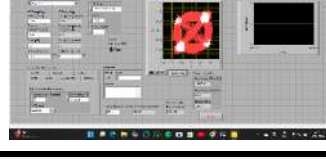
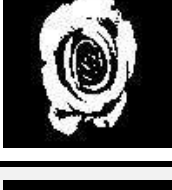
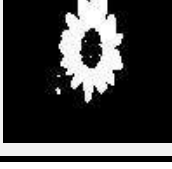
Image No.	Transmitted Image	Set Gain Value (dB)	Tx Front Panel	Rx Front Panel	Received Image
Image 1 (P1)		30			
Image 1 (P2)		40			
Image 1 (P3)		50			
Image 2 (P4)		30			
Image 2 (P5)		40			
Image 2 (P6)		50			
Image 3 (P7)		30			

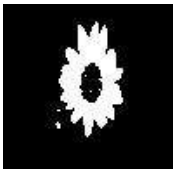
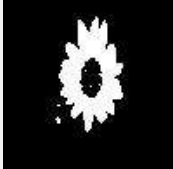
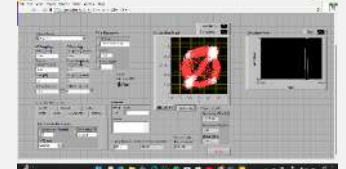
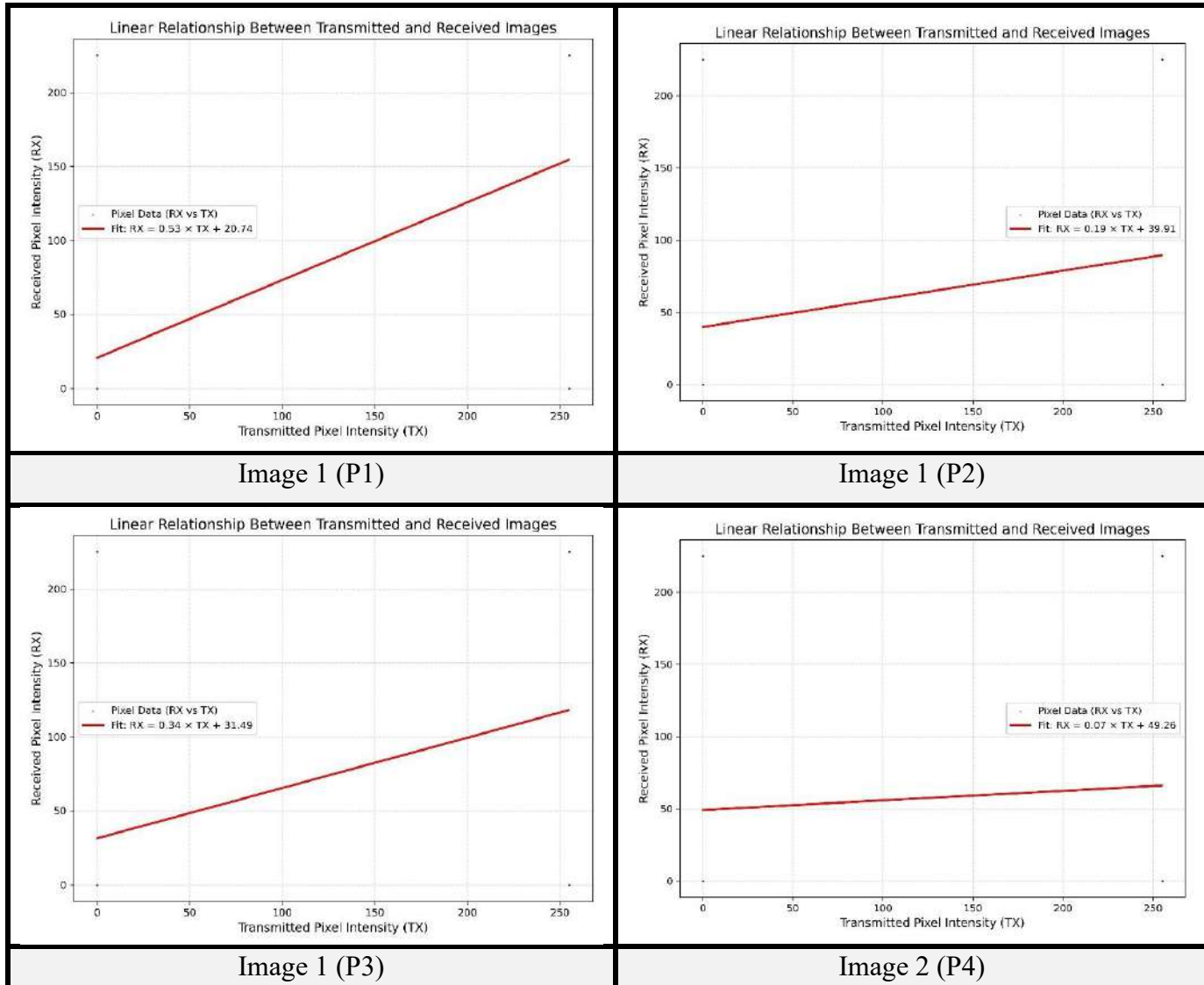
Image 3 (P8)		40			
Image 3 (P9)		50			

Table 4.29 Linearity Graph Properties (Two USRPs Patch Antenna - LOS 195 cm)



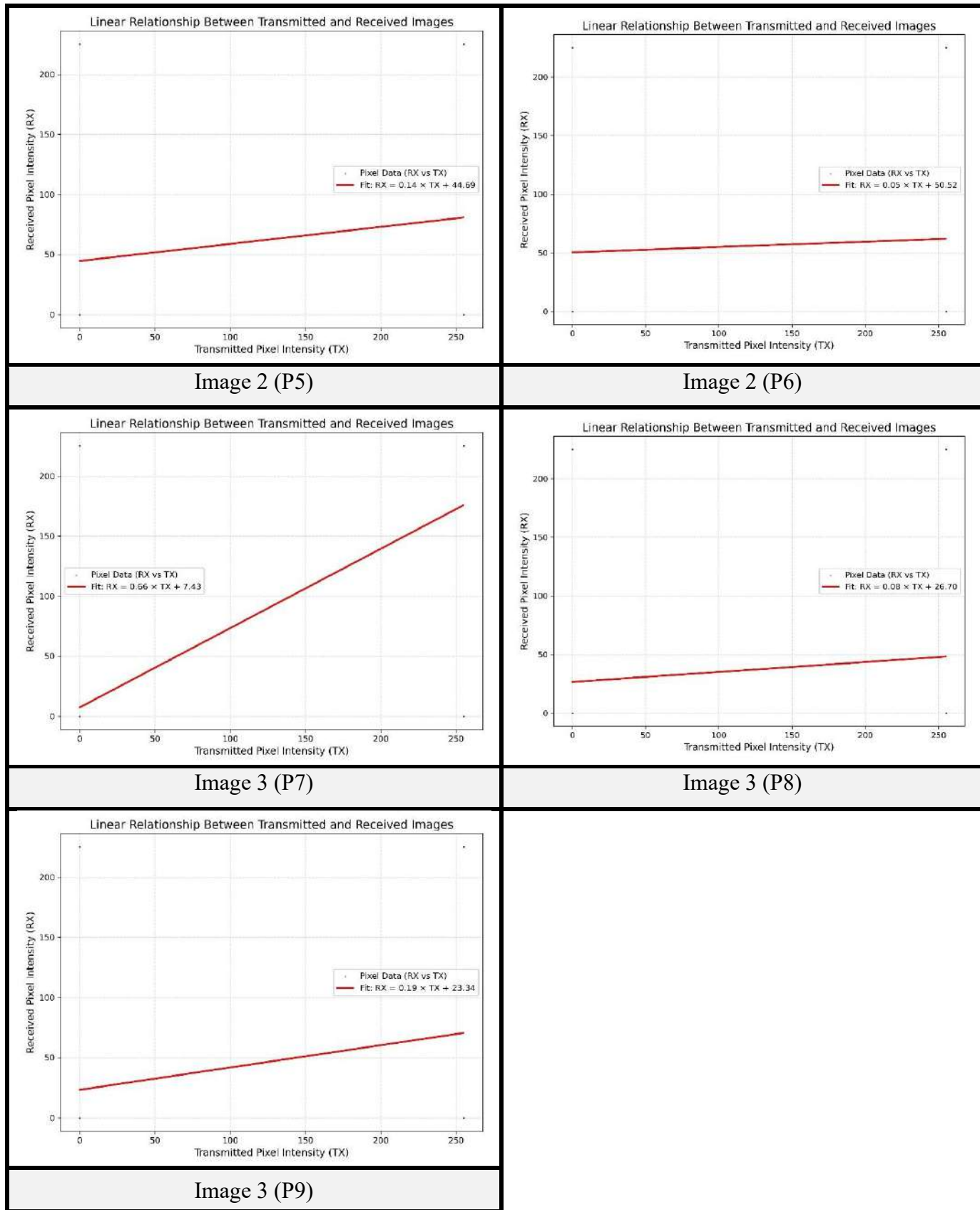


Table 4.30 Quantitative Performance Metrics (Two USRPs Patch Antenna - LOS 195 cm)

Image No.	Set Gain value (dB)	Pearson Correlation Coefficient	RMSE	PSNR (dB)	Normalized Cross-Correlation (NCC)	SSIM	Linear Fit Slope (m)	Linear Fit Intercept (c)
Image 1 (P1)	30	0.595116	5.87118 4	32.756 29	0.595116	0.5123 32	0.525102	20.74323
Image 1 (P2)	40	0.220939	6.20889 7	32.270 51	0.220939	0.3848 48	0.194946	39.91325
Image 1 (P3)	50	0.385281	6.06288 7	32.477 21	0.385281	0.4243 47	0.339954	31.49359
Image 2 (P4)	30	0.075125	6.45016 3	31.939 39	0.075125	0.3090 29	0.066287	49.25652
Image 2 (P5)	40	0.160916	6.37523 3	32.040 88	0.160916	0.3675 06	0.141984	44.68754
Image 2 (P6)	50	0.051325	6.47079 6	31.911 65	0.051325	0.3167 97	0.045287	50.52404
Image 3 (P7)	30	0.748379	4.37161 3	35.317 97	0.748379	0.7539 94	0.660334	7.433521
Image 3 (P8)	40	0.096092	4.87070 8	34.378 96	0.096092	0.5689 12	0.084787	26.7037
Image 3 (P9)	50	0.210067	4.78725 4	34.529 07	0.210067	0.6149 84	0.185353	23.33659

➤ **Experiment 2 [Fixed DNI Tx, Varied Rx Antennas (Slant LOS 240 cm Inside Lab)]:**

This experiment looked into how image transfer performed at a slanted line-of-sight distance of 140 cm from the transmitter, still within the laboratory. The Metamaterial Double Negative Index (DNI) antenna remained fixed as the transmitting antenna. The IQ Sampling Rate was fixed at 250k S/sec, and only the gain was changed (30 dB, 40 dB, 50 dB). The conceptual diagram for this setup is shown in Figure 4.16.

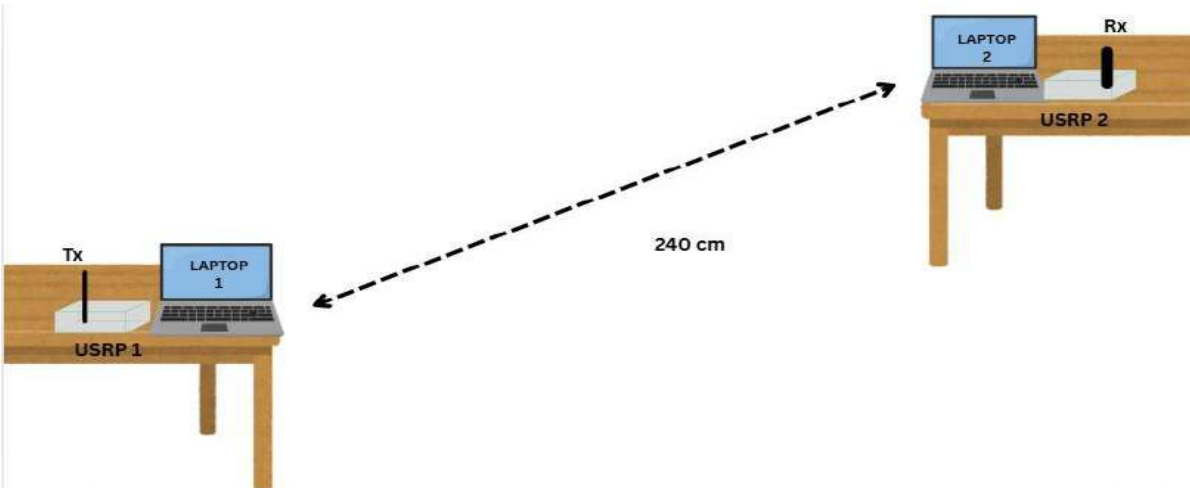


Fig. 4.16 Conceptual Diagram

- **For Metamaterial Epsilon Near Zero (ENZ) Receive Antenna:** The on-site experimental setup for this antenna is shown in Figure 4.17. Visual results are presented in Table 4.31. Linearity graph properties are provided in Table 4.32. Quantitative performance metrics are in Table 4.33.



Fig. 4.17 On-site Experimental Setup

Table 4.31 Visual Experiment Results (Two USRPs ENZ Antenna - Slant LOS 240 cm)

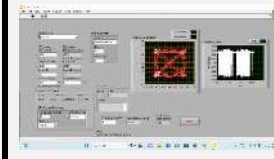
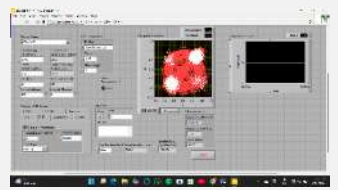
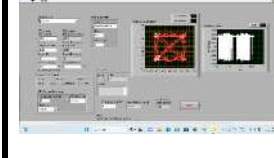
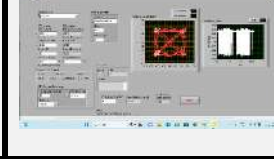
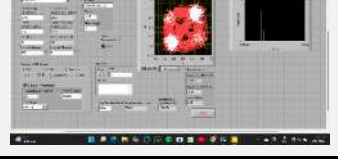
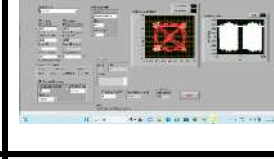
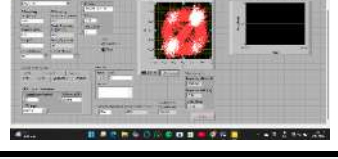
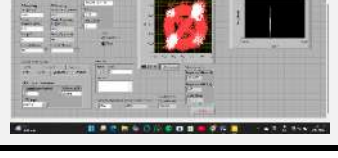
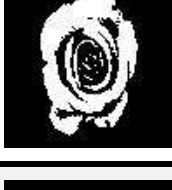
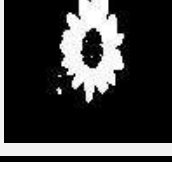
Image No.	Transmitted Image	Set Gain Value (dB)	Tx Front Panel	Rx Front Panel	Received Image
Image 1 (E1)		30			
Image 1 (E2)		40			
Image 1 (E3)		50			
Image 2 (E4)		30			
Image 2 (E5)		40			
Image 2 (E6)		50			
Image 3 (E7)		30			

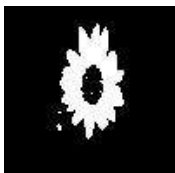
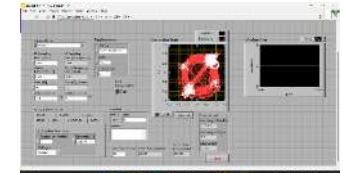
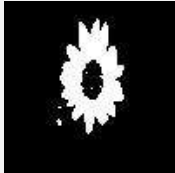
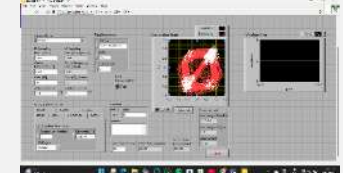
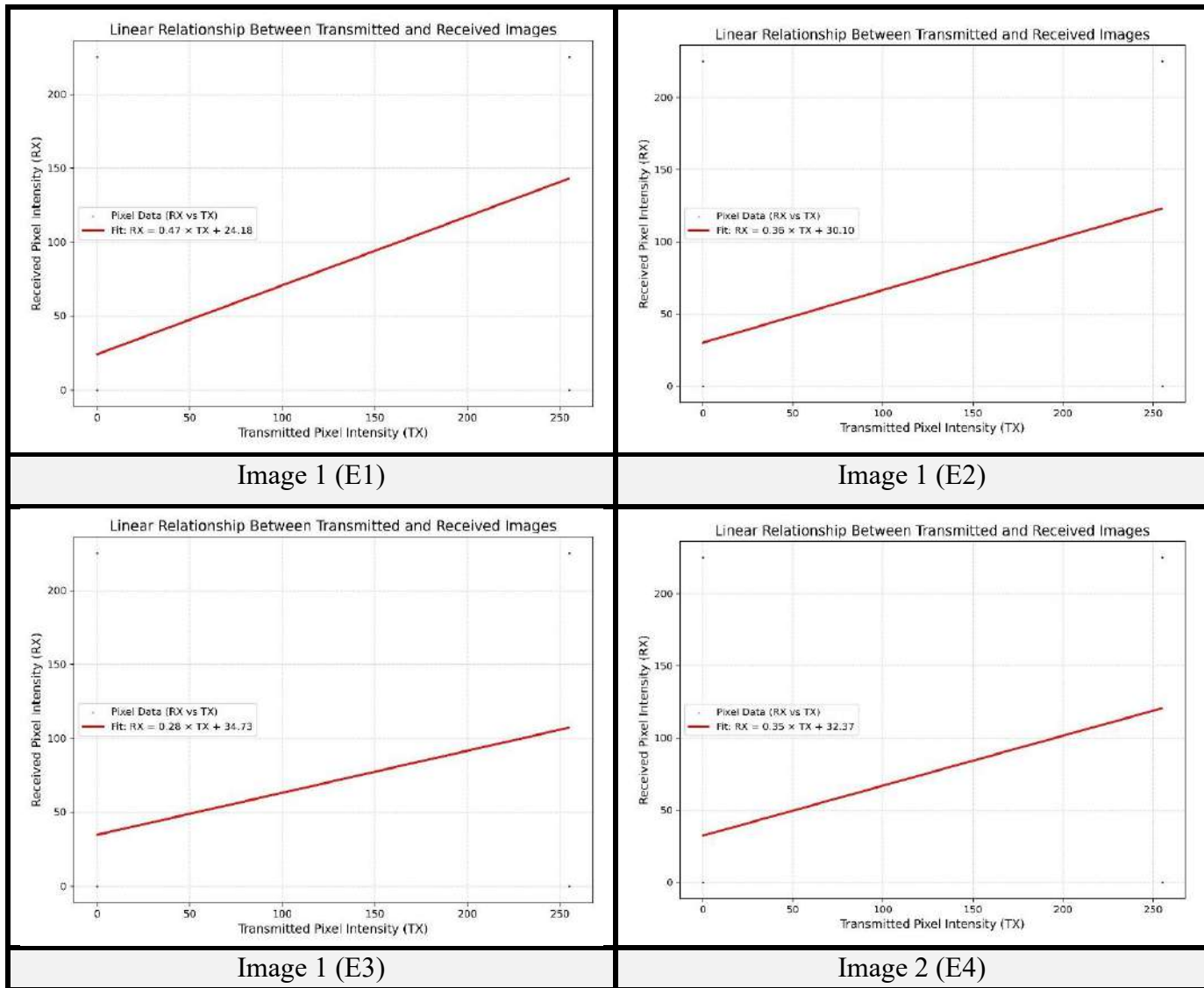
Image 3 (E8)		40			
Image 3 (E9)		50			

Table 4.32 Linearity Graph Properties (Two USRPs ENZ Antenna - Slant LOS 240 cm)



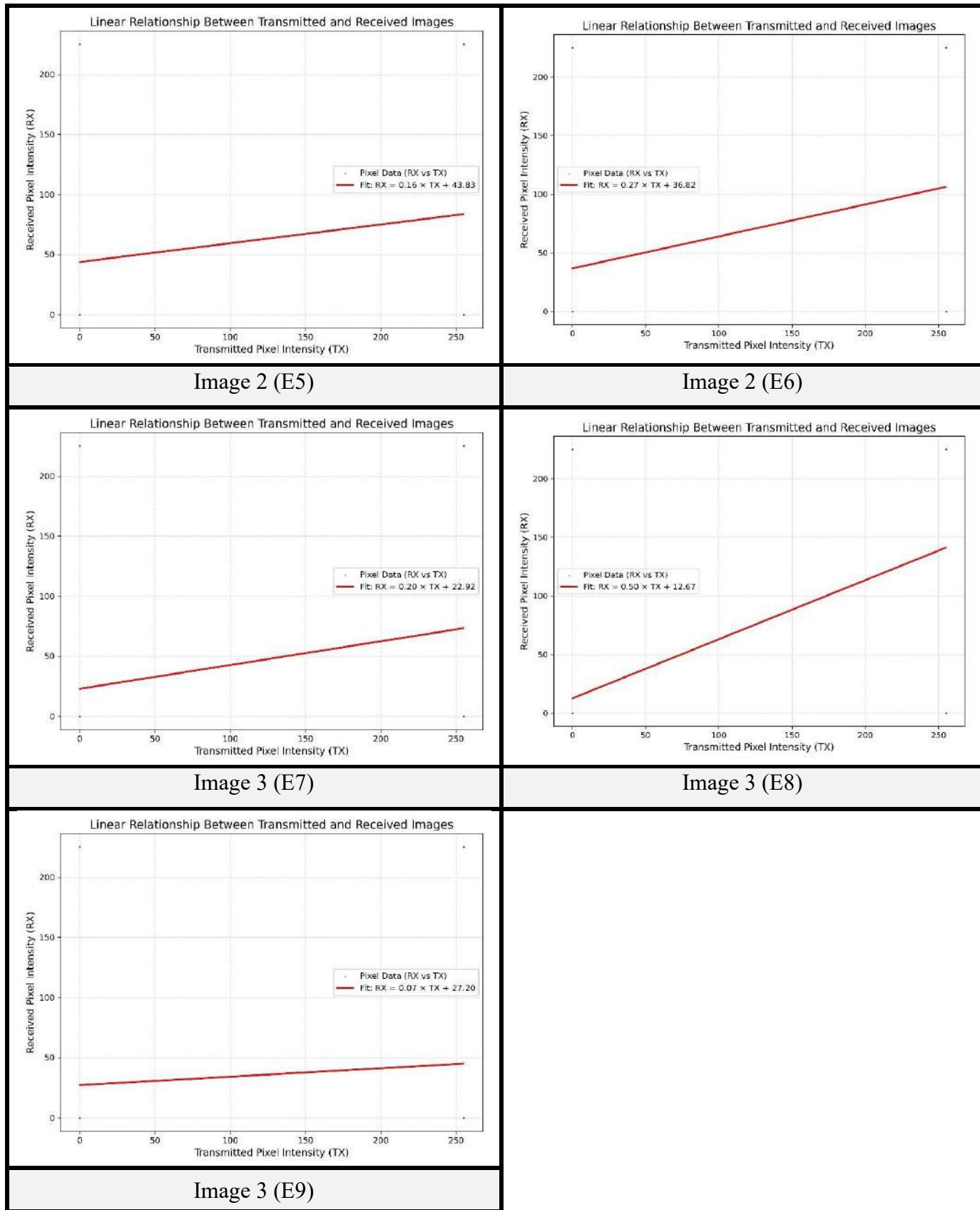


Table 4.33 Quantitative Performance Metrics (Two USRPs ENZ Antenna - Slant LOS 240 cm)

Image No.	Set Gain value (dB)	Pearson Correlation Coefficient	RMSE	PSNR (dB)	Normalized Cross-Correlation (NCC)	SSIM	Linear Fit Slope (m)	Linear Fit Intercept (c)
Image 1 (E1)	30	0.528014	5.93316 1	32.665 08	0.528014	0.4864 87	0.465895	24.18102
Image 1 (E2)	40	0.413327	6.04046 4	32.509 4	0.413327	0.4376 64	0.364813	30.09517
Image 1 (E3)	50	0.32216	6.11937 9	32.396 66	0.32216	0.4062 5	0.284259	34.72744
Image 2 (E4)	30	0.392273	6.16863	32.327 03	0.392273	0.4551 72	0.346123	32.36604
Image 2 (E5)	40	0.176967	6.36111 6	32.060 14	0.176967	0.3715 83	0.156147	43.8327
Image 2 (E6)	50	0.308696	6.24405 3	32.221 47	0.308696	0.4285 31	0.272379	36.81711
Image 3 (E7)	30	0.224095	4.77688 2	34.547 91	0.224095	0.6053 85	0.197731	22.92218
Image 3 (E8)	40	0.571279	4.51258 2	35.042 3	0.571279	0.7151 92	0.50407	12.66548
Image 3 (E9)	50	0.079434	4.88278 6	34.357 45	0.079434	0.5536 35	0.070089	27.19581

- **For Slot Cut Patch Antenna (Rogers RO3003):** The on-site experimental setup for this antenna is shown in Figure 4.18. Visual results are presented in Table 4.34. Linearity graph properties are provided in Table 4.35. Quantitative performance metrics are in Table 4.36.



Fig. 4.18 On-site Experimental Setup

Table 4.34 Visual Experiment Results (Two USRPs Slot Cut Patch Antenna - Slant LOS 240 cm)

Image No.	Transmitted Image	Set Gain Value (dB)	Tx Front Panel	Rx Front Panel	Received Image
Image 1 (S1)		30			
Image 1 (S2)		40			
Image 1 (S3)		50			

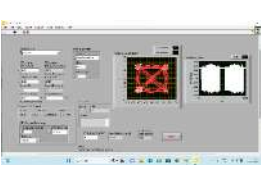
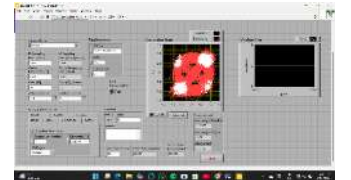
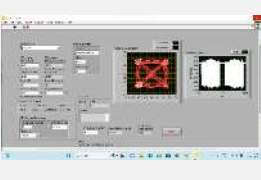
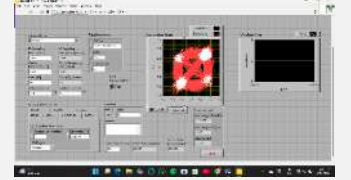
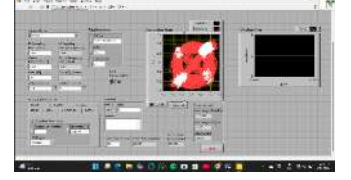
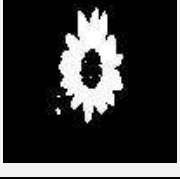
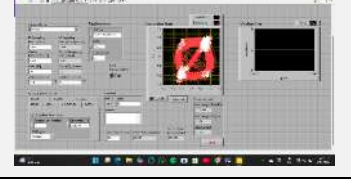
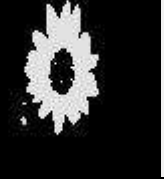
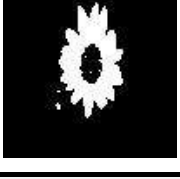
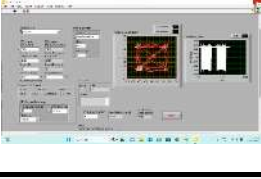
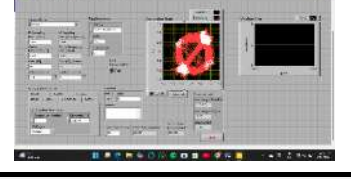
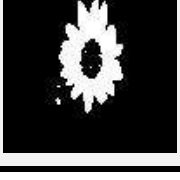
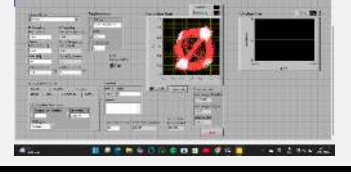
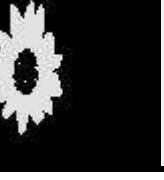
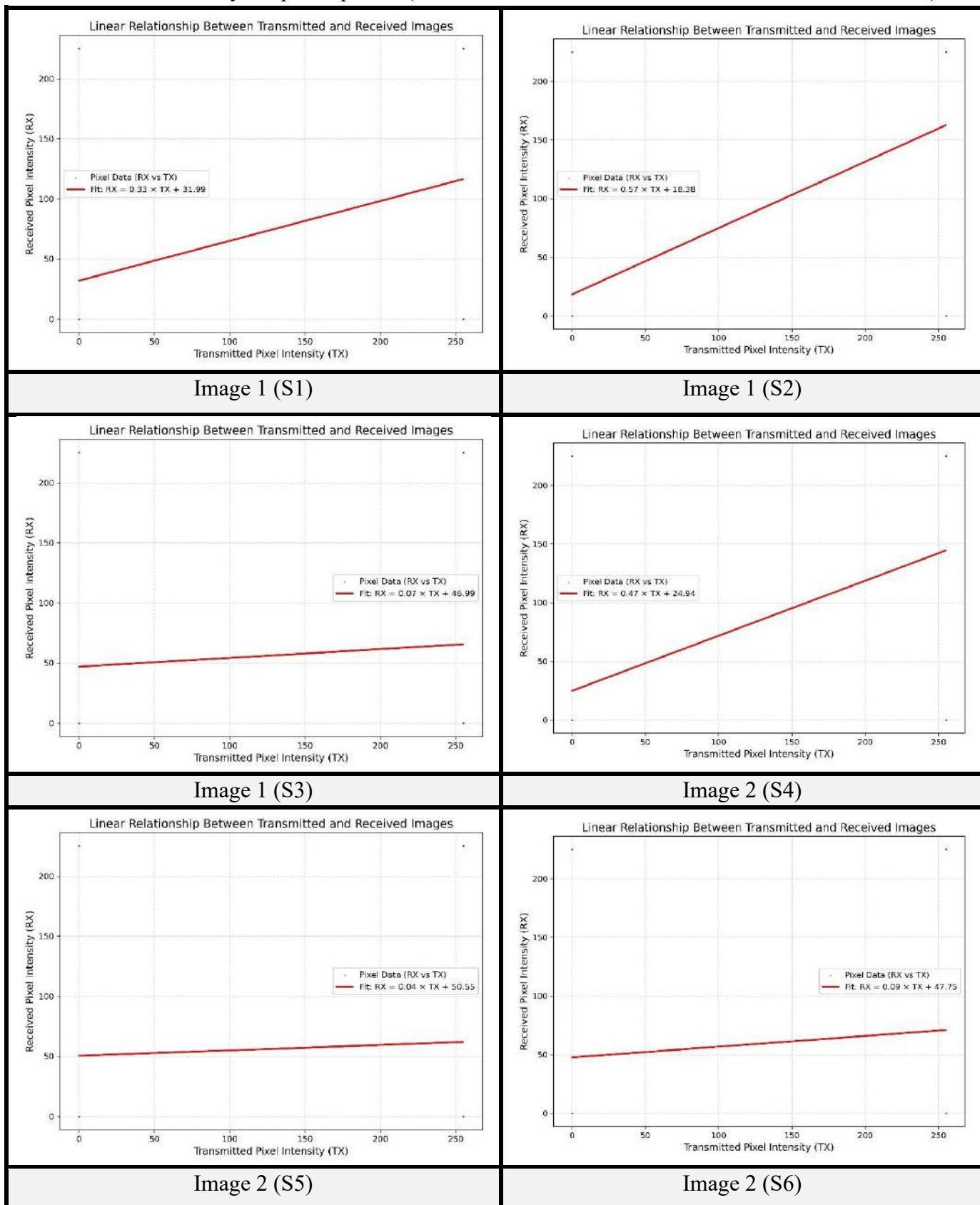
Image 2 (S4)		30			
Image 2 (S5)		40			
Image 2 (S6)		50			
Image 3 (S7)		30			
Image 3 (S8)		40			
Image 3 (S9)		50			

Table 4.35 Linearity Graph Properties (Two USRPs Slot Cut Patch Antenna - Slant LOS 240 cm)

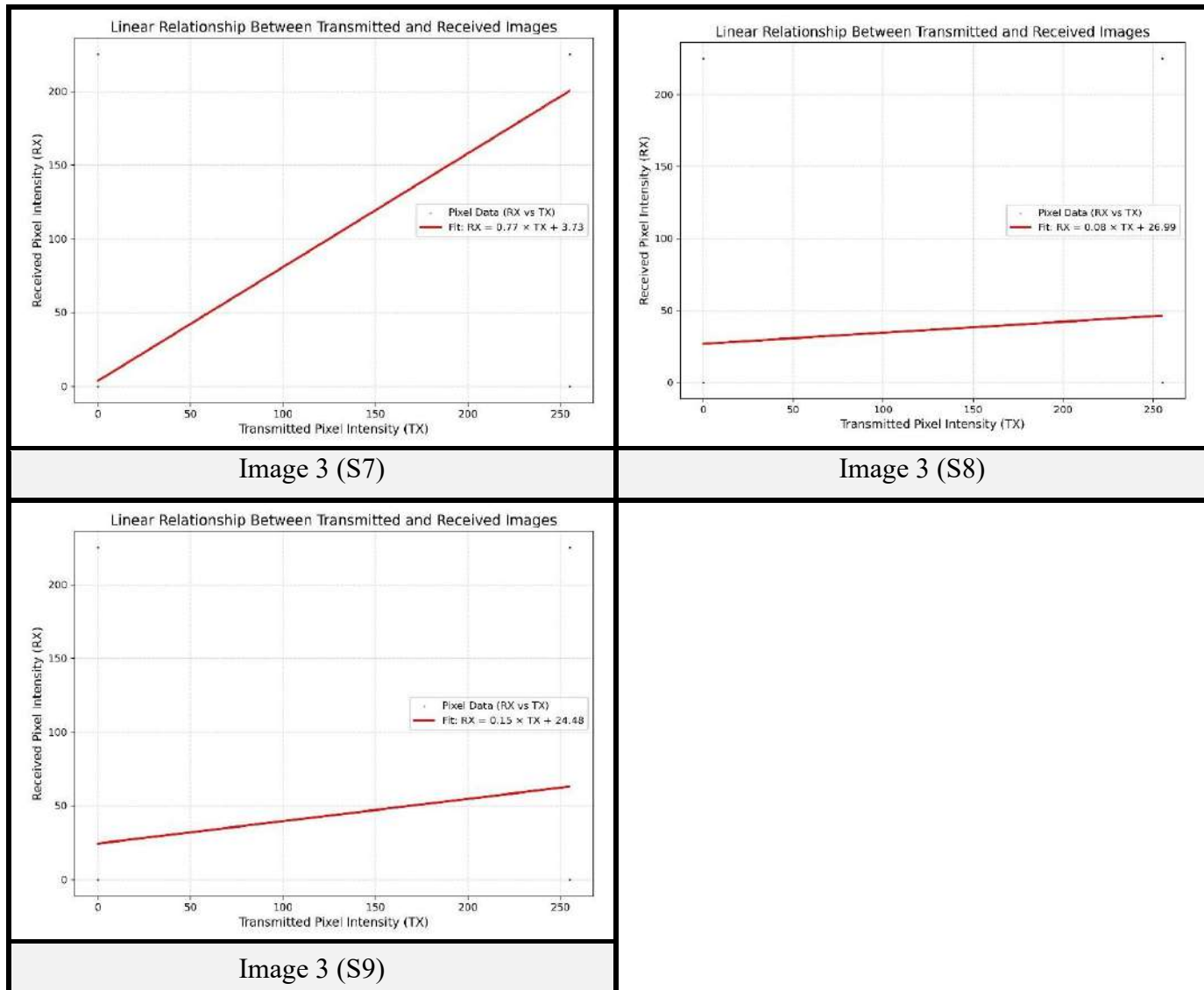


Table 4.36 Quantitative Performance Metrics (Two USRPs Slot CutAntenna - Slant LOS 240 cm)

Image No.	Set Gain value (dB)	Pearson Correlation Coefficient	RMSE	PSNR (dB)	Normalized Cross-Correlation (NCC)	SSIM	Linear Fit Slope (m)	Linear Fit Intercept (c)
Image 1 (S1)	30	0.375614	6.071573	32.46478	0.375614	0.416316	0.331424	31.98886
Image 1 (S2)	40	0.641177	5.828259	32.82003	0.641177	0.55417	0.565744	18.3834
Image 1 (S3)	50	0.082755	6.32906	32.10402	0.082755	0.352941	0.073019	46.99275

Image 2 (S4)	30	0.531751	6.040662	32.50911	0.531751	0.498418	0.469192	24.93777
Image 2 (S5)	40	0.050772	6.471275	31.91101	0.050772	0.306132	0.044799	50.55352
Image 2 (S6)	50	0.103353	6.425605	31.97252	0.103353	0.326487	0.091194	47.75318
Image 3 (S7)	30	0.873751	4.269005	35.52427	0.873751	0.840063	0.770957	3.729711
Image 3 (S8)	40	0.086448	4.877704	34.36649	0.086448	0.556573	0.076278	26.9886
Image 3 (S9)	50	0.171491	4.815662	34.47768	0.171491	0.589134	0.151316	24.47623

For Parasitic Patch Antenna (Rogers RO3003): The on-site experimental setup for this antenna is shown in Figure 4.19. Visual results are presented in Table 4.37. Linearity graph properties are provided in Table 4.38. Quantitative performance metrics are in Table 4.39.



Fig. 4.19 On-site Experimental Setup

Table 4.37 Visual Experiment Results (Two USRPs Parasitic Patch Antenna - Slant LOS 240 cm)

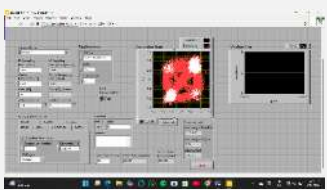
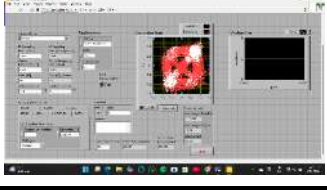
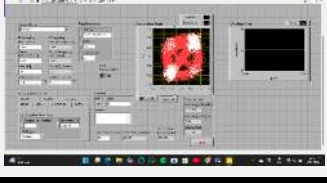
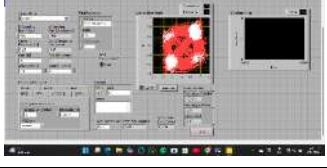
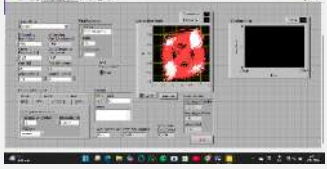
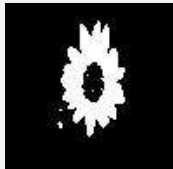
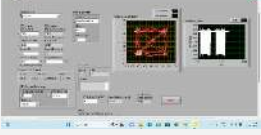
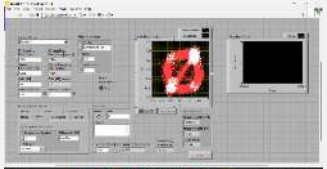
Image No.	Transmitted Image	Set Gain Value (dB)	Tx Front Panel	Rx Front Panel	Received Image
Image 1 (PP1)		30			
Image 1 (PP2)		40			
Image 1 (PP3)		50			
Image 2 (PP4)		30			
Image 2 (PP5)		40			
Image 2 (PP6)		50			
Image 3 (PP7)		30			

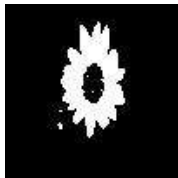
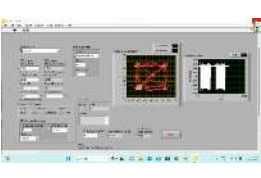
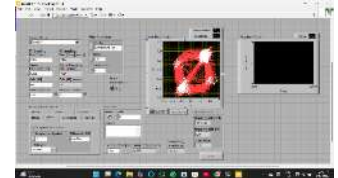
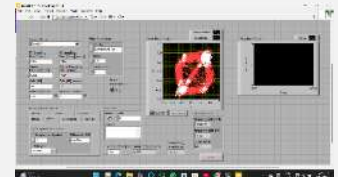
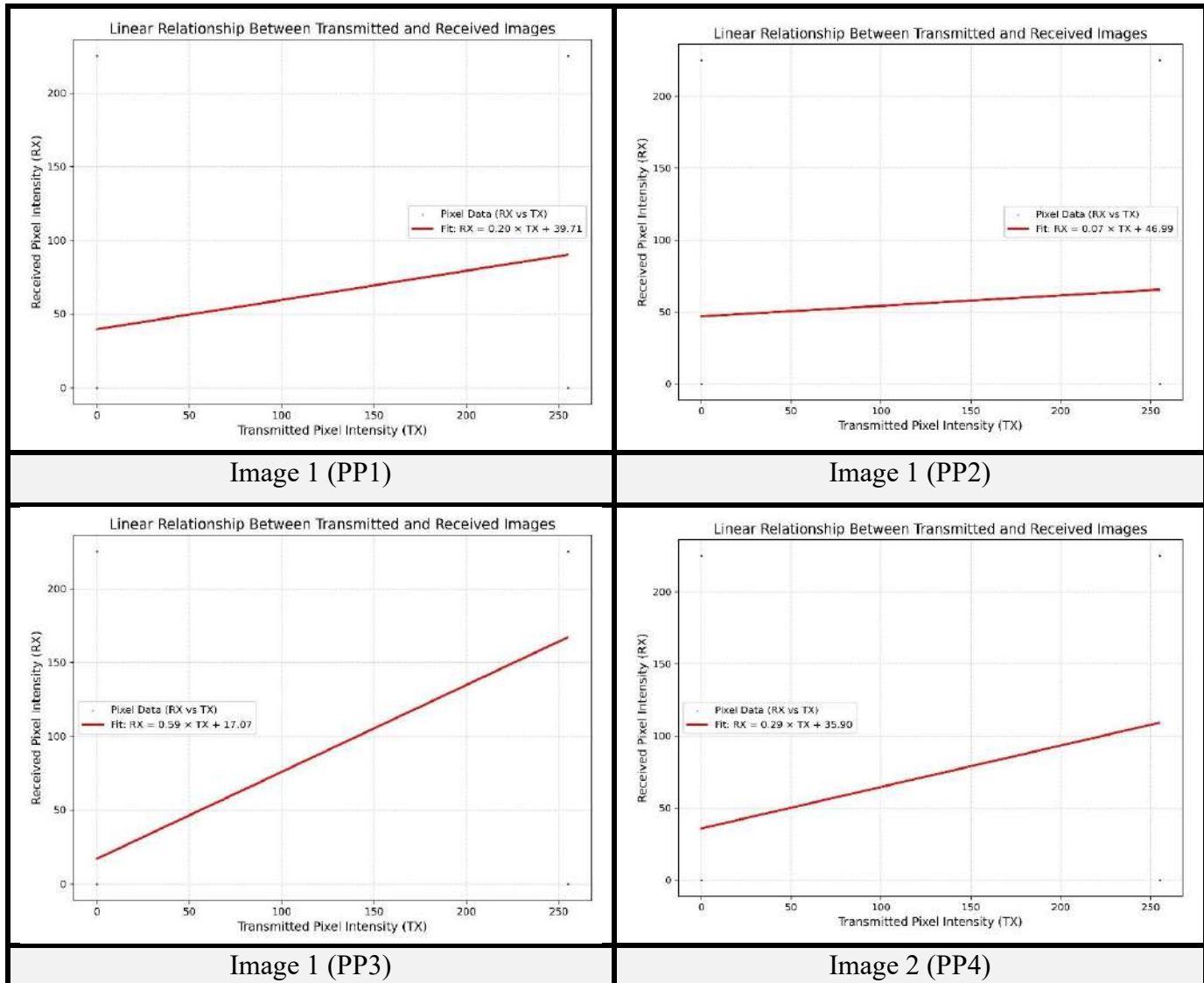
Image 3 (PP8)		40			
Image 3 (PP9)		50			

Table 4.38 Linearity Graph Properties (Two USRPs Parasitic Patch Antenna - Slant LOS 240 cm)



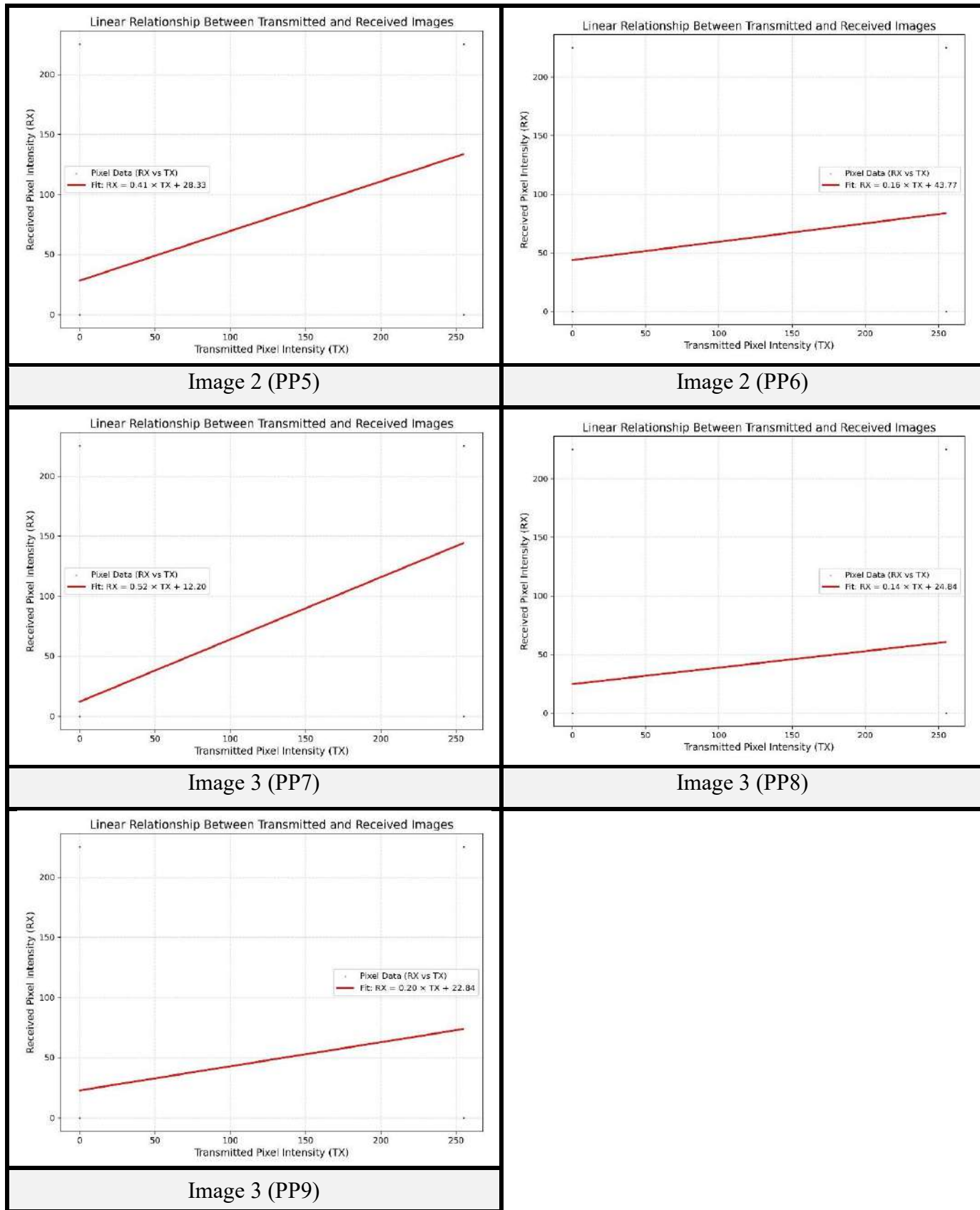


Table 4.39 Quantitative Performance Metrics (Parasitic Patch Antenna - Slant LOS 240 cm)

Image No.	Set Gain value (dB)	Pearson Correlation Coefficient	RMSE	PSNR (dB)	Normalized Cross-Correlation (NCC)	SSIM	Linear Fit Slope (m)	Linear Fit Intercept (c)
Image 1 (PP1)	30	0.22492	6.20540 1	32.2754 1	0.22492	0.38124 9	0.198458	39.70931
Image 1 (PP2)	40	0.082755	6.32906	32.1040 2	0.082755	0.34421 3	0.073019	46.99275
Image 1 (PP3)	50	0.666767	5.80427 4	32.8558 5	0.666767	0.56098 4	0.588323	17.07238
Image 2 (PP4)	30	0.325854	6.22864 4	32.2429 3	0.325854	0.40833 6	0.287519	35.90331
Image 2 (PP5)	40	0.4681	6.09939 3	32.4250 7	0.4681	0.46859 3	0.41303	28.32766
Image 2 (PP6)	50	0.178074	6.36014 2	32.0614 7	0.178074	0.35176 8	0.157124	43.77375
Image 3 (PP7)	30	0.587061	4.5002	35.0661 7	0.587061	0.69458 6	0.517995	12.19926
Image 3 (PP8)	40	0.159217	4.82466 6	34.4614 6	0.159217	0.58876 2	0.140485	24.83884
Image 3 (PP9)	50	0.226725	4.77493 5	34.5514 6	0.226725	0.60019 2	0.200051	22.84448

- **For Patch Antenna (FR4 Material):** The on-site experimental setup for this antenna is shown in Figure 4.20. Visual results are presented in Table 4.40. Linearity graph properties are provided in Table 4.41. Quantitative performance metrics are in Table 4.42.

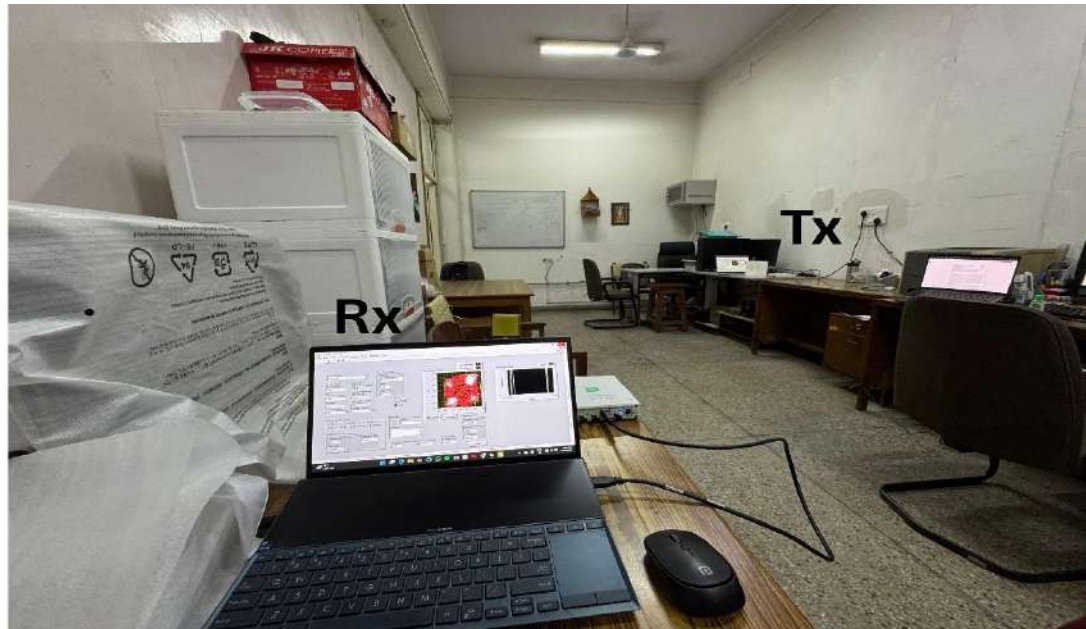


Fig. 20 On-site Experimental Setup

Table 4.40 Visual Experiment Results (Two USRPs Patch Antenna - Slant LOS 240 cm)

Image No.	Transmitted Image	Set Gain Value (dB)	Tx Front Panel	Rx Front Panel	Received Image
Image 1 (P1)		30			
Image 1 (P2)		40			
Image 1 (P3)		50			

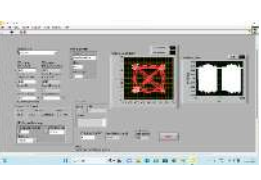
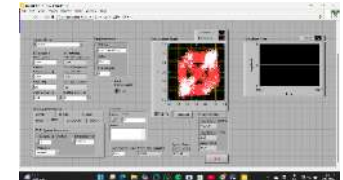
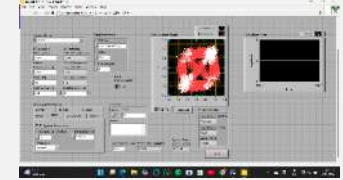
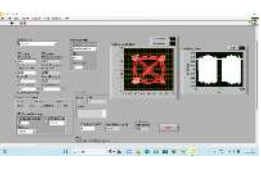
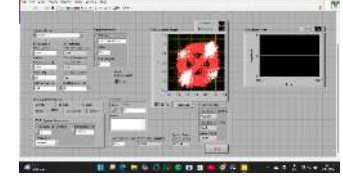
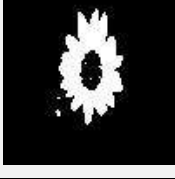
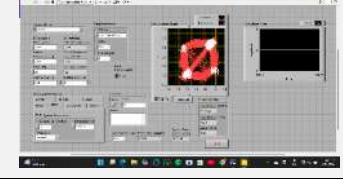
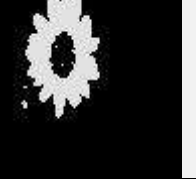
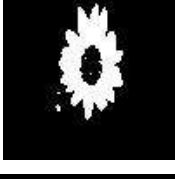
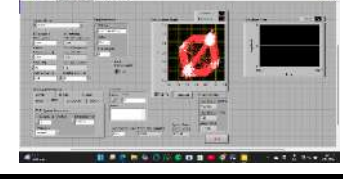
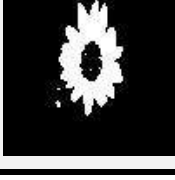
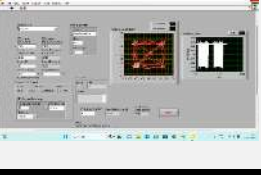
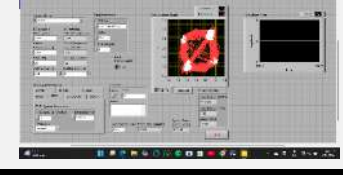
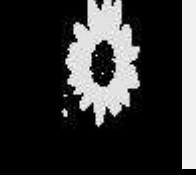
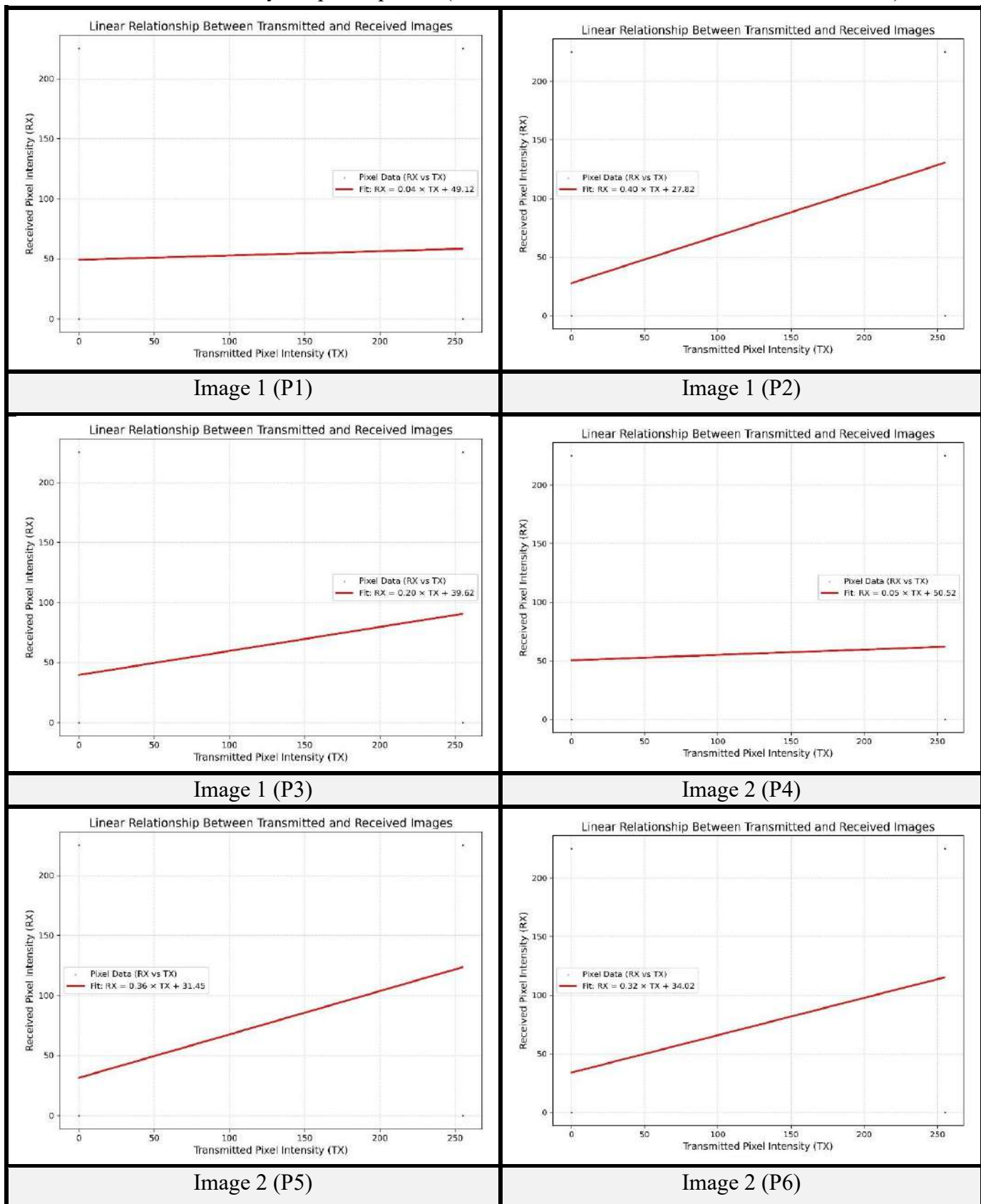
Image 2 (P4)		30			
Image 2 (P5)		40			
Image 2 (P6)		50			
Image 3 (P7)		30			
Image 3 (P8)		40			
Image 3 (P9)		50			

Table 4.41 Linearity Graph Properties (Two USRPs Patch Antenna - Slant LOS 240 cm)

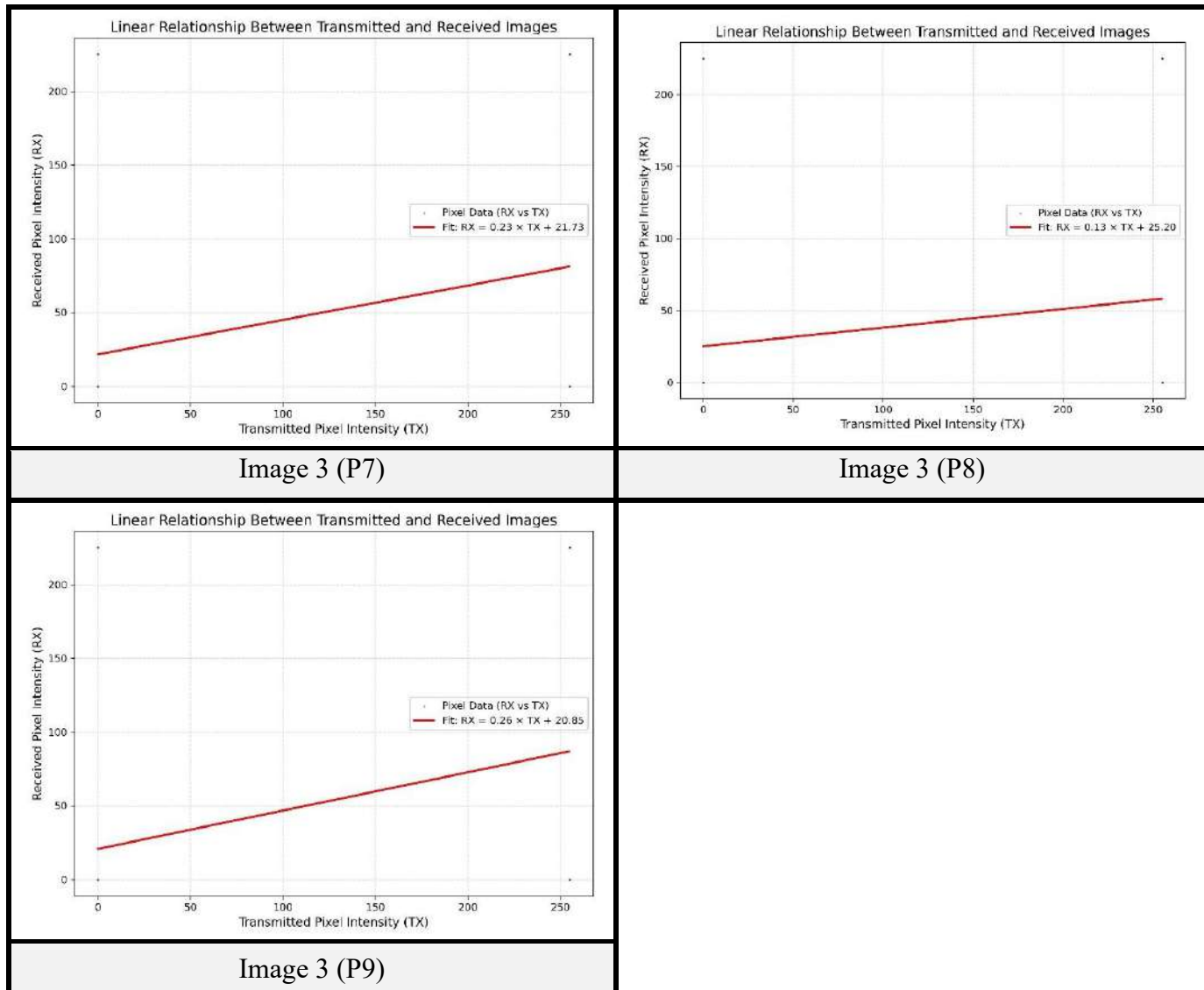


Table 4.42 Quantitative Performance Metrics (Two USRPs Patch Antenna - Slant LOS 240 cm)

Image No.	Set Gain value (dB)	Pearson Correlation Coefficient	RMSE	PSNR (dB)	Normalized Cross-Correlation (NCC)	SSIM	Linear Fit Slope (m)	Linear Fit Intercept (c)
Image 1 (P1)	30	0.041243	6.364715	32.05522	0.041243	0.331264	0.036391	49.11951
Image 1 (P2)	40	0.456563	5.997024	32.57209	0.456563	0.455098	0.402788	27.82274
Image 1 (P3)	50	0.226626	6.203902	32.27751	0.226626	0.371439	0.199964	39.62191

Image 2 (P4)	30	0.051325	6.47079 6	31.9116 5	0.051325	0.29681 5	0.045287	50.52404
Image 2 (P5)	40	0.409431	6.15303 2	32.3490 2	0.409431	0.45688 5	0.361262	31.45225
Image 2 (P6)	50	0.361277	6.19670 9	32.2875 8	0.361277	0.44632	0.318774	34.01677
Image 3 (P7)	30	0.264424	4.74693 6	34.6025 4	0.264424	0.62364 5	0.233315	21.73075
Image 3 (P8)	40	0.146943	4.83365 3	34.4452 9	0.146943	0.57990 2	0.129655	25.20145
Image 3 (P9)	50	0.294233	4.72468	34.6433 6	0.294233	0.62661 5	0.259617	20.85012

- **Experiment 3 [Fixed DNI Tx, Varied Rx Antennas (Outside Lab Ground Floor)]:** This experiment evaluated image transfer performance with the receiving USRP moved outside the laboratory on the ground floor. This setup required higher gains because signals tend to weaken more over longer distances and through obstacles (path loss). The Metamaterial Double Negative Index (DNI) antenna remained fixed as the transmitting antenna. The IQ Sampling Rate was fixed at 1M S/sec, and only the gain was changed (60 dB, 70 dB, 80 dB). The conceptual diagram for this setup is shown in Figure 4.21.

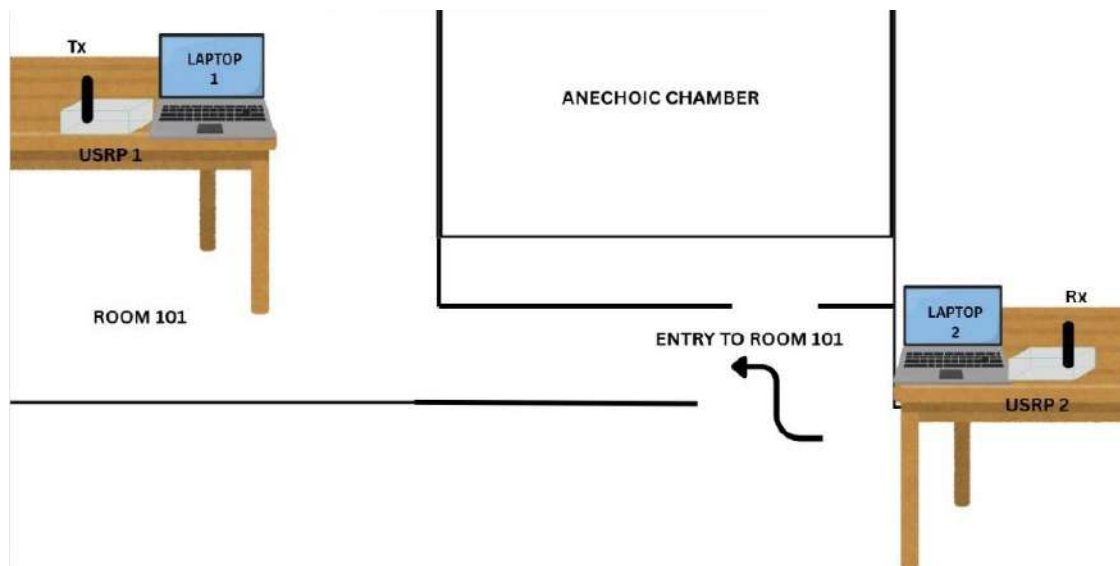


Fig. 4.21 Conceptual Diagram

- **For Metamaterial Epsilon Near Zero (ENZ) Receive Antenna:** The on-site experimental setup for this antenna is shown in Figure 4.22. Visual results are presented in Table 4.43. Linearity graph properties are provided in Table 4.44. Quantitative performance metrics are in Table 4.45.



Fig. 4.22 On-site Experimental Setup

Table 4.43 Visual Experiment Results (Two USRPs ENZ Antenna - Outside Lab Ground Floor)

Image No.	Transmitted Image	Set Gain Value (dB)	Tx Front Panel	Rx Front Panel	Received Image
Image 1 (E1)		60			
Image 1 (E2)		70			
Image 1 (E3)		80			

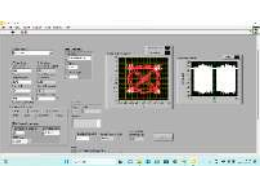
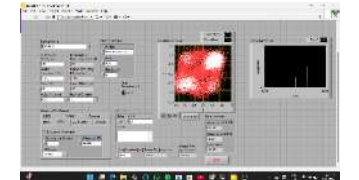
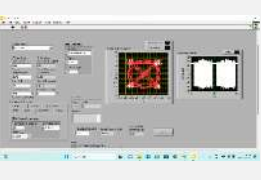
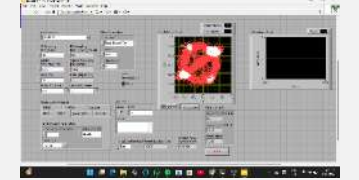
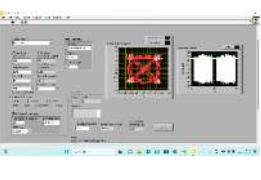
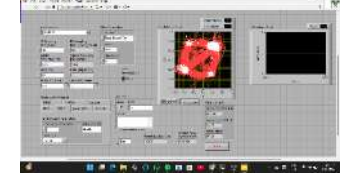
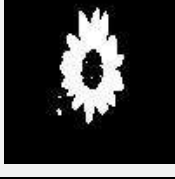
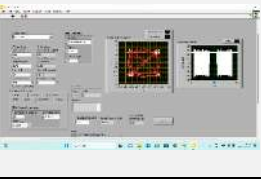
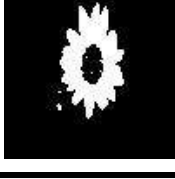
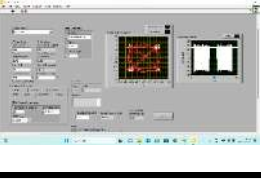
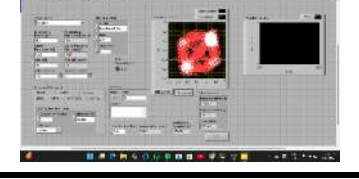
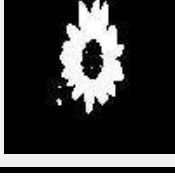
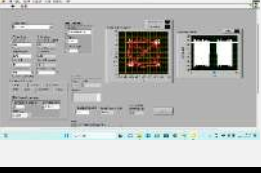
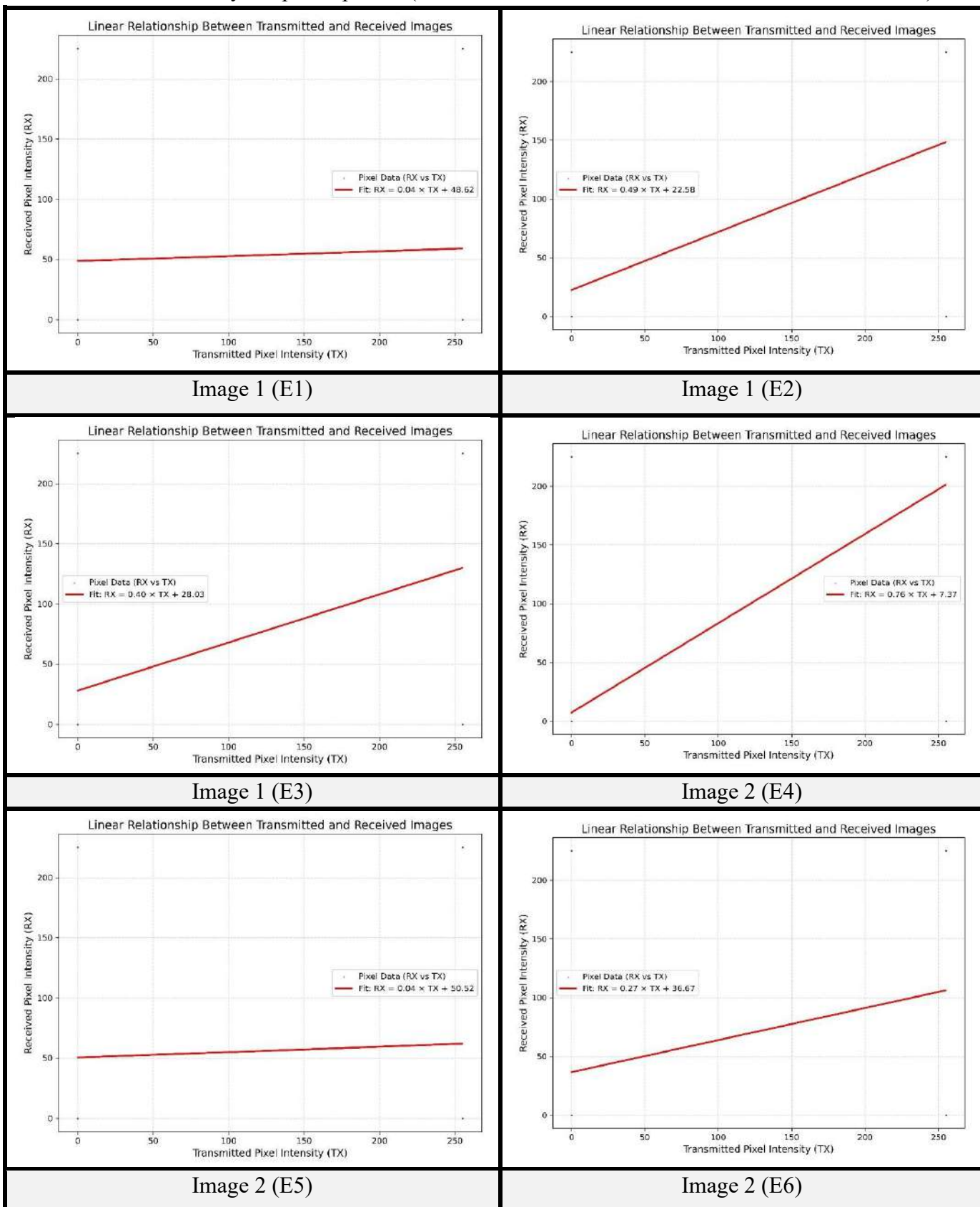
Image 2 (E4)		60			
Image 2 (E5)		70			
Image 2 (E6)		80			
Image 3 (E7)		60			
Image 3 (E8)		70			
Image 3 (E9)		80			

Table 4.44 Linearity Graph Properties (Two USRPs ENZ Antenna - Outside Lab Ground Floor)

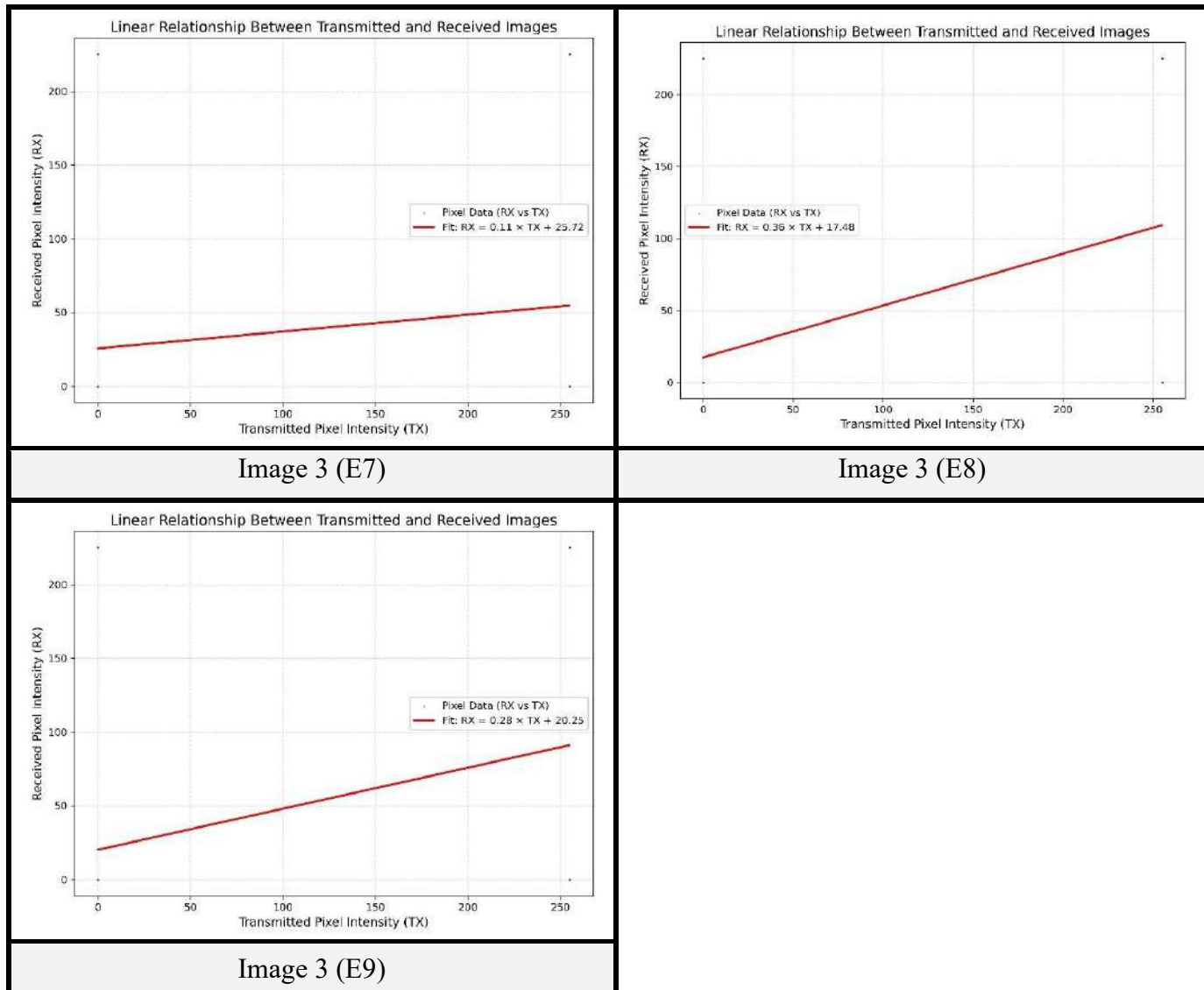


Table 4.45 Quantitative Performance Metrics (ENZ Antenna - Outside Lab Ground Floor)

Image No.	Set Gain value (dB)	Pearson Correlation Coefficient	RMSE	PSNR (dB)	Normalized Cross-Correlation (NCC)	SSIM	Linear Fit Slope (m)	Linear Fit Intercept (c)
Image 1 (E1)	60	0.046591	6.346117	32.08064	0.046591	0.328178	0.041046	48.62424
Image 1 (E2)	70	0.559643	5.905464	32.70572	0.559643	0.50139	0.493879	22.57866
Image 1 (E3)	80	0.452951	6.001733	32.56527	0.452951	0.458428	0.399663	28.02667

Image 2 (E4)	60	0.861629	5.72664	32.9728 1	0.861629	0.79406 5	0.76026	7.369317
Image 2 (E5)	70	0.05091	6.46978 4	31.9130 1	0.05091	0.31697 7	0.044914	50.52404
Image 2 (E6)	80	0.309577	6.23632 1	32.2322 3	0.309577	0.42845 4	0.272957	36.66972
Image 3 (E7)	60	0.129408	4.84646 3	34.4223 1	0.129408	0.57262 8	0.114183	25.71947
Image 3 (E8)	70	0.408208	4.63859 9	34.8030 7	0.408208	0.65510 6	0.360183	17.48302
Image 3 (E9)	80	0.315058	4.71095 5	34.6686 2	0.315058	0.63317 8	0.278082	20.2544

- **For Slot Cut Patch Antenna (Rogers RO3003):** The on-site experimental setup for this antenna is shown in Figure 4.23. Visual results are presented in Table 4.46. Linearity graph properties are provided in Table 4.47. Quantitative performance metrics are in Table 4.48.



Fig. 4.23 On-site Experimental Setup

Table 4.46 Visual Experiment Results (Slot Cut Patch Antenna - Outside Lab Ground Floor)

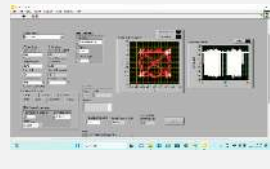
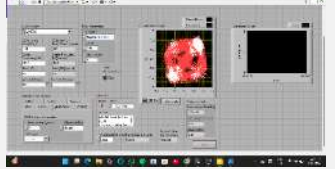
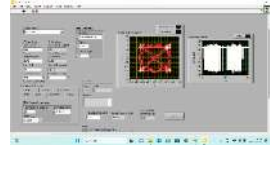
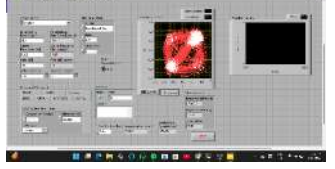
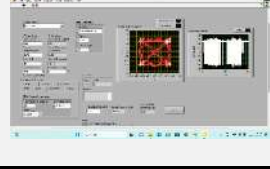
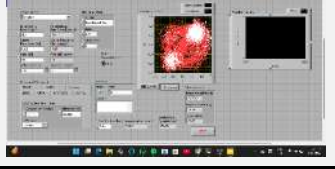
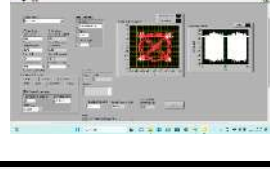
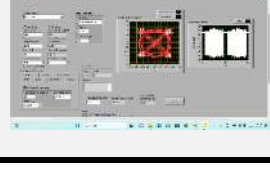
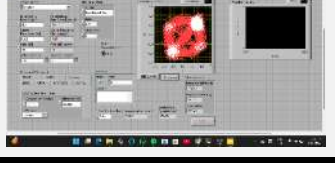
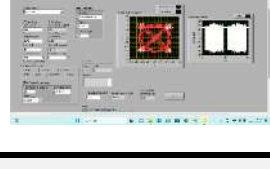
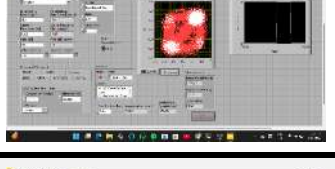
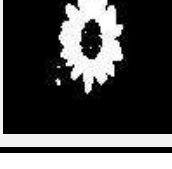
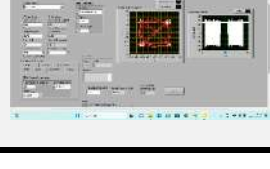
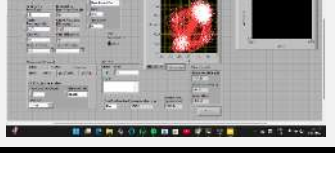
Image No.	Transmitted Image	Set Gain Value (dB)	Tx Front Panel	Rx Front Panel	Received Image
Image 1 (S1)		60			
Image 1 (S2)		70			
Image 1 (S3)		80			
Image 2 (S4)		60			
Image 2 (S5)		70			
Image 2 (S6)		80			
Image 3 (S7)		60			

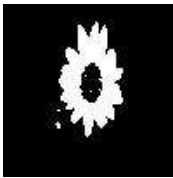
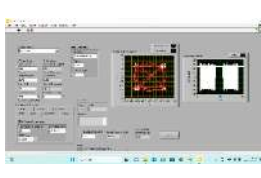
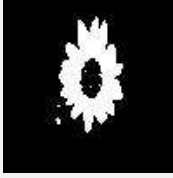
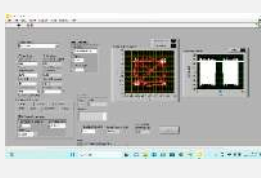
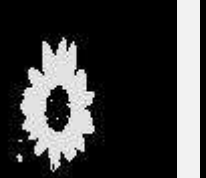
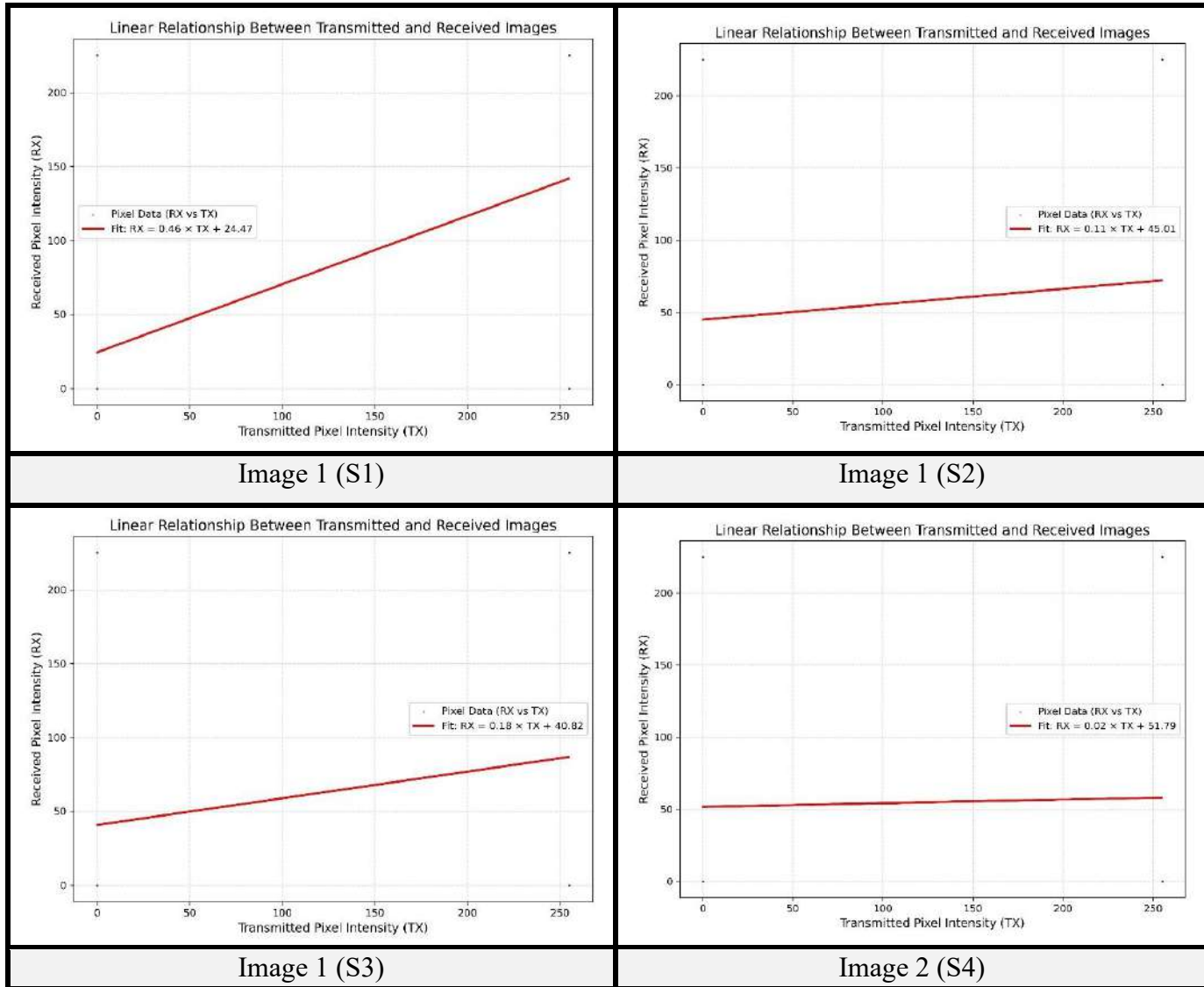
Image 3 (S8)		70			
Image 3 (S9)		80			

Table 4.47 Linearity Graph Properties (Slot Cut Patch Antenna - Outside Lab Ground Floor)



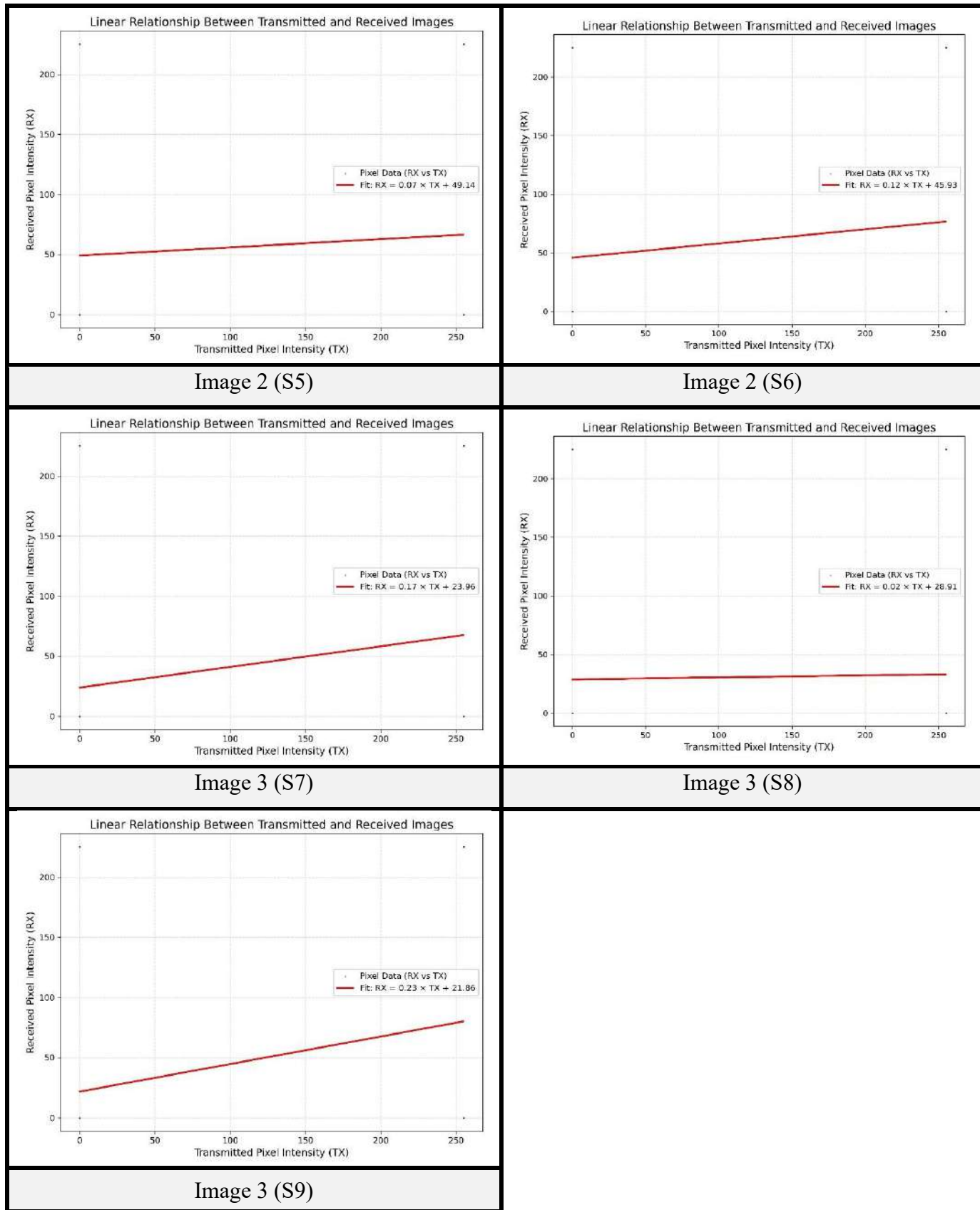


Table 4.48 Quantitative Performance Metrics (Slot Cut Antenna - Outside Lab Ground Floor)

Image No.	Set Gain value (dB)	Pearson Correlation Coefficient	RMSE	PSNR (dB)	Normalized Cross-Correlation (NCC)	SSIM	Linear Fit Slope (m)	Linear Fit Intercept (c)
Image 1 (S1)	60	0.521969	5.93728 1	32.6590 5	0.521969	0.49900 5	0.46049	24.47236
Image 1 (S2)	70	0.121003	6.29462 5	32.1514 1	0.121003	0.33477 4	0.106751	45.01165
Image 1 (S3)	80	0.204533	6.22751 2	32.2445 1	0.204533	0.36608	0.180554	40.81639
Image 2 (S4)	60	0.027944	6.49237 2	31.8827 4	0.027944	0.31546 4	0.02466	51.79156
Image 2 (S5)	70	0.07775	6.44925 6	31.9406 1	0.07775	0.33873 2	0.068613	49.13861
Image 2 (S6)	80	0.137267	6.39459 9	32.0145 4	0.137267	0.37397	0.1211	45.92559
Image 3 (S7)	60	0.193919	4.81230 7	34.4837 4	0.193919	0.57246 8	0.171491	23.95821
Image 3 (S8)	70	0.018548	4.91918 7	34.2929 4	0.018548	0.55277	0.016345	28.90526
Image 3 (S9)	80	0.259363	4.74882 1	34.5990 9	0.259363	0.62460 5	0.228776	21.86025

- **For Parasitic Patch Antenna (Rogers RO3003):** The on-site experimental setup for this antenna is shown in Figure 4.24. Visual results are presented in Table 4.49. Linearity graph properties are provided in Table 4.50. Quantitative performance metrics are in Table 4.51.



Fig. 4.24 On-site Experimental Setup

Table 4.49 Visual Experiment Results (Parasitic Patch Antenna - Outside Lab Ground Floor)

Image No.	Transmitted Image	Set Gain Value (dB)	Tx Front Panel	Rx Front Panel	Received Image
Image 1 (PP1)		60			
Image 1 (PP2)		70			
Image 1 (PP3)		80			

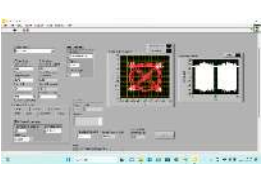
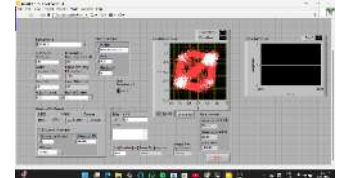
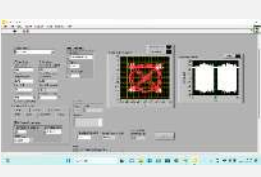
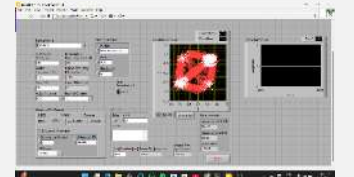
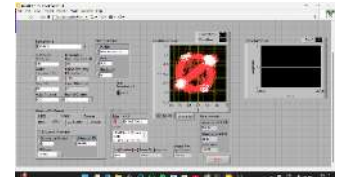
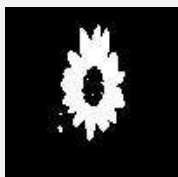
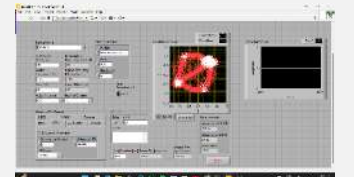
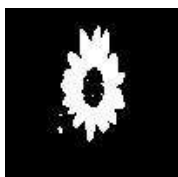
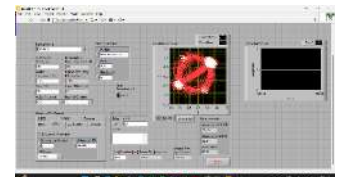
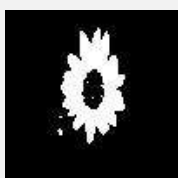
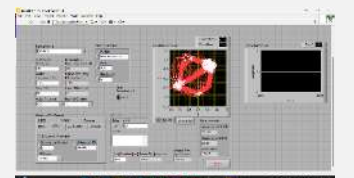
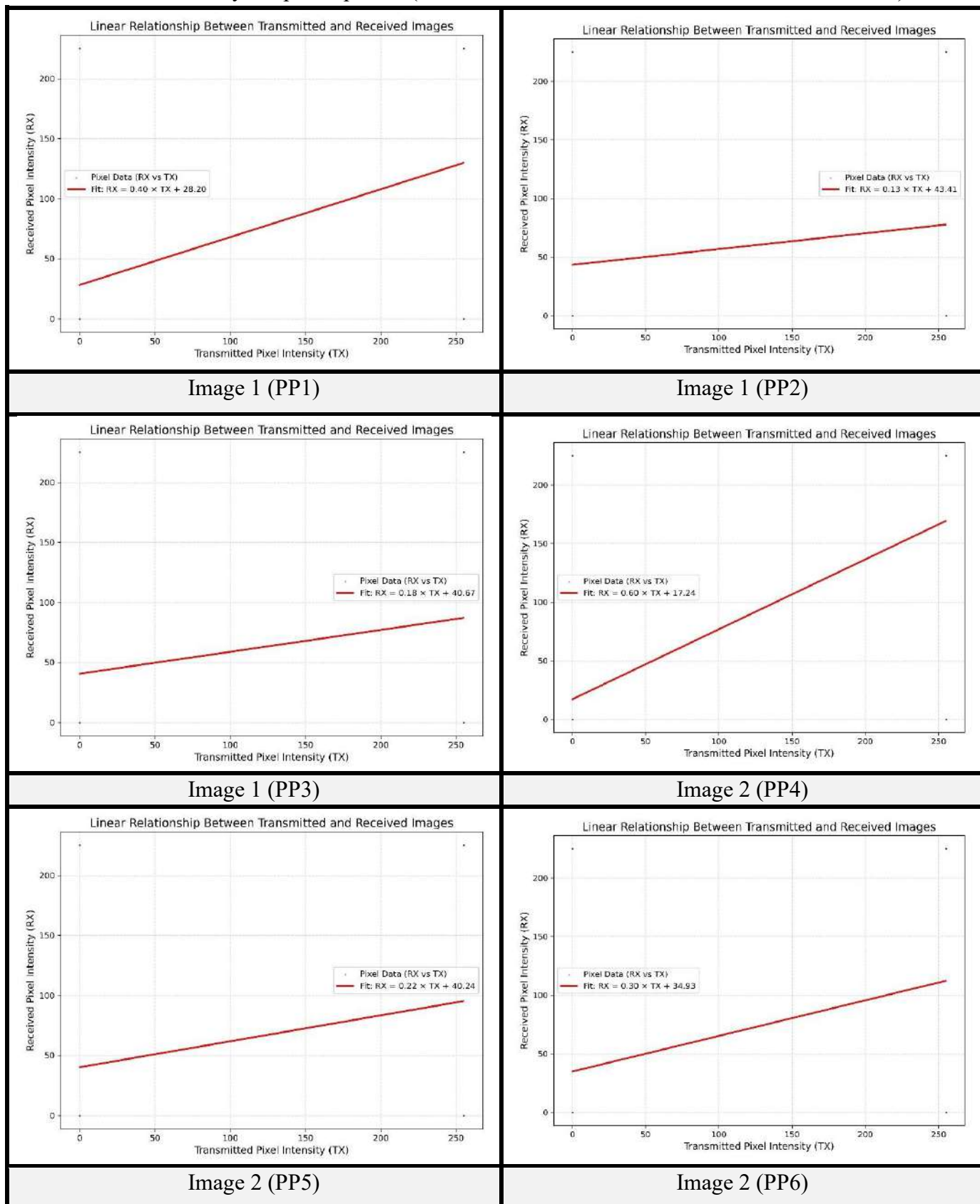
Image 2 (PP4)		60			
Image 2 (PP5)		70			
Image 2 (PP6)		80			
Image 3 (PP7)		60			
Image 3 (PP8)		70			
Image 3 (PP9)		80			

Table 4.50 Linearity Graph Properties (Parasitic Patch Antenna - Outside Lab Ground Floor)

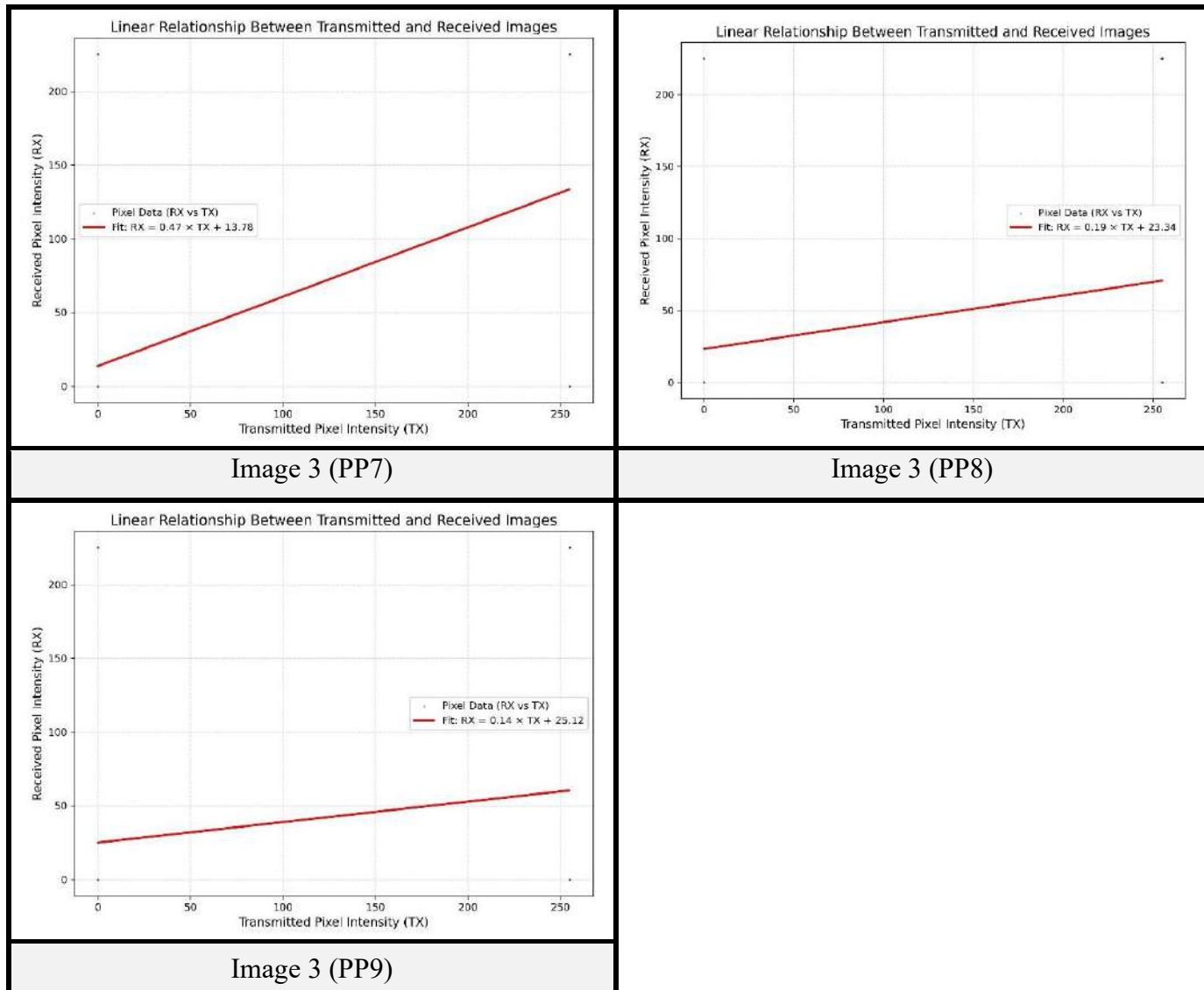


Table 4.51 Quantitative Performance Metrics (Parasitic Patch Antenna - Ground Floor)

Image No.	Set Gain value (dB)	Pearson Correlation Coefficient	RMSE	PSNR (dB)	Normalized Cross-Correlation (NCC)	SSIM	Linear Fit Slope (m)	Linear Fit Intercept (c)
Image 1 (PP1)	60	0.451386	6.010283	32.55291	0.451386	0.447348	0.39859	28.20148
Image 1 (PP2)	70	0.1527	6.268525	32.1875	0.1527	0.358025	0.134735	43.4093
Image 1 (PP3)	80	0.206561	6.222917	32.25092	0.206561	0.366199	0.182288	40.67072

Image 2 (PP4)	60	0.676211	5.90520 1	32.7061 1	0.676211	0.59639 1	0.596657	17.2442
Image 2 (PP5)	70	0.244879	6.30242	32.1406 6	0.244879	0.38869 9	0.216101	40.23647
Image 2 (PP6)	80	0.344119	6.21219 8	32.2659	0.344119	0.41633 9	0.303635	34.93056
Image 3 (PP7)	60	0.532991	4.54058 4	34.9885 7	0.532991	0.68689	0.470134	13.77921
Image 3 (PP8)	70	0.210761	4.78862 2	34.5265 9	0.210761	0.60407 9	0.186025	23.33659
Image 3 (PP9)	80	0.156684	4.84526 6	34.4244 5	0.156684	0.58087 8	0.138696	25.12375

- **For Patch Antenna (FR4 Material):** The on-site experimental setup for this antenna is shown in Figure 4.25. Visual results are presented in Table 4.52. Linearity graph properties are provided in Table 4.53. Quantitative performance metrics are in Table 4.54.

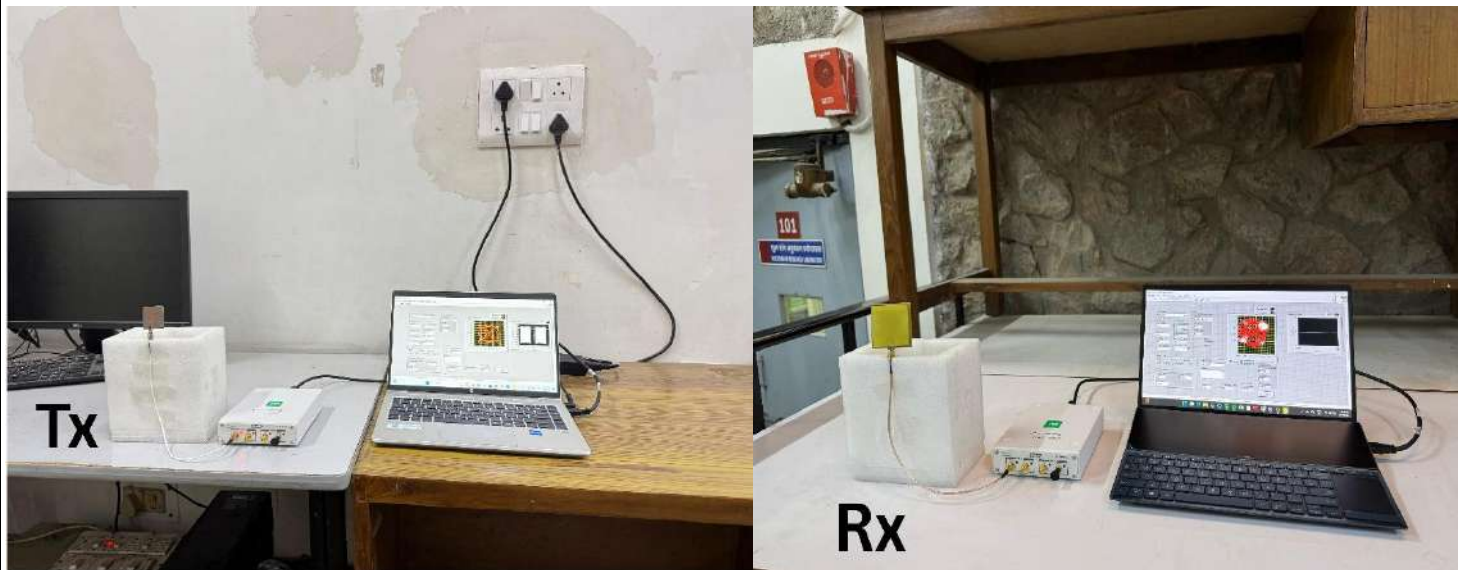


Fig. 4.25 On-site Experimental Setup

Table 4.52 Visual Experiment Results (Patch Antenna - Outside Lab Ground Floor)

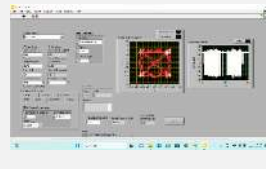
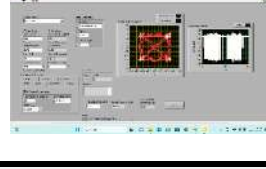
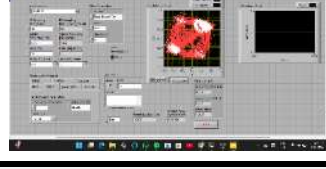
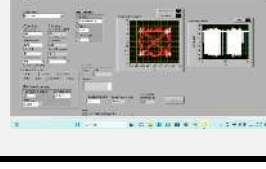
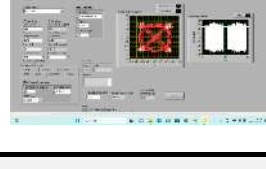
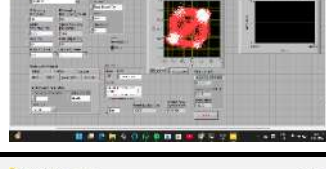
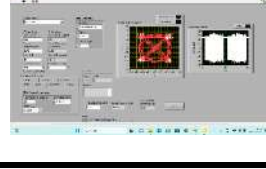
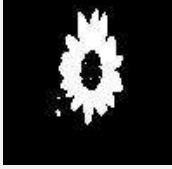
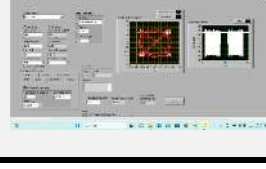
Image No.	Transmitted Image	Set Gain Value (dB)	Tx Front Panel	Rx Front Panel	Received Image
Image 1 (P1)		60			
Image 1 (P2)		70			
Image 1 (P3)		80			
Image 2 (P4)		60			
Image 2 (P5)		70			
Image 2 (P6)		80			
Image 3 (P7)		60			

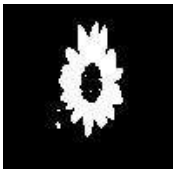
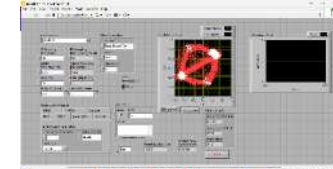
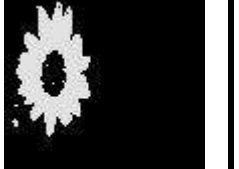
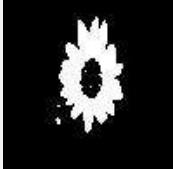
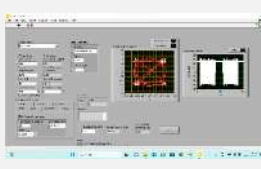
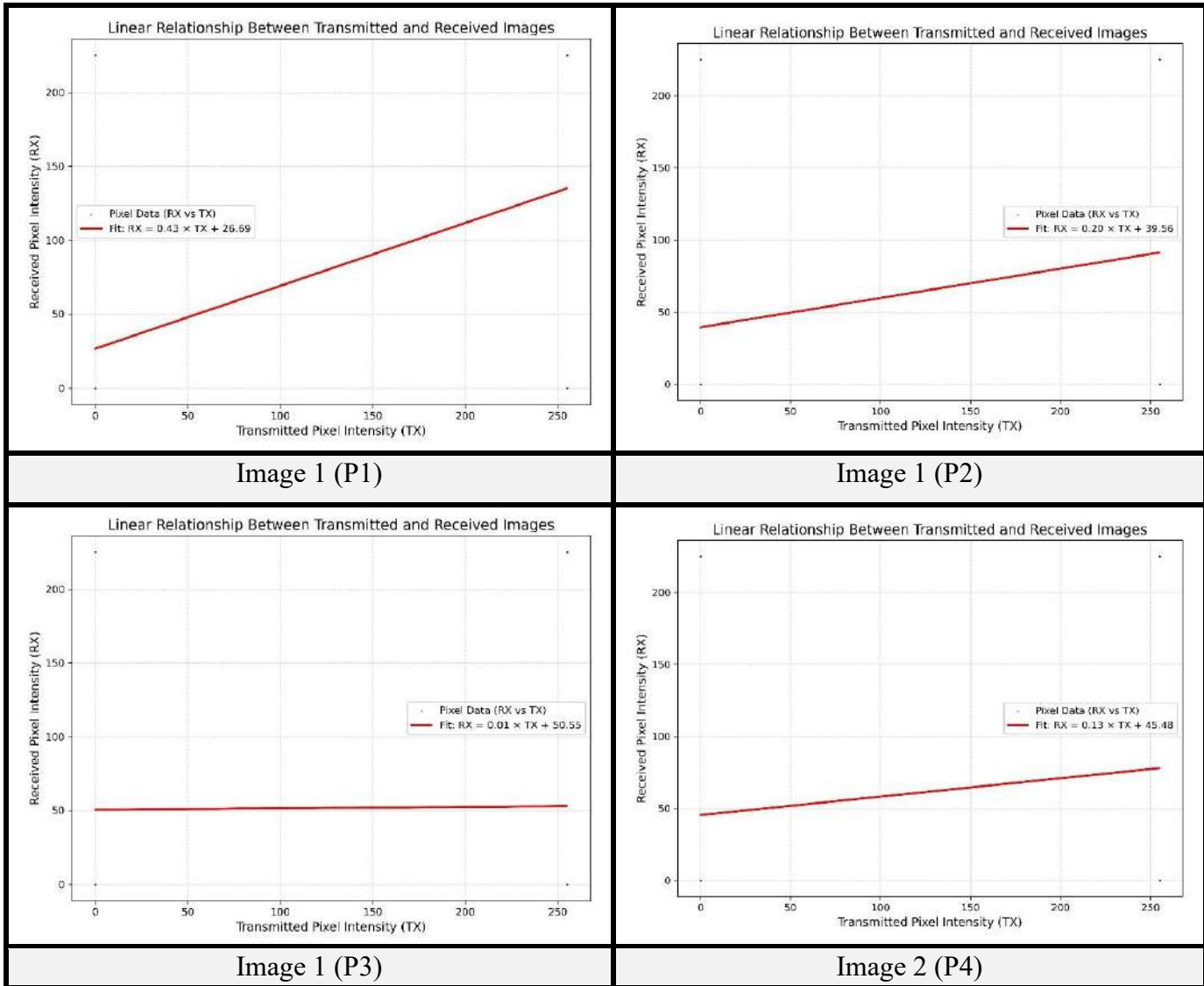
Image 3 (P8)		70			
Image 3 (P9)		80			

Table 4.53 Linearity Graph Properties (Two USRPs Patch Antenna - Outside Lab Ground Floor)



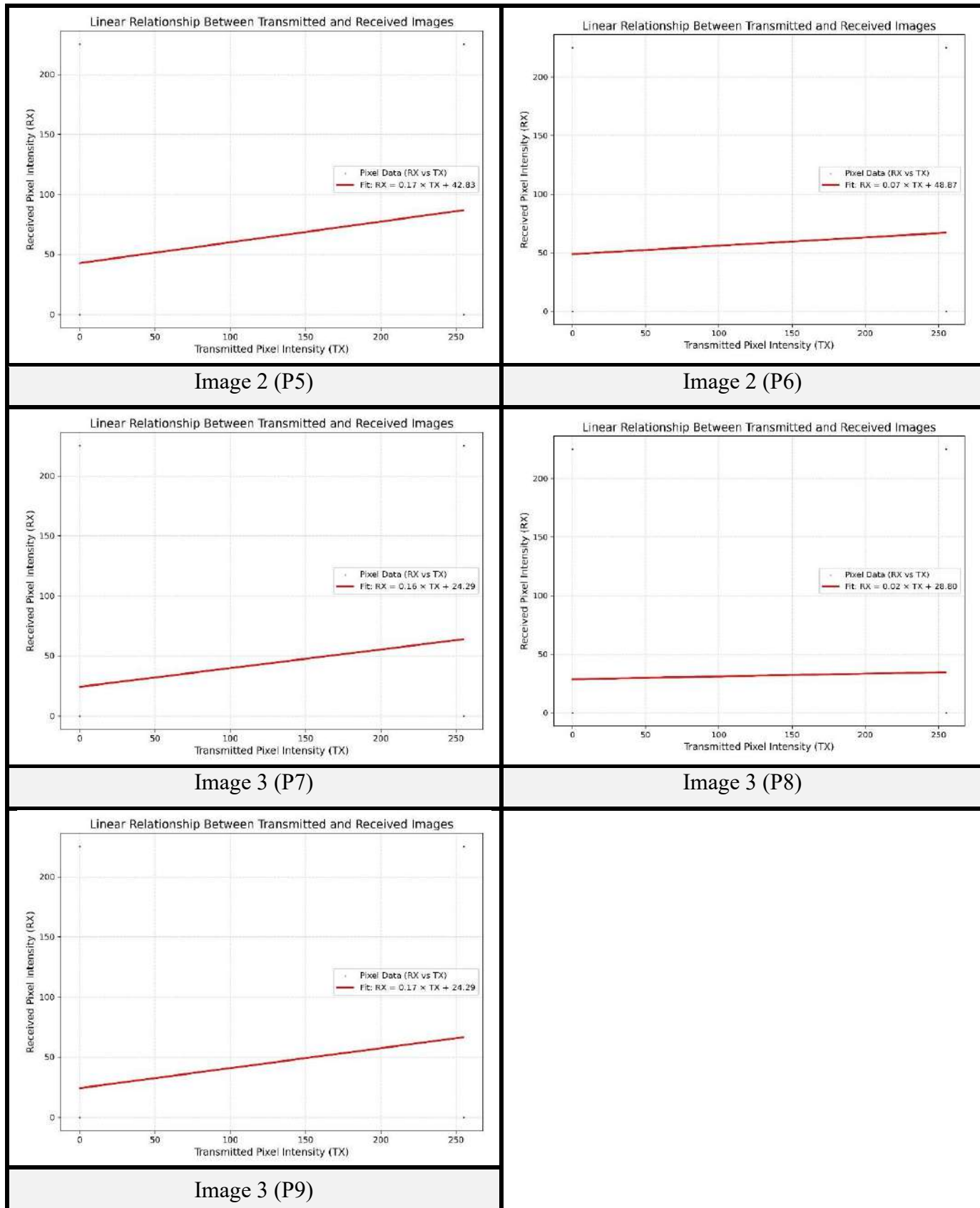


Table 4.54 Quantitative Performance Metrics (Patch Antenna - Outside Lab Ground Floor)

Image No.	Set Gain value (dB)	Pearson Correlation Coefficient	RMSE	PSNR (dB)	Normalized Cross-Correlation (NCC)	SSIM	Linear Fit Slope (m)	Linear Fit Intercept (c)
Image 1 (P1)	60	0.481298	5.98449 7	32.5902 5	0.481298	0.48007 2	0.425069	26.68652
Image 1 (P2)	70	0.229781	6.20818	32.2715 2	0.229781	0.36572 8	0.202905	39.56364
Image 1 (P3)	80	0.010754	6.38238 2	32.0311 5	0.010754	0.30902 4	0.00948	50.54707
Image 2 (P4)	60	0.144767	6.38527 2	32.0272 2	0.144767	0.36889 1	0.12768	45.48343
Image 2 (P5)	70	0.195785	6.34452 5	32.0828 2	0.195785	0.38590 1	0.172752	42.83047
Image 2 (P6)	80	0.081089	6.44086 2	31.9519 2	0.081089	0.29853 3	0.071517	48.87331
Image 3 (P7)	60	0.176219	4.80843	34.4907 4	0.176219	0.58703 1	0.155387	24.29492
Image 3 (P8)	70	0.02583	4.92332 2	34.2856 4	0.02583	0.53416 3	0.022799	28.80166
Image 3 (P9)	80	0.187446	4.83017 6	34.4515 4	0.187446	0.58976	0.166139	24.29492

- **Experiment 4 [Fixed DNI Tx, Varied Rx Antennas (First Floor)]:** This experiment checked image transfer performance with the receiving USRP placed on the first floor. This meant there was a vertical distance of 310 cm from the ground floor laboratory where the transmitter was located. The Metamaterial Double Negative Index (DNI) antenna stayed as the transmitting antenna. The IQ Sampling Rate was fixed at 1M S/sec, and only the gain was changed (60 dB, 70 dB, 80 dB). The conceptual diagram for this setup is shown in Figure 4.26.

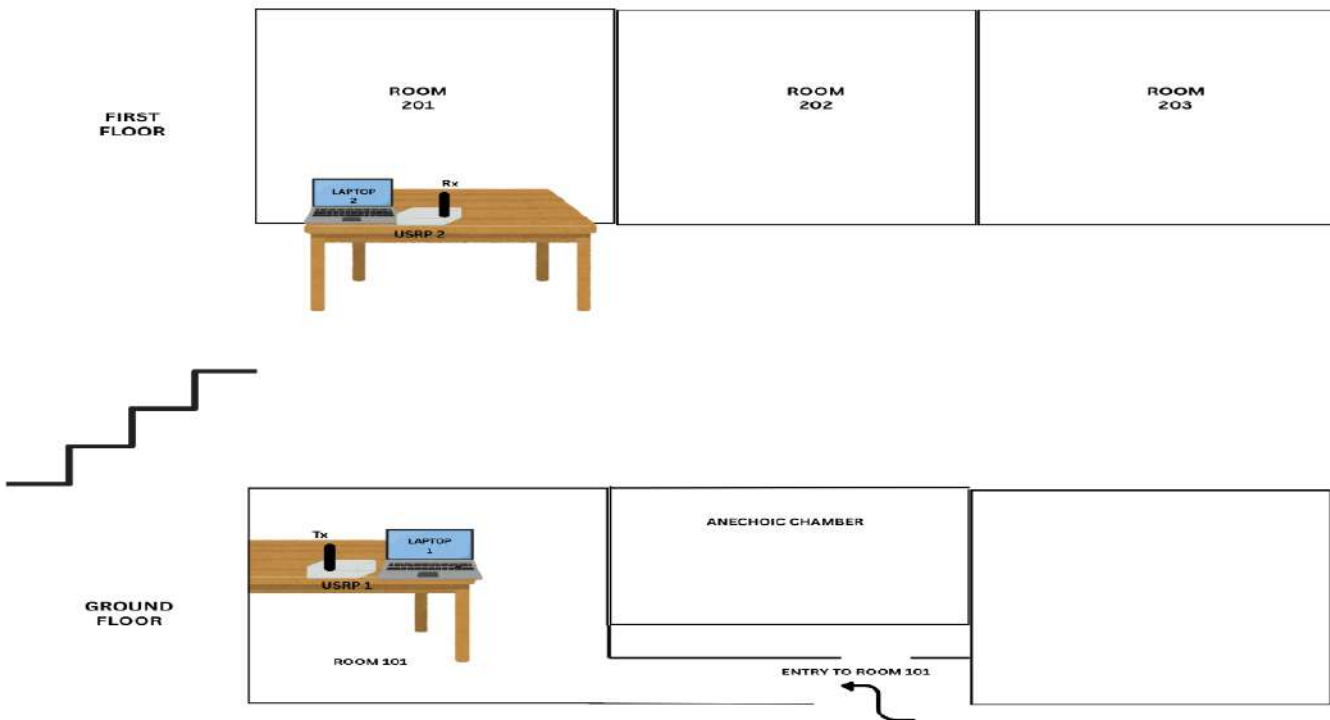


Fig. 4.26 Conceptual Diagram

- For Metamaterial Epsilon Near Zero (ENZ) Receive Antenna:** The on-site experimental setup for this antenna is shown in Figure 4.27. Visual results are presented in Table 4.55. Linearity graph properties are provided in Table 4.56. Quantitative performance metrics are in Table 4.57.



Fig. 4.27 On-site Experimental Setup

Table 4.55 Visual Experiment Results (Two USRPs ENZ Receive Antenna - First Floor)

Image No.	Transmitted Image	Set Gain Value (dB)	Tx Front Panel	Rx Front Panel	Received Image
Image 1 (E1)		60			
Image 1 (E2)		70			
Image 1 (E3)		80			

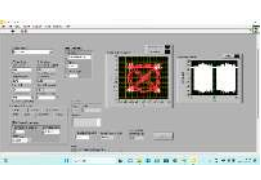
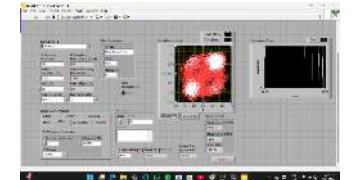
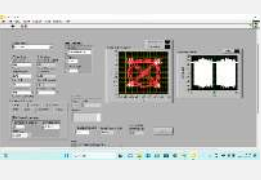
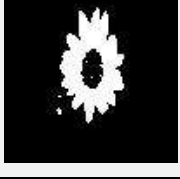
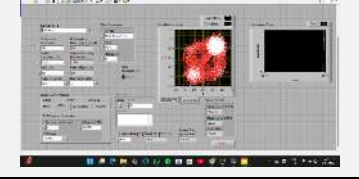
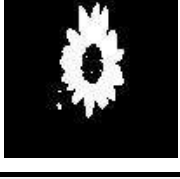
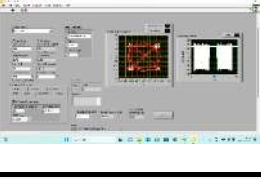
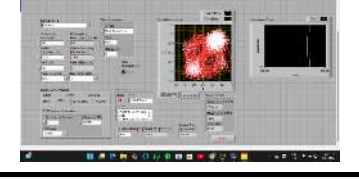
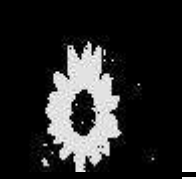
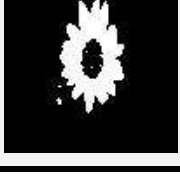
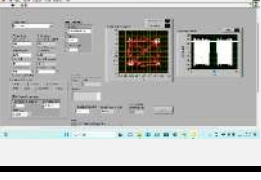
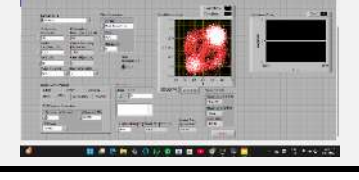
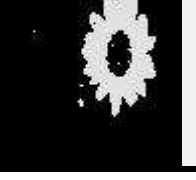
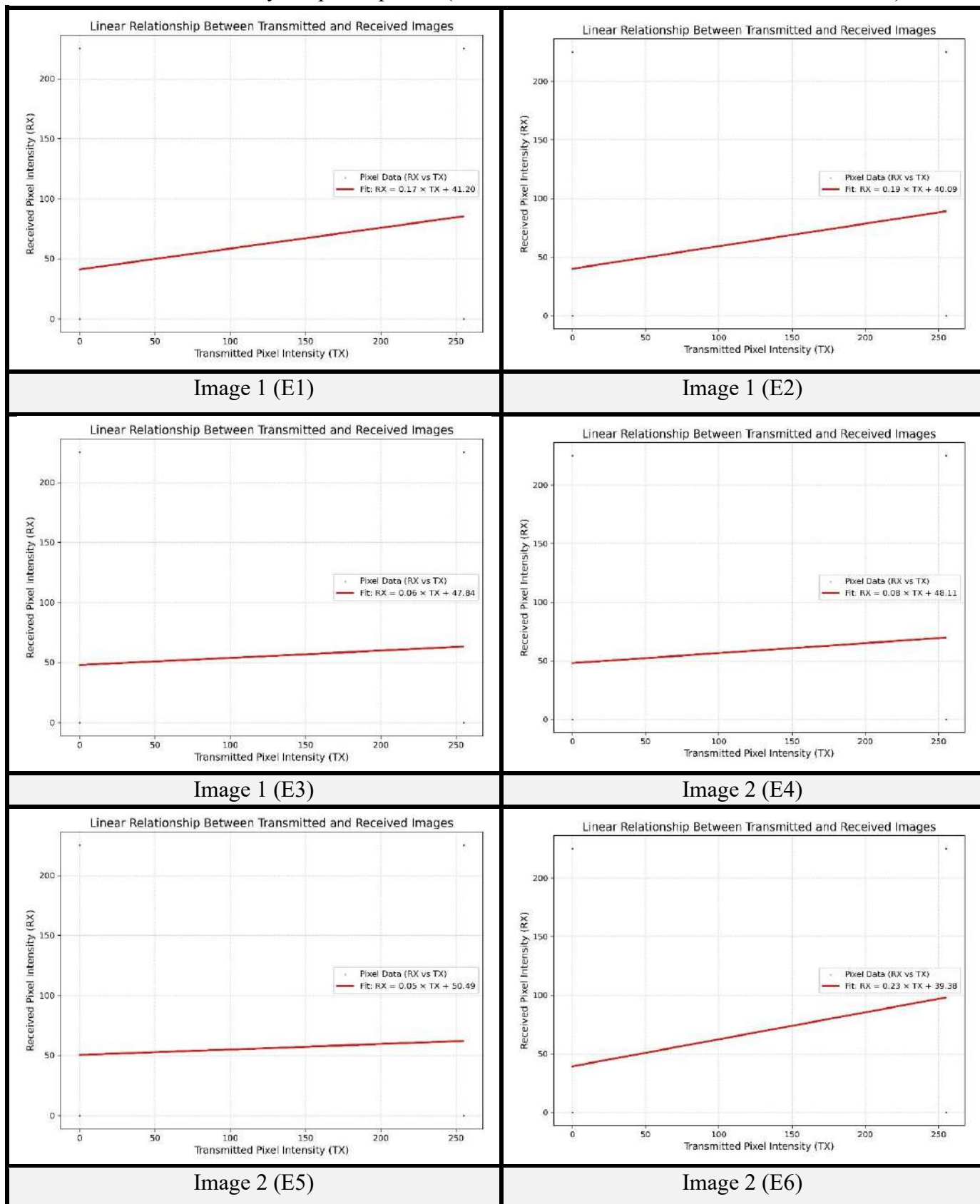
Image 2 (E4)		60			
Image 2 (E5)		70			
Image 2 (E6)		80			
Image 3 (E7)		60			
Image 3 (E8)		70			
Image 3 (E9)		80			

Table 4.56 Linearity Graph Properties (Two USRPs ENZ Receive Antenna - First Floor)

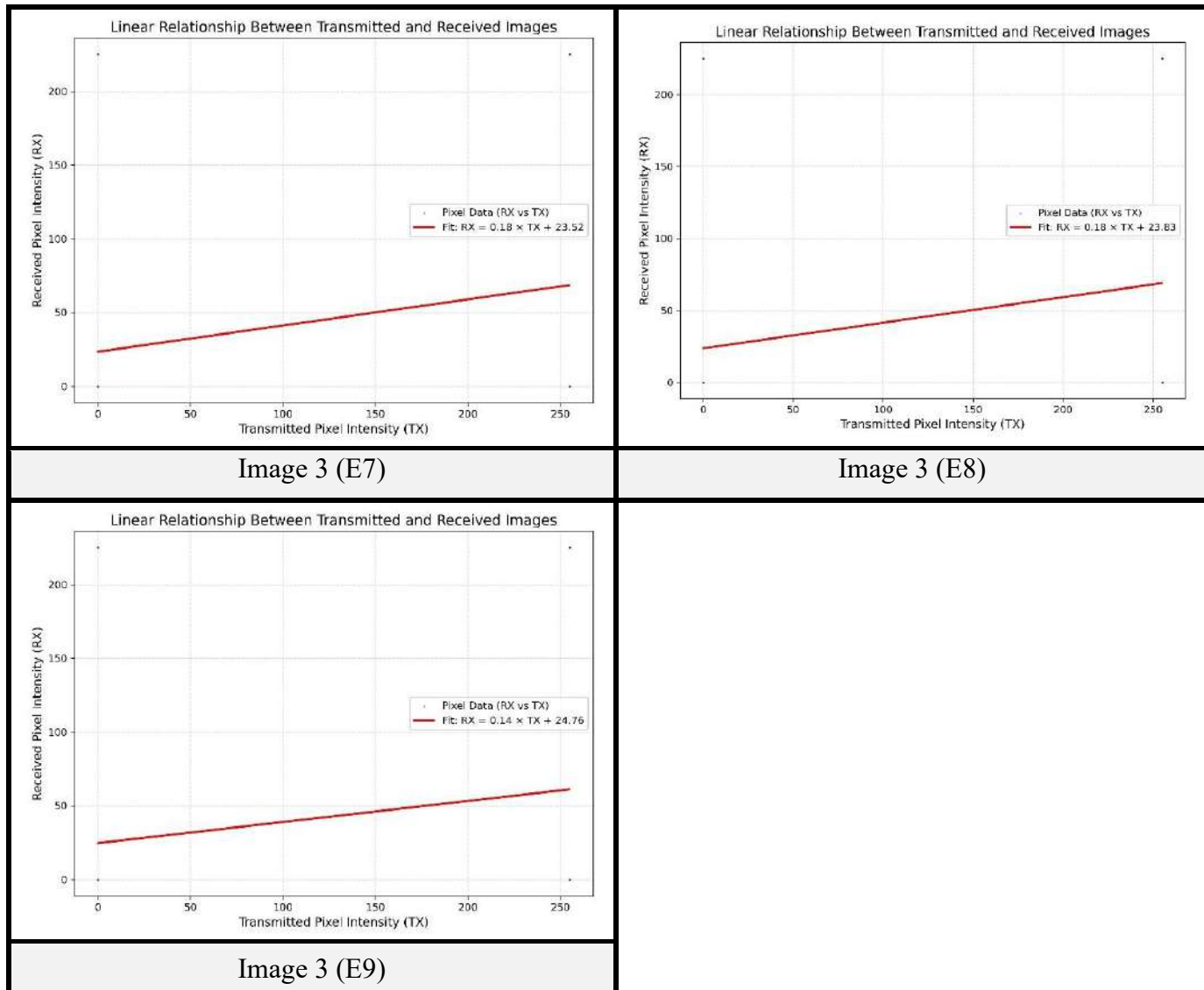


Table 4.57 Quantitative Performance Metrics (Two USRPs ENZ Receive Antenna - First Floor)

Image No.	Set Gain value (dB)	Pearson Correlation Coefficient	RMSE	PSNR (dB)	Normalized Cross-Correlation (NCC)	SSIM	Linear Fit Slope (m)	Linear Fit Intercept (c)
Image 1 (E1)	60	0.196327	6.231878	32.23843	0.196327	0.374059	0.173256	41.19513
Image 1 (E2)	70	0.217932	6.212946	32.26485	0.217932	0.417973	0.192323	40.08805
Image 1 (E3)	80	0.068407	6.348409	32.07751	0.068407	0.307975	0.060406	47.83763

Image 2 (E4)	60	0.096303	6.430373	31.96608	0.096303	0.338858	0.084961	48.1069
Image 2 (E5)	70	0.051464	6.469304	31.91365	0.051464	0.341895	0.045403	50.49456
Image 2 (E6)	80	0.260927	6.28814	32.16036	0.260927	0.43069	0.230264	39.38163
Image 3 (E7)	60	0.201144	4.786314	34.53078	0.201144	0.611896	0.17725	23.5179
Image 3 (E8)	70	0.20038	4.813169	34.48218	0.20038	0.602197	0.177375	23.82871
Image 3 (E9)	80	0.161847	4.822738	34.46493	0.161847	0.581907	0.142806	24.76114

- **For Slot Cut Patch Antenna (Rogers RO3003):** The on-site experimental setup for this antenna is shown in Figure 4.28. Visual results are presented in Table 4.58. Linearity graph properties are provided in Table 4.59. Quantitative performance metrics are in Table 4.60.



Fig. 4.28 On-site Experimental Setup

Table 4.58 Visual Experiment Results (Two USRPs Slot Cut Patch Antenna - First Floor)

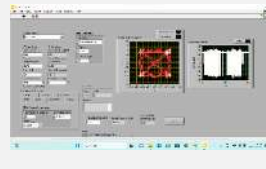
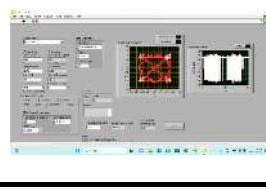
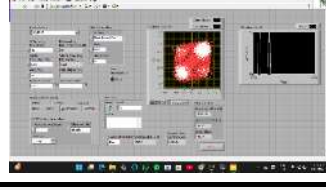
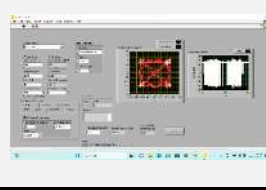
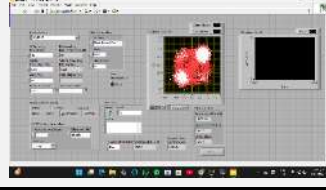
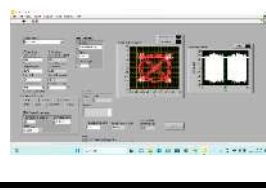
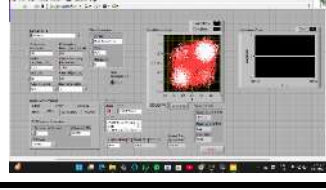
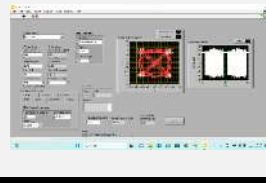
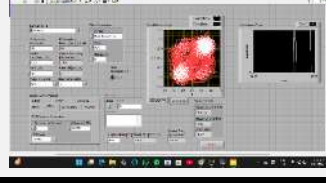
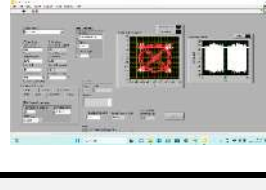
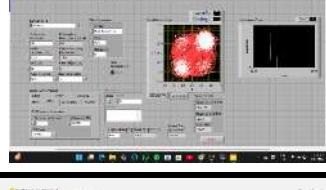
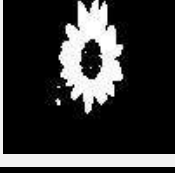
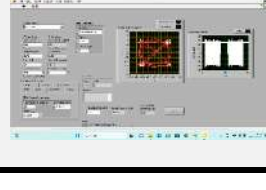
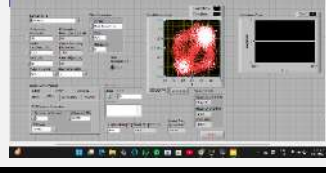
Image No.	Transmitted Image	Set Gain Value (dB)	Tx Front Panel	Rx Front Panel	Received Image
Image 1 (S1)		60			
Image 1 (S2)		70			
Image 1 (S3)		80			
Image 2 (S4)		60			
Image 2 (S5)		70			
Image 2 (S6)		80			
Image 3 (S7)		60			

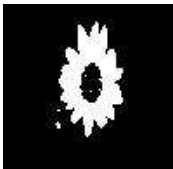
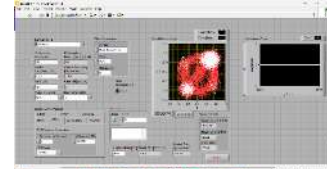
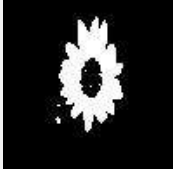
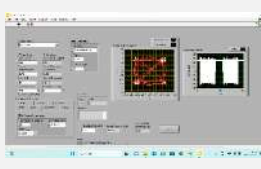
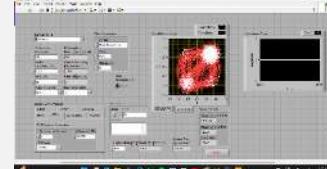
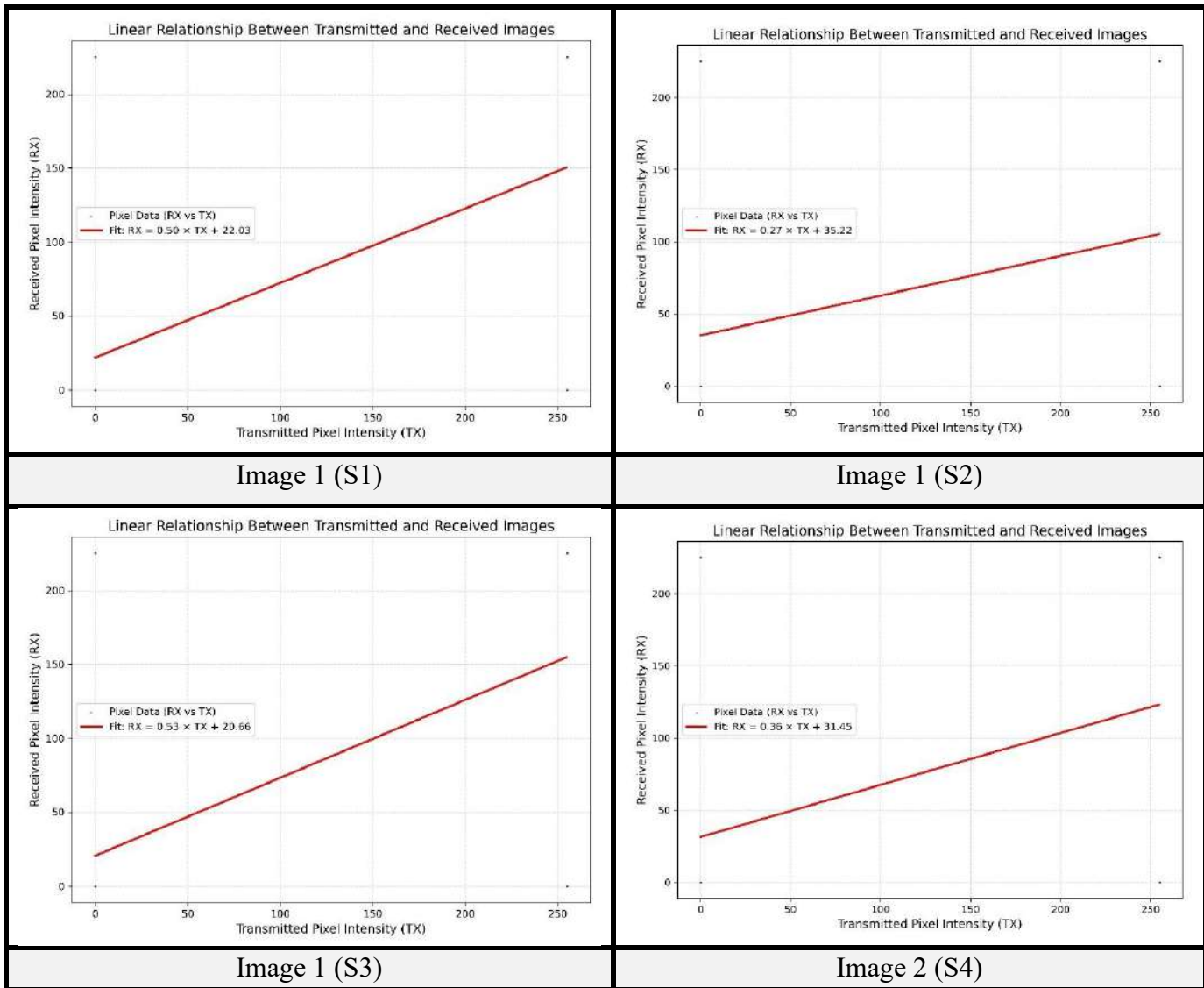
Image 3 (S8)		70			
Image 3 (S9)		80			

Table 4.59 Linearity Graph Properties (Two USRPs Slot Cut Patch Antenna - First Floor)



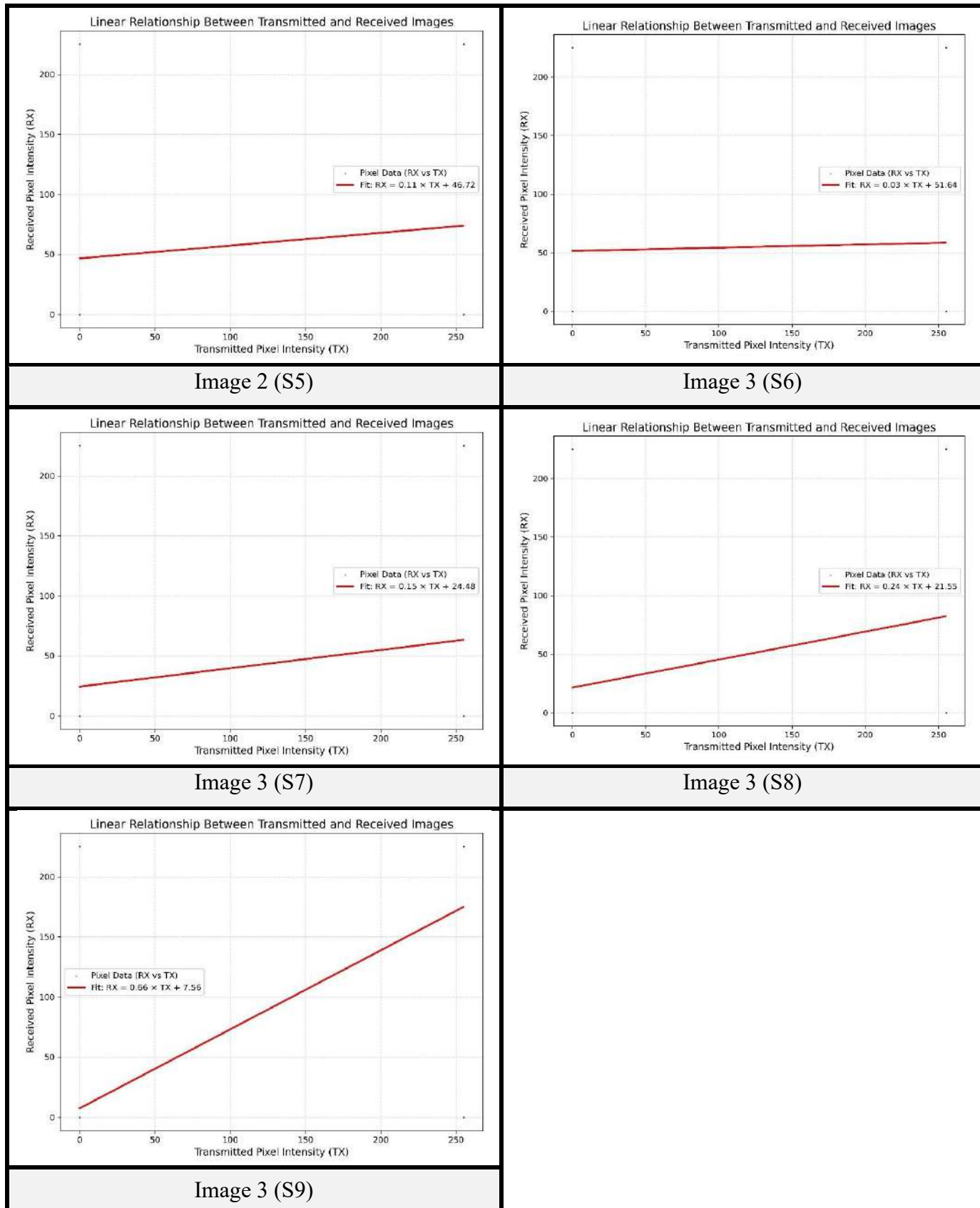


Table 4.60 Quantitative Performance Metrics (Two USRPs Slot Cut Patch Antenna - First Floor)

Image No.	Set Gain value (dB)	Pearson Correlation Coefficient	RMSE	PSNR (dB)	Normalized Cross-Correlation (NCC)	SSIM	Linear Fit Slope (m)	Linear Fit Intercept (c)
Image 1 (S1)	60	0.570796	5.896592	32.71878	0.570796	0.491726	0.5038	22.02512
Image 1 (S2)	70	0.311711	6.125847	32.38748	0.311711	0.397009	0.274954	35.22271
Image 1 (S3)	80	0.596822	5.8696	32.75863	0.596822	0.517736	0.526607	20.65583
Image 2 (S4)	60	0.408342	6.149837	32.35353	0.408342	0.45357	0.360144	31.45225
Image 2 (S5)	70	0.121106	6.404608	32.00095	0.121106	0.370044	0.106796	46.72147
Image 2 (S6)	80	0.030711	6.489985	31.88593	0.030711	0.331492	0.027102	51.64418
Image 3 (S7)	60	0.172902	4.818381	34.47278	0.172902	0.566216	0.15266	24.47623
Image 3 (S8)	70	0.270561	4.742362	34.61091	0.270561	0.630819	0.238731	21.54944
Image 3 (S9)	80	0.743995	4.375157	35.31093	0.743995	0.757924	0.656466	7.563025

- **For Parasitic Patch Antenna (Rogers RO3003):** The on-site experimental setup for this antenna is shown in Figure 4.29. Visual results are presented in Table 4.61. Linearity graph properties are provided in Table 4.62. Quantitative performance metrics are in Table 4.63.



Fig. 4.29 On-site Experimental Setup

Table 4.61 Visual Experiment Results (Two USRPs Parasitic Patch Antenna - First Floor)

Image No.	Transmitted Image	Set Gain Value (dB)	Tx Front Panel	Rx Front Panel	Received Image
Image 1 (PP1)		60			
Image 1 (PP2)		70			
Image 1 (PP3)		80			

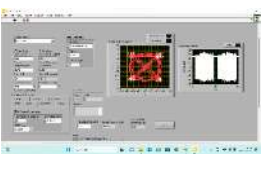
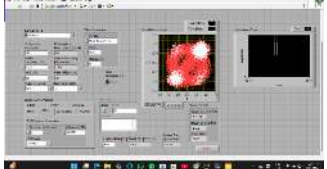
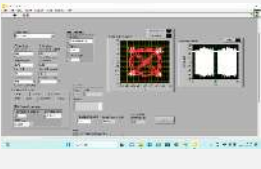
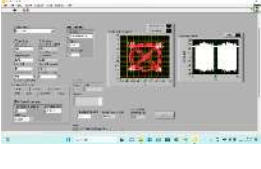
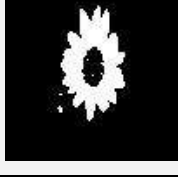
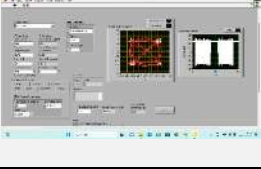
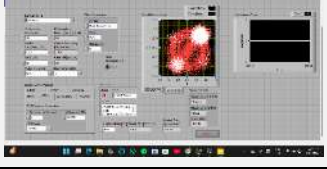
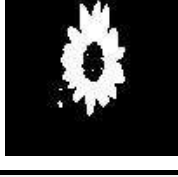
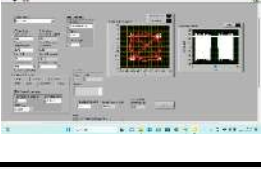
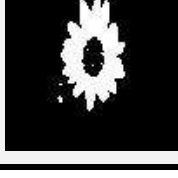
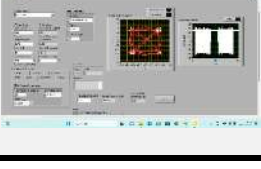
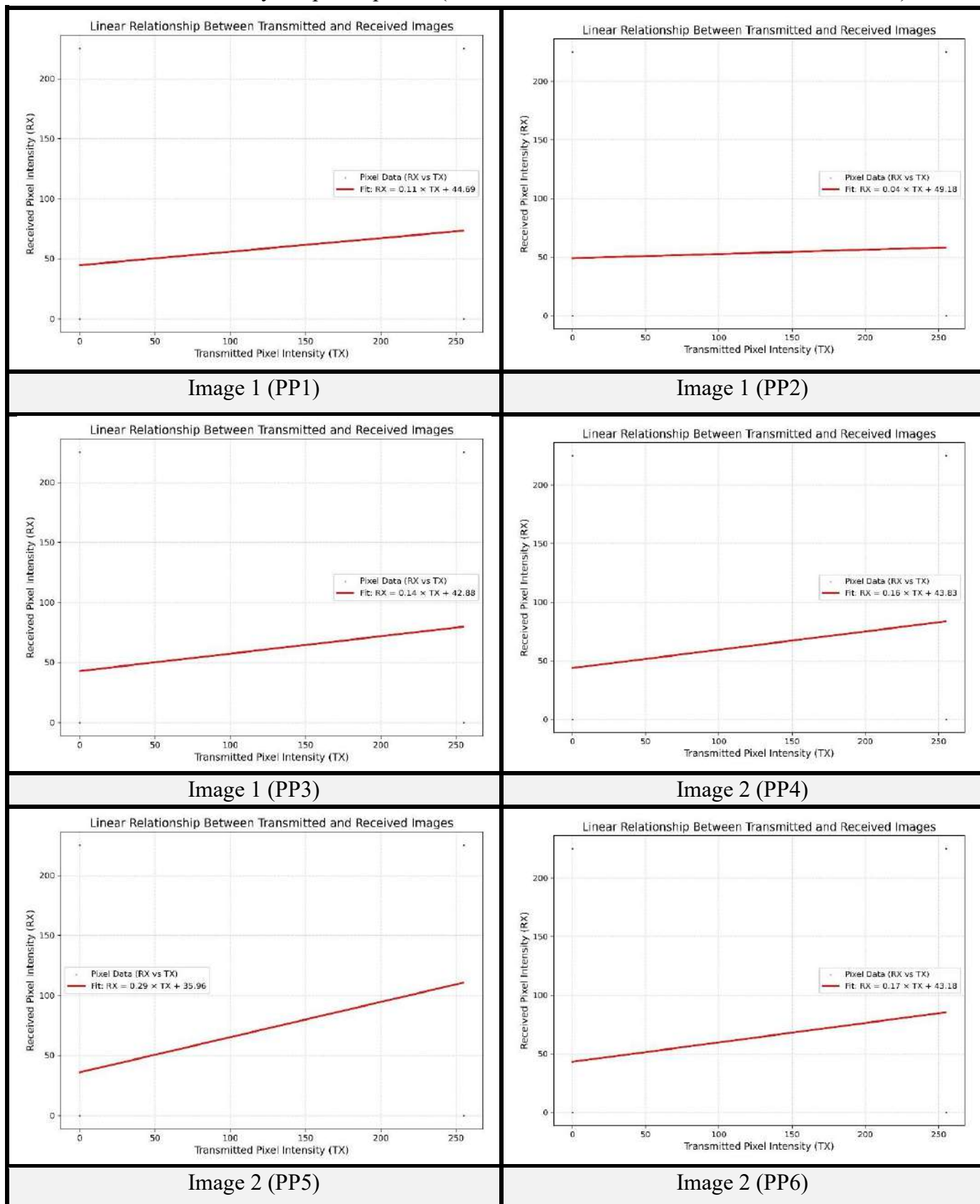
Image 2 (PP4)		60	 	
Image 2 (PP5)		70	 	
Image 2 (PP6)		80	 	
Image 3 (PP7)		60	 	
Image 3 (PP8)		70	 	
Image 3 (PP9)		80	 	

Table 4.62 Linearity Graph Properties (Two USRPs Parasitic Patch Antenna - First Floor)

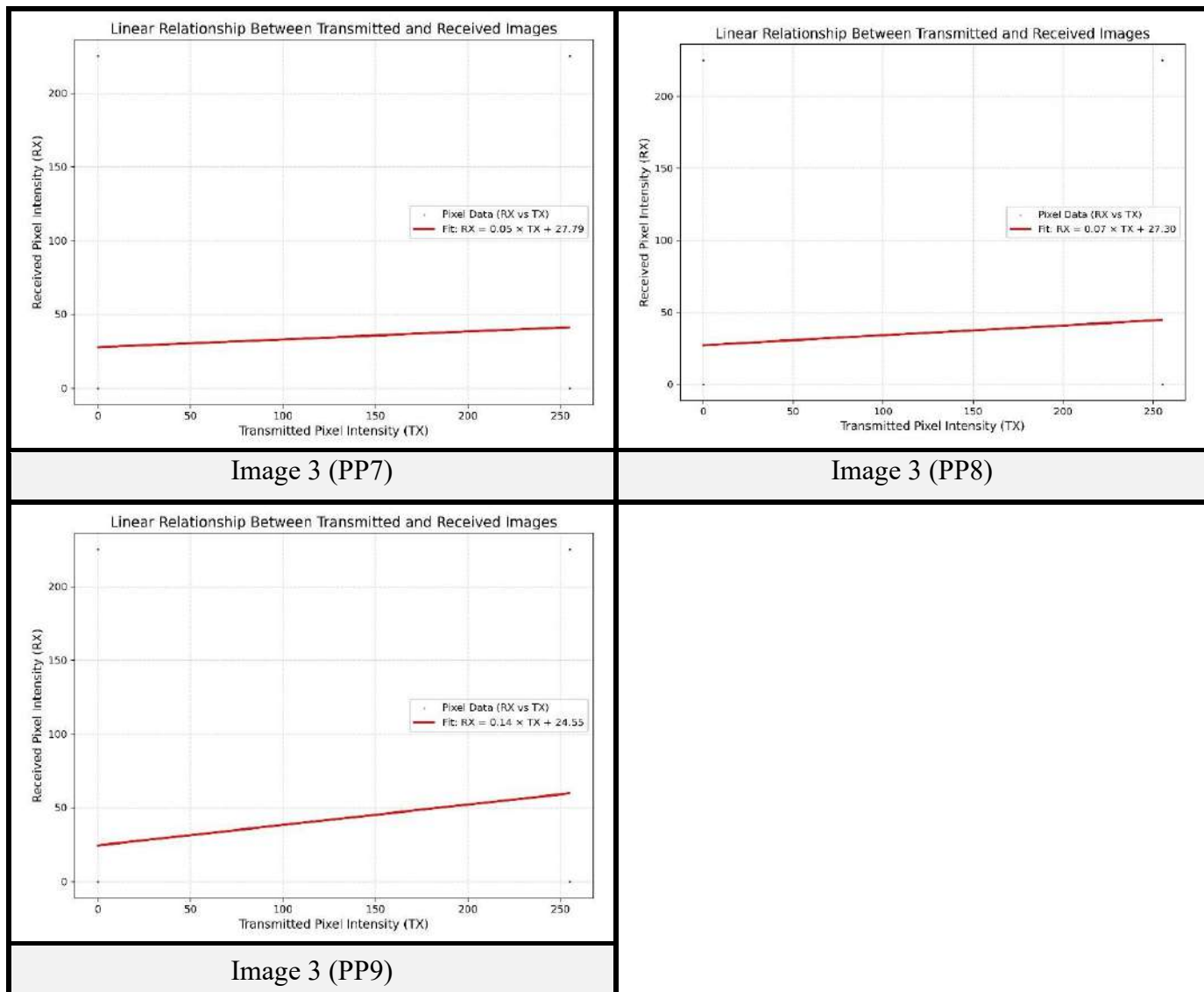


Table 4.63 Quantitative Performance Metrics (Two USRPs Parasitic Patch Antenna - First Floor)

Image No.	Set Gain value (dB)	Pearson Correlation Coefficient	RMSE	PSNR (dB)	Normalized Cross-Correlation (NCC)	SSIM	Linear Fit Slope (m)	Linear Fit Intercept (c)
Image 1 (PP1)	60	0.127679	6.290246	32.15745	0.127679	0.346574	0.112658	44.69118
Image 1 (PP2)	70	0.040106	6.365689	32.05389	0.040106	0.329819	0.035387	49.17778
Image 1 (PP3)	80	0.164177	6.262755	32.1955	0.164177	0.349199	0.144929	42.88489

Image 2 (PP4)	60	0.176967	6.36111 6	32.0601 4	0.176967	0.37675 7	0.156147	43.8327
Image 2 (PP5)	70	0.331486	6.24853 6	32.2152 4	0.331486	0.42224 3	0.293252	35.96227
Image 2 (PP6)	80	0.187958	6.34729 1	32.0790 4	0.187958	0.38212 3	0.165773	43.1842
Image 3 (PP7)	60	0.060012	4.89870 4	34.3291 8	0.060012	0.54771 9	0.052969	27.79153
Image 3 (PP8)	70	0.077401	4.88800 6	34.3481 7	0.077401	0.52588 5	0.068339	27.29941
Image 3 (PP9)	80	0.157493	4.79579	34.5136	0.157493	0.58012	0.138243	24.55393

- **For Patch Antenna (FR4 Material):** The on-site experimental setup for this antenna is shown in Figure 4.30. Visual results are presented in Table 4.64. Linearity graph properties are provided in Table 4.65. Quantitative performance metrics are in Table 4.66.



Fig. 4.30 On-site Experimental Setup

Table 4.64 Visual Experiment Results (Two USRPs Patch Antenna - FR4 Material - First Floor)

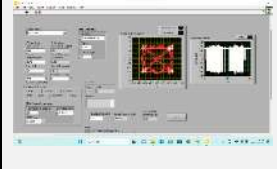
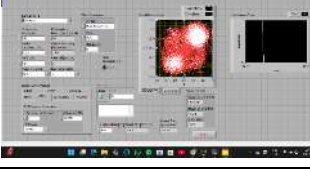
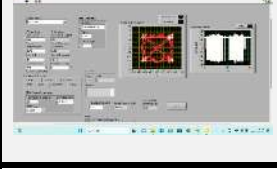
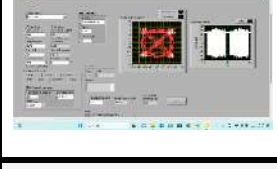
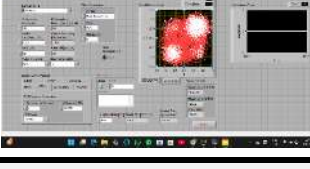
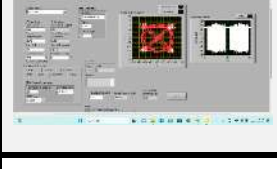
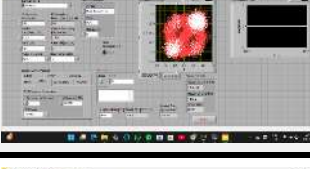
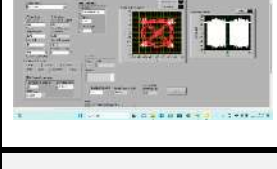
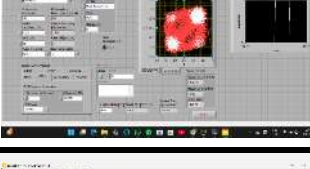
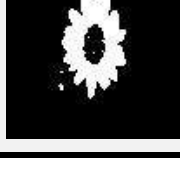
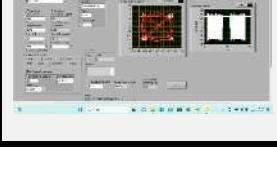
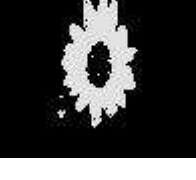
Image No.	Transmitted Image	Set Gain Value (dB)	Tx Front Panel	Rx Front Panel	Received Image
Image 1 (P1)		60			
Image 1 (P2)		70			
Image 1 (P3)		80			
Image 2 (P4)		60			
Image 2 (P5)		70			
Image 2 (P6)		80			
Image 3 (P7)		60			

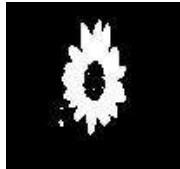
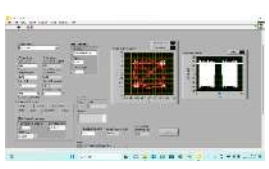
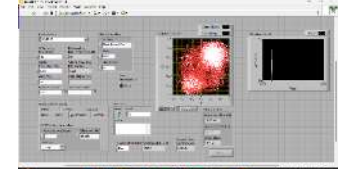
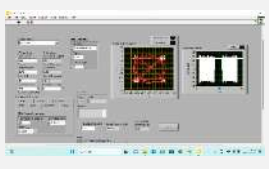
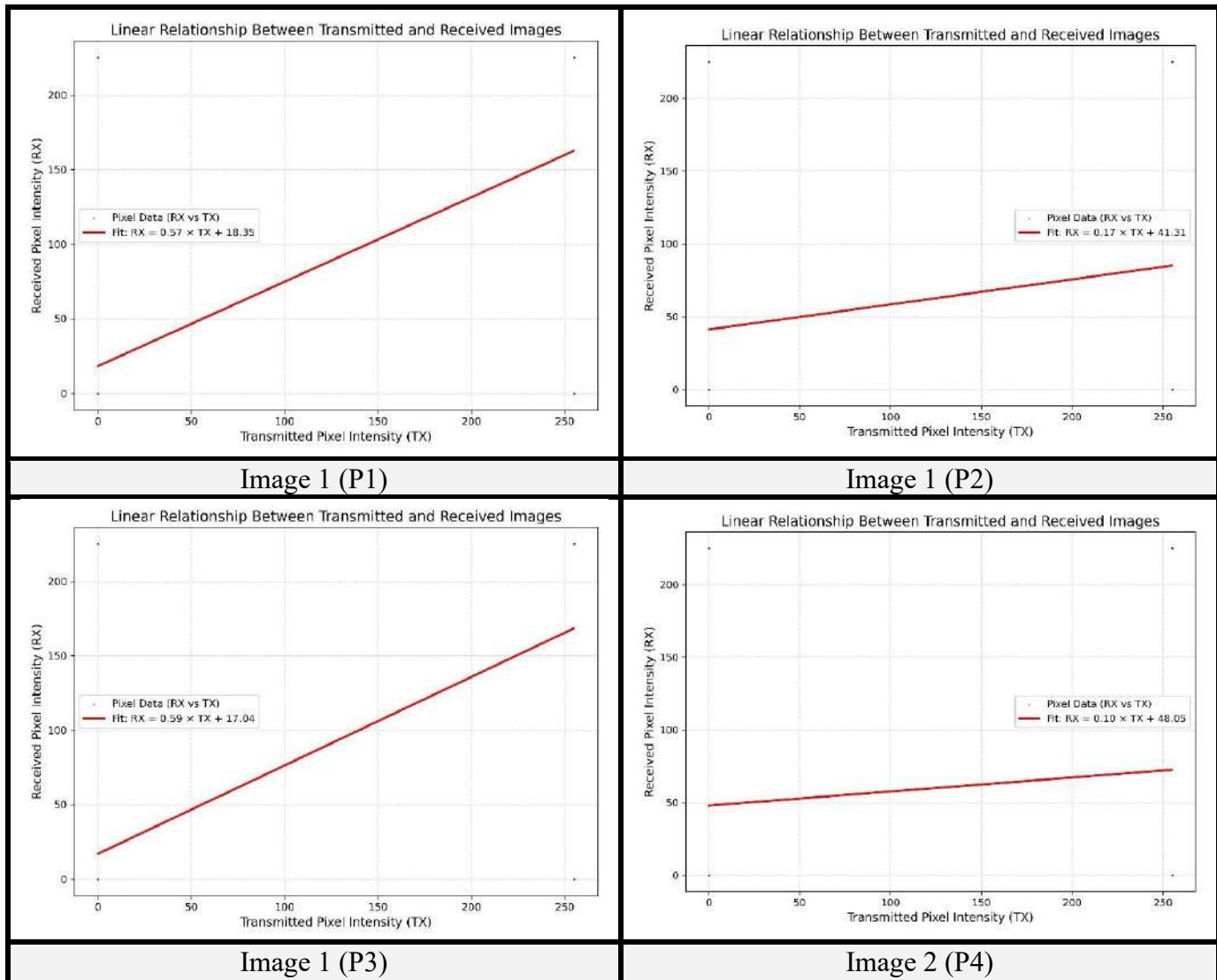
Image 3 (P8)		70			
Image 3 (P9)		80			

Table 4.65 Linearity Graph Properties (Two USRPs Patch Antenna - FR4 Material - First Floor)



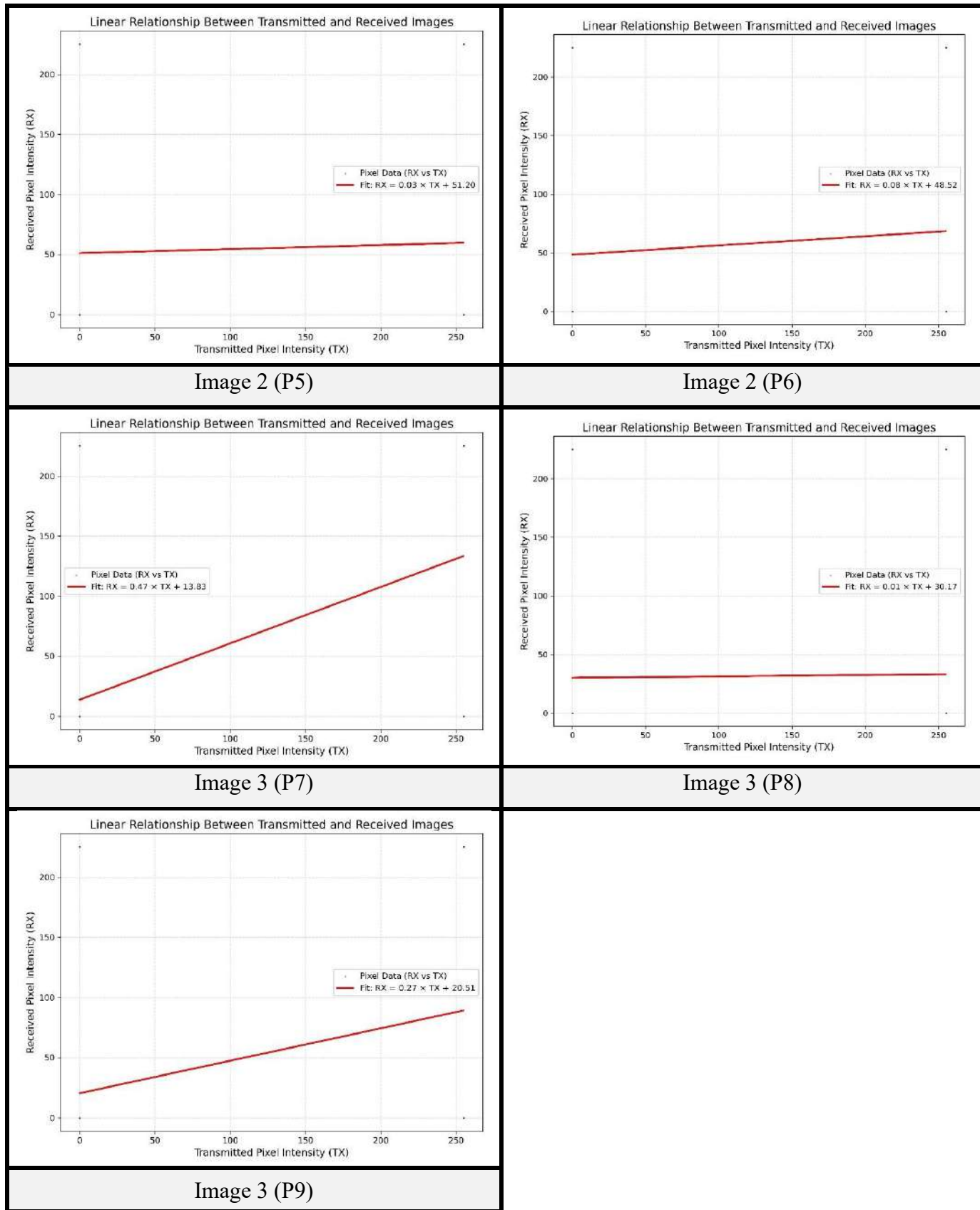


Table 4.66 Quantitative Performance Metrics (Two USRPs Patch Antenna - First Floor)

Image No.	Set Gain value (dB)	Pearson Correlation Coefficient	RMSE	PSNR (dB)	Normalized Cross-Correlation (NCC)	SSIM	Linear Fit Slope (m)	Linear Fit Intercept (c)
Image 1 (P1)	60	0.641406	5.82660 3	32.8225	0.641406	0.53937 8	0.565859	18.35427
Image 1 (P2)	70	0.19487	6.23596 8	32.2327 3	0.19487	0.32938 9	0.172024	41.31167
Image 1 (P3)	80	0.671697	5.81839 3	32.8347 4	0.671697	0.55339 5	0.593863	17.04325
Image 2 (P4)	60	0.1088	6.45787 1	31.9290 2	0.1088	0.31815 7	0.096375	48.04795
Image 2 (P5)	70	0.038178	6.48079 5	31.8982 4	0.038178	0.30707 4	0.033682	51.20202
Image 2 (P6)	80	0.088962	6.43813 6	31.9556	0.088962	0.34821 9	0.078496	48.51959
Image 3 (P7)	60	0.531827	4.54339 1	34.9832	0.531827	0.68975 7	0.469259	13.83101
Image 3 (P8)	70	0.013448	5.01569 5	34.1241 8	0.013448	0.39904 2	0.01204	30.1744
Image 3 (P9)	80	0.305631	4.71614 2	34.6590 7	0.305631	0.63981 8	0.269674	20.51341

➤ **Experiment 5 [Fixed DNI Tx, Varied Rx Antennas (Second Floor)]**

This experiment aimed to check image transfer performance at a significant vertical distance of 700 cm on the second floor from the ground floor laboratory where the transmitter was located. The Metamaterial Double Negative Index (DNI) antenna stayed as the transmitting antenna. The IQ Sampling Rate was fixed at 1M S/sec. Images were sent with varying gain settings: Image 1 with 60 dB, Image 2 with 70 dB, and Image 3 with 80 dB. However, reliable image transfer was not consistently achieved in this scenario. The conceptual diagram for this setup is shown in Figure 4.31.

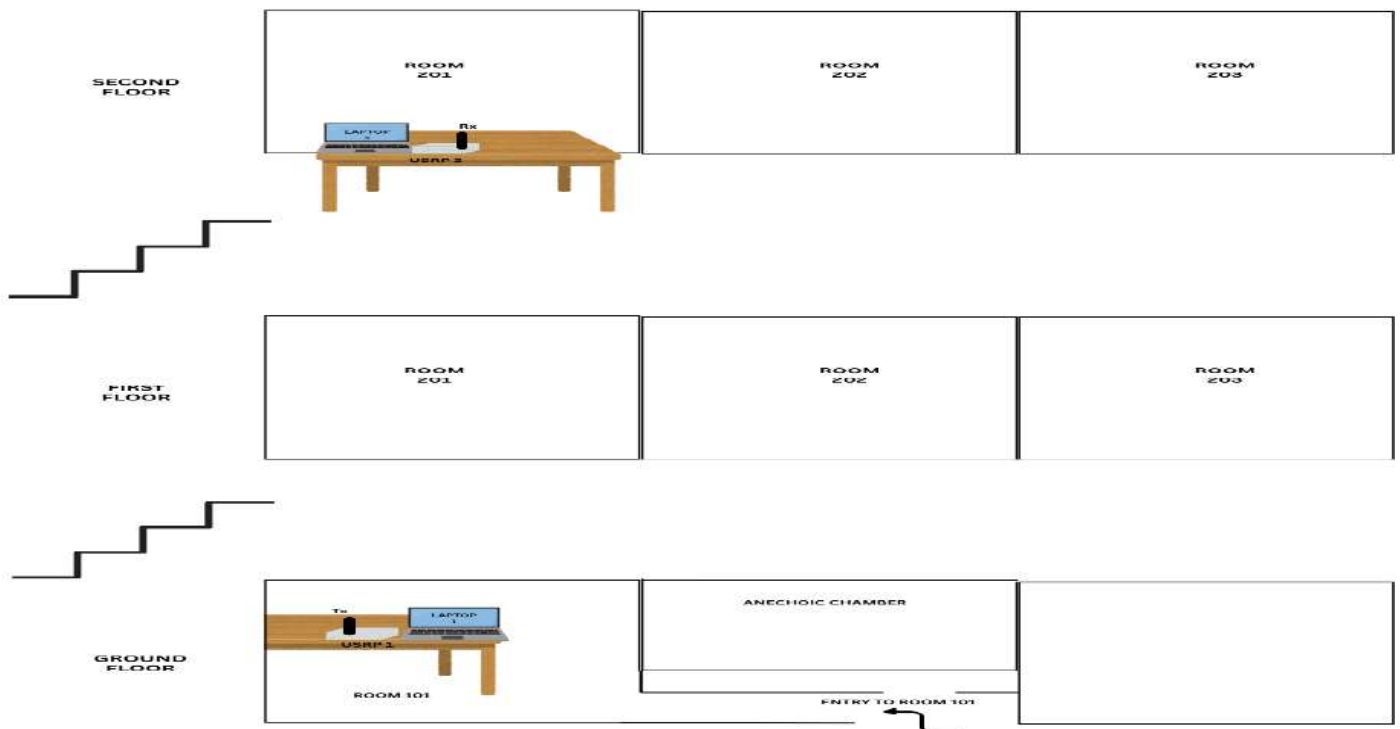


Fig. 4.31 Conceptual Diagram

- **For Metamaterial Epsilon Near Zero (ENZ) Receive Antenna:** The on-site experimental setup for this antenna is shown in Figure 4.32. Visual results are presented in Table 4.67.



Fig. 4.32 On-site Experimental Setup

Table 4.67 Visual Experiment Results (Two USRPs ENZ Receive Antenna - Second Floor)

Image No.	Transmitted Image	Set Gain Value (dB)	Tx Front Panel	Rx Front Panel	Received Image
Image 1		60			
Image 2		70			
Image 3		80			

- **For Slot Cut Patch Antenna (Rogers RO3003):** The on-site experimental setup for this antenna is shown in Figure 4.33. Visual results are presented in Table 4.68.



Fig. 4.33 On-site Experimental Setup

Table 4.68 Visual Experiment Results (Two USRPs Slot Cut Patch Antenna - Second Floor)

Image No.	Transmitted Image	Set Gain Value (dB)	Tx Front Panel	Rx Front Panel	Received Image
Image 1		60			
Image 2		70			
Image 3		80			

- For Parasitic Patch Antenna (Rogers RO3003): For Parasitic Patch Antenna (Rogers RO3003) The on-site experimental setup for this antenna is shown in Figure 4.34. Visual results are presented in Table 4.69.



Fig. 4.34 On-site Experimental Setup

Table 4.69 Visual Experiment Results (Two USRPs Parasitic Patch Antenna - Second Floor)

Image No.	Transmitted Image	Set Gain Value (dB)	Tx Front Panel	Rx Front Panel	Received Image
Image 1		60			
Image 2		70			
Image 3		80			

- **For Patch Antenna (FR4 Material):** The on-site experimental setup for this antenna is shown in Figure 4.35. Visual results are presented in Table 4.70.

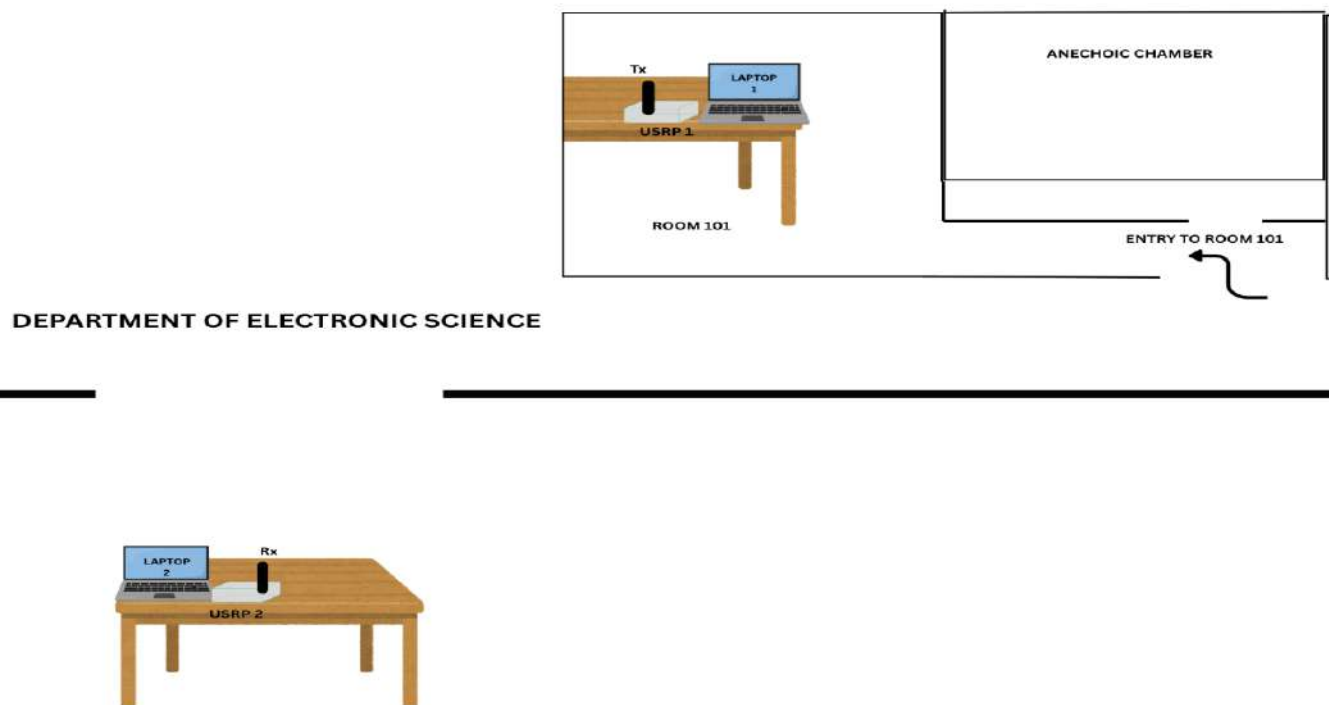


Fig. 4.35 On-site Experimental Setup

Table 4.70 Visual Experiment Results (Two USRPs Patch Antenna - Second Floor)

Image No.	Transmitted Image	Set Gain Value (dB)	Tx Front Panel	Rx Front Panel	Received Image
Image 1		60			
Image 2		70			
Image 3		80			

- **Experiment 6 [Fixed DNI Tx, Varied Rx Antennas (Outside Department Main Gate)]:** This experiment took the assessment to an outdoor location near the department's main gate, where there was no direct line of sight. The Metamaterial Double Negative Index (DNI) antenna remained fixed as the transmitting antenna. The IQ Sampling Rate was fixed at 1M S/sec, and the only gain setting attempted was 80 dB (for Image 1). However, in this location, transmission was very poor, meaning a reliable wireless connection could not be made under these tough conditions. The conceptual diagram for this setup is shown in Figure 4.36.



- **For Metamaterial Epsilon Near Zero (ENZ) Receive Antenna:** The on-site experimental setup for this antenna is shown in Figure 4.37. Visual results are presented in Table 4.71.



Fig. 4.37 On-site Experimental Setup

Table 4.71 Visual Experiment Results (ENZ Receive Antenna - Outside Department Main Gate)

Image No.	Transmitted Image	Set Gain Value (dB)	Tx Front Panel	Rx Front Panel	Received Image
Image 1		80			

- For Slot Cut Patch Antenna (Rogers RO3003): The on-site experimental setup for this antenna is shown in Figure 4.38. Visual results are presented in Table 4.72.



Fig. 4.37 On-site Experimental Setup

Table 4.72 Visual Experiment Results (Slot Cut Patch Antenna - Outside Department Main Gate)

Image No.	Transmitted Image	Set Gain Value (dB)	Tx Front Panel	Rx Front Panel	Received Image
Image 1		80			

- **For Parasitic Patch Antenna (Rogers RO3003):** The on-site experimental setup for this antenna is shown in Figure 4.39. Visual results are presented in Table 4.73.



Fig. 4.39 On-site Experimental Setup

Table 4.73 Visual Experiment Results (Parasitic Patch Antenna - Outside Department Main Gate)

Image No.	Transmitted Image	Set Gain Value (dB)	Tx Front Panel	Rx Front Panel	Received Image
Image 1		80			

- **For Patch Antenna (FR4 Material):** The on-site experimental setup for this antenna is shown in Figure 4.40. Visual results are presented in Table 4.74.



Fig. 4.40 On-site Experimental Setup

Table 4.74 Visual Experiment Results (Patch Antenna - Outside Department Main Gate)

Image No.	Transmitted Image	Set Gain Value (dB)	Tx Front Panel	Rx Front Panel	Received Image
Image 1		80			

4.3 Discussion and Comparative Analysis

This section discusses and compares the results from our wireless image transfer experiments. We will first explain how image quality is measured in this study. After that, we will show graphs that compare how well different antennas performed in various tests.

4.3.1 Understanding Image Quality Metrics

Several measurements were used to evaluate how well the wireless image transfer system performed. These measurements came from Python-based analysis of the transmitted and received images. These metrics provide objective ways to judge how true the received image is to the original and how similar its structure is.

- **Peak Signal-to-Noise Ratio (PSNR):** PSNR measures image quality by comparing the strongest possible power of a signal to the power of the unwanted noise affecting it. It's expressed in decibels (dB). A higher PSNR value means there's less noise and the image quality is better.
- **Structural Similarity Index (SSIM):** SSIM checks image quality by looking at changes in structural information, brightness, and contrast between the original and the rebuilt images. Its value usually goes from -1 to 1, with a value closer to 1 meaning higher structural similarity and better perceived visual quality.
- **Root Mean Squared Error (RMSE):** RMSE measures the average size of the difference between the pixel values of the original and the rebuilt images. It's calculated as the square root of the average of the squared differences between the two images. A lower RMSE value means better image accuracy.
- **Normalized Cross-Correlation (NCC):** NCC measures how similar the overall pattern and shape are between the original and received image signals. Its value ranges from -1 to 1, where a value closer to 1 shows a stronger positive correlation and higher signal similarity.

- **Pearson Correlation Coefficient:** This coefficient measures the linear relationship between the pixel strengths of the transmitted and received images. A value close to 1 indicates a strong positive linear correlation, meaning the pixel values are reproduced with high accuracy.

- **Linear Fit Slope (m) and Intercept (c):** These numbers come from a straight-line (linear regression) model ($RX = m \times TX + c$) applied to a scatter plot where received pixel strength is plotted against transmitted pixel strength. The Slope (m) tells us how much the received pixel values scale compared to the transmitted ones; an ideal value is 1. The Intercept (c) represents any constant shift in received pixel values when the transmitted value is zero; an ideal value is 0. Slope values near 1 and intercept values near 0 show that the image transfer is very linear and faithful.

For visual performance comparisons in this study, the Structural Similarity Index (SSIM) is chosen as the main parameter for showing results in graphs. SSIM provides a strong and visually relevant way to measure image quality.

4.3.2 Graphical Performance Comparisons

This part presents graphs that compare the performance for the relevant experimental setups, showing the trends for different antenna arrangements. For experiments where multiple receiving antennas were used, each graph will have four distinct lines, representing the performance of the Metamaterial Epsilon Near Zero (ENZ), Parasitic Patch, Slot Cut Patch, and Patch FR4 receiving antennas. The X-axis will represent the varying gain (in dB), and the Y-axis will represent the SSIM values.

Exclusions for Graphing: Graphs will not be created for the "Initial Testing" phases (both single and two USRP setups), as these were basic checks. Graphs will also be left out for Experiment 5 (Second Floor) and Experiment 6 (Outside Department Main Gate), because wireless signal transmission was not consistently achieved or was very poor in these challenging conditions, making it impossible to get meaningful numbers for analysis.

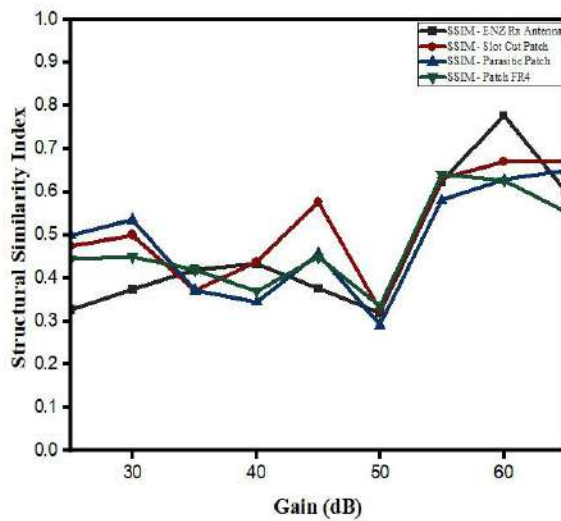


Fig. 4.41 SSIM Performance (Single USRP)

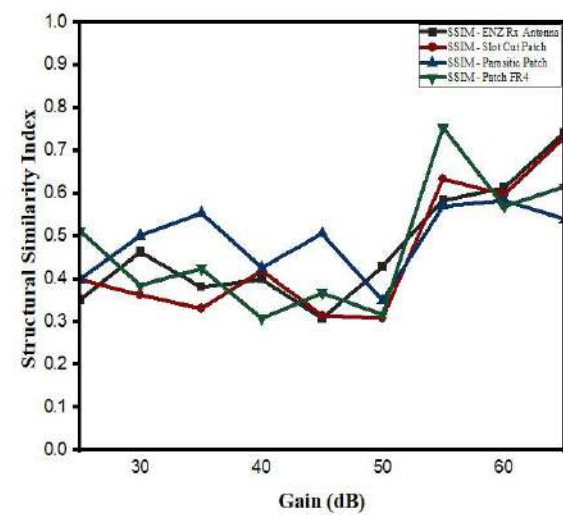


Fig. 4.42 SSIM Performance (LOS 195 cm)

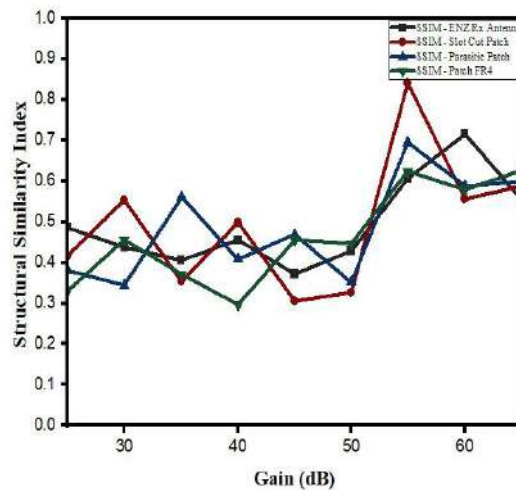


Fig. 4.43 SSIM Performance (Slant LOS 195 cm)

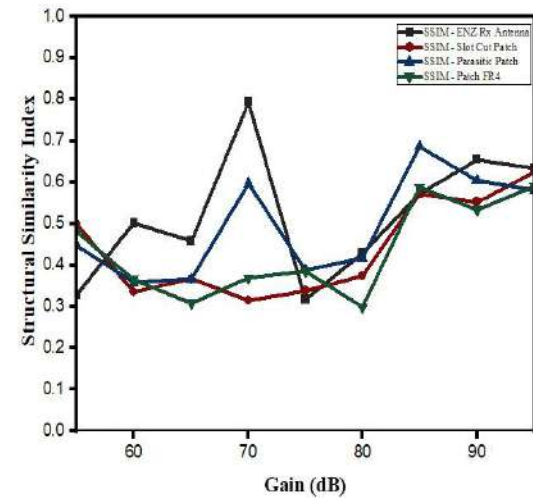


Fig. 4.44 SSIM Performance (Ground Floor)

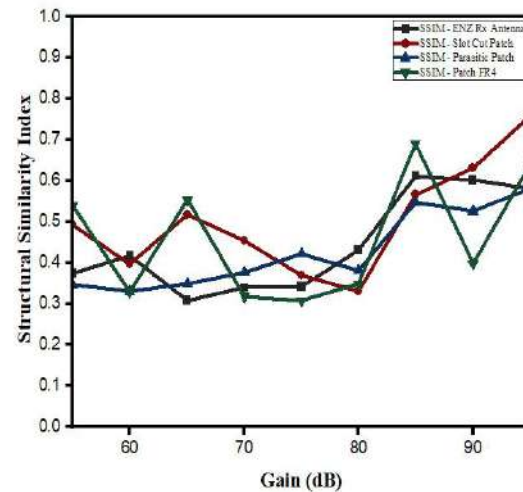


Fig. 4.45 SSIM Performance (First Floor)

4.3.3 Overall Discussion of Antenna Performance

The comparison across various challenging conditions shows clear differences in how the receiving antennas performed, especially when looking at SSIM, which directly shows image quality.

In the single USRP setup, where the IQ sampling rate was 250k S/sec and gain changed from 30 dB to 50 dB, the Parasitic Patch antenna generally showed the highest SSIM values. The Slot Cut Patch antenna also performed very well, often coming very close to the Parasitic Patch. Both the Metamaterial Epsilon Near Zero (ENZ) Rx Antenna and the Patch FR4 antenna showed lower SSIM values in this situation. As the gain increased, all antennas generally showed an improvement in SSIM.

Moving to the two USRPs setup in a direct line-of-sight (LOS) condition at 195 cm with an IQ sampling rate of 250k S/sec, the Parasitic Patch antenna and Slot Cut Patch antenna continued to perform strongly, often getting higher SSIM values than the ENZ Rx Antenna and Patch FR4 antenna. While the ENZ Rx Antenna showed competitive results, the Patch FR4 antenna consistently had the lowest image quality in this setup.

Under a slanted line-of-sight condition at 140 cm inside the lab with two USRPs and an IQ sampling rate of 250k S/sec, the overall SSIM values were generally lower than in direct LOS. This reflects the increased difficulty. In this setup, the Slot Cut Patch antenna and ENZ Rx Antenna showed the best performance, keeping higher SSIM values. The Parasitic Patch antenna had moderate performance, while the Patch FR4 antenna consistently showed the lowest image quality.

For the outdoor ground floor situation, using two USRPs with an IQ sampling rate of 1M S/sec and higher gains (60-80 dB), the ENZ Rx Antenna and Parasitic Patch antenna generally kept the highest SSIM values. The Slot Cut Patch antenna showed competitive performance, but the Patch FR4 antenna struggled the most in this environment, giving the lowest SSIM.

Finally, at the first-floor location, which involved a vertical distance of 310 cm, the ENZ Rx Antenna consistently showed the best performance in terms of SSIM, especially at higher gain levels. The Parasitic Patch antenna and Slot Cut Patch antenna also performed acceptably, but the Patch FR4 antenna continued to show the lowest SSIM values. The SSIM values at this vertical distance were even lower compared to ground floor or LOS experiments, which shows how much vertical distance and obstacles (like floors) affect signal quality.

In summary, across various challenging conditions, the ENZ Rx Antenna, Parasitic Patch antenna, and Slot Cut Patch antenna generally performed better in terms of SSIM compared to the Patch FR4 antenna, with their specific strengths changing a little depending on the environment and gain levels. Higher gain levels generally led to better SSIM for all antennas, but the impact of distance and obstacles had a big effect on the overall image quality.

CHAPTER 5

CONCLUSION AND FUTURE WORK

5.1 Conclusion

This project successfully built and tested a system that can send images wirelessly using Software Defined Radio (SDR) principles. We used USRP hardware, controlled by LabVIEW, and analyzed the results with Python. The main goal was to see how well different antennas would work for sending images wirelessly at the 5.8 GHz frequency, which is useful for communication systems where dependable data transfer is key.

We were able to achieve stable wireless image transfer with our system. Our tests clearly showed that the choice of antenna made a big difference in how well the system performed. For example, the Parasitic Patch and Slot Cut Patch antennas generally gave better image quality, shown by higher SSIM values, when tested in the lab. The Metamaterial Epsilon Near Zero (ENZ) Rx Antenna also performed well, especially in tests where there was a clear line of sight and when the antennas were at a slight angle to each other.

We also found that the quality of the image got worse as the distance between the antennas increased or when there were obstacles in the way. This happened even when we used higher power settings. In very difficult places, like on the second floor of a building or outside the department gate, it was either very hard to send images wirelessly or completely impossible to establish a reliable connection.

Overall, this project successfully demonstrated how to create and evaluate a wireless image transfer system. It also helped us identify which antennas work best in different environments for this kind of application.

5.2 Future Work

Based on what we learned from this study, there are several areas where future work could be done:

- **Antenna Design Improvements:** We could look for ways to make the metamaterial antennas smaller while still keeping their high performance. Another idea is to develop antennas that can change their shape or direction to adapt to how signals are moving.
- **System Robustness:** We could try testing other types of modulation techniques (besides QPSK) or more advanced error-correction methods. This would help improve image quality even in very noisy environments.
- **Real-time Video:** A big next step would be to expand this system to send live video streams. This would involve managing a lot more data at a much faster rate.
- **Extended Range Tests:** It would be helpful to do more outdoor experiments over longer distances and in different types of terrain. This would give us a better understanding of the limits and challenges in real-world situations.

REFERENCES

- [1] A. Doufexi, A. Nix, and D. Bull, "Robust Wireless Image Transmission using Jointly-Optimized Modulation and Source Coding," in *Proc. IEEE 51st Vehicular Technology Conference (VTC)*, Tokyo, Japan, 2000, vol. 3, pp. 2039-2043.
- [2] G. Kolumbán, T. I. Krébesz, and F. C. M. Lau, "Theory and Application of Software Defined Electronics: Design Concepts for the Next Generation of Telecommunications and Measurement Systems," *IEEE Circuits and Systems Magazine*, vol. 12, no. 2, pp. 8-34, 2012.
- [3] T. B. Welch and S. Shearman, "LabVIEW, the USRP, and their Implications on Software Defined Radio," in *Proc. ASEE Annual Conference & Exposition*, Vancouver, BC, Canada, 2011, pp. 22.998.1-22.998.13.
- [4] T. B. Welch and S. Shearman, "Teaching software defined radio using the USRP and LabVIEW," in *Proc. IEEE International Conference on Acoustics, Speech, and Signal Processing (ICASSP)*, Kyoto, Japan, 2012, pp. 2789-2792.
- [5] K. C.-M. Teng, "The Design and Evaluation of a 5.8 GHz Laptop-Based Radar System," Master's Thesis, Purdue University, West Lafayette, IN, 2013. [Online].
- [6] M. Chandra, D. Agarwal, and A. Bansal, "Image Transmission through Wireless Channel: A Review," in *1st IEEE International Conference on Power Electronics, Intelligent Control and Energy Systems (ICPEICES-2016)*, Delhi, India, 2016, pp. 1-4.
- [7] R. S. Chadhar and A. Rai, "An Efficient Digital Modulation Technique for Image Transmission over Wireless Channel," *International Journal of Scientific Progress and Research (IJSR)*, vol. 24, no. 01, 2016.
- [8] S. A. Aliesawi, D. S. Alani, and A. M. Awad, "Secure image transmission over wireless network," *International Journal of Engineering & Technology*, vol. 7, no. 4, pp. 2758-2764, 2018.
- [9] A. Mishra and C. Li, "A Low Power 5.8-GHz ISM-Band Intermodulation Radar System for Target Motion Discrimination," *IEEE Sensors Journal*, vol. 19, no. 19, pp. 8839-8846, Oct. 2019.
- [10] H. Ö. Yilmaz and F. Yaman, "Meta-material Antenna Designs for a 5.8 GHz Doppler Radar," *IEEE Transactions on Instrumentation and Measurement*, vol. 69, no. 4, pp. 1775-1782, Apr. 2020.
- [11] M. J. Mohsin, W. K. Saad, B. J. Hamza, and W. A. Jabbar, "Performance analysis of image transmission with various channel conditions/modulation techniques," *TELKOMNIKA Telecommunication, Computing, Electronics and Control*, vol. 18, no. 3, pp. 1158-1168, 2020.
- [12] J. Merlo, S. Vakalis, C. Hilton, and J. Randall, "5.8-GHz FMCW Radar System for Drone Tracking," Unpublished Project Report.
- [13] S. N, N. T. K. Reddy, E. S. Tarun, K. S. Eswar, and P. Nagendra, "Image Transmission using USRP through LabVIEW," in *2022 IEEE North Karnataka Subsection Flagship International Conference (NKCon)*, 2022, pp. 1-6.
- [14] S. P. Giri, D. Vyshnavi, S. Devi R. V., P. Mathur and D. G. Kurup, "Non-Linear Modeling of Radio Frequency Impairments in Software Defined Radio (SDR)," in *Proc. International Conference on Emerging Trends in Networks & Internet of Things (IENT)*, 2024.

- [15] G. Rai, P. Sehgal, and K. Patel, "Wireless image transfer by various antennas using transmitter and receiver modules at 5.8 GHz," *International Journal of Microwave and Wireless Technologies*, vol. 16, no. 7, pp. 1248-1259, 2024.
- [16] A. Shams, P. Naugain, M. K. Khandelwal, A. Kumar, B. Mukherjee, and K. Patel, "Analysis and Performance of High Gain Receiver Antenna," Unpublished M.Tech Project Report, Department of Electronic Science, University of Delhi South Campus, New Delhi, India.
- [17] P. Naugain, A. Shams, M. K. Khandelwal, A. Kumar, B. Mukherjee, and K. Patel, "Compact Parasitic Based High Gain Antenna with Frequency Selective Surface for RADAR Applications," Unpublished Project Paper Draft, Department of Electronic Science, University of Delhi South Campus, New Delhi, India.
- [18] A. Shams, P. Naugain, M. K. Khandelwal, A. Kumar, B. Mukherjee, and K. Patel, "Compact Slot Based High Gain Patch Antenna for RADAR Application," Unpublished Project Paper Draft, Department of Electronic Science, University of Delhi South Campus, New Delhi, India.